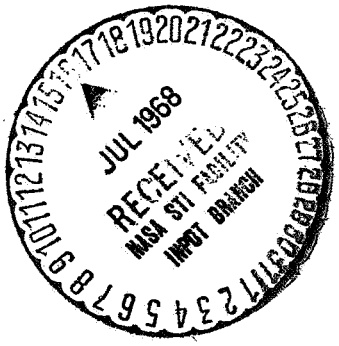


MERRICK ENGINEERING INC.

Nashville, Tennessee

FINAL REPORT

DEVELOPMENT OF WELD INTELLIGENCE SYSTEM AND CONTROLS

Contract No. NAS8-11808

Prepared For
George C. Marshall Space Flight Center
National Aeronautics and Space Administration

August, 1967

Prepared by: George E. Cook
George E. Cook, Vice President
And Director of Engineering

Approved by: George J. Merrick
George J. Merrick, President

FACILITY FORM 602
N68-32052 (ACCESSION NUMBER)
289 (PAGES)
CR-61921 (NASA CR OR TMX OR AD NUMBER)
(THRU) 1
(CODE) 17
(CATEGORY)

502-52598

ADMINISTRATIVE INFORMATION

This report was prepared by Merrick Engineering Inc. under contract NAS8-11808, "Development of Weld Intelligence System and Controls", for Marshall Space Flight Center, National Aeronautics and Space Administration.

The work was administered under the technical direction of the Manufacturing Engineering Laboratory with Mr. William M. McCampbell (R-ME-ME) as technical representative for Merrick Engineering Inc. Dr. George E. Cook served as project manager.

ABSTRACT

The objective of this program was to improve the properties of 2219 aluminum weldments by adaptively controlling the workpiece temperature in the vicinity of the molten puddle. Constraints placed on the scope of the program were: (1) the transducer utilized had to be of the temperature sensing type capable of providing intelligence related to the heat pattern about the molten puddle, (2) emphasis would be placed on transducers operating from the arc-side of the workpiece, (3) all experimentation would be conducted with the Gas Tungsten Arc process, (4) the transducer had to be of such size and shape as not to obstruct the welding operation, and (5) the material considered would be restricted to 2219 aluminum.

During the program, a hybrid thermocouple probe assembly was designed and fabricated to provide an accurate and simple method of monitoring workpiece temperature during the welding process. The system was demonstrated to: (1) be insensitive to radiated arc interference and the effect of variations in surface emissivity, (2) provide an essentially instantaneous response, and (3) be free from interference due to surface oxides.

An adaptive controller was designed and fabricated to amplify the hybrid thermocouple signal and actuate a small instrument servo motor, which was geared to a potentiometer for varying either the travel speed or weld current. The adaptive system was demonstrated to be capable of providing accurate and stable control of temperature at the probe position for wide variations in fitup, fixture, and material thickness.

Experimentation was conducted to demonstrate that the hybrid thermocouple signal was proportional to penetration on partial or full penetration welds made on

0.090 inch thick 2219 aluminum samples. On all of these experiments automatic voltage control was used to maintain constant arc voltage, and the transducer signal was used to automatically alter the weld current in such a manner as to maintain the mean temperature (and hence depth of penetration), at the probe, constant. While experimentation was limited to 0.090 inch thick samples, it was concluded that similar results could be achieved on all samples less than approximately 0.125 inch thickness.

Results of experimentation conducted on samples of 0.250 and 0.312 inch thickness indicated that the hybrid thermocouple signal could be correlated with partial penetration for varying conditions of heat sink. The system was found to operate with only marginal satisfaction, however, on the 0.250 and 0.312 inch thick samples when 100% penetration was attempted.

Experiments were conducted to establish the feasibility of utilizing a continuous intrinsic thermocouple in conjunction with a backup bar for penetration control on welds requiring backup for chilling purposes. Also, preliminary investigation was conducted to determine the feasibility of a recently developed thermocouple wire, trademarked Magic Wire, being used in the backup bar type of control.

TABLE OF CONTENTS

Page

1.0 INTRODUCTION ----------1

1.1 Purpose----------1

1.2 Approach----------2

1.3 Results----------4

2.0 PHASE I - INVESTIGATION OF TEMPERATURE SENSING METHODS----------7

2.1 Arc-Side Sensing----------7

2.1.1 Infrared Temperature Sensing Equipment----------7

2.1.2 Eddy Current Temperature Transducer----------23

2.1.3 Hybrid Thermocouple Surface - Temperature Transducer-------26

2.1.4 Summary----------43

2.2 Backside Sensing----------44

2.2.1 Application----------44

2.2.2 Intrinsic Thermocouple----------44

2.2.3 Magic Wire Thermocouple----------47

3.0 PHASE II - EXPERIMENTATION TO DETERMINE FEASIBILITY OF OBTAINING INTELLIGENT INFORMATION FROM TEMPERATURE TRANSDUCER----------49

3.1 Arc-Side Sensing----------51

3.1.1 Initial - Phase Fixture, Power Source and Instrumentation--51

3.1.2 Initial - Phase Hybrid Probe Assembly----------51

3.1.3 Sensitivity of Transducer Signal Versus Controllable Weld Variables----------57

3.2 Backside Sensing----------90

3.2.1 Modified, Intrinsic Thermocouple Control From Backside of Weld Plate----------90

3.2.2 Experiments with Magic Wire Sensing----------98

4.0 PHASE III - IMPLEMENTATION OF ADAPTIVE FEEDBACK CONTROL----------103

4.1 Introduction----------103

4.2 Servomechanism For Speed Control----------103

4.3 Penetration Control----------110

4.4 Initial Tests With Servo Compensation, Speed Control----------112

4.5 Experiments Run To Determine Functional Weld Penetration------118

4.6 Servomechanism Evaluation, Speed Control----------122

4.7 Equivalent Resistance of Aluminum-Constantan Hybrid Thermocouple Probe----------123

4.8 Sensitivity of Servo Amplifier-Motor Combination----------127

4.9 Test Samples with Pre-Positioned Heat Sinks----------127

4.10 Experiments with Large Heat Sinks, Speed Control----------130

4.11 Overall Closed-Loop Stability of System, Speed Control-------130

4.12 Reduction of Noise Effects----------133

4.13 Experimental Setups to Approximate Ideal Conditions----------133

4.14 System Modification For Current Control----------135

4.15 Response To Force Changes In Current, Current Control--------138

4.16 Stepped-Plate Weld (Increasing Thickness, Current Control)---138

4.17 Stepped-Plate Weld (Decreasing Thickness, Current Control)----139

4.18 System Response Time, Current Control----------139

4.19 Out-of-Position Welding, Current Control----------139

5.0 PHASE IV - COMPLETE SYSTEM EXPERIMENTATION----------139

5.1 Equipment----------139

5.1.1 Power Source----------139

5.1.2 Voltage Control Head----------142

5.1.3 Travel Speed Recorder----------142
5.1.4 Weld Current Recorder----------142
5.1.5 Arc Voltage Recorder----------142
5.1.6 Thermocouple Recorder----------142
5.1.7 Miscellaneous Recording----------142
5.1.8 Rotary Positioner----------142
5.1.9 Fixture----------142
5.1.10 Hybrid Probe Assembly----------142
5.1.11 Adaptive Controller----------152
5.2 Thick-Plate Experiments----------152
5.2.1 Thermocouple Output Versus Penetration----------152
5.2.2 Penetration Control, Partial Penetration Welds----------165
5.3 Thin-Plate Experiments----------187
5.3.1 Test Numbers 1T, 2T, 3T, 4T----------205
5.3.2 Test Numbers 5T and 6T----------205
5.3.3 Test Number 7T, 8T, and 9T----------205
5.3.4 Test Numbers 10T, 11T, 12T, 13T, 14T----------230
5.3.5 Test Number 15T----------230
5.3.6 Discussion----------230
6.0 CONCLUSIONS AND RECOMMENDATIONS----------230
7.0 REFERENCES----------270
8.0 PUBLICATIONS, PATENTS, AND PRESENTATIONS----------270
9.0 PERSONNEL AND ACKNOWLEDGEMENTS----------272

LIST OF FIGURES AND ILLUSTRATIONS

Figure 1 - Black Body Radiation Characteristics----------11

Figure 2 - Representative GTA Weld Bead on 0.250 Inch Thick, 2219 Aluminum Plate----------14

Figure 3 - Representative GTA Weld Bead on 0.250 Inch Thick, 2219 Aluminum Plate With Stepped Changes in Welding Current------15

Figure 4 - Cross Sections of Samples Shown in Figure 3----------16

Figure 5 - Method of Measuring Beadwidth----------17

Figure 6 - Beadwidth Versus Weld Current For Sample Show In Figure 3----18

Figure 7 - Beadwidth Versus Penetration For Sample Show In Figure 3-----19

Figure 8 - Eddy Current Transducer Principle----------25

Figure 9 - Basic Thermocouple Temperature Monitoring System----------27

Figure 10 - Hybrid Thermocouple Temperature Monitoring System----------30

Figure 11 - Experimental Simulation Of Radiated Interference From Torch-33

Figure 12 - Thermocouple Calibration Apparatus----------34

Figure 13 - Effect of Change In Reference Junction Temperature---------41

Figure 14 - NASA Memo On Intrinsic Thermocouple System----------45

Figure 15 - Simplified View of Instrinsic Thermocouple System----------46

Figure 16 - Simplified Equivalent Circuit Of Magic Wire Thermocouple----48

Figure 17 - Placement of Magic Wire In Backup Bar----------50

Figure 18 - Torch and AVC Assembly----------52

Figure 19 - Fixture and Instrumentation----------53

Figure 20 - Torch and Hybrid Probe Assembly----------54

Figure 21 - Torch and Hybrid Probe Assembly During Weld----------55

Figure 22 - Prototype Probe Assembly----------56
Figure 23 - Thermocouple Output Versus Weld Position----------59
Figure 24 - Thermocouple Output Versus Weld Position----------60
Figure 25 - Thermocouple Output Versus Weld Position----------61
Figure 26 - Thermocouple Output Versus Arc Voltage Variation----------64
Figure 27 - Thermocouple Response Versus Current Variation, Uncooled Plates----------67
Figure 28 - Thermocouple Response Versus Current Variation, Water cooled Plates----------68
Figure 29 - Thermocouple Response Versus Speed Variation----------69
Figure 30 - Thermocouple Signal Versus Probe Position----------70
Figure 31 - Thermocouple Output Versus Current Variation, Uncleaned Plates-72
Figure 32 - Thermocouple Output Versus Current Variation, Uncleaned Plates-73
Figure 33 - Average Change In Thermocouple Output Versus Current Variation, Uncleaned Plates----------74
Figure 34 - Thermocouple Output Versus Current Variation, Plates Wire Brushed Prior To Weld----------75
Figure 35 - Thermocouple Output Versus Current Variation, Plates Wire Brushed Prior To Weld----------76
Figure 36 - Average Change In Thermocouple Output Versus Current Variation, Plates Wire Brushed Prior To Weld----------77
Figure 37 - Average Change In Thermocouple Output Versus Current Variation, Cleaned and Uncleaned Plates----------78
Figure 38 - Heat Gradient Test----------80
Figure 39 - Heat Gradient Test----------81

Figure 40 - Instrumentation For Thermocouple Stability Tests----------83

Figure 41 - Typical Set of Welding Isotherms----------87

Figure 42 - Response Speed Tests----------88

Figure 43 - Experiment To Determine If Intrinsic Thermocouple Would Adhere To Molten Aluminum----------91

Figure 44 - Parallel Thermocouples----------92

Figure 45 - Experiment To Determine The Effect Of Loading On Thermocouple Junction----------94

Figure 46 - Simulation of Backside Instrinsic Thermocouple Method--------96

Figure 47 - Backside Sensing, Intrinsic Thermocouple----------97

Figure 48 - Magic Wire Thermocouple Experiment----------99

Figure 49 - Magic Wire Temperature Response----------101

Figure 50 - Magic Wire Response Time Characteristics----------104

Figure 51 - Chassis Layout, Prototype Control System----------105

Figure 52 - Prototype Control System----------106

Figure 53 - Schematic Diagram, Prototype Control System----------108

Figure 54 - Block Diagram, Speed Control System----------109

Figure 55 - Sample Welds, Speed Control----------113

Figure 56 - Travel Speed Charts, Speed Control----------114

Figure 57 - Stepped Plate Samples, Speed Control----------116

Figure 58 - Travel Speed Charts For Stepped Plate Welds With Speed Control----------117

Figure 59 - Weld Samples With Speed Control And Two Thermocouple Sensors----------119

Figure 60 - Speed Charts For Samples Made Using Two Thermocouple Sensors----------120
Figure 61 - Test Setup To Determine Functional Weld Penetration----------121
Figure 62 - Instrumentation To Determine Equivalent Resistance Of Aluminum-Constantan Hybrid Thermocouple Probe----------124
Figure 63 - Thevenin Equivalent Circuit----------125
Figure 64 - Test Setup, Experiments With Speed Control----------128
Figure 65 - Test Setup, Experiments with Speed Control----------131
Figure 66 - Feedback Control System Block Diagram, Speed Control---------132
Figure 67 - Test Setup, Experiments To Approximate Ideal Conditions------134
Figure 68 - Gear Train Assembly, Prototype Control System----------136
Figure 69 - Power Supply, Instrumentation, And Test Fixture----------137
Figure 70 - System Response Time, Current Control----------140
Figure 71 - Welding Station For Complete System Experimentation----------141
Figure 72 - ESR400 Programmable Power Source----------143
Figure 73 - Programming Modules And Control Panel, ESR400----------144
Figure 74 - Gas Panel And Impulse Starter Panel, ESR400----------145
Figure 75 - Test Fixture----------146
Figure 76 - Cylindrical Fixture With Clamping Arms Extended----------147
Figure 77 - Cylindrical Fixture And Recording Equipment----------148
Figure 78 - Cylindrical Fixture With Parts Clamped In Place----------149
Figure 79 - Rear View Of Cylindrical Fixture With Parts Clamped In Place----------150
Figure 80 - Cylindrical Fixture, Rear View----------151
Figure 81 - Torch, Hybrid Probe, And Adaptive Feedback Controller--------153

Figure 82 - Hybrid Probe Assembly, Vernier Scale Adjustment----------154
Figure 83 - Hybrid Probe Assembly, Vernier Scale Adjustment----------155
Figure 84 - Position Of Hybrid Probe With Respect To Electrode----------156
Figure 85 - Hybrid Probe And Torch Assembly During Weld----------157
Figure 86 - Hybrid Probe, Torch, And Adaptive Controller
During Weld----------158
Figure 87 - Adaptive Controller Layout----------159
Figure 88 - Front Panel, Adaptive Controller----------160
Figure 89 - Front Panel, Adaptive Controller----------161
Figure 90 - Top View, Adaptive Controller----------162
Figure 91 - Bottom View, Adaptive Controller----------163
Figure 92 - Rear View, Adaptive Controller----------164
Figure 93 - Hybrid Thermocouple Output, Test Number 40----------165
Figure 94 - Welding Current, Test Number 40----------166
Figure 95 - Weld Bead, Arc-Side, Test Number 40----------168
Figure 96 - Backside of Test Number 40----------169
Figure 97 - Cross Sections Of Test Number 40----------170
Figure 98 - Hybrid Thermocouple Output, Test Number 41----------171
Figure 99 - Welding Current, Test Number 41----------172
Figure 100 - Weld Bead, Arc-Side, Test Number 41----------173
Figure 101 - Backside of Test Number 41----------174
Figure 102 - Cross Sections Of Test Number 41----------175
Figure 103 - Hybrid Thermocouple Output, Test Number 42----------176
Figure 104 - Welding Current, Test Number 42----------177
Figure 105 - Weld Bead, Arc-Side, Test Number 42----------178

Figure 106 - Backside Of Test Number 42----------179
Figure 107 - Cross Sections Of Test Number 42----------180
Figure 108 - Hybrid Thermocouple Output, Test Number 28----------181
Figure 109 - Welding Current, Test Number 28----------182
Figure 110 - Hybrid Thermocouple Output, Test Number 29----------183
Figure 111 - Welding Current, Test Number 29----------184
Figure 112 - Welding Current, Test Number 27----------185
Figure 113 - Cross Sections, Test Numbers 27, 28, 29----------186
Figure 114 - Hybrid Thermocouple Output, Test Number 30----------188
Figure 115 - Welding Current, Test Number 30----------189
Figure 116 - Cross Sections, Test Number 30----------190
Figure 117 - Hybrid Thermocouple Output, Test Number 31----------191
Figure 118 - Cross Sections, Test Number 31----------192
Figure 119 - Hybrid Thermocouple Output, Test Number 33----------193
Figure 120 - Welding Current, Test Number 33----------194
Figure 121 - Cross Sections, Test Number 33----------195
Figure 122 - Hybrid Thermocouple Output, Test Number 34----------196
Figure 123 - Welding Current, Test Number 34----------197
Figure 124 - Cross Sections, Test Number 34----------198
Figure 125 - Hybrid Thermocouple Ouput, Test Number 35----------199
Figure 126 - Welding Current, Test Number 35----------200
Figure 127 - Cross Sections, Test Number 35----------201
Figure 128 - Hybrid Thermocouple Output, Test Number 36----------202
Figure 129 - Welding Current, Test Number 36----------203
Figure 130 - Cross Sections, Test Number 36----------204

Figure 131 - Hybrid Thermocouple Output, Test Number 1T----------206
Figure 132 - Weld Bead, Arc side, Test Number 1T----------207
Figure 133 - Weld Bead, Backside, Test Number 1T----------208
Figure 134 - Cross Sections, Test Number 1T----------209
Figure 135 - Hybrid Thermocouple Output, Test Number 2T----------210
Figure 136 - Weld Bead, Arc Side, Test Number 2T----------211
Figure 137 - Weld Bead, Backside, Test Number 2T----------212
Figure 138 - Cross Sections, Test Number 2T----------213
Figure 139 - Hybrid Thermocouple Output, Test Number 3T----------214
Figure 140 - Weld Bead, Arc Side, Test Number 3T----------215
Figure 141 - Weld bead, Backside, Test Number 3T----------216
Figure 142 - Cross Sections, Test Number 3T----------217
Figure 143 - Hybrid Thermocouple Output, Test Number 4T----------218
Figure 144 - Weld Bead, Arc Side, Test Number 4T----------219
Figure 145 - Weld Bead, Backside, Test Number 4T----------220
Figure 146 - Cross Sections, Test Number 4T----------221
Figure 147 - Hybrid Thermocouple Output, Test Number 5T----------222
Figure 148 - Weld Bead, Arc Side, Test Number 5T----------223
Figure 149 - Weld Bead, Backside, Test Number 5T----------224
Figure 150 - Cross Sections, Test Number 5T----------225
Figure 151 - Hybrid Thermocouple Output, Test Number 6T----------226
Figure 152 - Weld Bead, Arc Side, Test Number 6T----------227
Figure 153 - Weld Bead, Backside, Test Number 6T----------228
Figure 154 - Cross Sections, Test Number 6T----------229
Figure 155 - Hybrid Thermocouple output, Test Number 7T----------231

Figure 156 - Weld Bead, Arc Side, Test Number 7T----------232
Figure 157 - Weld Bead, Backside, Test Number 7T----------233
Figure 158 - Cross Sections, Test Number 7T----------234
Figure 159 - Hybrid Thermocouple Output, Test Number 8T----------235
Figure 160 - Weld Bead, Arc Side, Test Number 8T----------236
Figure 161 - Weld Bead, Backside, Test Number 8T----------237
Figure 162 - Cross Sections, Test Number 8T----------238
Figure 163 - Hybrid Thermocouple Output, Test Number 9T----------239
Figure 164 - Weld Bead, Arc Side, Test Number 9T----------240
Figure 165 - Weld Bead, Backside, Test Number 9T----------241
Figure 166 - Cross Sections, Test Number 9T----------242
Figure 167 - Hybrid Thermocouple Ouput, Number 10T----------243
Figure 168 - Weld Bead, Arc Side, Test Number 10T----------244
Figure 169 - Weld Bead, Backside, Test Number 10T----------245
Figure 170 - Cross Sections, Test Number 10T----------246
Figure 171 - Hybrid Thermocouple Output, Test Number 11T----------247
Figure 172 - Weld Bead, Arc Side, Test Number 11T----------248
Figure 173 - Weld Bead, Backside, Test Number 11T----------249
Figure 174 - Cross Sections, Test Number 11T----------250
Figure 175 - Hybrid Thermocouple Output, Test Number 12T----------251
Figure 176 - Weld Bead, Arc Side, Test Number 12T----------252
Figure 177 - Weld Bead, Backside, Test Number 12T----------253
Figure 178 - Cross Sections, Test Number 12T----------254
Figure 179 - Hybrid Thermocouple Output, Test Number 13T----------255
Figure 180 - Weld Bead, Arc Side, Test Number 13T----------256

Figure 181 - Weld Bead, Backside, Test Number 13T----------257

Figure 182 - Cross Sections, Test Number 13T----------258

Figure 183 - Hybrid Thermocouple Output, Test Number 14T----------259

Figure 184 - Weld Bead, Arc Side, Test Number 14T----------260

Figure 185 - Weld Bead, Backside, Test Number 14T----------261

Figure 186 - Cross Sections, Test Number 14T----------262

Figure 187 - Hybrid Thermocouple Output, Test Number 15T, Preheat Pass----263

Figure 188 - Hybrid Thermocouple Ouput, Test Number 15T----------264

Figure 189 - Weld Bead, Arc Side, Test Number 15T----------265

Figure 190 - Weld Bead, Backside, Test Number 15T----------266

Figure 191 - Cross Sections, Test Number 15T----------267

LIST OF TABLES

Table No. Page No.

I - Thermoelectric Sensitivity of Materials Against Platinum----------31

II - Calibration of Aluminum-Constantan Thermocouple----------36

III - Weld Parameter Values----------58

IV - Weld Parameter Values----------62

V - Thermocouple Signal (millivolts) Versus Current Variation----------65

VI - Thermocouple Signal (millivolts) Versus Current Variation-
Water Cooled Specimens----------65

VII - Thermocouple Signal (millivolts) Versus Speed Variation----------66

VIII - Weld Parameters, Tests With Servo Compensation----------112

IX - Weld Parameters, With Servo Compensation----------115

X - Weld Parameters, With Servo Compensation----------118

XI - Thermocouple Variation, Speed Control----------122

XII - Thermocouple Variation, Speed Control----------123

XIII - Thermocouple Variation, Speed Control----------123

CONTRACT NAS8-11808

DEVELOPMENT OF WELD INTELLIGENCE SYSTEM AND CONTROLS

1.0 INTRODUCTION

1.1 PURPOSE

Conventional arc welding systems depend upon control of certain variables; among them arc voltage, current, travel speed, and wire feed rate. These are called, for purposes of comparison, the controllable weld variables. For a given weld, when all weld variables (both controllable and uncontrollable) are constant, certain direct weld characteristics may be expected to remain constant. These include bead width, buildup, nugget consistency, and penetration. However, when one or more of the weld variables other than those subject to precision control (for example, atmospheric conditions) may vary, or in welds involving changes in thickness or contour, a poor weld may result. A sufficiently skilled operator may reduce the occurrance of poor welds by rapidly identifying degradations in the direct weld characteristics and manually modifying one or more of the controllable variables to adapt the welding system to the changing environment. With the increasing demands for high quality welds by the Aerospace Industry, however, and with the increasing costs incurred by a single weld failure in a large complex weld, the need to eliminate the human operator from the feedback path for correction of the welding process has become evident.

Of the several manufacturing technologies, welding alone has defied true adaptive automation. Even with excellent controllers for the several controllable variables, the human operator still provides in most present welding systems the only feedback loop between the direct weld characteristics and the controllable variables. In a typical programmed machine tool operation, position

transducers provide a continuous, accurate feedback on the location of the tool. But in a typical fusion welding process control, no such intelligence is available. It is still usually necessary to have the human operator monitor the weld in progress and make corrections to compensate for minor variations in joint fit-up, plate thickness, variations in shield or one or more of several of the uncontrollable variables.

The purpose of this program was to: (1) investigate the feasibility of developing a transducer that would directly or indirectly sense one or more of the direct weld characteristics, (2) conduct experimentation to substantiate the transducer's ability to provide a useful signal proportional to direct weld characteristics, and (3) develop a prototype, automatic feedback control system that would utilize the information obtained from the transducer to make the necessary modifications in one or more of the controllable variables to maintain the mean output of the transducer constant.

Constraints placed on the scope of the program were[1]: (1) the transducer had to be of the temperature sensing type capable of providing information related to the heat pattern about the molten puddle, (2) emphasis would be placed on transducers operating from the arc-side of the workpiece, (3) all experimentation would be conducted with the Gas Tungsten Arc (GTA) process, (4) the transducer had to be of such size and shape as not to obstruct the welding operation, and (5) the material considered would be restricted to 2219 aluminum. While all experimentation under this program was limited to GTA welding of 2219 aluminum, the techniques developed should prove helpful in other welding processes and different materials as well.

1.2 APPROACH

Based on the results of earlier work [2] utilizing infrared scanning techniques it was concluded at the offset that the transducer should be of the temperature sensing type. The first phase of the program therefore consisted of a general investigation of applicable temperature sensing devices. The types of temperature

transducers investigated were those based on: (1) infrared principles, (2) eddy current techniques, and (3) modifications of the simple thermocouple. After extensive research into the advantages and disadvantages of these three general methods of temperature sensing, it was concluded that a hybrid thermocouple utilizing the aluminum workpiece as one half of the thermocouple junction was superior in terms of accuracy, size, simplicity and cost. The limitations of the hybrid thermocouple probe were: (1) it required direct physical contact with the workpiece, and (2) it was only capable of measuring temperatures outside the molten puddle.

The second phase of the program consisted of experimentation under practical GTA weld conditions to: (1) determine the feasibility of obtaining intelligent information from the hybrid thermocouple transducer, (2) determine the sensitivity of transducer signal versus controllable weld variables, (3) determine optimum locations of the sensing probe under varying weld conditions and material thickness, and (4) determine under what conditions the transducer output could be correlated with one or more of the direct weld characteristics such as penetration.

The third phase of the program was to design and construct a prototype automatic feedback control system and to conduct experimentation under complete system feedback conditions. The automatic feedback control system was designed such that it could be used with any programmable power source and/or travel speed controller. The experimentation was directed toward determining the classes of welding conditions under which the system would perform satisfactory, and determining what percentage of change in uncontrollable variables could be tolerated for stable operation.

In addition to the three phases of work described above, experimentation was conducted concurrently with backside temperature sensing techniques. Two methods were employed, both being modifications of the standard thermocouple principle. Since backside sensing was considered a secondary objective of this program, experimentation was limited to feasibility studies with no complete system experimentation being conducted.

1.3 RESULTS

1.3.1 A hybrid thermocouple probe assembly was designed and constructed to provide: (1) constant probe pressure against the workpiece regardless of vertical torch movement or surface irregularities, (2) accurate control of the probe position relative to the puddle during normal torch motion due to automatic voltage control, (3) vernier adjustments of the probe position, and (4) rigid mechanical operation to avoid fluctuations in location during a weld program. The assembly was designed such that it could be easily clamped to most commercial welding torches.

1.3.2 Utilizing the hybrid thermocouple concept, a simple, positive, and accurate method of monitoring workpiece temperature was developed. By allowing the aluminum workpiece to form one half of the thermocouple junction, radiated torch interference and the effect of variations in surface emissivity were eliminated. The response to temperature changes was essentially instantaneous because the constantan probe was designed to draw negligible heat away from the junction before reaching equilibrium. Further, tests with aluminum plates both chemically cleaned and not cleaned showed no effect from oxide films on the workpiece surface when using the single wire technique.

In the majority of experiments conducted under this program, the temperature at a single point, located with respect to the molten puddle, was monitored. However, a dual probe could be easily implemented such that a continuous measure of a temperature gradient could be obtained; thereby providing a continuous signal proportional to thermal transients in the workpiece. This signal could then be used in a feedback loop to control an auxiliary workpiece cooling system [3]; and hence provide automatic control of the time-temperature relationship in the vicinity of the molten puddle.

The result would be better control of the grained cast structure and heat affected zones in the weldment.

1.3.3 A prototype adaptive control system was designed and constructed to amplify the hybrid thermocouple signal and actuate a small instrument servo motor, which was geared to a potentiometer for varying either the travel speed or weld current. The control system was demonstrated to be capable of providing accurate and stable control of temperature at the probe position for wide variations in fitup, fixture, and material thickness. Controls were provided for ease in initial setup and activation of the adaptive loop.

1.3.4 Experimentation was conducted to demonstrate that the hybrid thermocouple signal was proportional to penetration on partial or full penetration welds made on 0.090 inch thick aluminum samples. On all of these experiments automatic voltage control was used to maintain constant arc voltage, and the transducer signal was used to automatically alter the welding current in such a manner as to maintain the mean temperature (and hence weld penetration), at the probe, constant. Variations in heat sink were simulated by backup aluminum blocks, and welds were made with and without adaptive feedback to demonstrate the improvement in penetration consistency with closed-loop control.

While experimentation was limited to 0.090 inch thick samples, it is felt that similiar results can be achieved on thinner sections such as thin-walled tubing. Experimentation with samples thicker than 0.090 inch is described below.

1.3.5 Results of experimentation conducted on samples of 0.250 and 0.312 inch thickness indicated that the hybrid thermocouple signal could be correlated with penetration on welds of less than 100% penetration and could therefore be utilized to control depth of penetration for varying conditions of heat sink. The system was found to operate with only marginal satisfaction, however, on the 0.250 and

0.312 inch thick samples when 100% penetration was attempted. The reason for this was traced to the relatively large changes in tungsten-to-work proximity (for varying heat sink conditions) due to automatic voltage control action. These changes in proximity produced significant changes in the arc-side bead-width and hence produced error in the probe output (the transducer signal being proportional to the puddle edge-to-probe distance). This effect was found to be insignificant on the 0.090 inch samples (see section 1.3.4) and hence did not degrade system performance even for 100% penetration.

It should be noted that penetration control systems designed to operate from a signal proportional to tungsten-to-work variations, under constant automatic voltage control, perform optimally on thicker materials with 100% penetration because of the more pronounced signal change available. On thin materials or on thick materials with less than 100% penetration, this type penetration control system does not operate well because of the small signal available (tungsten-to-work distance being essentially constant). Since the temperature-control system developed under this program operates optimally when the tungsten-to-work distance is essentially constant, it fills a gap heretofore missing with the proximity-operated penetration control device.

Limited experimentation was conducted on 0.250 and 0.312 inch samples with 100% penetration utilizing proximity control rather than arc voltage control, and utilizing the temperature control system to vary current in such a manner as to maintain temperature constant. The results were satisfactory but rather critical in setup.

1.3.6 Experimentation was conducted to establish the feasibility of utilizing a continuous intrinsic thermocouple in conjunction with a backup bar for penetration control (from the backside) on welds requiring backup for chilling purposes.

1.3.7 Preliminary investigation was conducted to determine the feasibility of a recently developed thermocouple wire[4] (trademarked "Magic Wire") being utilized in the backup bar type of control (see section 1.3.6).

2.0 PHASE I- INVESTIGATION OF TEMPERATURE SENSING METHODS

As a preliminary phase of this program, an evaluative investigation was undertaken to resolve the type of temperature transducer that would be utilized. For arc side sensing, three general types of transducers were considered: (1) transducers based on the infrared principles, (2) eddy current devices, and (3) transducers based on modifications of the simple thermocouple. These transducers are discussed below in section 2.1. For backside sensing, two methods were investigated; both being modifications of the standard thermocouple principle: (1) intrinsic thermocouple, and (2) "Magic Wire" thermocouple. The backside sensing techniques are discussed in section 2.2.

2.1 ARC-SIDE SENSING

2.1.1 INFRARED TEMPERATURE SENSING EQUIPMENT

As a result of a report entitled "Infrared Temperature Sensing Systems For Automatic Fusion Welding"[2] by Ramsey, Chyle, Kuhr, Myers, and Groth of research performed under Contract NAS8-1593 for the National Aeronautics And Space Administration, infrared temperature-sensing techniques were the first to be conconsidered. A summary of the conclusions reached in this report are listed below in section 2.1.1.1.

2.1.1.1 CONCLUSIONS REACHED IN REPORT, "INFRARED TEMPERATURE SENSING SYSTEMS FOR AUTOMATIC FUSION WELDING"

2.1.1.1.1 It was concluded that commercial fixed infrared radiometers did not appear feasible for monitoring weld bead or adjacent areas for control purposes, primarily because of arc area radiation and variable emissivity of the viewed surface.

2.1.1.1.2 It was concluded that a scanning type infrared radiometer (arranged to periodically scan across the weld centerline) appeared to offer considerable promise for GTA welding control by providing signals whose width is related

to radiation profiles across the weld bead.

2.1.1.1.3 Infrared scanning behind the arc was found preferable to other locations.

2.1.1.1.4 Mechanical shielding of electrode radiation from the scanned area did not appear practical.

2.1.1.2 FURTHER INVESTIGATION OF INFRARED TRANSDUCERS

Encouraged by the conclusions reached in the report referenced in section 2.1.1 above, additional investigation was undertaken to determine: (1) whether or not fixed point monitoring could be made feasible by utilization of various filtering techniques or specialized instrument design; and (2) whether or not information obtained from scanning equipment could be correlated in a meaningful way with uniformity of weld characteristics.

2.1.1.2.1 REASONS FOR INTERFERENCE WITH FIXED POINT MONITORING

The difficulty of using an infrared radiometer to measure the surface temperature from the arc side of the workpiece at a fixed point adjacent to the molten puddle is due primarily to: (1) direct or reflected radiation from the much hotter tungsten tip and associated arc plasma, and (2) variation in surface emissivity due to oxidation. The reasons for these difficulties are as follows:

2.1.1.2.1.1 The heat transmitted to the infrared transducer will consist of three components; (1) that due to direct radiation from the surface of the workpiece, (2) that due to reflected radiation from the arc plasma, and (3) that due to direct radiation from the arc plasma.

2.1.1.2.1.2 Of the three components stated in paragraph 2.1.1.2.1.1. above, only the first is indicative of the true surface temperature of the workpiece. If the other two components are not eliminated or accounted for, an erroneous signal will be obtained from the radiometer.

2.1.1.2.1.3 The desired component due to direct radiation from the surface of the workpiece will have an intensity given by the Stefan-Boltzman Law

$$W = \varepsilon\sigma\,(T_1^4 - T_0^4) \qquad (1)$$
$$\tilde{=} \varepsilon\sigma T_1^4, \text{for } T_1 \gg T_0$$

Where W = intensity of radiation

σ = proportionality constant

T_1 = surface temperature of workpiece

T_0 = environmental temperature

ε = emissivity of workpiece surface (the emissivity is defined as the ratio of the radiance of an object at temperature T to the radiance of a blackbody at the same temperature. The emissivity is thus 1.0 for an ideal blackbody and less than 1.0 for any other object.)

The emissivity ε of aluminum is approximately 0.1 prior to welding. The exact value depends on the type of cleaning immediately preceeding the weld. During and after welding the emissivity of the aluminum workpiece in the vicinity of the molten puddle may increase by as much as five time, ε= 0.5, due to oxidation of the aluminum surface. Thus from equation (1) we see that the intensity of radiation may vary as much as 500% even though the surface temperature is completely constant.

2.1.1.2.1.4 Assuming an emissivity of 0.1 for the aluminum surface, the reflectivity will then be 0.9. Thus energy will be reflected from the workpiece with 9 times the magnitude of an equal amount of energy directly radiated.

2.1.1.2.1.5 The temperature of the aluminum surface at the point of interest will normally be between 600°F and 1000°F (see section 3.0), while the plasma temperature may be as high as 35,000°F([5]). The much higher temperature of the plasma combined with the high reflectivity of the aluminum surface means that the plasma heat energy reflected into the focal cone of the infrared radiometer is likely to be many times the intensity of the direct radiation component.

2.1.1.2.1.6 If one could assume that the reflected component from the arc plasma were constant, then this component could be cancelled at the voltage output of the radiometer, leaving only

the component due to direct radiation. This assumption is not valid, however, because of: (1) the turbulency of the arc plasma, (2) the "wandering" of the tungsten "cathode spot", and (3) the varying surface conditions of the workpiece.

2.1.1.2.1.7 The reflected component from the arc plasma will be more intense at some angles than others. However, due to the turbulency of the arc plasma and the relatively rough reflecting surface of the aluminum workpiece, it would be expected that some energy would be reflected in all directions.

2.1.1.2.1.8 Radiation will be transmitted directly from the arc plasma in roughly all directions.

2.1.1.2.2 TECHNIQUES FOR REDUCING INTERFERENCE WITH FIXED POINT MONITORING

2.1.1.2.2.1 The problem of variation in emissivity at the workpiece surface can be reduced by: (1) focusing the radiometer at a point where oxide accumulation is small and/or (2) painting a graphite strip parallel to the weld joint to provide a greater and more constant emissivity in the radiometer's target zone. The latter is undesirable from the standpoint of: (1) time and expense of painting graphite strip on workpiece, (2) possibility of graphite particles dropping into the weld zone producing contamination, and (3) usual necessity of removing graphite after weld is completed.

2.1.1.2.2.2 Because of the much greater temperature of the arc plasma as compared to the temperature of the aluminum workpiece, direct and reflected radiation from the plasma can be reduced in intensity by choosing an infrared radiometer that operates in the long wavelength region. Shown in Figure 1 is the black body radiation characteristics for several valves of temperature. We note that a peak in radiant intensity occurs as a function of wavelength, and that further, the peak occurs at progressively lower wavelengths as the temperature increases. Thus in order to measure the relatively low surface temperature of a material in the presence of a high temperature reflection, a long wavelength radiometer should be used. The desired long wavelength characteristics

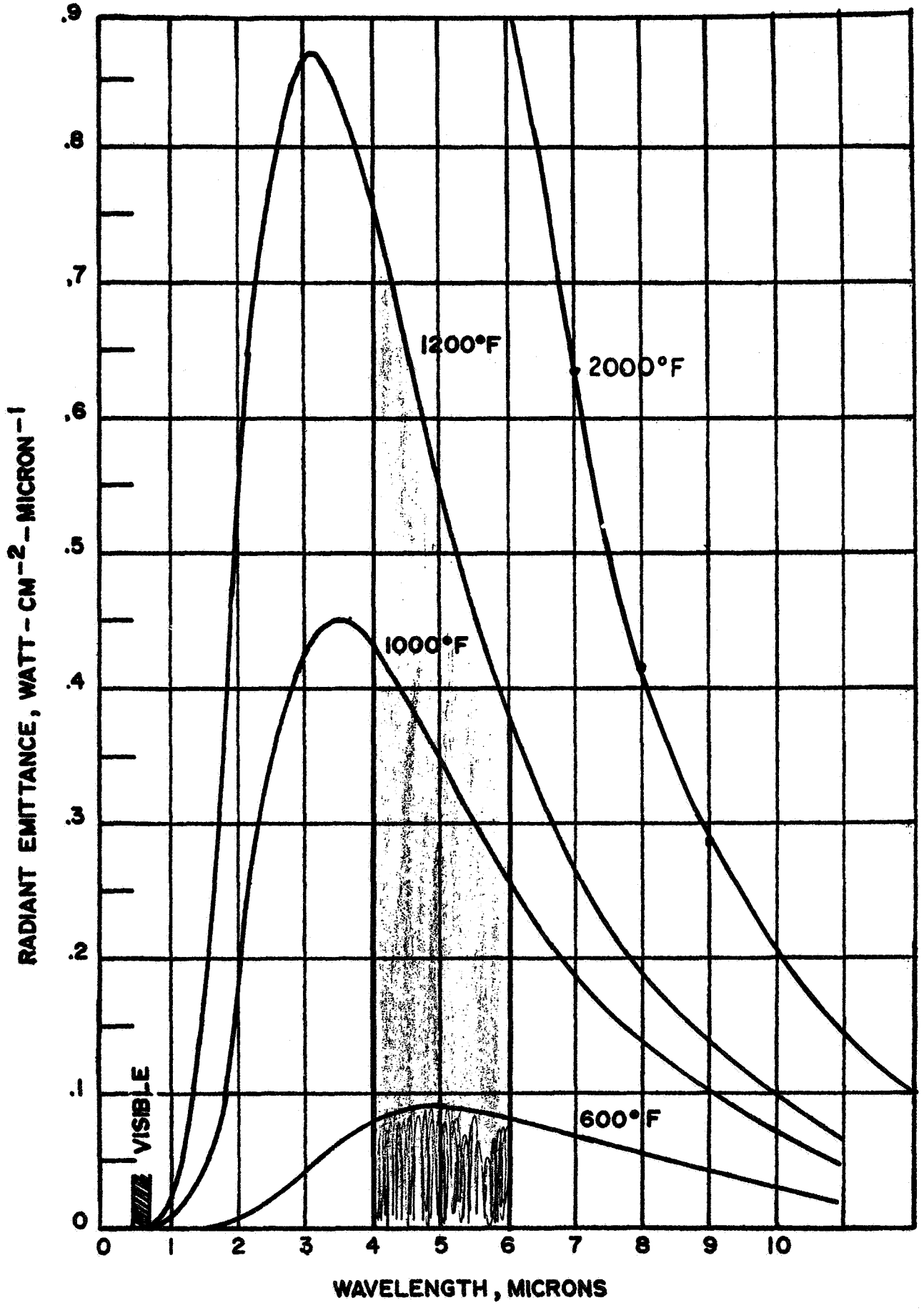


FIG. 1 – BLACK BODY RADIATION CHARACTERISTICS

of the radiometer can be achieved by utilization of the proper detection element, or the proper filter, or both.

In the report referenced in section 2.1.1, a Thermistor Bolometer type detector was used in the radiometer. In addition a germanium absorption-edge filter was used to eliminate radiation of wavelengths shorter than 1.8 microns. Also an experiment was reported in which an InSb filter was placed in the optical axis to prevent transmission of wavelengths below 7.5 microns. The combined attenuation of the germanium and InSb filters was so great, however, the signal to noise ratio was reduced to an unuseable level. The signal to noise ratio could be greatly increased by use of a solid state or quantum detector choosen for the long wavelength spectral range of interest, thereby eliminating the necessity of additional filters and their associated attenuation.

2.1.1.2.2.3 To reduce reflection interference from the tungsten electrode and associated arc plasma, the angular positioning of the sensing head is of the utmost importance. If the optical line of sight of the infrared detector is arranged at an angle where emission from the arc reflects out into space, a considerable advantage can be gained.

2.1.1.2.2.4 One possible means of reducing reflection interference would be to utilize a split beam principle that would divide the energy radiated from a small diameter spot onto two separate detectors. The difference in the reflected energy from these two spots would presumably be very slight; thus the possibility of cancelling out the effect of the reflected energy would have a better opportunity of success.

2.1.1.2.2.5 A number of means are available for mechanically shielding the field of view of the infrared radiometer from arc and electrode radiation. Devices considered in this respect have been ceramic skirts, graphite baffles in the form of thin chissels, and critical placement of masks between the weldment and the radiometer. All such devices greatly reduce visual and physical access to the torch area, and none provide complete shielding of the electrode and plasma radiation.

2.1.1.2.3 FEASIBILITY OF INFRARED SCANNING

2.1.1.2.3.1 A typical GTA weld bead on 0.250 inch thick 2219 aluminum plate is shown in Figure 2. It is seen that a definite oxide strip exists on each side of the weld bead. Due to the increased emissivity of the oxide, the scanner signal will be very pronounced at each of the oxide strips. Thus the scan signal width will be a function of the oxide strip's position, distinction, and width. These characteristics of the oxide strips are, however, very dependent on the arc voltage, gas type, gas flow, welding current, and position of welding.

2.1.1.2.3.2 A representative GTA weld bead on 0.250 inch thick 2219 aluminum plate for stepped increases in current is shown in Figure 3. On this sample, the type shielding gas was Helium, the gas flow was 100CFH, the arc voltage was held constant at 12 volts, and the sample position was horizontal. Cross-sections of the sample are shown in Figure 4. With beadwidth measurements made as shown in Figure 5, a plot of beadwidth versus weld current is presented in Figure 6. A similar plot of beadwidth versus penetration is shown in Figure 7. In both figures, we see that the beadwidth is very dependent on whether full or partial penetration is present; the slope of the beadwidth curve actually changing from positive to negative at the point of full penetration. It should be noted that this effect is less for thinner plates, and for plates of 0.125 inch thickness or less is negligible; the beadwidth having a positive slope versus current for all desired levels of penetration.

2.1.1.2.3.4 Based on the results presented in section 2.1.1.2.3.1 and 2.1.1.2.3.2 it is concluded that a scan signal will not be useable to indicate or control penetration except on thin sheets or on thick sheets where less than full penetration is desired.

2.1.1.3 CONSULTATION WITH MANUFACTURERS

Several manufacturers of infrared equipment were consulted in regard to equipment specifications and recommendations. A listing of companies and summary of equipment specifications is presented below.

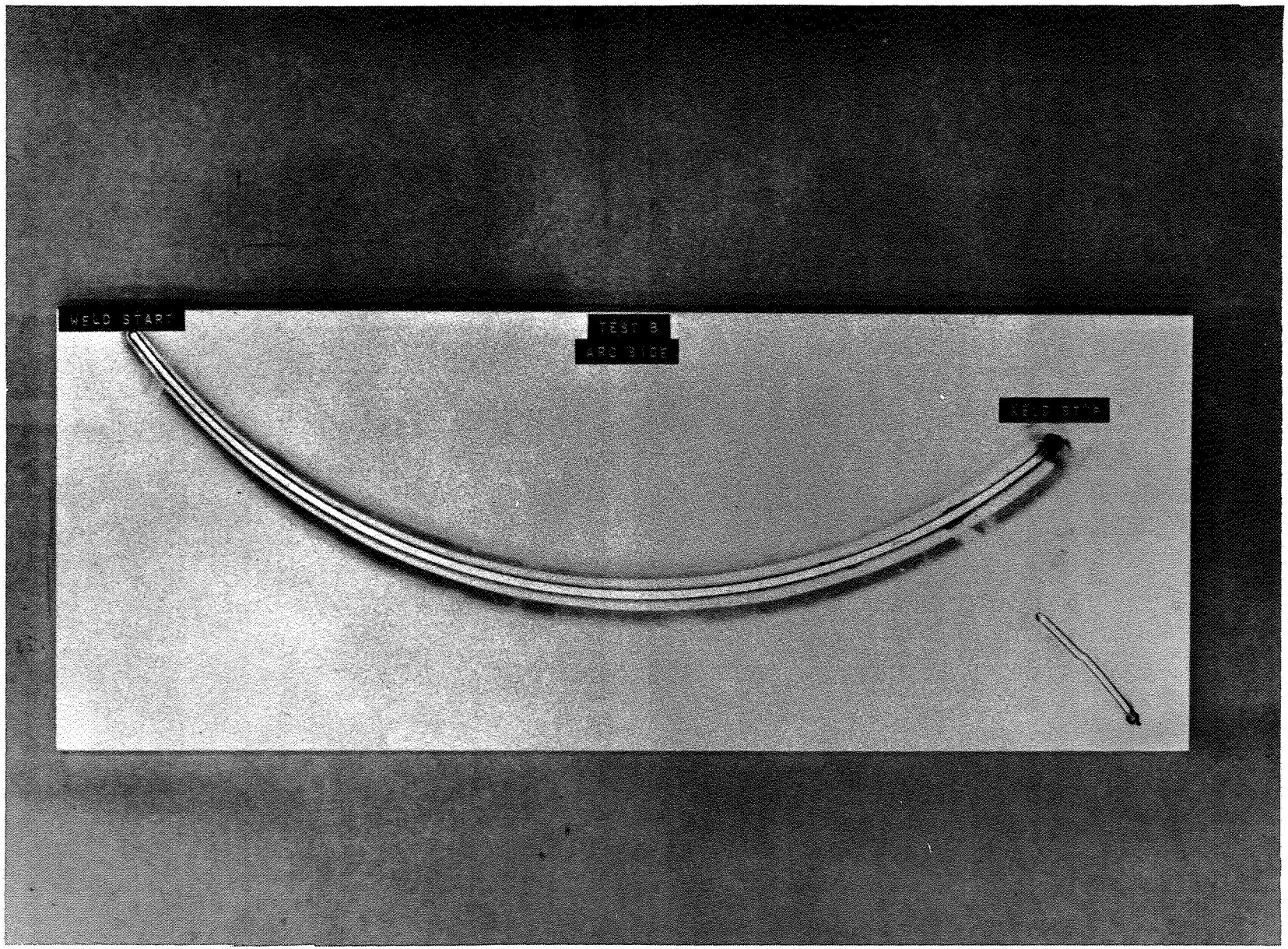


Figure 2: Representative GTA Weld bead on 0.250 inch thick, 2219 aluminum plate.

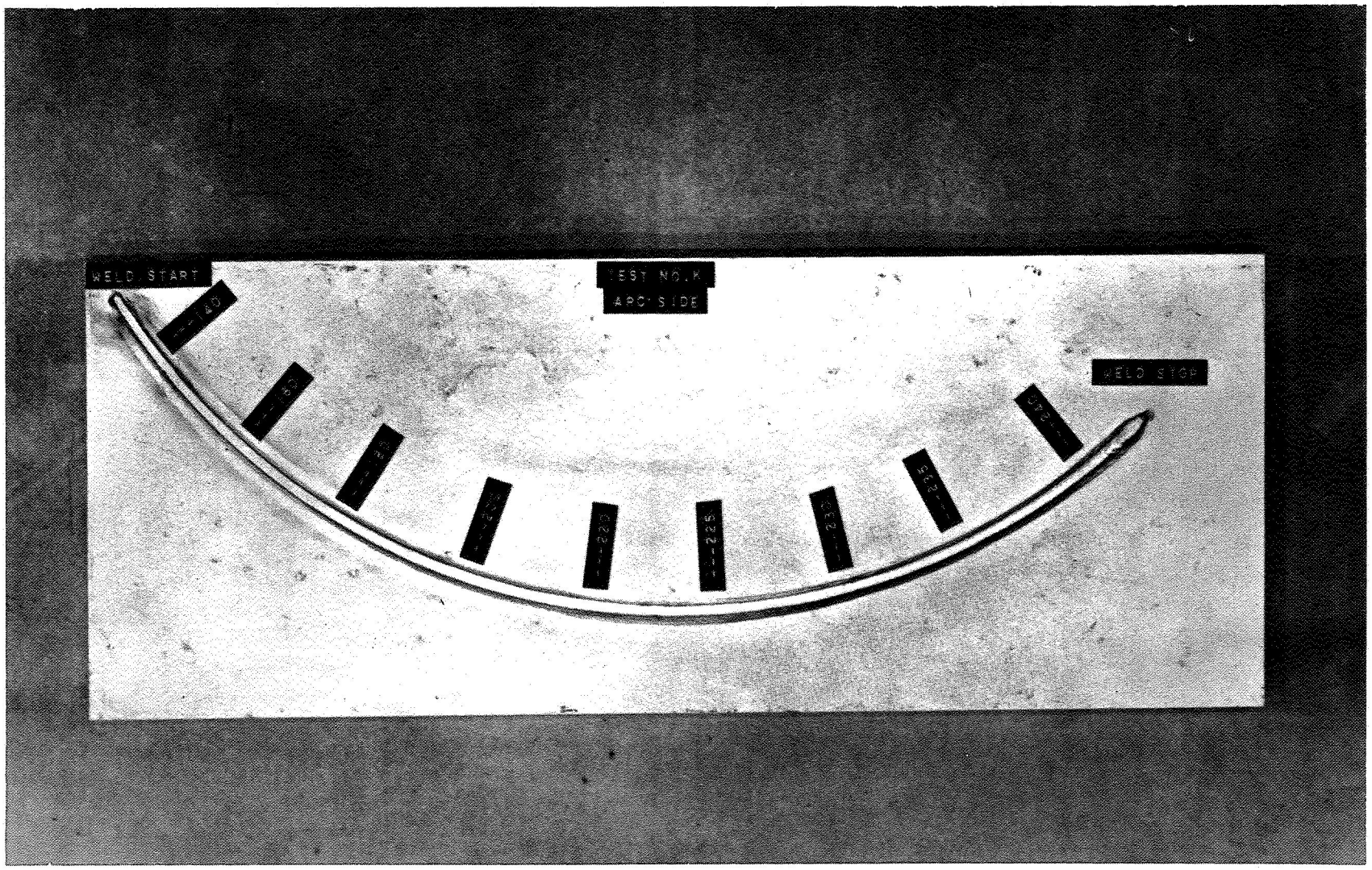


Figure 3: Representative GTA weld bead on 0.250 inch thick, 2219 aluminum plate with stepped changes in welding current.

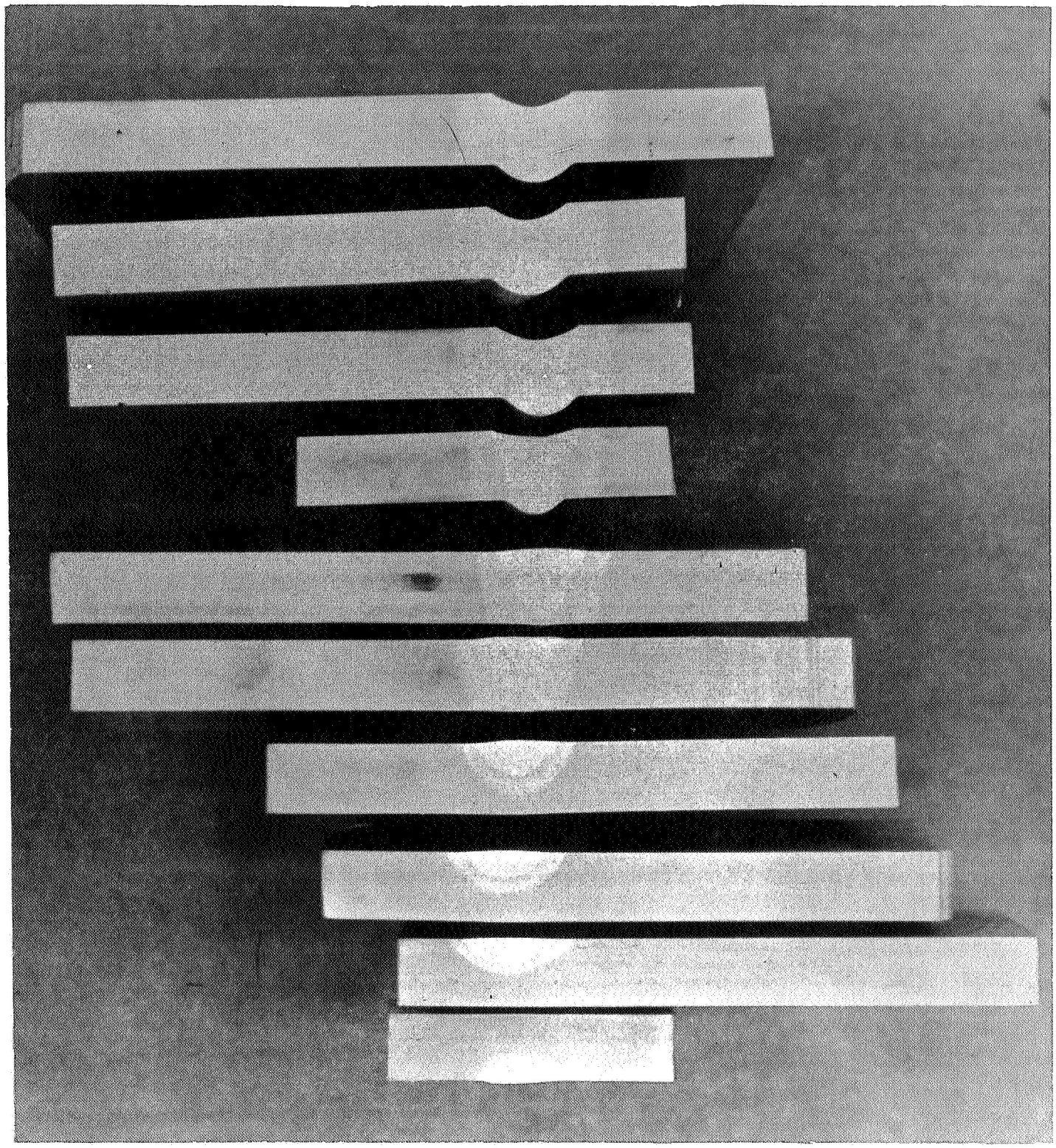


Figure 4: Cross/sections of sample shown in Figure 3.

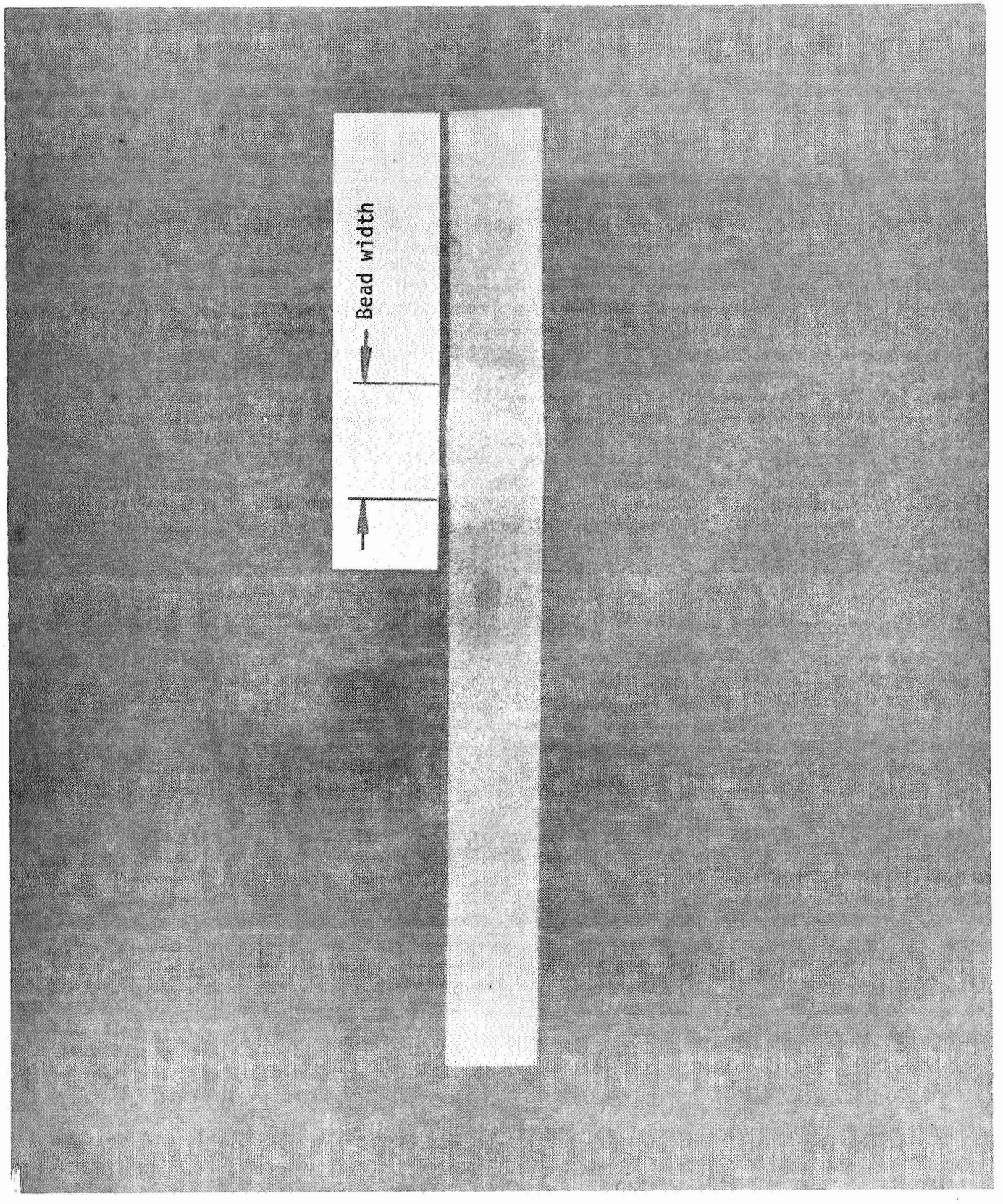


Figure 5: Method of measuring beadwith

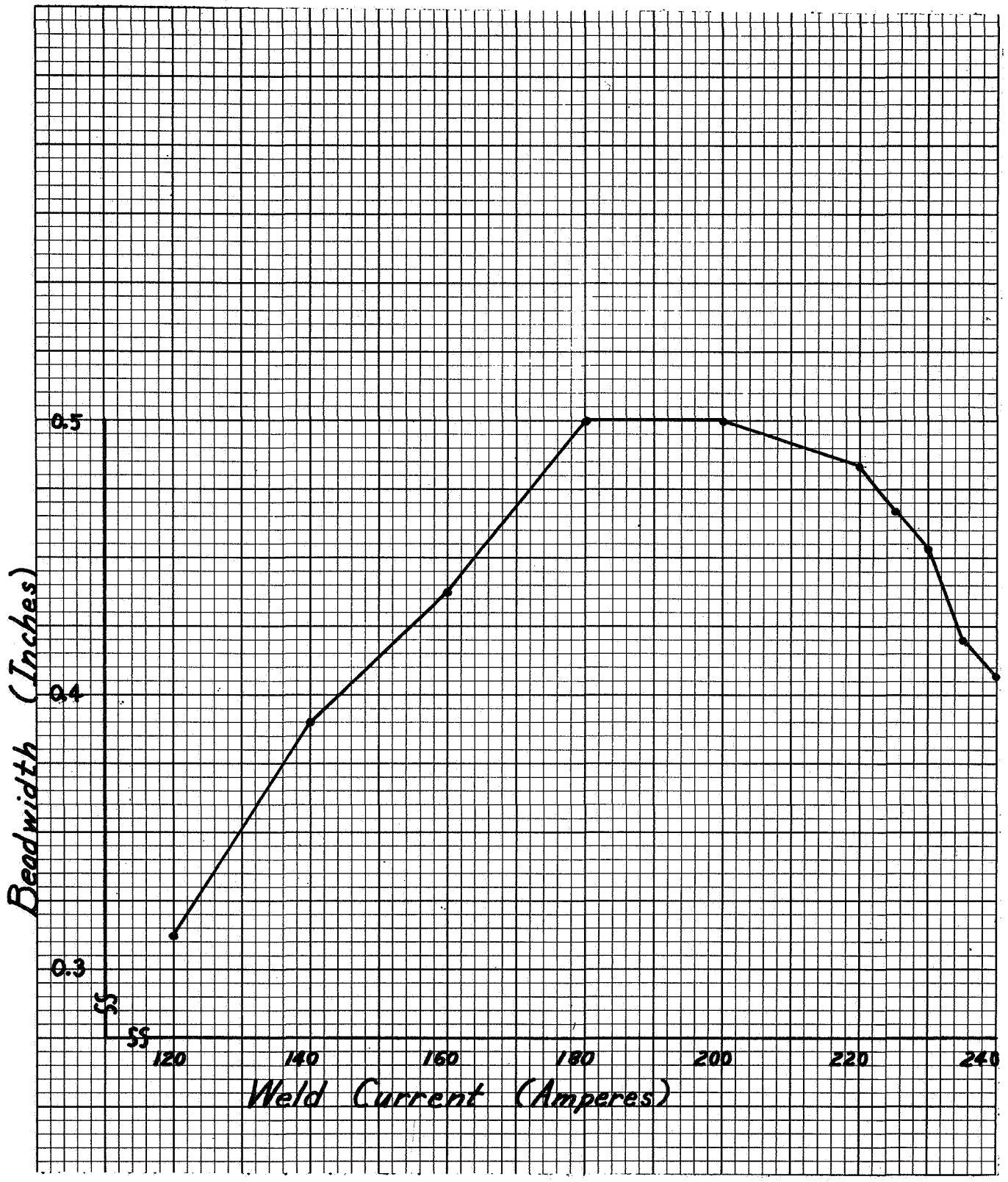


Figure 6: Beadwidth versus weld current for sample shown in figure 3.

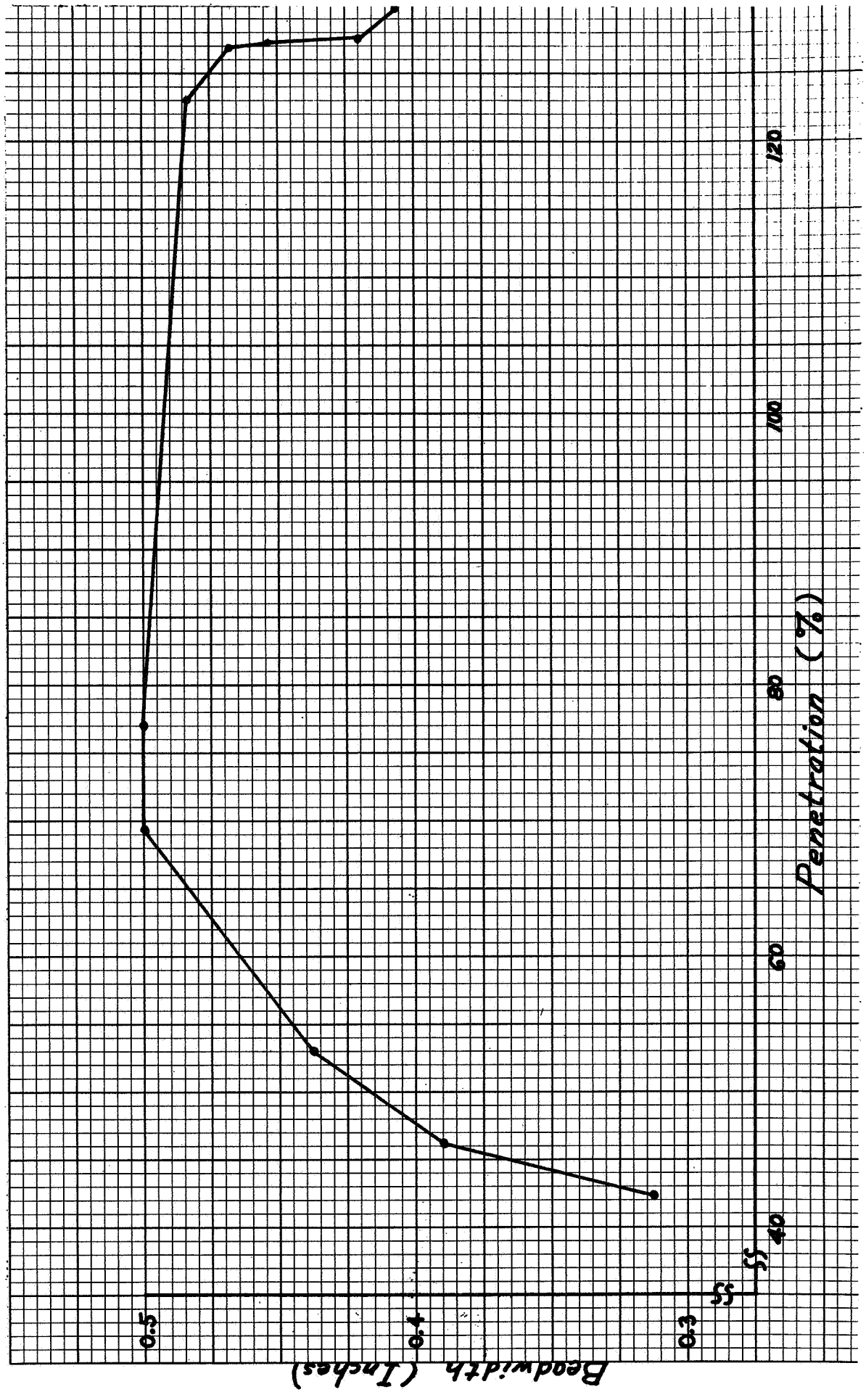


Figure 7: Beadwidth versus penetration for sample shown in Figure 3.

2.1.1.3.1 BARNES ENGINEERING COMPANY

2.1.1.3.1.1 Barnes' Model R-4D1 uses 2 matched thermistors connected in a bridge circuit across a source of constant voltage. One element provides compensation for ambient effects. A germanium filter is used to eliminate radiation below 1.8 microns. The incoming radiation is chopped at 150 cps by a rotating, notched disc. The optical system consists of an aluminized mirror telescope focusing from 2 feet to infinity. The amplifier contains a voltmeter, synchronous rectifier circuit, temperature monitoring circuit, power supply and means for testing and calibrating. The detector head measures 6 inches by 6.5 inches by 17.5 inches and weighs 15 pounds.

2.1.1.3.1.2 The Barnes Scanning Radiometer uses a lead sulfide detector and a germanium objective lens. Radiation is focused onto the plane of a rotating reticle beneath a slotted mask. A field lens collects the moving beam and focuses it on the detector. The same amplifier is used as with the R-4D1.

2.1.1.3.1.3 The Barnes' Model UV-1 uses a photomultiplier tube and a quartz objective lens. Since this instrument operates in the shorter wavelengths it takes advantage of the high power of "T" to become independent of emissivity. The target area, however, is quite large so that it is not applicable to the specific need of this program.

2.1.1.3.1.4 Barnes' Models R-4F, R-8B and R-1ZA all use the bolometer principle with mirror optics. They detect within the range of interest but are all much too bulky.

2.1.1.3.1.5 Barnes' Model RRT-4 uses a thermistor detector with an indium antimonide filter. The resulting bandpass is restricted to 8 to 14 microns. The detection range is 11 degrees F. to 110 degrees F. The target area is too large and the range too limited for the specific application.

2.1.1.3.1.6 For fixed-point scanning, Barnes recommended model R-4D1 with possibly the germanium filter replaced with an indium antimonide filter with approximately 4 micron cutoff.

2.1.1.3.2 IRCON INC.

2.1.1.3.2.1 Ircon Series 100 operates in the short wavelength area, with 1200°F minimum. It uses a photovoltaic detector and has no moving parts. The size is 2 inch diameter by 5.75 inches long. The weight is 1 pound. Response time is 50 microseconds. Target area 0.050 inch diameter minimum. Focal length is 8 inches to infinity.

2.1.1.3.2.2 Ircon Series 300 uses a lead sulfide detector and is responsive in the 2.0-2.6 micron spectral band. Optical chopping rate is 500 cps. The optical system consists of an objective lens, a dichroic mirror and a multilayer interference filter. Response time is 0.1 second to 1 second depending upon the temperature range. Focusing range is 20 inches to infinity. Size and weight of optical head is 10.5 inches by 5.5 inches by 3.75 inches and 6.5 lbs. The temperature range is from 170°F to 5000°F. Minimum target size equals distance from target divided by 100.

2.1.1.3.2.3 Ircon Series 700 is similiar to the 300 series except that is uses an indium antimonide detector and operates in the 4.8-5.6 micron band.

2.1.1.3.2.4 Ircon recommended their model 700 for fixed point monitoring. This was because the model 700 operates at longer wavelengths where the radiance of the hot tungsten drops considerably relative to that of the aluminum. Also, the model 700 was reported to have a low temperature range and high signal-to-noise ratio even for the very low emittances of aluminum.

For scanning applications, Ircon recommended an oscillating mechanism manufactured by Leeds and Northrup Company. The model 700 optical head would then be mounted to the rotating shaft.

2.1.1.3.3 PHILCO CORPORATION

Model GPC-215 uses a germanium detector with a barium floride window. The spectral range is 1-10 microns. The unit requires refrigeration and is much too bulky for the application.

2.1.1.3.4 LAND PYROMETERS, LTD.

2.1.1.3.4.1 The Land Continuous Optical Pyrometer uses a silicon "solar cell" as its quantitative detector, producing a DC voltage proportional to the intensity of the light falling upon it. Ambient temperature compensation is accomplished by the use of a thermistor and manganim resistors. The optical system consists of an objective lens, protected by a Pyrex window, and an internal calibrating aperture.

2.1.1.3.4.2 Target size can vary from 0.20 inches to 4.30 inches with the larger sizes required for the lower temperatures. 700^{o}C is the lowest practical temperature measurable without interference from daylight or shop lighting.

2.1.1.3.4.3 The Land engineers did not recommend their equipment because of the arc interference and the low plate temperature associated with this study.

2.1.1.3.5 EPPLEY LABORATORY INC.

2.1.1.3.5.1 The Eppley infrared detector operates on the "Golay" principle of gas expansion. An infrared absorbing film is located in the center of a small gas chamber and heats the gas in this chamber when exposed to infrared radiation. The resulting expansion of the gas distends a small flexible mirror. As this mirror moves in and out of focus it modulates the amount of light reaching the light sensitive cell, thus changing its signal output.

2.1.1.3.5.2 Eppley can supply an external beam chopper, which is necessary to avoid drift, and optical systems to facilitate focusing on a target.

2.1.1.3.5.3 The Golay detector is an excellent instrument for detecting radiation and because it covers the entire infrared spectrum it is particularly adaptable to spectrometric applications. However, like all other infrared instruments investigated, it does not discriminate between reflected and emitted energy.

2.1.1.3.6 MILLETRON INC.

2.1.1.3.6.1 Milletron's "Infrared Eye" utilizes the two-color pyrometer principle. Where gray body conditions exists, it

measures temperatures independent of changes in emissivity.

2.1.1.3.6.2 Milletron did not feel that an infrared radiometer would accurately measure temperatures in the range of 500°F to 1100°F where direct reflection of the welding electrode and the plasma arc itself were viewed by the sensing head.

2.1.1.4 ADVANTAGES AND DISADVANTAGES OF INFRARED SENSORS

2.1.1.4.1 ADVANTAGES

The principle advantages of the infrared temperature transducer are that: (1) it does not require direct contact with the work, and (2) it can measure temperatures of the molten puddle itself, provided interference can be eliminated.

2.1.1.4.2 DISADVANTAGES

2.1.1.4.2.1 The radiant energy seen by the infrared radiometer is proportional to the emissivity of the workpiece surface. For aluminum this emissivity is very low, 0.1 typical, prior to welding and, due to oxidation, may increase by as much as a factor of 5 after the weld is completed.

2.1.1.4.2.2 Due to the very high temperature of the electrode and associated arc plasma, as compared to the workpiece, it is extremely difficult to shield the radiometer's optical line of sight from direct and reflected radiation from the arc.

2.1.1.4.2.3 To be effective, any shielding devices utilized must be in the near proximity of the arc area. This, however, reduces the accesibility to the arc area for other functions such as wire feed, head pivot, etc.

2.1.1.4.2.4 Most of the infrared optical heads investigated were rather large and bulky and would definitely require special fixturing to mount the infrared head to the torch carriage.

2.1.1.4.2.5 Relative to the hybrid-thermocouple, see section 2.1.3, infrared equipment is more expensive and more difficult to use.

2.1.2 EDDY CURRENT TEMPERATURE TRANSDUCER

2.1.2.1 INTRODUCTION

Eddy current techniques for measuring temperature variations of electrically conductive objects was proposed in

1934[6]. This application was extremely limited in the past, however, one reason being the particular type of instrumentation problem presented by the technique. The method has the advantage of being noncontacting, emissivity-free, and independent of gases or liquids between the probe and the workpiece.

2.1.2.2 TECHNICAL DESCRIPTION

A qualitative explanation of the technique can be made by referring to Figure 8. The material, whose temperature is being measured, forms the yoke of an iron core inductor L from which it is separated by a small air gap d. A variation of the eddy current losses resulting from a temperature change of the part affects the magnitude of the magnetic flux and is reflected in a change of the resistive components of L, which can be detected in subsequent stages. The magnitude of the impedance changes is determined by a number of factors among which are: the inductor design, the excitation characteristics (frequency and voltage), the characteristics of any object placed in the inductor field, and the relative position of the object and the inductor.

For a given inductor design and a given excitation, the impedance variation is a function of the object temperature and its relative position with respect to the coil. The basic instrumentation problem is to design a circuit that will discriminate between the impedance changes due to the sample temperature variations T and those originating in fluctuations of the inductor-to-surface spacing d, and provide an output function of the plate temperature only. An impedance comparison bridge that discriminates between unbalanced voltages originating in temperature variation, and those originating in distance variations was reported on by R. J. Mouly of the Corning Glass Works in 1962[7]. This device is patented to Corning Glass Works under patent number 3,071,967.

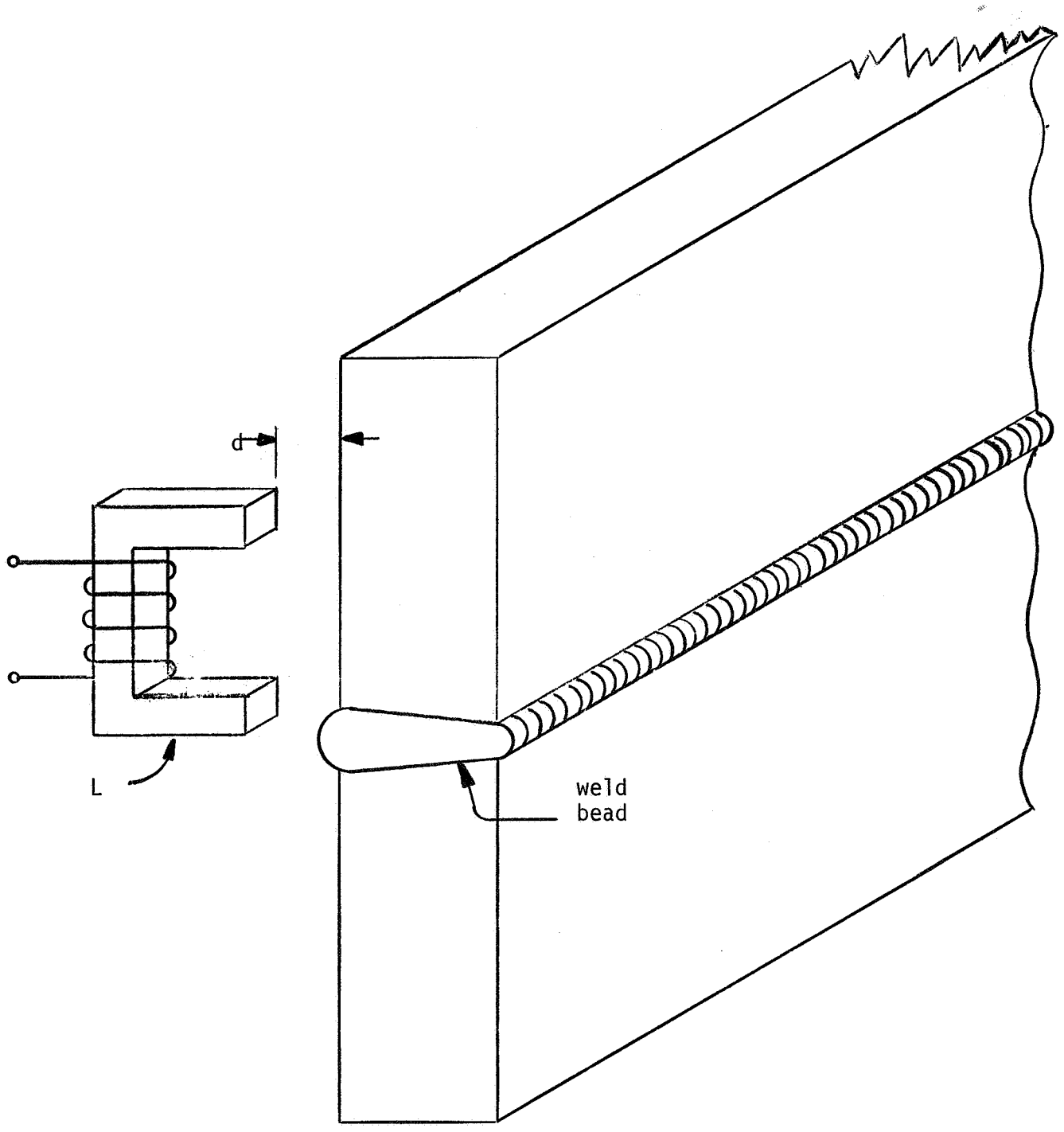


FIGURE 8: EDDY CURRENT TRANSDUCER PRINCIPLE

2.1.2.3 ADVANTAGES AND DISADVANTAGES

2.1.2.3.1 ADVANTAGES

2.1.2.3.1.1 The transducer head does not require direct contact with the workpiece.

2.1.2.3.1.2 Measurements are not affected by the presence of gases or liquids between the probe and the workpiece.

2.1.2.3.1.3 The method is emissivity-free.

2.1.2.3.1.4 The speed of response is inherently high.

2.1.2.3.2 DISADVANTAGES

2.1.2.3.2.1 The structural state of the workpiece must be known in order to avoid confusing temperature variations with structural changes.

2.1.2.3.2.2 The area of the point of detection is limited by the physical size of the sensing inductor.

2.1.2.3.2.3 The probe is bulky and would be difficult to mount to most existing weld heads.

2.1.2.3.2.4 The complete system, including probe and instrumentation, is relatively expensive and critical of adjustment.

2.1.3 HYBRID THERMOCOUPLE SURFACE-TEMPERATURE TRANSDUCER

2.1.3.1 INTRODUCTION

It is well known that when two wires of different material, i.e., iron-constantan, copper-constantan, chromel-alumel, etc., are joined together at two ends and exposed to different temperatures an emf output (Seebeck effect) is generated causing an electric current to flow continuously through the circuit. In practical useage one joint is generally made by welding the two thermocouple wires together to form a thermocouple bead. This bead is placed in contact with the material whose temperature is to be measured. The opposite ends of the thermocouple wires are normally connected to copper leads which in turn are connected to a meter, amplifier, or other monitoring device to complete the circuit (see Figure 9). The junction between the thermocouple wires and the copper wires is defined as the reference junction and is usually maintained at a fixed temperature T_1 so that the emf generated will be proportional to the tem-

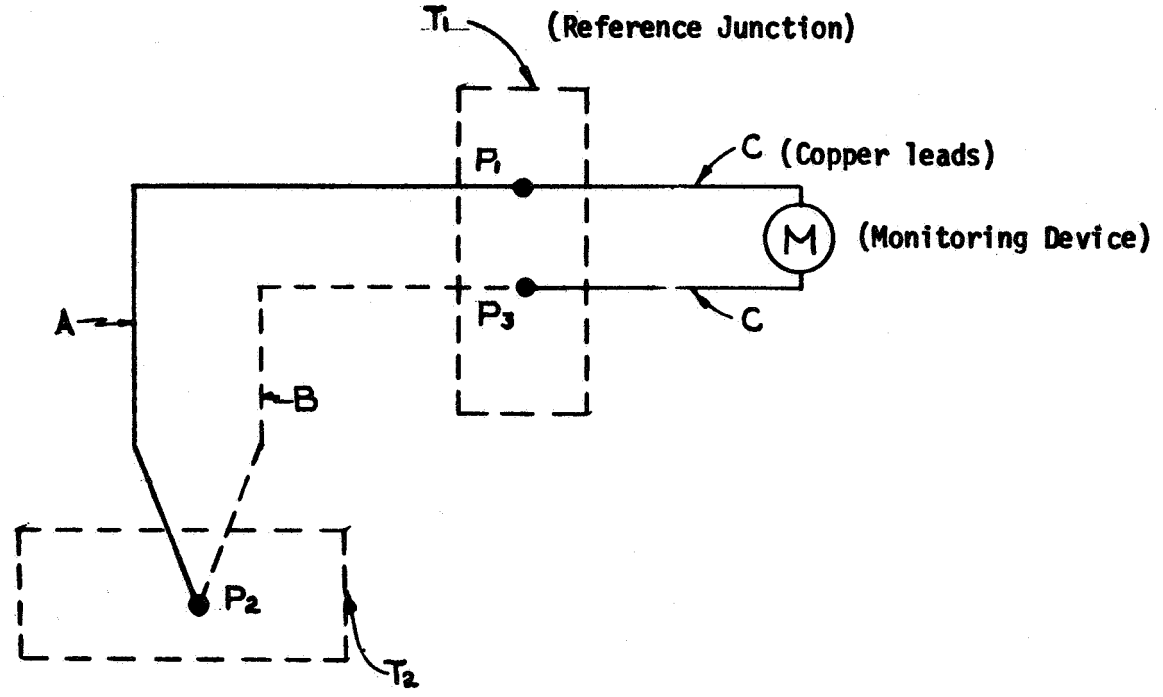


Figure 9: Basic thermocouple temperature monitoring system.

perature of the thermocouple bead T_2.

It would thus seem obvious that the surface temperature of the workpiece at a fixed position with respect to the tungsten electrode could be continuously measured by mounting the thermocouple bead in a rigid probe assembly, which would be mechanically fastened to the welding torch, and hence allowed to move with the torch. By allowing the thermocouple bead to project out the end of the probe assembly and drag on the surface of the workpiece, a continuous measurement of the surface temperature at the point of contact between the bead and workpiece (fixed position with respect to tungsten tip) should be obtainable. There are two distinct disadvantages to this idea, however, which are:

(1) The thermocouple bead will have a definite thermal time constant associated with it and hence there will be a corresponding time lag between surface temperature variation and emf output of the thermocouple system. The smaller the thermocouple bead the shorter the thermal time constant will be; however, at some point a compromise will have to be made between response time and mechanical rigidity and reliability. In any event, some time delay will always be present.

(2) The temperature of the thermocouple bead will not only be a function of the temperature of the workpiece (contacting one side of the bead) but will also be a function of direct and reflected radiation from the tungsten tip. Thus, it can not be assumed that the thermocouple's emf output will be indicative of the true surface temperature of the workpiece. Shielding could be incorporated to reduce interference from direct and reflected hot tungsten radiation; however, this would further clutter the weld area and also would not completely eliminate the problem.

2.1.3.2 HYBRID THERMOCOUPLE TRANSDUCER

The two disadvantages stated above were alleviated by allowing the 2219 aluminum workpiece to form one half of the thermocouple junction, as shown in Figure 10. A constantan wire was mounted in the probe assembly and allowed to drag on the surface of the workpiece in the same manner as the thermocouple bead discussed previously. Now, however, the thermocouple junction is at the point of contact of the dragging constantan wire; hence, an aluminum-constantan thermocouple is formed. Since the thermocouple so formed differs from the normal two-wire bead type, it will be referred to hereafter as a hybrid thermocouple transducer.

A constantan wire was chosen as the second half of the hybrid thermocouple because of its high thermoelectric sensitivity with respect to aluminum. A list of the thermoelectric sensitivities against Platinum is presented in Table I for several materials. We see that the sensitivity of constantan versus Platinum is -35 $\mu V/^{o}C$ and that the sensitivity of aluminum versus Platinum is + 3.5 $\mu V/^{o}C$. Therefore the sensitivity of constantan versus aluminum is

$$-35-(+3.5) = -38.5\ \mu V/^{o}C.$$

A quick check of Table I reveals that no other materials possessing the same durability, flexibility, and availability as constantan have as high a sensitivity versus aluminum.

Because the thermocouple junction of the hybrid transducer is the workpiece, itself,at the point of contact with the constantan probe, response time to variations in workpiece temperature are instantaneous. Furthermore, for the same reason, interference due to direct or reflected radiation from the hot tungsten is completely eliminated. This is because only radiation that directly affects the surface temperature will be measured and this is precisely what is desired.

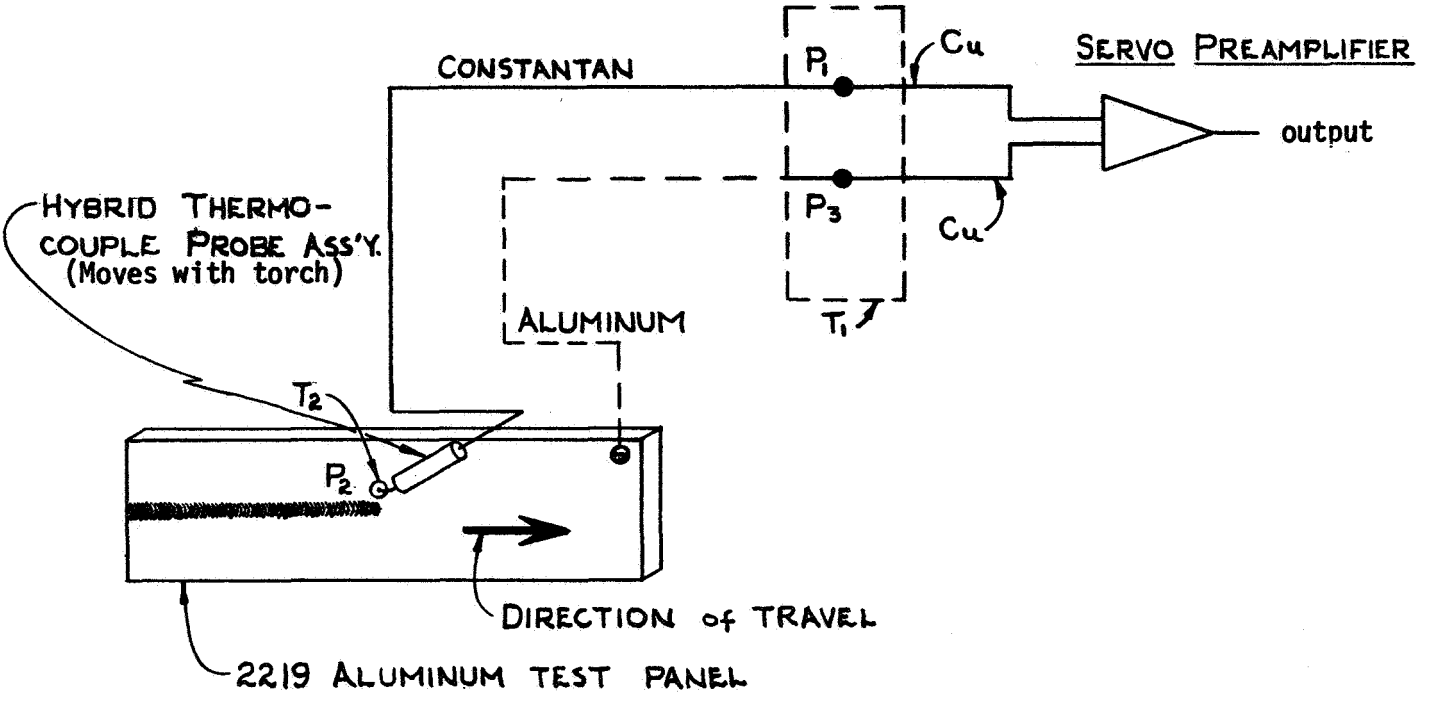


Figure 10: Hybrid thermocouple temperature monitoring system.

Table 1

Thermoelectric Sensitivity of Materials Against Platinum

Material	S_{μ} V/°C	Material	S_{μ} V/°C
Bismuth	-72	Silver	+6.5
Constantan	-35	Copper	+6.5
Nickel	-15	Gold	+6.5
Potassium	- 9	Tungsten	+7.5
Sodium	- 2	Cadmium	+7.5
Platinum	0	Iron	+18.5
Mercury	+0.6	Nichrome	+25
Carbon	+3	Antimony	+47
Aluminum	+3.5	Germanium	+300
Lead	+4	Silicon	+440
Tantalum	+4.5	Tellurium	+500
Rhodium	+6	Selenium	+900

To further prove that the hybrid thermocouple transducer would read true surface temperature and not be affected by direct or reflected radiation from the torch, an experiment was run with the physical setup shown in Figure 11. Torch interference was simulated by heating the constantan lead with an oxy-acetylene torch as shown in the figure. With T_1 = 20mv and T_2 = 18mv, heat was slowly applied to the constantan lead until it eventually burned in half. No variation was observed in the millivolt reading of T_2 until the constantan lead had been melted.

A series of tests (discussed later in report) were also run to determine what effect, if any, surface oxides would have on the hybrid thermocouple's emf output. No effect was observed. This is attributed to the fact that the sharp-pointed constantan probe scratches through the oxides continuously as the weld is made.

2.1.3.3 ALUMINUM-CONSTANTAN THERMOCOUPLE CALIBRATION

2.1.3.3.1 The equipment used in obtaining an aluminum-constantan thermocouple calibration chart was as follows:

2.1.3.3.1.1 Rosemount Variable Temperature Oil Bath, Model 910A.

2.1.3.3.1.2 Rosemount Resistance Bridge, Model 400A.

2.1.3.3.1.3 Rosemount Platinum Resistance Sensor, Model 124M24CBC.

2.1.3.3.2 A schematic diagram of the equipment assembly is shown in Figure 12.

2.1.3.3.3 Referring to Figure 12, a Heath Recorder and Tetronix Oscilloscope were connected to the output of the bridge circuit. Both instruments were adjusted to zero with the sensor in ice water before each temperature reading. Each reading shown in the data below (See part 2.1.3.3.4) was verified at least three time, i.e., ice water to oil bath. The aluminum-constantan thermocouple was monitored without amplification.

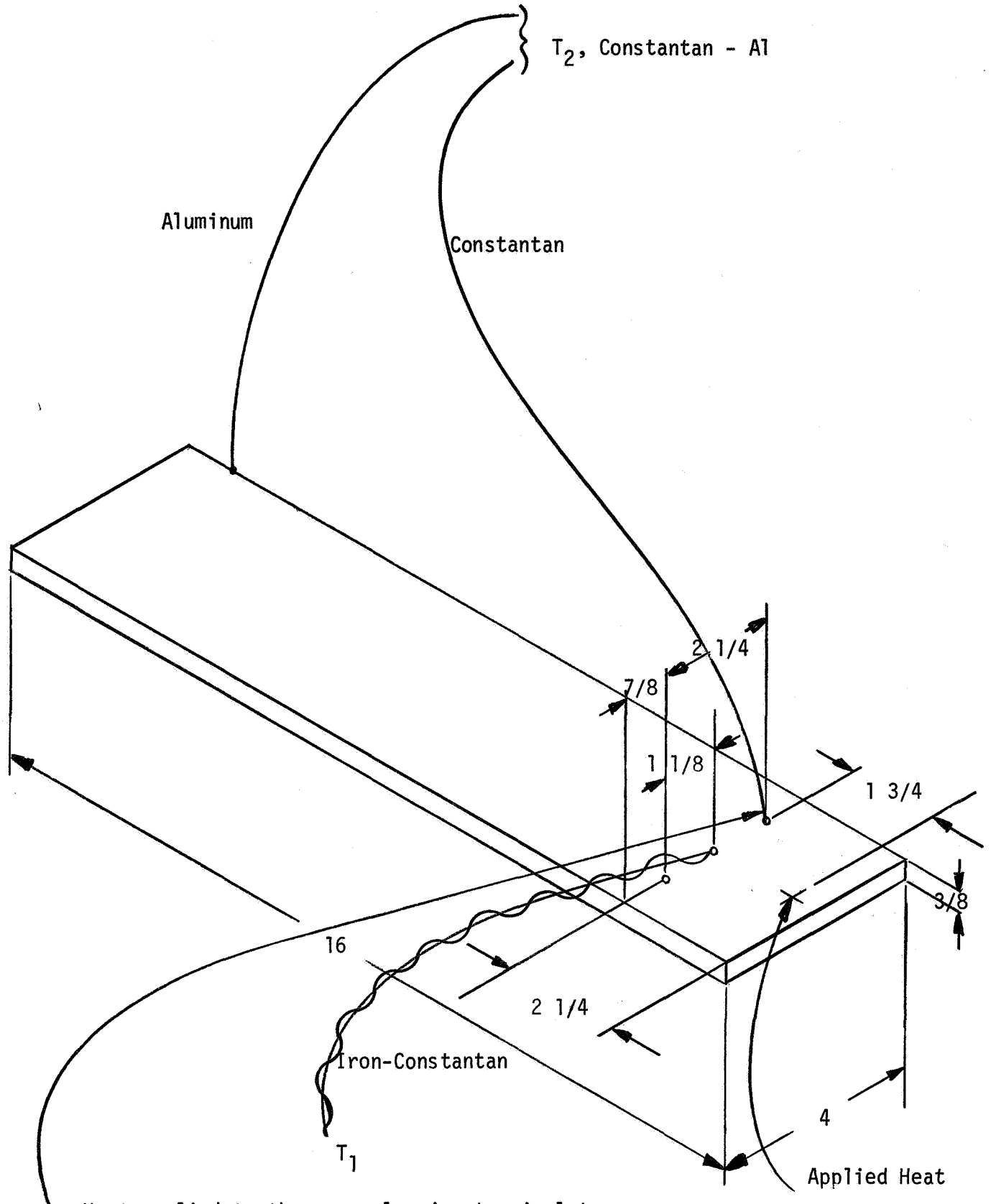


Figure 11: Experimental simulation of radiated interference from torch.

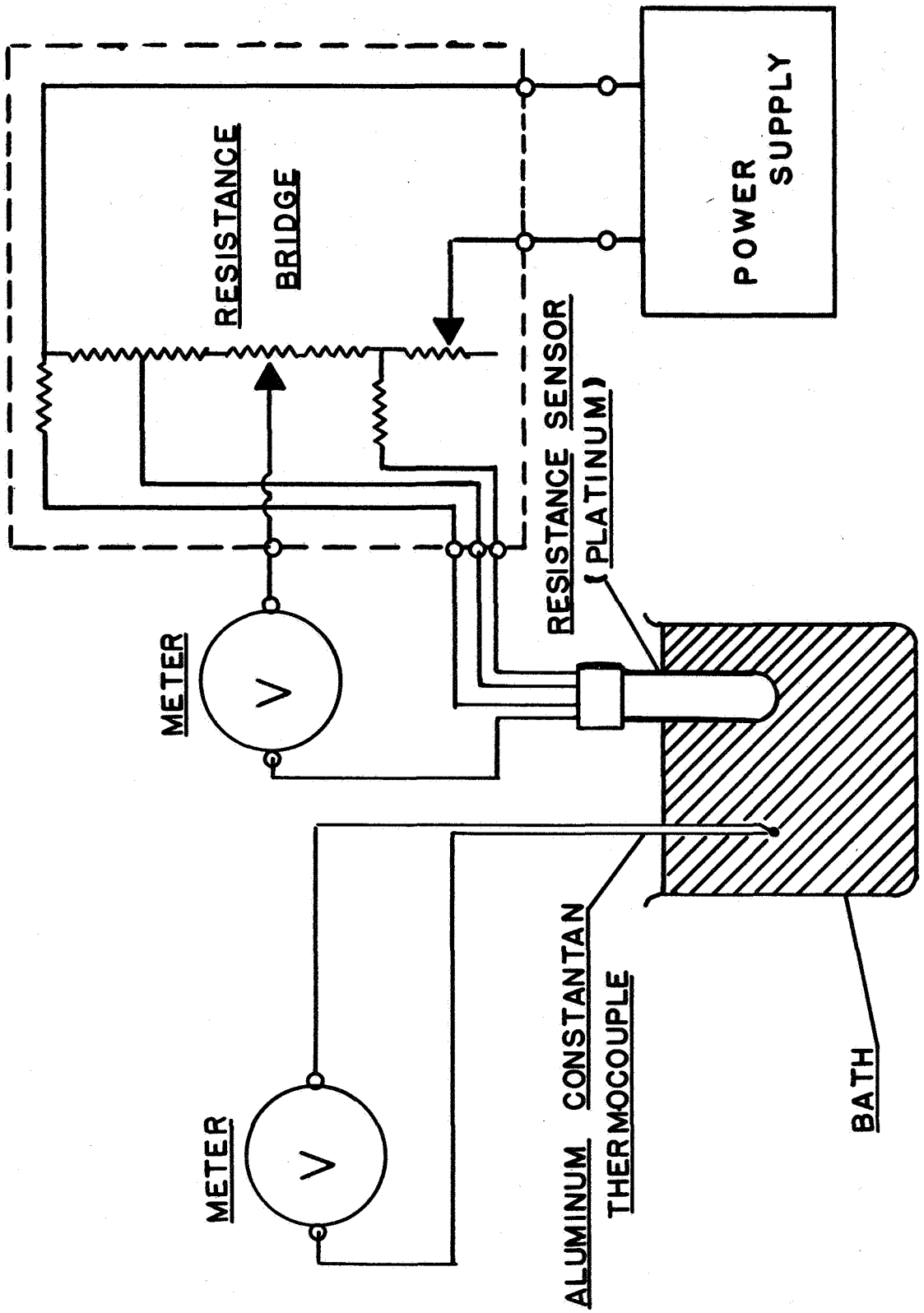


FIGURE 12 · THERMOCOUPLE CALIBRATION APPARATUS

2.1.3.3.4 The data taken in this test is given below:

Coarse Dial Setting of Temp. Bath	Calibration Temp.	Bridge Output		Thermocouple Output	
		Oscilloscope	Heath Recorder	Oscilloscope	Heath Recorder
600	255°	13.5 m.v.	13.5 m.v.	5.0 m.v.	4.5 m.v.
630	340	18.5	19.0	7.5	7.5
653	410	23.0	24.5	10.0	10.0
658	438	24.0	25.75	10.5	11.0
670	500	27.5	29.0	12.0	12.5

2.1.3.3.5 Using an extrapolation process and the above data a calibration chart for the aluminum-constantan thermocouple was made. This data is presented in Table II.

2.1.3.4 EFFECT OF REFERENCE TEMPERATURE VARIATION ON HYBRID-THERMOCOUPLE SENSOR OUTPUT

As stated previously, a basic thermoelement system is shown in Figure 9. The junction point P2 is at the temperature t_2, which is the temperature to be measured. The thermocouple wires A and B are connected, with a wire C made from a third material, to the meter M. The junction points P_1 and P_3 are at the same temperature t_1, which is the reference temperature of the system. The magnitude of the thermal emf is independent of the presence of the third metal C as long as the contact points P_1 and P_3 are at the same temperature. This temperature must be known, however, in order to determine the temperature t_2 of the measuring junction P_2; the meter reading, being to a first approximation, proportional to t_2 minus t_1.

A pictorial representation of the hybrid thermocouple sensor is shown in Figure 10. The measuring junction P_2 is at the sliding contact point of the hybrid-sensor tip and the aluminum workpiece. The temperature at this point is T_2.

TABLE II

CALIBRATION OF ALUMINUM-CONSTANTAN THERMOCOUPLE

Aluminum 4043 (5.0% S_1)

Temperature in Degree F. Reference Junction at 32° F.

MILLIVOLTS

Degrees F.	0	1	2	3	4	5	6	7	8	9	10
30			0.00								
100	1.45										
200	3.68	3.71	3.74	3.77	3.80	3.83	3.86	3.89	3.92	3.95	3.99
300	5.95	5.98	6.02	6.05	6.08	6.11	6.14	6.17	6.20	6.23	6.26
400	8.80	8.83	8.85	8.88	8.90	8.93	8.95	8.98	9.00	9.03	9.05
410	9.05	9.08	9.10	9.13	9.15	9.18	9.20	9.23	9.25	9.27	9.29
420	9.29	9.32	9.35	9.38	9.41	9.44	9.47	9.50	9.53	9.55	9.57
430	9.57	9.60	9.63	9.66	9.69	9.72	9.75	9.78	9.81	9.84	9.86
440	9.86	9.89	9.92	9.95	9.98	10.01	10.04	10.07	10.10	10.13	10.15
450	10.15	10.18	10.21	10.24	10.27	10.30	10.33	10.36	10.39	10.42	10.44
460	10.44	10.47	10.50	10.53	10.56	10.59	10.62	10.65	10.68	10.71	10.73
470	10.73	10.76	10.79	10.82	10.85	10.88	10.91	10.94	10.97	11.00	11.02
480	11.02	11.05	11.08	11.11	11.14	11.17	11.20	11.23	11.26	11.29	11.31
490	11.31	11.34	11.37	11.40	11.43	11.46	11.49	11.52	11.55	11.58	11.60
500	11.60	11.63	11.66	11.69	11.72	11.75	11.78	11.81	11.84	11.87	11.89
510	11.89	11.92	11.95	11.98	12.01	12.03	12.06	12.09	12.12	12.15	12.17
520	12.17	12.20	12.23	12.26	12.29	12.32	12.35	12.38	12.41	12.44	12.46
530	12.46	12.49	12.51	12.54	12.57	12.60	12.63	12.66	12.69	12.72	12.74
540	12.74	12.77	12.80	12.83	12.86	12.89	12.92	12.95	12.98	13.01	13.03
550	13.03	13.06	13.09	13.11	13.14	13.17	13.20	13.23	13.26	13.29	13.31
560	13.31	13.34	13.37	13.40	13.43	13.46	13.49	13.52	13.55	13.58	13.60
570	13.60	13.63	13.65	13.68	13.71	13.74	13.77	13.80	13.83	13.86	13.88
580	13.88	13.90	13.93	13.96	13.99	14.02	14.05	14.07	14.10	14.13	14.15
590	14.15	14.18	14.21	14.23	14.26	14.29	14.31	14.33	14.38	14.40	14.42
600	14.42	14.45	14.48	14.50	14.53	14.56	14.59	14.62	14.65	14.68	14.70
610	14.70	14.73	14.75	14.78	14.81	14.84	14.87	14.90	14.93	14.96	14.98
620	14.98	15.01	15.04	15.07	15.10	15.12	15.15	15.18	15.21	15.23	15.25
630	15.25	15.28	15.30	15.33	15.36	15.38	15.41	15.44	15.47	15.50	15.52
640	15.52	15.55	15.58	15.60	15.62	15.65	15.68	15.70	15.72	15.75	15.77
650	15.77	15.80	15.83	15.85	15.88	15.90	15.93	15.96	15.99	16.02	16.04
660	16.04	16.07	16.09	16.12	16.15	16.17	16.20	16.23	16.26	16.29	16.31
670	16.31	16.33	16.36	16.39	16.42	16.44	16.47	16.50	16.53	16.56	16.58
680	16.58	16.61	16.63	16.66	16.69	16.71	16.74	16.76	16.79	16.82	16.84
690	16.84	16.87	16.90	16.92	16.95	16.98	17.00	17.02	17.05	17.08	17.10

	0	1	2	3	4	5	6	7	8	9	10
700	17.10	17.13	17.15	17.18	17.21	17.23	16.26	17.29	17.31	17.34	17.36
710	17.36	17.39	14.41	17.44	17.47	17.49	17.52	17.55	17.57	17.60	16.62
720	17.62	17.65	17.67	17.70	17.73	17.75	17.78	17.81	17.83	17.86	17.88
730	17.88	17.91	17.93	17.96	17.99	18.01	18.04	18.07	18.09	18.12	18.14
740	18.14	18.17	18.19	18.22	18.25	18.27	18.30	18.33	18.35	18.38	18.40
750	18.40	18.43	18.45	18.48	18.51	18.53	18.56	18.59	18.61	18.64	18.66
760	18.66	18.69	18.71	18.74	18.77	18.79	18.82	18.85	18.87	18.90	18.92
770	18.92	18.95	18.97	19.00	19.03	19.05	19.08	19.11	19.13	19.16	19.18
780	19.18	19.21	19.24	19.27	19.30	19.32	19.35	19.38	19.40	19.43	19.45
790	19.45	19.48	19.50	19.53	19.56	19.58	19.61	19.64	19.67	19.70	19.72
800	19.72	19.75	19.78	19.81	19.84	19.86	19.89	19.91	19.94	19.97	19.99
810	19.99	20.01	20.04	20.06	20.09	20.11	20.14	20.17	20.20	20.23	20.25
820	20.25	20.28	20.30	20.33	20.35	20.38	20.41	20.44	20.47	20.50	20.52
830	20.52	20.55	20.57	20.60	20.63	20.65	20.67	20.70	20.73	20.76	20.78
840	20.78	20.81	20.84	20.86	20.89	20.92	20.95	20.98	21.00	21.03	21.05
850	21.05	21.08	21.11	21.13	21.16	21.19	21.22	21.25	21.27	21.30	21.32
860	21.32	21.35	21.38	21.40	21.43	21.46	21.49	21.52	21.54	21.57	21.59
870	21.59	21.62	21.65	21.67	21.70	21.72	21.75	21.78	21.80	21.83	21.85
880	21.85	21.88	21.90	21.93	21.96	21.99	22.02	22.04	22.07	22.10	22.12
890	22.12	22.15	22.17	22.20	22.23	22.25	22.28	22.30	22.33	22.36	22.38
900	22.38	22.41	22.44	22.46	22.49	22.52	22.55	22.57	22.60	22.63	22.65
910	22.65	22.68	22.71	22.73	22.76	22.79	22.81	22.84	22.86	22.89	22.91
920	22.91	22.94	22.97	22.99	23.02	23.04	23.07	23.10	23.13	23.16	23.18
930	23.18	23.21	23.24	23.26	23.29	23.31	23.34	23.36	23.39	23.42	23.44
940	23.44	23.47	23.50	23.52	23.55	23.57	23.60	23.63	23.66	23.69	23.71
950	23.71	23.74	23.77	23.79	23.82	23.84	23.87	23.90	23.92	23.95	23.97
960	23.97	24.00	24.03	24.05	24.08	24.10	24.13	24.16	24.19	24.22	24.24
970	24.24	24.27	24.30	24.32	24.36	24.38	24.41	24.43	24.46	24.49	24.51
980	24.51	24.54	24.56	24.59	24.62	24.65	24.68	24.70	24.73	24.76	24.78
990	24.78	24.81	24.84	24.86	24.89	24.91	24.94	24.96	24.99	25.02	25.04
1000	25.04	25.07	25.09	25.12	25.15	25.17	25.20	25.23	25.26	25.29	25.31
1010	25.31	25.34	25.37	25.39	25.42	25.44	25.47	25.49	25.52	25.55	25.57
1020	25.57	25.60	25.63	25.65	25.68	25.70	25.73	25.76	25.79	25.82	25.84
1030	25.84	25.87	25.90	25.92	25.95	25.97	26.00	26.03	26.06	26.09	26.11
1040	26.11	26.14	26.17	26.19	26.22	26.24	26.27	26.29	26.32	26.35	26.37
1050	26.37	26.40	26.43	26.45	26.48	26.50	26.53	26.56	26.59	26.62	26.64
1060	26.64	26.67	26.70	26.72	26.75	26.77	26.80	26.83	26.86	26.89	26.91
1070	26.91	26.94	26.97	26.99	27.02	27.04	27.07	27.09	27.12	27.15	27.17

	0	1	2	3	4	5	6	7	8	9	10
1080	27.17	27.20	27.23	27.25	27.28	27.31	27.34	27.36	27.39	27.42	27.44
1090	27.44	27.47	27.50	27.53	27.55	27.57	27.60	27.63	27.66	27.69	27.71
1100	27.71	27.74	27.77	27.79	27.82	27.85	27.87	27.90	27.93	27.96	27.98
1110	27.98	28.01	28.04	28.06	28.09	28.12	28.14	28.17	28.20	28.23	28.25
1120	28.25	28.28	28.31	28.33	28.36	28.39	28.41	28.44	28.47	28.50	28.52
1130	28.52	28.55	28.58	28.60	28.63	28.66	28.68	28.71	28.74	28.77	28.79
1140	28.79	28.82	28.85	28.87	28.90	28.93	28.95	28.98	29.01	29.04	29.06
1150	29.06	29.09	29.12	29.14	29.17	29.19	29.22	29.25	29.28	29.31	29.33
1160	29.33	29.36	29.39	29.41	29.44	29.47	29.49	29.52	29.55	29.58	29.60
1170	29.60	29.63	29.66	29.68	29.71	29.74	29.76	29.80	29.83	29.86	29.88
1180	29.88	29.91	29.94	29.96	29.99	30.02	30.05	30.08	30.11	30.14	30.16
1190	30.16	30.19	30.22	30.24	30.27	30.30	30.33	30.36	30.39	30.42	30.44
1200	30.44										

Referring to Figure 10, the thermocouple output voltage is, to a first approximation

$$e_t = K_t (t_2 - t_1), \qquad (1)$$

where e_t = Thermocouple output voltage (input to servo control system).

k_t = Proportionality constant.

t_2 = Temperature to be measured (in centigrade).

t_1 = Reference temperature (in centigrade).

If we assume that the reference temperature is increased by an amount Δt_1, then the thermocouple output voltage will decrease by an amount Δe_t so that equation (1) becomes:

$$e_t - \Delta e_t = k_t \; t_2 - (t_1 + \Delta t_1), \qquad (2)$$

where Δe_t = Change in thermocouple output voltage.

Δt_1 = Change in reference temperature, $t_1 - t_1'$ where t_1 is new reference temperature.

Substituting equation (1) into equation (2), and solving for Δe_t, we get

$$\Delta e_t = k_t \, \Delta t_1. \qquad (3)$$

We can determine the per unit change in the thermocouple voltage by dividing equation (3) by equation (1) to get

$$\frac{\Delta e_t}{e_t} = \frac{\Delta t_1}{t_2 - t_1} \qquad (4)$$

By multiplying the right side of equation (4) by t_1/t_1, we get an equation of per unit voltage change versus per unit temperature change:

$$\frac{\Delta e_t}{e_t} = \left(\frac{\Delta t_1}{t_2 - t_1}\right) \frac{\Delta t_1}{t_1} \quad , \qquad (5)$$

where $\frac{\Delta e_t}{e_t}$ = per unit change in thermocouple output voltage.

$\frac{\Delta t_1}{t_1}$ = per unit change in reference junction temperature.

Expressing Δt_1 as $t_1 - t_1'$ where t_1' is the new reference temperature and expressing the per unit changes as percent changes, euqation (5) becomes

$$\left[\frac{\Delta e_t}{e_t} \times 100\%\right] = \left(\frac{t_1}{t_2 - t_1}\right) \left[\frac{t_1 - t_1'}{t_1} \times 100\%\right] \quad . \qquad (6)$$

The temperatures in equation (6) are in degrees centigrade. However, by substituting the conversion equation,

$$tc = \frac{5}{9} \quad (t_f - 32) \ ,$$

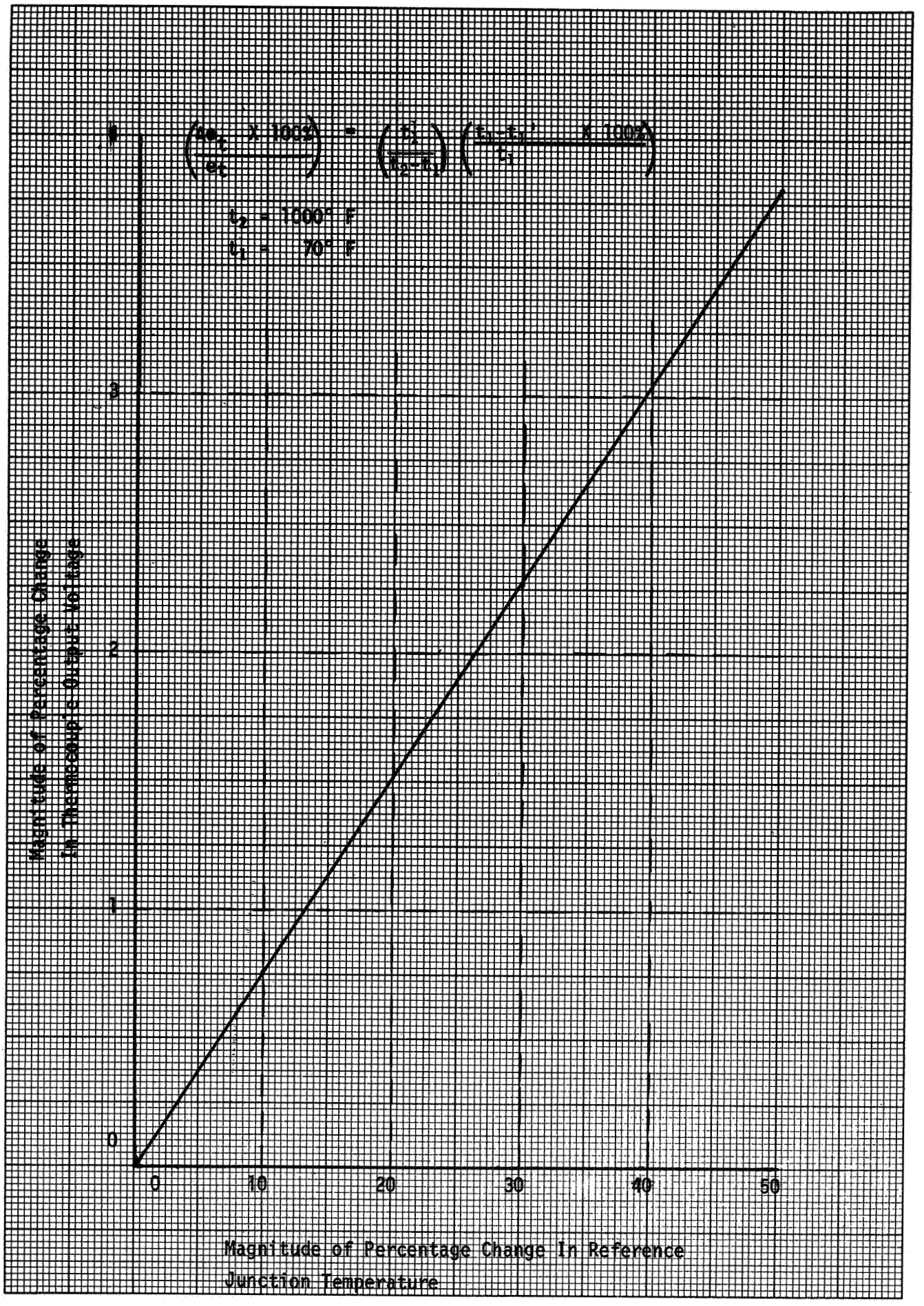
into equation (6), it is evident that the resulting equation in terms of degrees fahrenheit is identical to that in degrees centigrade.

Assuming an average room temperature of $t_1 = 70^{\circ}$ F and a measured temperature of $t_2 = 1000^{\circ}$ F (typical of welding conditions), equation (6) is plotted in figure 13. As an example, we see that a 30% change in the reference junction temperature (change of 21° F) produces a 2.26% change in the thermocouple output voltage, that is

$$\frac{\Delta e_t}{e_t} \times 100 = 2.26\%. \qquad (7)$$

A measuring junction temperature of 1000° F corresponds to a thermocouple output voltage of approximately 25 mv (see Table II)

12-282



20 Squares to the Inch

Figure 13: Effect of change in reference junction temperature.

Thus, the thermocouple voltage is,

$$e_t = 25 \text{ mv.}$$

Therefore from equation (7), the change in thermocouple voltage corresponding to a 30% change in reference junction temperature is

$$\Delta e_t = \frac{2.26(25)}{100} \text{ mv,}$$

$$\Delta e_t = 0.565 \text{ mv.}$$

In order to see what change will result in welding conditions for this change in the sensor output voltage, the following welding parameters are assumed:
Arc voltage = 10 volts, weld current = 300 amperes, travel speed = 3 inches/minute, aluminum, test plate dimension - 3/8" X 4" X 20", and hybrid sensor tip location = 3/8" above centerline of electrode.
For these welding conditions, the sensitivity of the hybrid thermocouple sensor is approximately 0.071 mv/ampere change (see section 3.1.5). Thus a 30% change in the reference junction temperature corresponds to a change of

$$0.565 \text{ mv} \div 0.071 \text{ mv/ampere} = 8 \text{ amperes}$$

in the welding current. An 8 ampere change in welding current, however, is equivalent to a 2.7% change in the heat input to the weld, which is sufficient to produce a definite visual change in penetration.
While these calculations have been made for specific parameters, it is evident that, under very adverse conditions of room temperature variations, the reference junction temperature can produce distinct changes in system accuracy unless it is stabilized and maintained constant. Thus, in conclusion it is obvious that a temperature-regulated sink should be provided for the reference junction if wide variations in the environmental temperature are expected. All weld tests presented in this report were conducted in a controlled-temperature environment.

2.1.3.5 ADVANTAGES AND DISADVANTAGES OF HYBRID THERMOCOUPLE TRANSDUCER

2.1.3.5.1 ADVANTAGES

2.1.3.5.1.1 The transducer is independent of surface emissivity and variations thereof.

2.1.3.5.1.2 The transducer is independent of direct or reflected radiation from the hot electrode and associated arc plasma.

2.1.3.5.1.3 The one wire thermocouple is unaffected by oxide films on the surface of the aluminum workpiece.

2.1.3.5.1.4 The Hybrid thermocouple transducer is relatively inexpensive (including mounting bracket) and is easy to set up.

2.1.3.5.1.5 The system is small and can therefore be connected to the torch without excessive physical interference in the arc area.

2.1.3.5.2 DISADVANTAGES

The principle disadvantages of the hybrid thermocouple transducer are:

2.1.3.5.2.1 Direct contact with the workpiece is required. This does not cause any undesirable effects on the weld process, however, provided the point of contact lies outside the molten-puddle zone.

2.1.3.5.2.2 Workpiece surface temperatures can only be measured outside of the molten puddle. Puddle temperature can not be measured with the hybrid thermocouple approach.

2.1.4. SUMMARY

As reviewed in the preceeding sections, the infrared and eddy current transducers have primarily two advantages relative to the hybrid thermocouple transducer. These are: (1) direct contact with the workpiece is not required, and (2) puddle temperature can be measured, provided direct and reflected arc interference can be eliminated.

It was decided at the offset that direct contact with the workpiece would not be objectionable, provided no weld zone interference

resulted. It was also concluded that desired temperature information could be obtained from measurements outside the molten puddle. Since. all other characteristics of the hybrid thermocouple transducer were found to be preferable to those of the infrared and eddy current transducers, the hybrid thermocouple was selected for use with all system experimentation.

2.2 BACKSIDE SENSING

2.2.1 APPLICATION

Two distinct methods were investigated for utilizing the thermocouple effect to continuously monitor the temperature on the backside of the workpiece and to utilize this intelligence to maintain constant "fall-through" on full penetration welds. Both methods are applicable to weld conditions in which a backup bar is feasible and/or necessary. They both are an integrable but removable part of the back up bar. The potential advantages over infrared sensing of the molten fall-through on the backside of the weldment are:

2.2.1.1 Additional fixturing is not necessary to synchronize motion between the welding torch and the infrared sensing head on the backside.

2.2.1.2 The two methods are applicable to weldments requiring a backup bar, where infrared sensing is not possible because of optical blocking of the molten fallthrough by the backup.

2.2.2 INTRINSIC THERMOCOUPLE

2.2.2.1 In NASA Memo No. R-ME-ME-198-64 [8], the possibility of using one thermocouple wire placed in an insulated backup bar to produce a signal by contacting the molten "fall-through" was suggested. The paragraphs including this suggestion from Mr. W. M. McCampbell of NASA and Detail A which shows the implementation of this suggestion are presented in Figure 14.

An alternate representation of this technique is shown in Figure 15, where the insulated backup bar is not included for the sake of clarity. The weld is assumed to be in progress, having started at point A and progressed to point B. Between points A and B the constantan wire is in contact with the fall-through of the weld. Between points B and C the weld has not yet been completed, and there is no contact between the constantan.

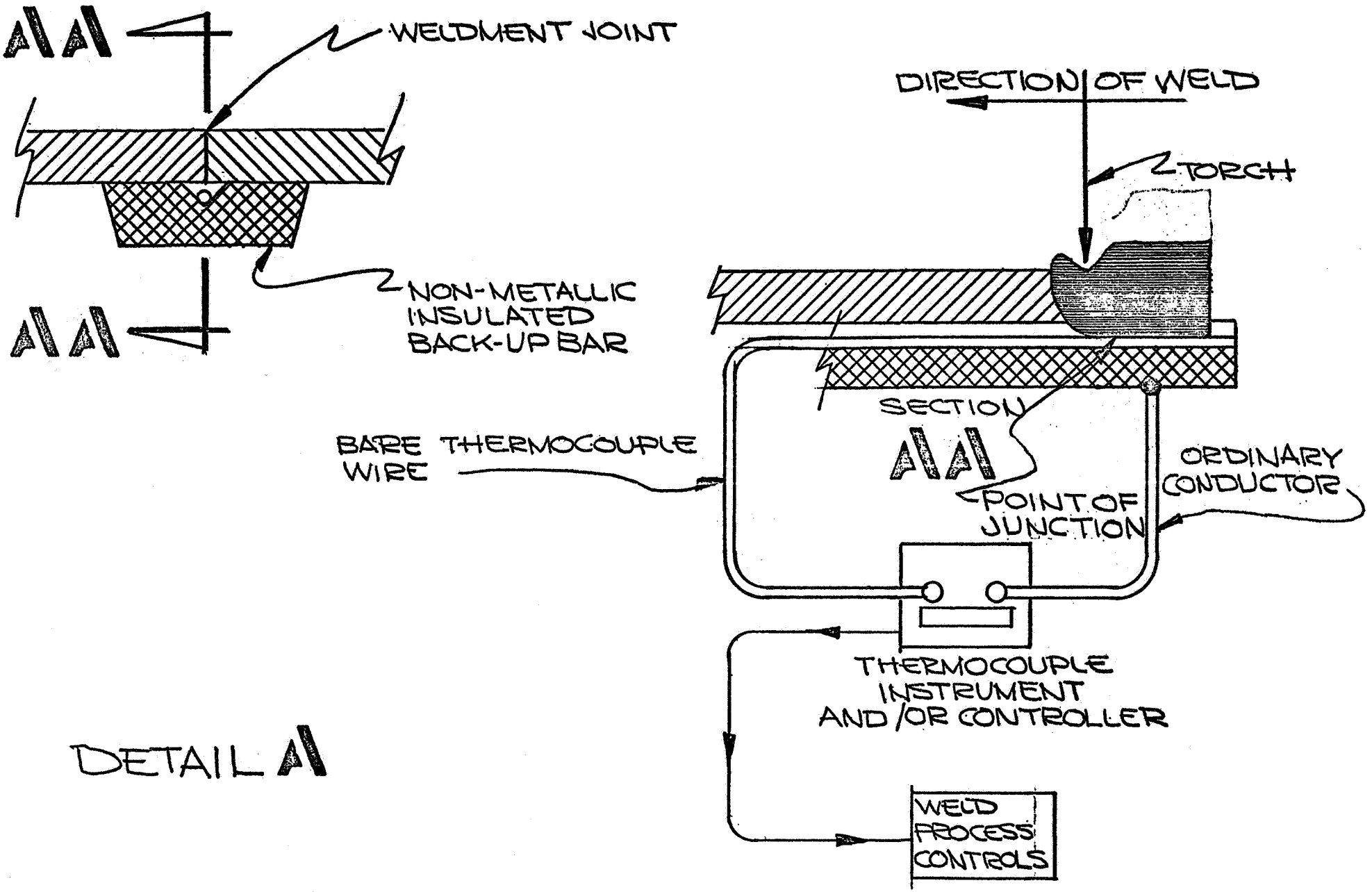


Figure 14: NASA Memo on Intrinsic thermocouple system.

Back-up Bar Not Shown

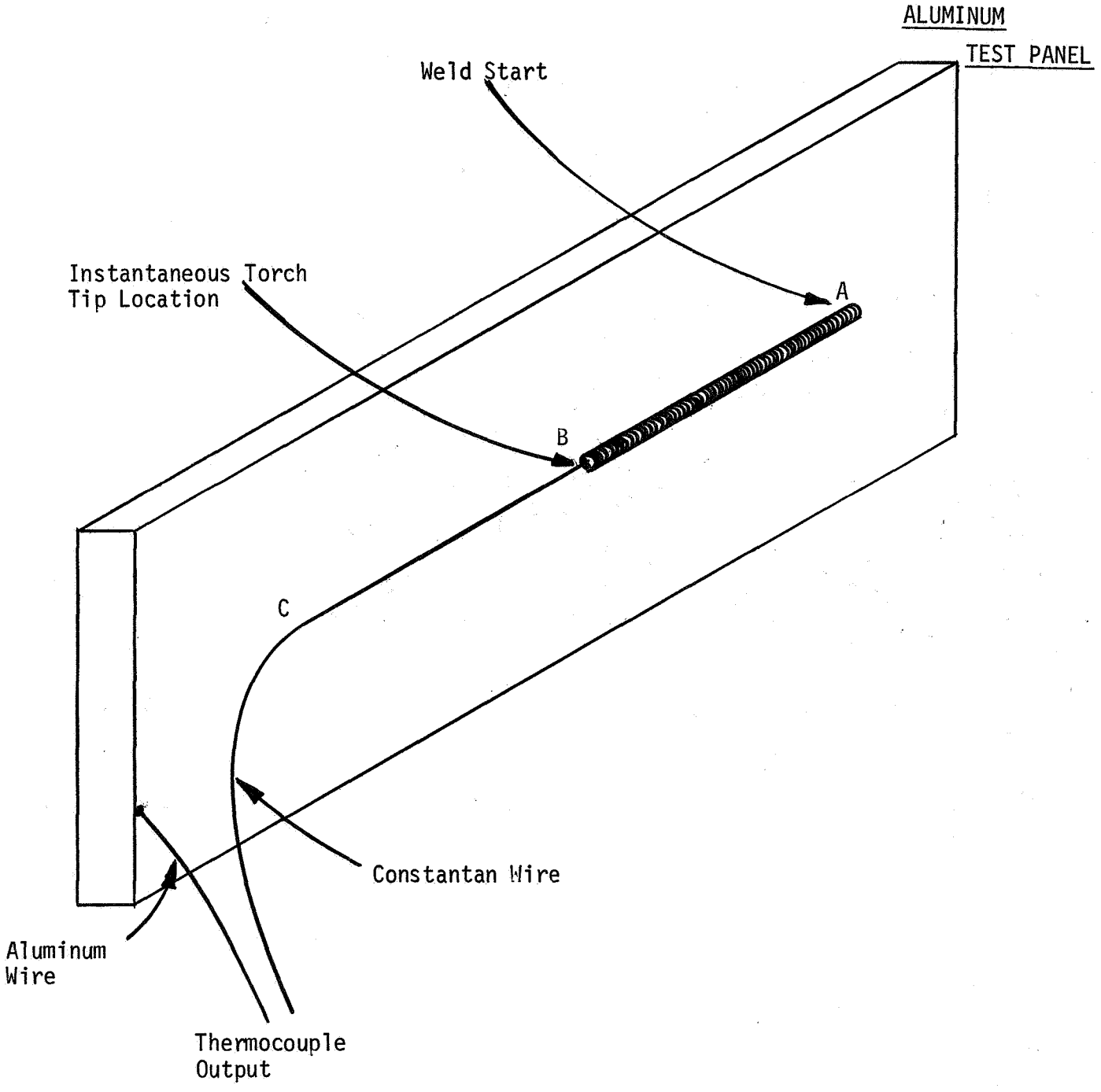


Figure 15: Simplified view of intrinsic thermocouple system.

wire and the weld specimen. Thus, the effective thermocouple junction exists between points A and B and progressively increases in length as the weld is made.

2.2.2.2 In order to determine the feasibility of the technique discussed above, the following problem areas were investigated.

2.2.2.2.1 Referring to Figure 15, the thermocouple output must be indicative of the temperature only at point B as it progressively moves down the weld path. Thus tests were run to determine the effect of the elongated junction behind point B extending to point A. These tests are explained in section 3.2.1.

2.2.2.2.2 A means must be provided for maintaining the constantan wire in tension and supported a fixed distance from the workpiece.

2.2.2.2.3 Assuming a metal backup bar, a means must be provided for insulating the constantan wire from the backup bar. The insulating material must be capable of withstanding temperatures in excess of 2000^{o} F. A summary of insulating materials evaluated is presented in section 3.2.1.

2.2.3 MAGIC WIRE THERMOCOUPLE

2.2.3.1 In February, 1966, Continental Sensing Inc. announced the development of a temperature measurement system based on an unique thermoelement pair designated Magic Wire[4]. The Magic Wire consists of a thermoelement pair, surrounded with a semiconductor insulator of controlled resistance-temperature coefficient; all of which has been uniformly compacted by means of swaging into an outer metallic sheath. A simplified equivalent circuit is shown in Figure 16.

As a peak temperature is applied to a discrete point along the length of Magic Wire, a localized thermoelectric junction is created. This junction produces a self-generating emf signal equivalent to standard millivolt output for the corresponding thermoelements (chromel-alumel) when subjected to the impressed temperature. The thermoelements are helically twisted in insulated spaced-apart relationship to eliminate noise pickup due to magnetic coupling.

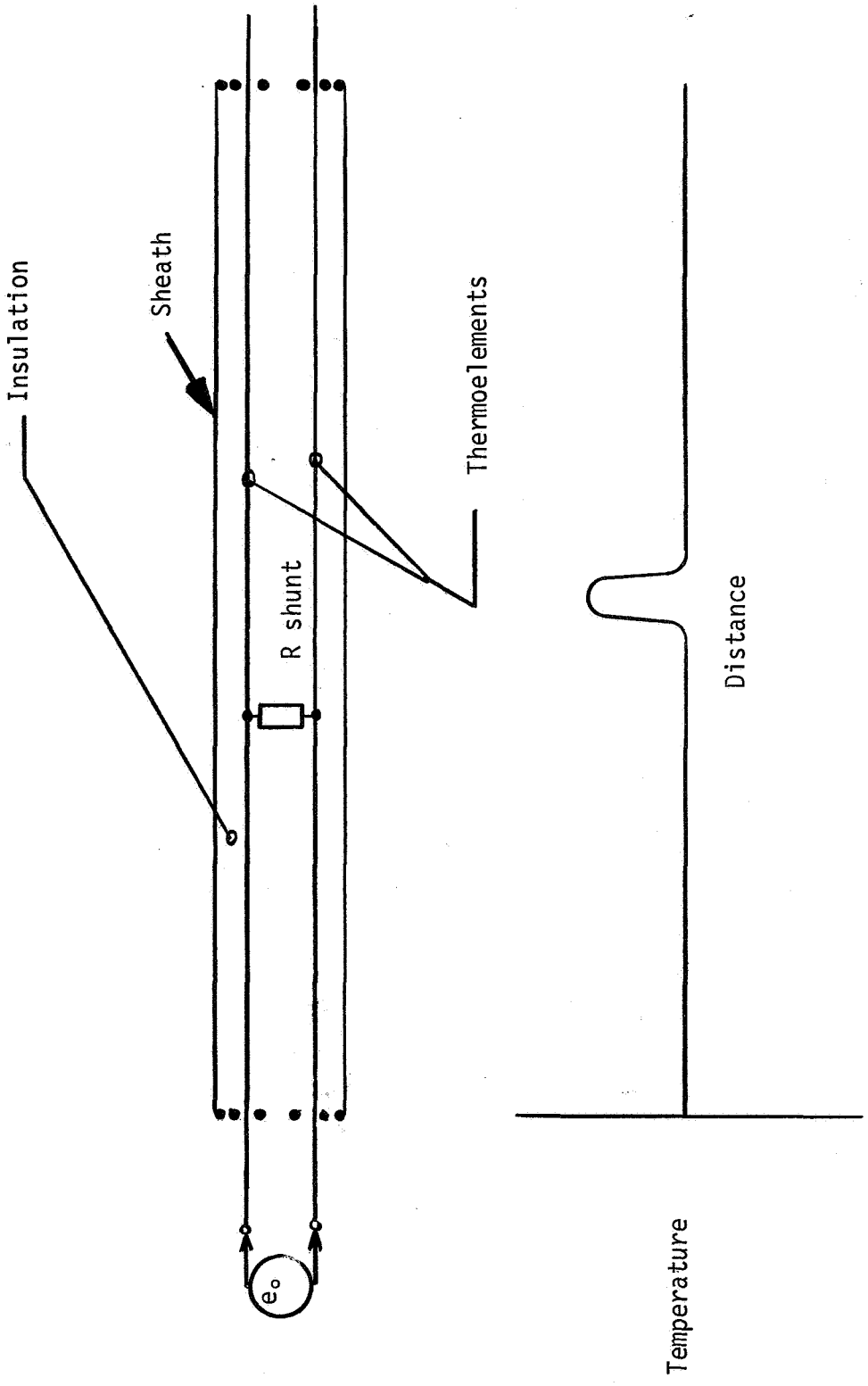


Figure 16: Simplified equivalent circuit of Magic Wire Thermocouple.

The metallic sheath itself reduces noise due to capacitive coupling thus insuring not only accurate temperature measurement but clear signal transmission of the measurement. Although the application of temperature creates a shunt resistance between the thermoelements, the design of the Magic Wire is such that a similar shunt does not occur between either of the wires and the sheath. Significant features of this wire which make it potentially feasible for the backup bar type of control are:

2.2.3.1.1 The construction of the transducer wire is such that even though various sections over the length of the transducer are exposed to different temperature conditions which tend to generate corresponding voltages, the output of the transducer will be the voltage signal indicative of the most extreme temperature condition to which the transducer has been exposed. Thus it is not necessary to insulate the thermocouple wire from the workpiece. The Magic Wire sheath can be positioned firmly against the workpiece parallel to the joint.

2.2.3.1.2 Since the Magic Wire can be placed firmly against the workpiece throughout its entire length and since shorting is no longer a problem, it can be held in place against the workpiece by means of an auxiliary grove machined into the backup bar as shown in Figure 17. Normal expansion of the wire is not detrimental because it is restricted to take place parallel to the joint.

2.2.3.2 Two nine (9) feet samples of Magic Wire, having a 304 stainless steel sheath with 0.100 inch O.D., were obtained from Continental Sensing, Inc. The following evaluation tests were conducted.

2.2.3.2.1 Speed-of-response tests were run to determine the amount of heat inertia that exists in the stainless steel sheath and semiconductor insulator. These tests are explained in section 3.2.2.

2.2.3.2.2 Tests were run to determine the peak temperature capabilities of the Magic Wire. These tests are also explained in section 3.2.2.

3.0 PHASE II - EXPERIMENTATION TO DETERMINE FEASIBILITY OF OBTAINING INTELLIGENT INFORMATION FROM TEMPERATURE TRANSDUCER

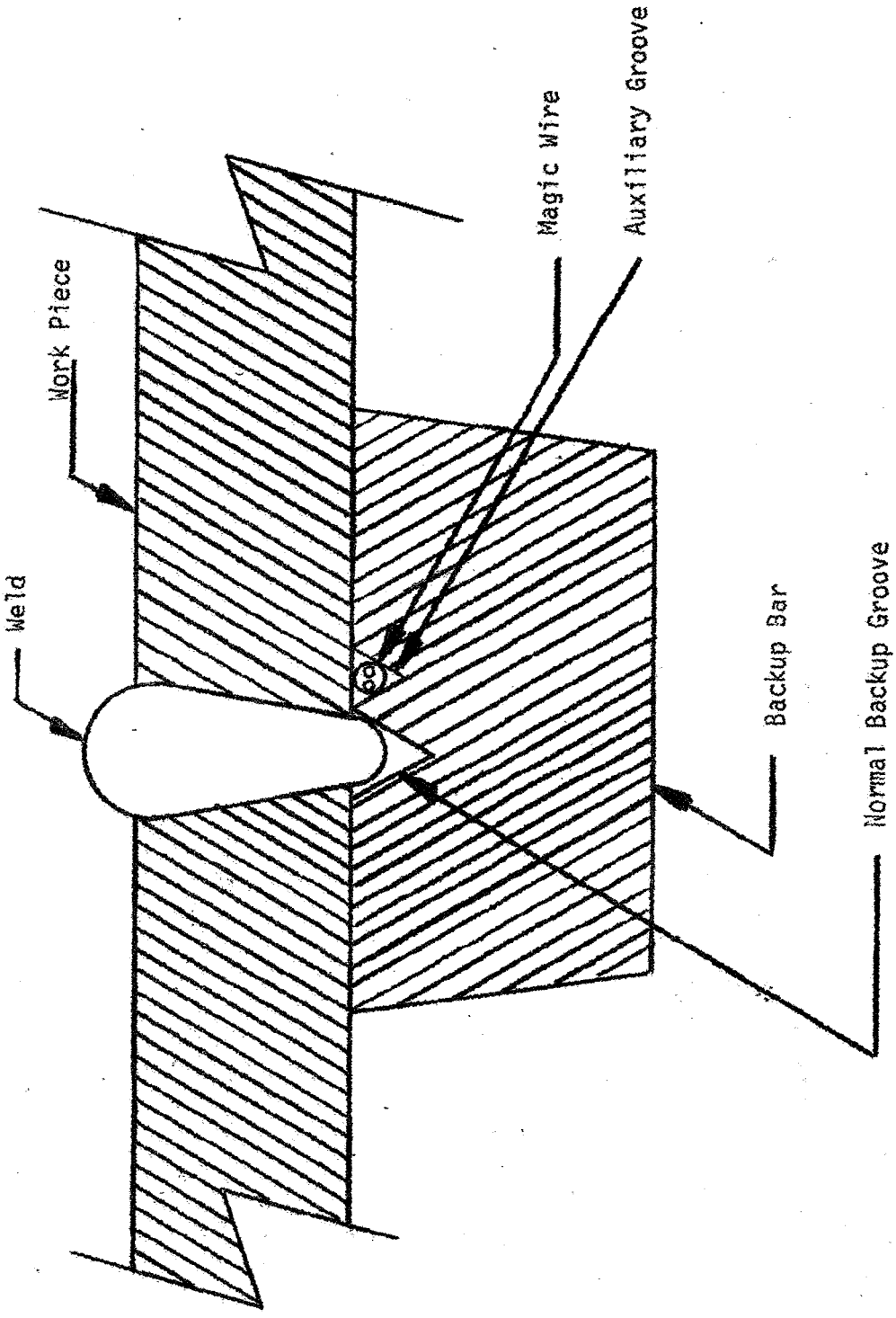


Figure 17: Placement of Magic Wire in Backup Bar

3.1 ARC-SIDE SENSING

In the second phase of this program extensive experimentation was conducted to determine the magnitude and behavior of the hybrid thermocouple signal under the influence of a welding arc. The primary emphasis of the early experimentation was to determine: (1) type design required of prototype probe assembly, (2) magnitude and intelligence of transducer signal, (3) sensitivity of transducer signal versus controllable weld variables, and (4) optimum location of transducer probe with respect to molten puddle.

3.1.1 INITIAL - PHASE FIXTURE, POWER SOURCE AND INSTRUMENTATION

A list of equipment used in the preliminary phases of this program is presented below.

3.1.1.1 Power source Vickers Controlarc #400 DC

3.1.1.2 Voltage Control Head Airco Model #HMH

3.1.1.3 Carriage governor: Linde Type EG-103

3.1.1.4 Weld Control Cabinet: Cayuga 9018A18

3.1.1.5 Speed Recorder: Esterline Angus Microammeter

3.1.1.6 Current Recorder: Esterline Angus Ammeter

3.1.1.7 Voltage Recorder: Esterline Angus Voltmeter

3.1.1.8 Signal Recorder: Heath Model EUW-20A

3.1.1.9 Thermocouple: .025 Constantan wire held in contact with the work by a phosphorbronze spring attached through a bracket to the voltage control head. The lead that connects the specimen to the recorder is made of aluminum so that there is no counter-thermocouple effect at the hot junction between the heated work and the lead wire.

3.1.1.10 Gas Regulator: Oxweld Type R 5007

3.1.1.11 Gas Supply 25% Argon - 75% Helium

3.1.1.12 Work holding fixture: Linde Sidebeam Carriage.

Photographs of the fixture, instrumentation, torch, and probe assembly are shown in Figures 18 through 21.

3.1.2 INITIAL - PHASE HYBRID PROBE ASSEMBLY

The prototype probe assembly used in initial experimentation is shown in Figure 22. As shown, a 0.025 inch diameter constantan wire was held in contact with the work by a phosphor bronze spring attached through a bracket to the voltage control head. The lead that connects the specimen

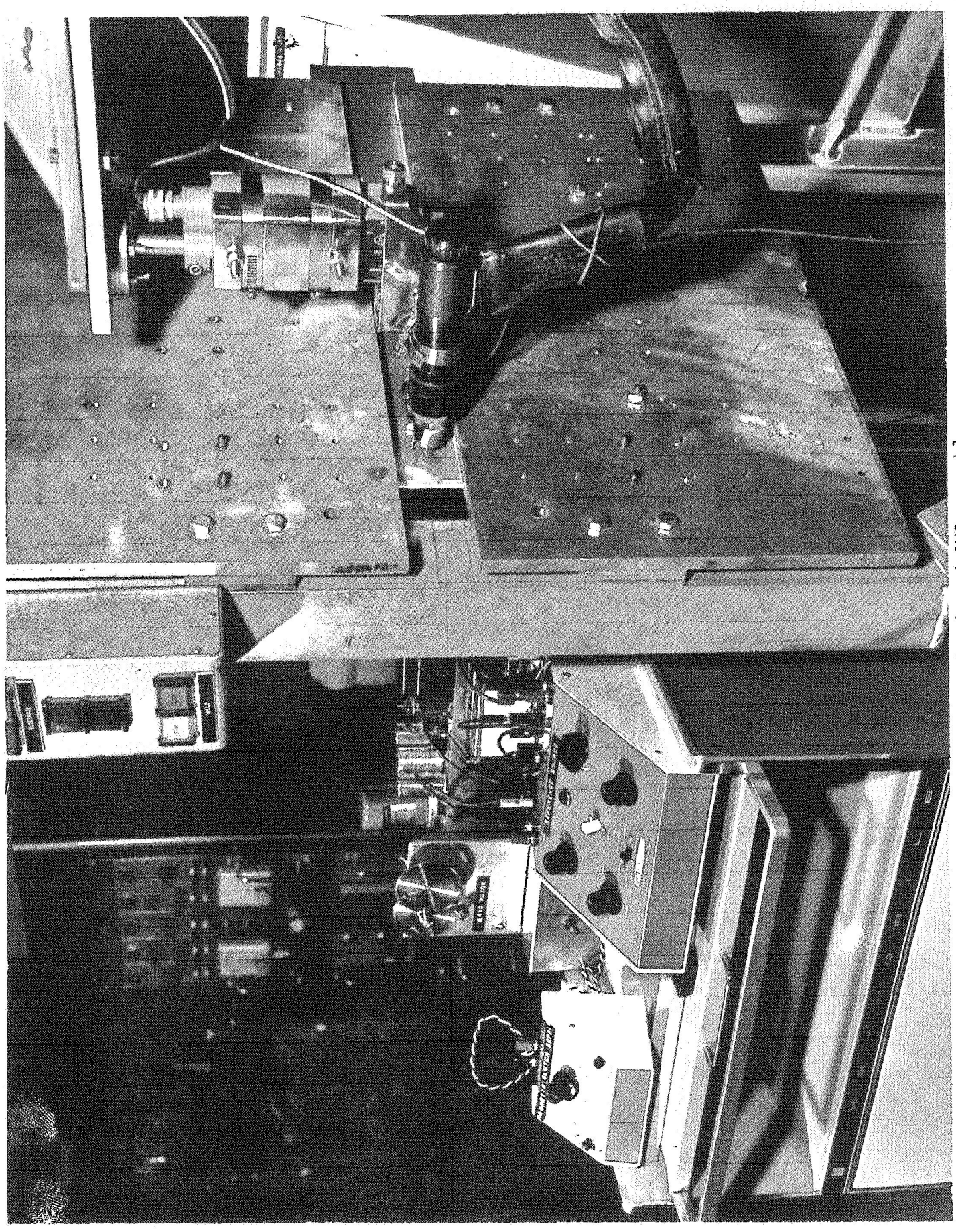


Figure 18: Torch and AVC assembly.

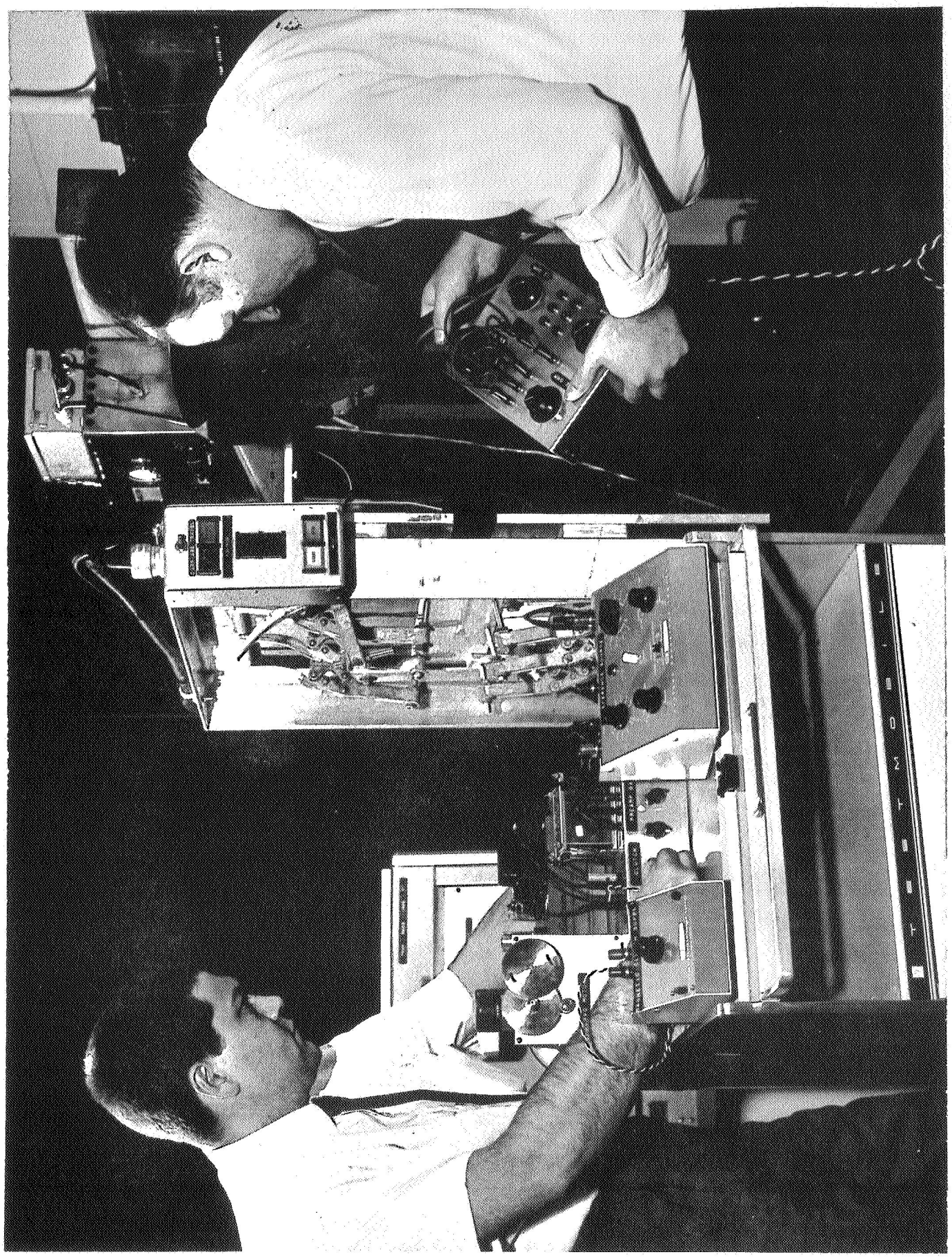


Figure 19: Fixture and instrumentation.

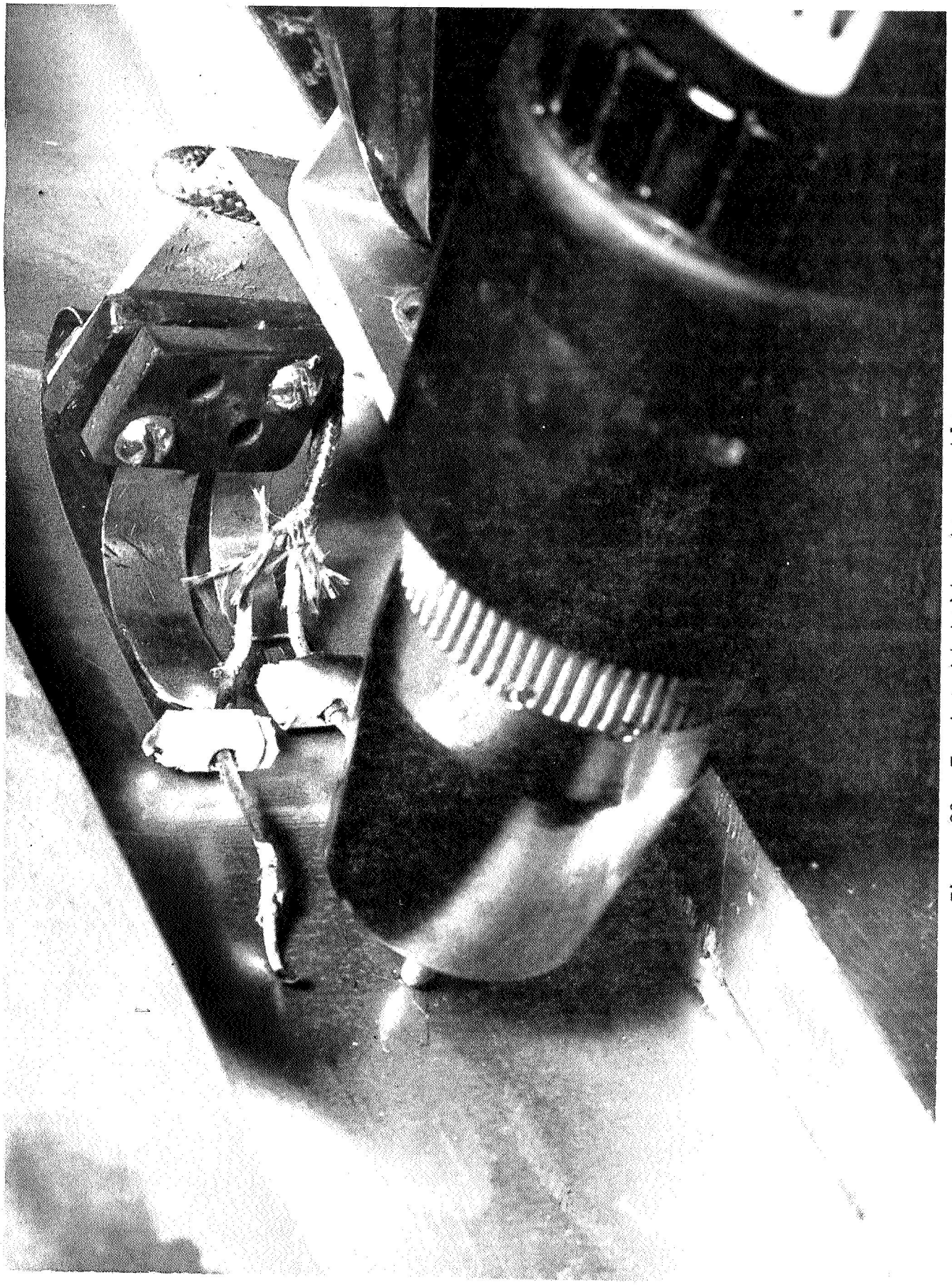


Figure 20: Torch and hybrid probe assembly.

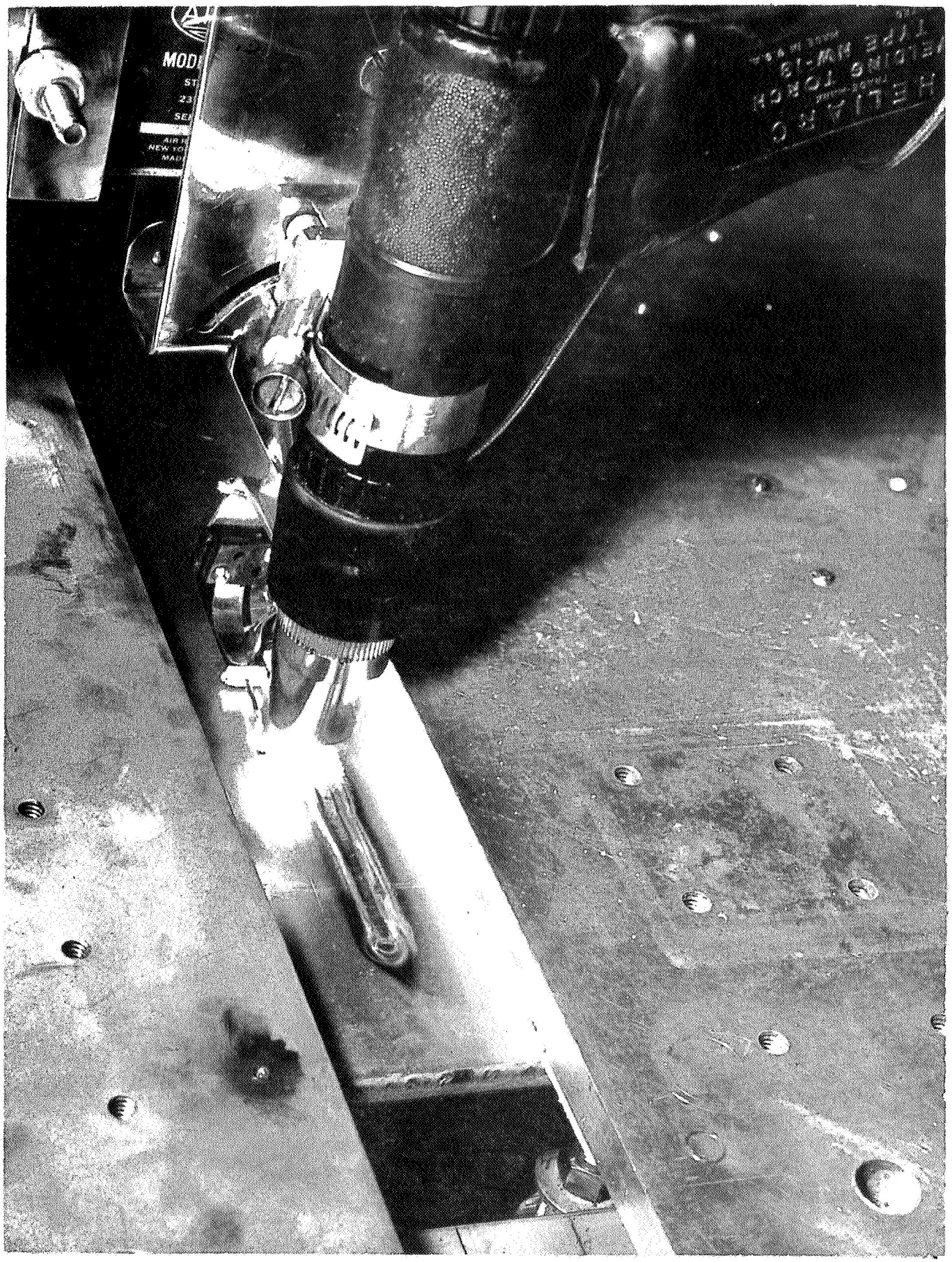


Figure 21: Torch and hybrid probe assembly during weld.

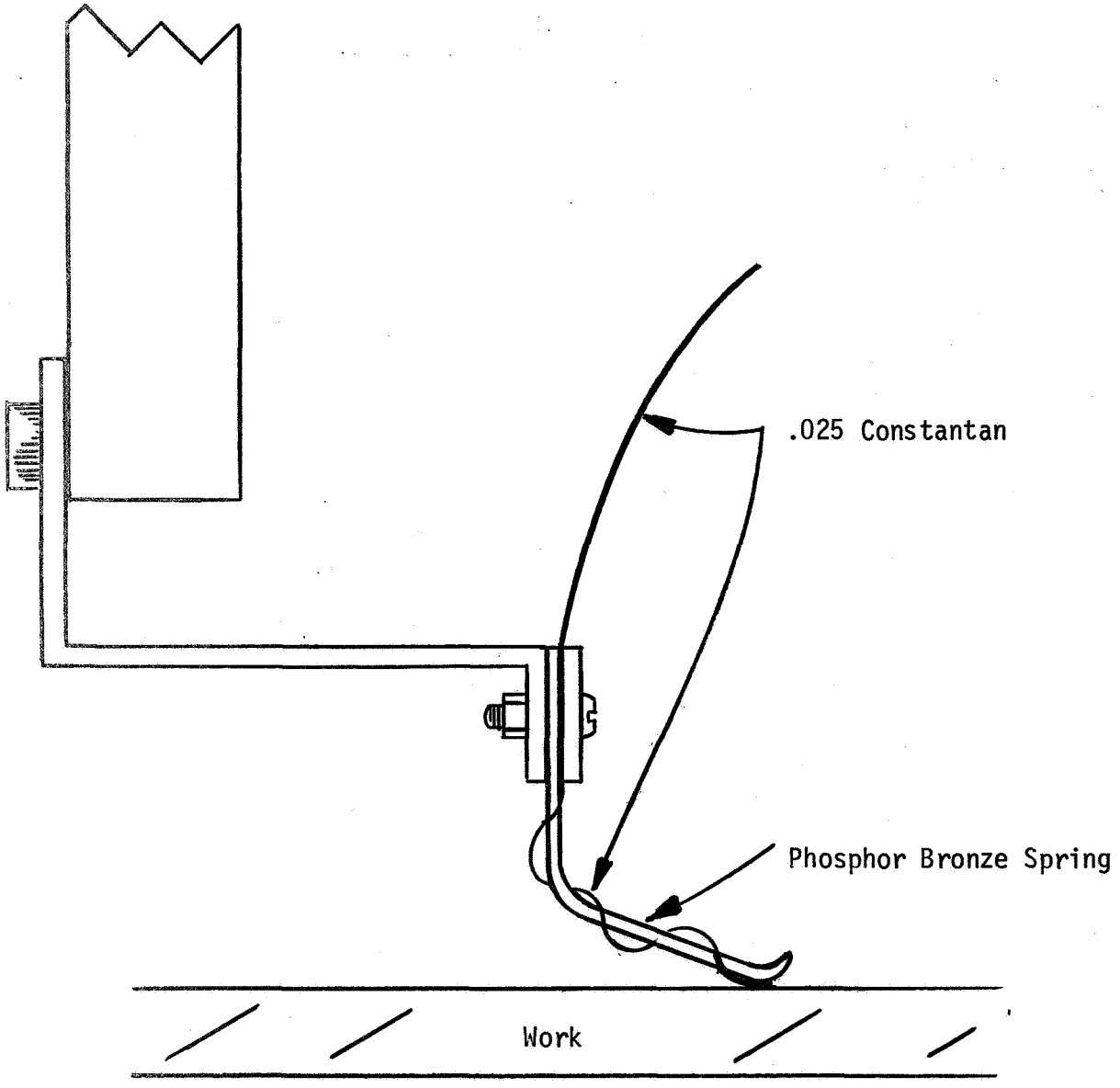


Figure 22: Prototype probe assembly.

to the recorder is made of aluminum so that there is no counter-thermocouple effect at the hot junction between the heated work and the lead wire.

3.1.3 SENSITIVITY OF TRANSDUCER SIGNAL VERSUS CONTROLLABLE WELD VARIABLES

3.1.3.1 EXPERIMENTS WITH 3/8" X 4" X 16" SPECIMENS

Most of the initial tests produced very erratic signals with very poor relationship between the weld and the signal and also poor repeatability. These earlier tests did, however, reflect instantaneous signal response to changes in speed, amperage and voltage, although there was no repeatability in their magnitude.

It was concluded that the lack of repeatability and erratic signal was caused by poor and erratic contact between the weld specimen and the work holding fixture. This condition could create a heat sink at points of contact, with no heat sink at other points.

The fixture was revised to incorporate 0.125 inch thick teflon strips to insulate the work from the fixture. Subsequent tests provided a more uniform signal. It was still possible to get a signal response during welding but only in the direction of increased temperature, i.e., increased voltage or amperage, or decreased speed. This indicated a buildup of heat in the specimen that could not dissipate fast enough to provide a decreasing signal. This problem was later alleviated with larger specimen size (see section 3.1.3.2).

3.1.3.1.1 PROCEDURE

3.1.3.1.1.1 The test specimen was clamped in the workholding fixture.

3.1.3.1.1.2 The torch was moved to a position one inch from the end of the specimen, then jogged down until the thermocouple wire was in contact with the work.

3.1.3.1.1.3 Pushing the start button initiated the weld start.

3.1.3.1.1.4 The torch was held in its original position until a puddle 3/8" in diameter appears on the back side of the specimen. The carriage was then started and allowed to proceed to within 1-1/2 inch from the end of the specimen. The thermocouple moved with the torch maintaining its original relationship throughout the entire weld.

3.1.3.1.1.5 All welds were made bead-on-plate.

3.1.3.1.2 A series of tests were made to determine the effect of speed on the thermocouple signal. In these tests the voltage and amperage were held constant. Table III lists the weld parameter value used.

Table III

Weld Parameter Values

Specimen Number	Voltage (volts)	Current (amperes)	Travel Speed (ipm)
50	10	330	5
51	10	330	4.5
52	10	330	4
53	10	330	3.5
54	10	330	5
55	10	330	4.5
56	10	330	4
57	10	330	3.5
58	10	330	3

In all of the welds listed in Table III, the shielding gas was 75-25 Argon-Helium and the thermocouple probe was positioned 5/16 inch abeam the center of the puddle. The thermocouple output versus position along the weld specimen is plotted in Figures 23 and 24 for specimens number 50, 51, 53, 54, 56, and 58.

3.1.3.1.3 Another series of tests were made in which the voltage and travel speed were held constant. Each test specimen was welded at a different amperage from 300 to 420 amperes in 20 ampere increments. Table IV lists the weld parameter values used. In all of the welds listed in Table IV, the shielding gas was 75-25 Argon-Helium and the thermocouple probe was positioned 3/8 inch abeam the center of the puddle. The thermocouple output versus position along the weld specimen is plotted in Figure 25 for specimens number 60 and 66.

NO. 340R-10 DIETZGEN GRAPH PAPER
10 X 10 PER INCH

EUGENE DIETZGEN CO.
MADE IN U. S. A.

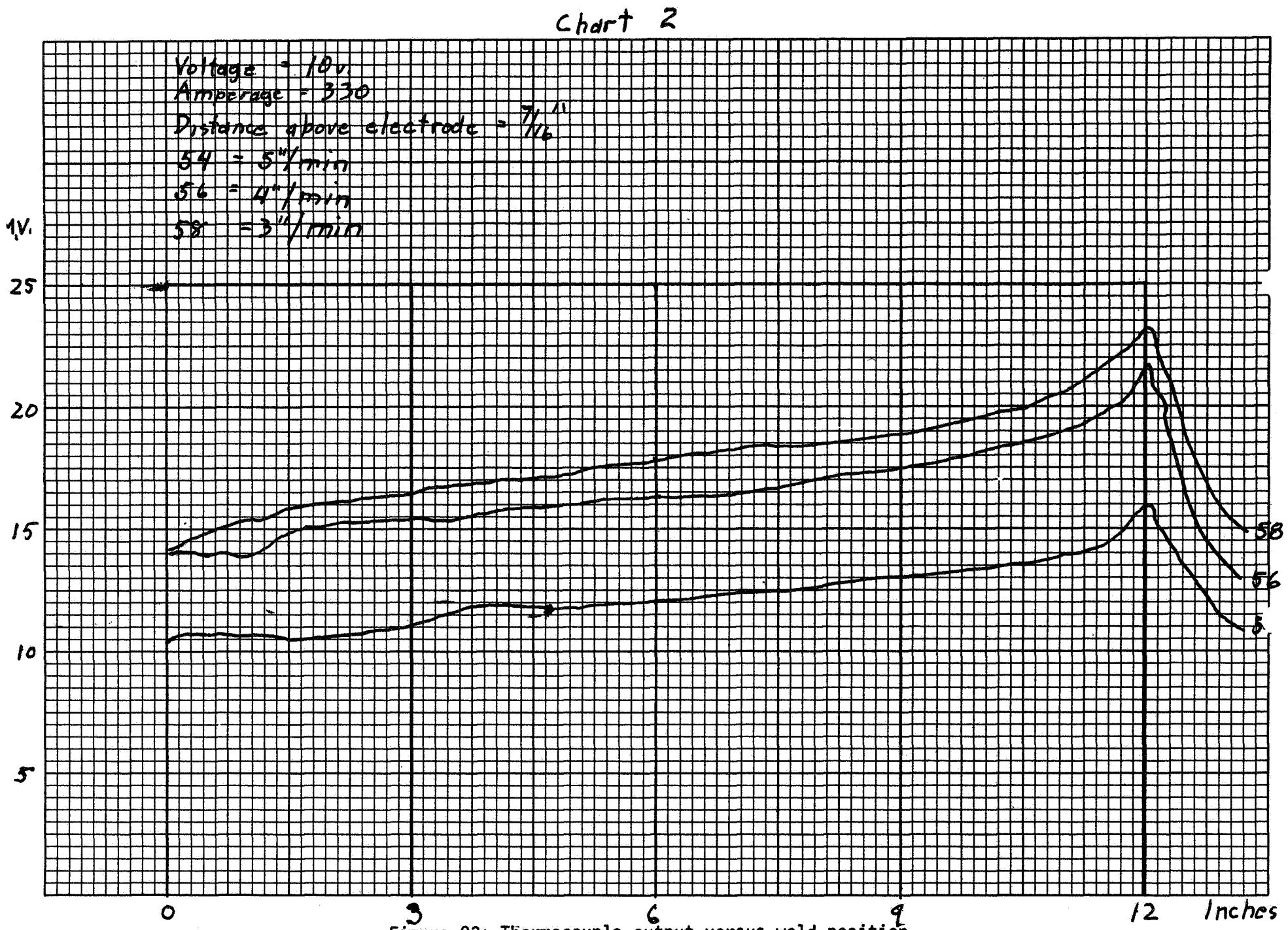


Figure 23: Thermocouple output versus weld position.

NO. 340R-10 DIETZGEN GRAPH PAPER
10 X 10 PER INCH

EUGENE DIETZGEN CO.
MADE IN U. S. A.

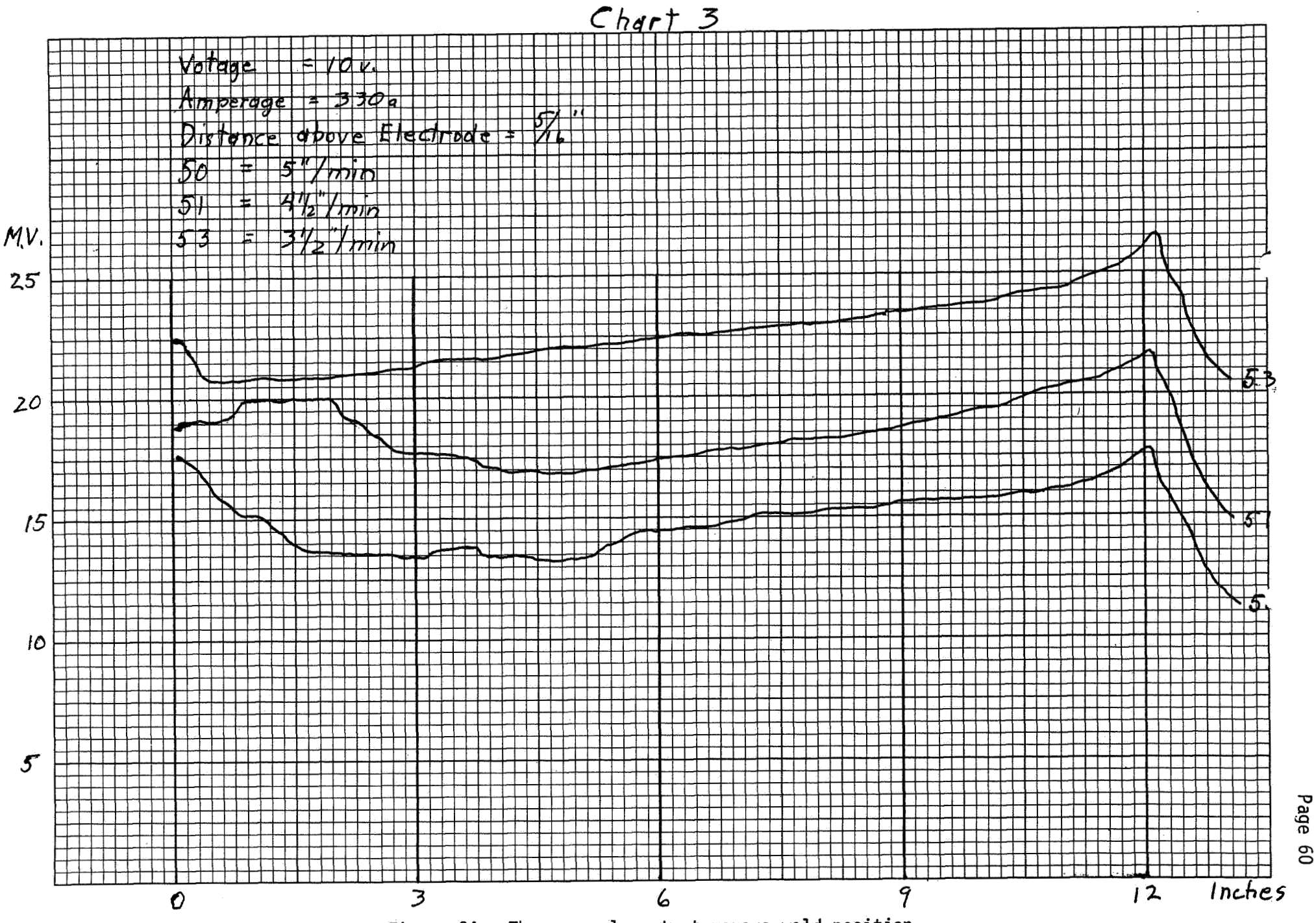


Figure 24: Thermocouple output versus weld position.

NO. 340R-10 DIETZGEN GRAPH PAPER
10 X 10 PER INCH

EUGENE DIETZGEN CO.
MADE IN U. S. A.

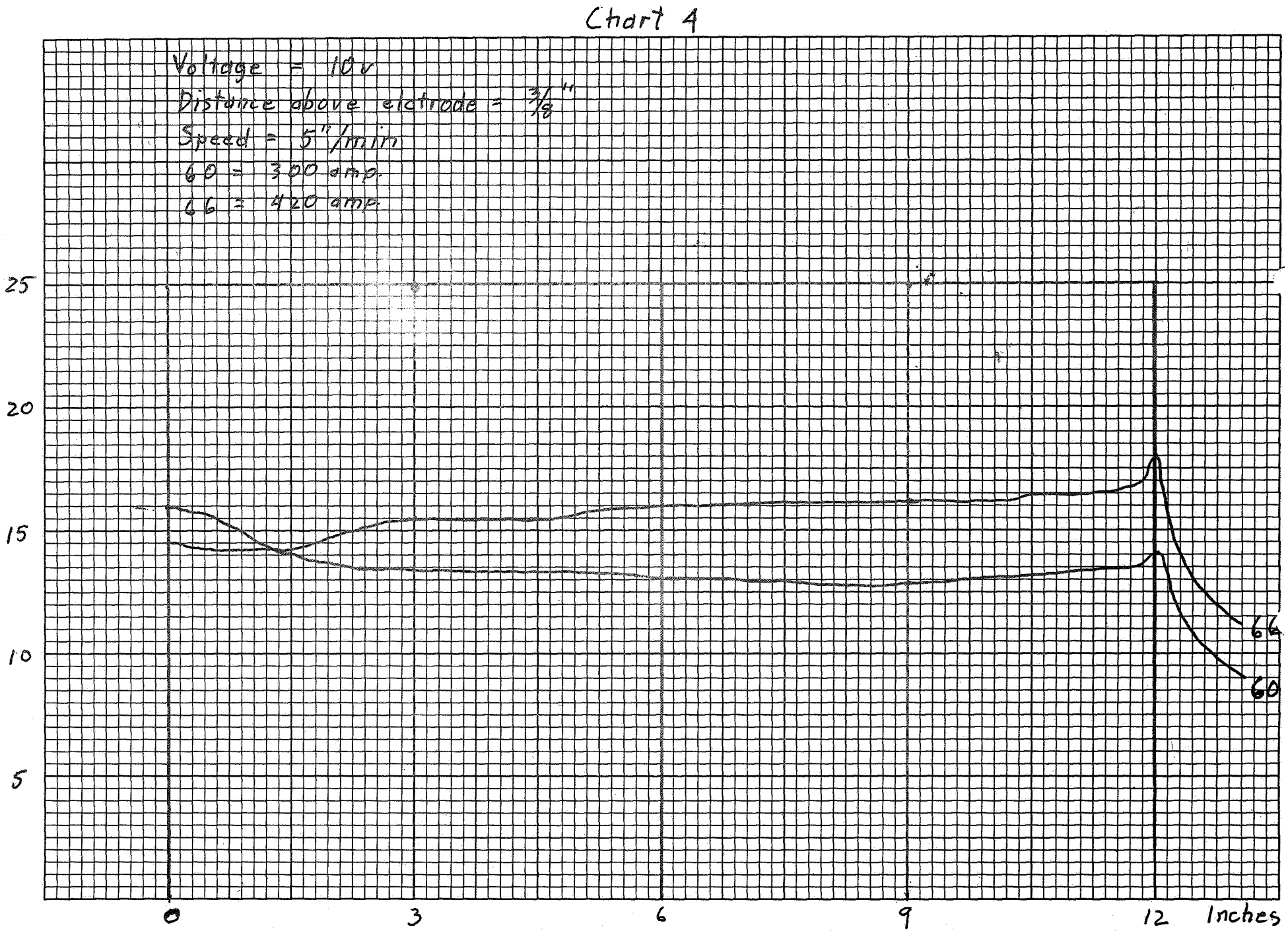


Figure 25: Thermocouple output versus weld position.

Table IV

Weld Parameter Values

Specimen Number	Voltage (volts)	Current (amperes)	Travel Speed (ipm)
60	10	300	5
61	10	320	5
62	10	340	5
63	10	360	5
64	10	380	5
65	10	400	5
66	10	420	5

3.1.3.1.4 Observation

3.1.3.1.4.1 It was possible to measure relative temperatures around a moving arc weld using the traveling single wire thermocouple.

3.1.3.1.4.2 Constantan versus aluminum provided a significant signal; approximately 25 mv at 1000° F.

3.1.3.1.4.3 Variations in voltage, amperage, speed and heat sink conditions did change the temperature signal.

3.1.3.1.4.4 There seems to be no adverse effects due to the proximity of the welding arc. Several tests were made where the wire was in the weld puddle itself, in which case the signal did oscillate, but within a 2 M.V. range.

3.1.3.1.4.5 It was concluded that a method needed to be developed for preventing the heat buildup in the test specimen, since this would be the only way of duplicating conditions that exist in a large structure. The problem was solved by using larger test specimens as explained in section 3.1.3.2.

3.1.3.2 EXPERIMENTATION WITH WATER-COOLED SPECIMENS AND 3/8" X 5" X 23" SPECIMENS

3.1.3.2.1 WATER-COOLED SPECIMENS

3.1.3.2.1.1 A hole was drilled longitudinally through a group of 1/2" X 4" X 12" plates and fitted with water connections.

3.1.3.2.1.2 With these specimens it was not possible to achieve penetration even at 450 amperes.

3.1.3.2.1.3 Because there was no buildup of heat in the specimen the signal changes were better defined than in the uncooled plates.

3.1.3.2.1.4 These tests were discontinued after the experiments described subsequenly because of the excessive cost for drilling, and the fact that there was no penetration to associate with the signal

3.1.3.2.2 LARGER SPECIMENS

Earlier tests using test specimens 3/8" thick, 4" wide, and 16" long produced a gradually rising signal peaking rapidly near the end. By increasing the length to 20 inches a more uniform signal was produced but there was still a rise toward the end. Therefore later test specimens were made 5" wide and 23" long. This seemed an ideal size for testing purposes.

3.1.3.2.3 VARIATION IN VOLTAGE

Only two tests were made varying voltage in one (1) volt increments. The results were quite different, although all conditions were the same. On one specimen the average signal was 6.14 millivolts per volt. On the other it was 3.5 millivolts per volt. On these tests, the weld parameters were: amperage, 450 amperes; travel speed, 3 imp; voltage, 10 volts, shielding gas, 75-25 Aragon-Helium, specimen size, 3/8" X 4" X 20", and probe position, 3/8" abeam center of puddle. The results for test specimen number 88 are shown in Figure 26.

3.1.3.2.4 VARIATION IN CURRENT

3.1.3.2.4.1 Eleven test welds were made varying the amperage with all other conditions constant. In all of these tests the weld parameters were: travel speed, 3 ipm, arc voltage, 10 volts; shielding gas, 75-25, Argon-Helium; welding current, 250 to 450 amperes in 50 ampere increments. Table V lists the thermocouple probe output signal versus current variation for specimens number 96 through 100. Each of these specimens were 3/8" X 4" X 20". All welds were bead on plate. Table VI lists the thermocouple probe output signal versus current variation for specimens number 102 through 107. Each of these specimens were water cooled and 1/2" X 4" X 12". All welds were again bead on plate.

NO. 340R-10 DIETZGEN GRAPH PAPER
10 X 10 PER INCH

EUGENE DIETZGEN CO.
MADE IN U. S. A.

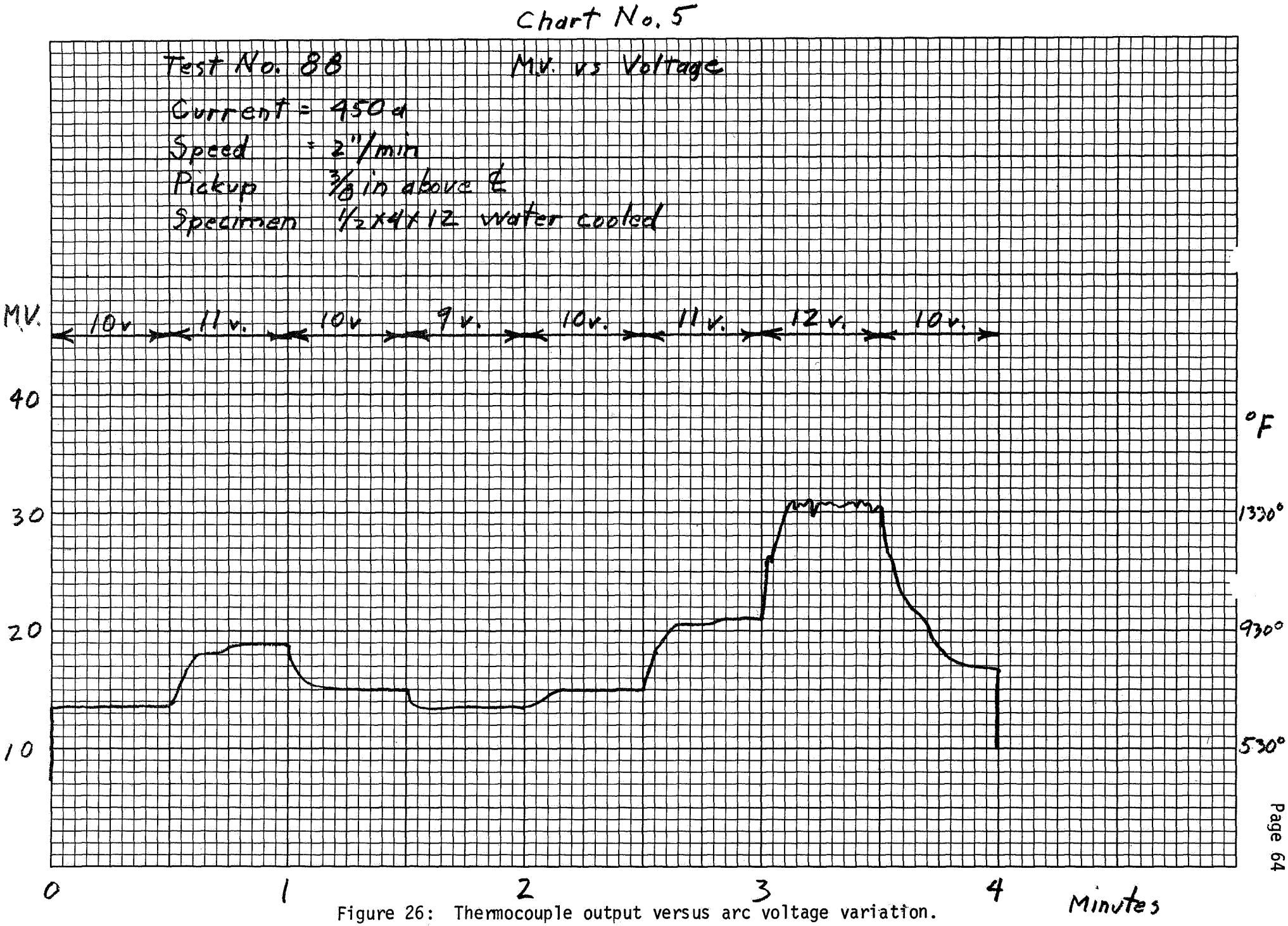


Figure 26: Thermocouple output versus arc voltage variation.

Table V.

Thermocouple Signal (millivolts)
Versus Current Variation

Current	Specimen Number				
	96	97	98	99	100
300	22.5 mv	24 mv	25.5 mv	25 mv	25mv
350	28	26	32.5	31	29.5
400	29	28	33	32	31.5
350	27.5	25.5	33	29	29.5
300	25.5	25	29	27	28
250	20	20.5	21.5	22	24.5
300	24	24	28	26.5	31
350	26.5	25.5	32	29.5	31.5
300	24.5	20	28	27	28
250	20	15.5	21.5	22	23.5

Table VI
Thermocouple Signal (millivolts)
Versus Current Variation-Water
Cooled Specimens

Current	Specimen Number					
	102	103	104	105	106	107
300	13 mv	14 mv	13.5 mv	14 mv	13.5 mv	13 mv
350	14	15	15	17	16	15
400	17	18	19	20	20	18
450	19	21	21.5	22	22	21
400	18	19.5	21	19.5	18.5	18
350	16	17	17	17.5	15.5	15.5
300	--	14.5	15	15	13.5	13.5
250	--	12	12	--	11	12

3.1.3.2.4.2 Although the recorded signals were similar they were not accurately repeatable. The maximum range from one sample to another for the same temperature was 4.5 millivolts.

3.1.3.2.4.3 The average response for the uncooled plates was 0.071 millivolts per ampere. The response for speciman number 99 is plotted in Figure 27.

3.1.3.2.4.4 The average response for the water cooled plates was 0.048 millivolts per ampere. The response for speciman number 107 is plotted in Figure 28.

3.1.3.2.5 VARIATION IN SPEED

3.1.3.2.5.1 Five test welds were made varying speed with all other parameters constant. The weld parameters were: travel speed, 1 to 5 ipm; current, 300 amperes; arc voltage, 9 volts; shielding gas, 75-25 Argon Helium; specimen size, 3/8"X5"X23"; probe position, 3/8" abeam center of puddle. Table VII lists the thermocouple probe output signal versus speed variation for specimens number 115 through 119. All welds were bead on plate.

Table VII

Thermocouple Signal (millivolts)

Versus Speed Variation

Speed (ipm)	Specimen Number 115	116	117	118	119
2	25.5 mv	25 mv	27 mv	26.5 mv	27
3	24.5	24.5	26	25.5	26
4	22.5	22	23	22.5	23
5	19.5	19.5	20	19.5	20
4	19.5	19.5	20	19	20
3	21.5	21	21.5	21	22
2	24	23.5	24.5	23.5	24.5
1	27.5	27	27	27	27

3.1.3.2.5.2 The maximum range for a given speed was 2.0 millivolts.

3.1.3.2.5.3 The average response was 2.014 millivolts per ipm. The response for speciman number 116 is plotted in Figure 29.

3.1.3.2.6 LOCATION OF THERMOCOUPLE

A series of tests were run to determine the variation in thermocouple output versus probe position with respect to the puddle. On these tests the weld parameters were: travel speed, 2 ipm; arc voltage, 9 volts; specimen size, 3/8"X5"X23", and weld current, 250 to 350 amperes in 50 ampere increments. The results for specimens number 140, 142, 143, and 154 are presented in Figure 30. As expected the thermocouple output progressively decreases as the distance of the probe away from the torch centerline increases.

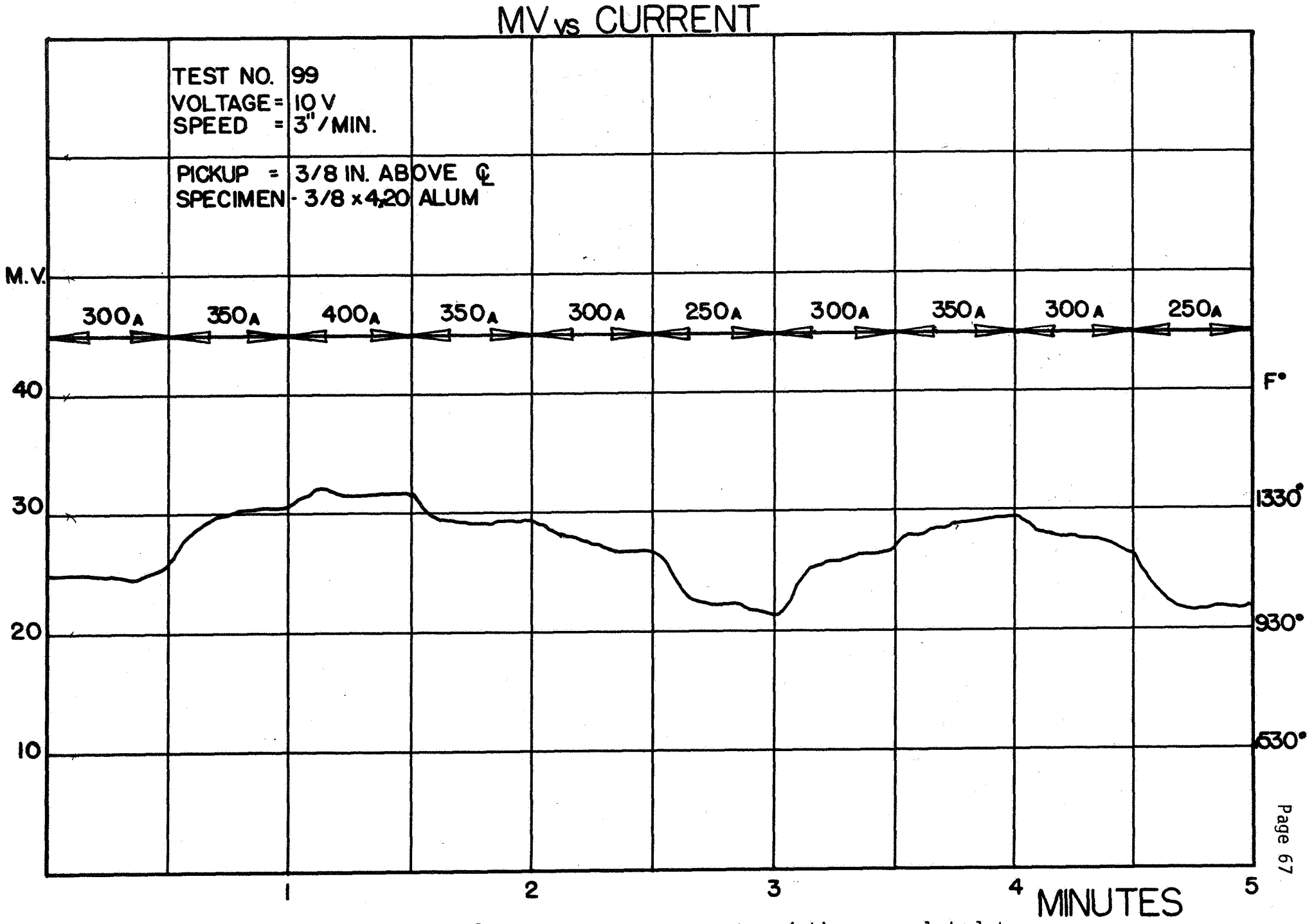


Figure 27: Thermocouple response versus current variation, uncooled plates.

NO. 340R-10 DIETZGEN GRAPH PAPER
10 X 10 PER INCH

EUGENE DIETZGEN CO.
MADE IN U. S. A.

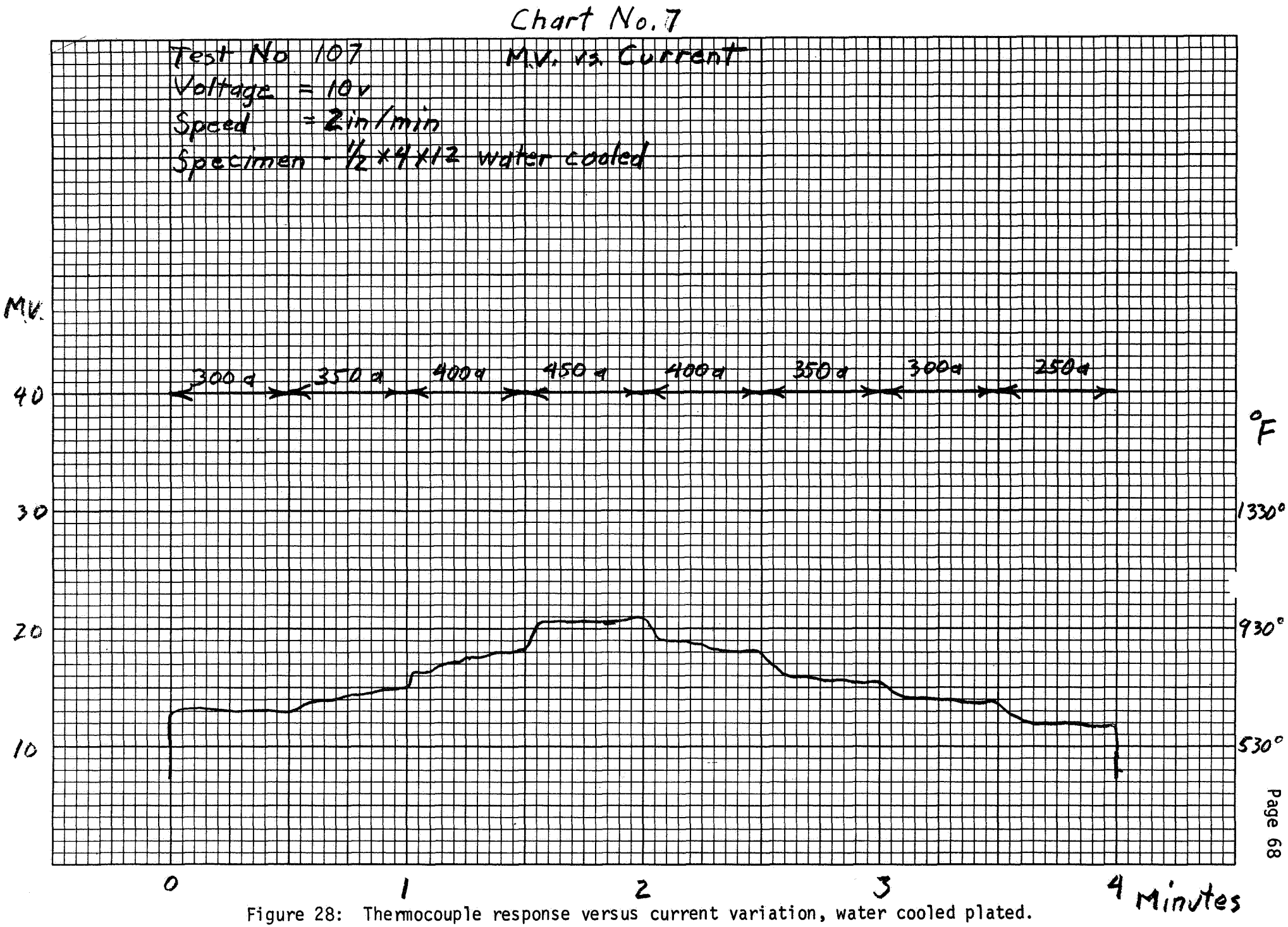


Figure 28: Thermocouple response versus current variation, water cooled plated.

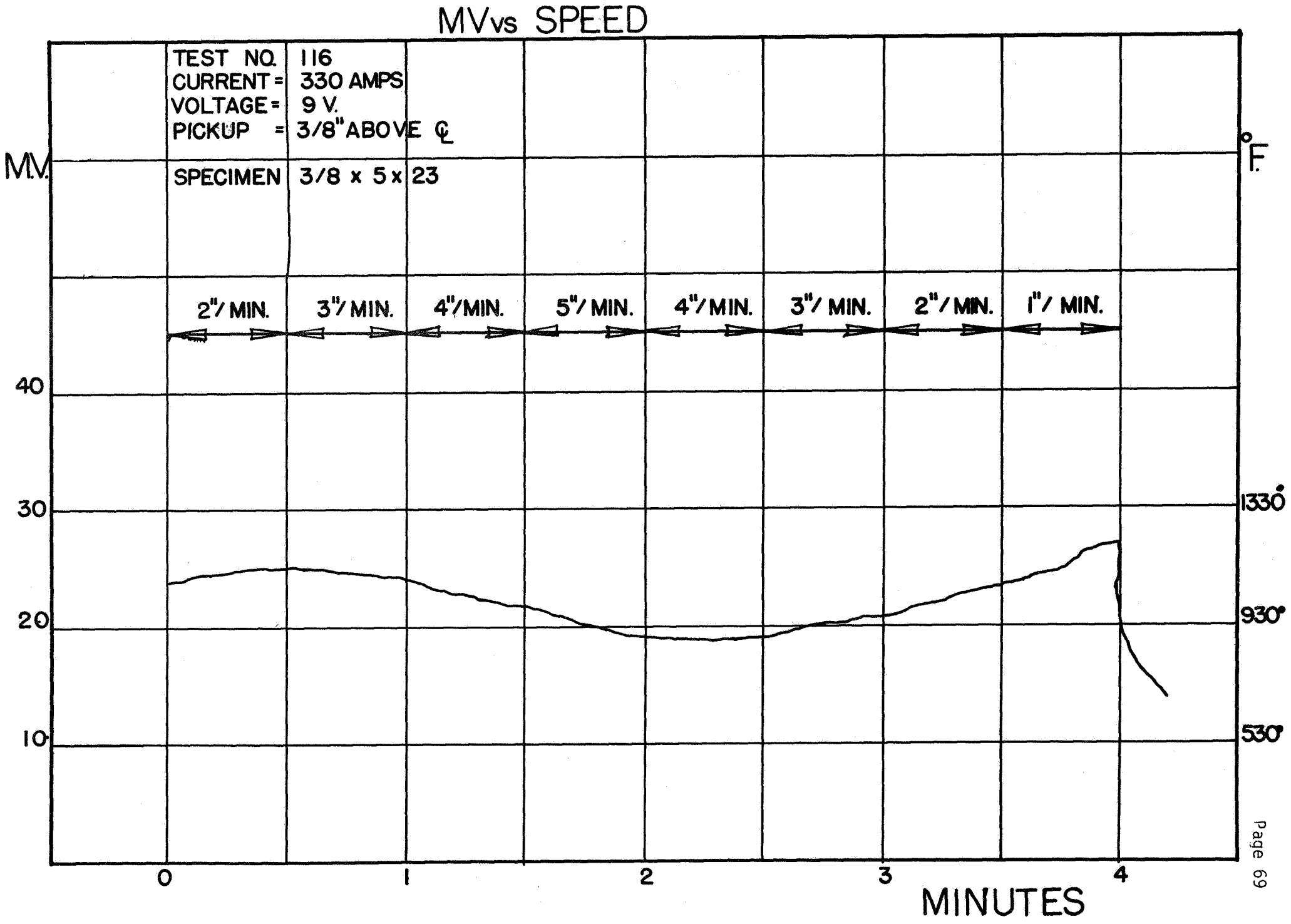


FIGURE 29: THERMOCOUPLE OUTPUT VARIATIONS IN RESPECT TO STEP CHANGES IN WELD SPEED

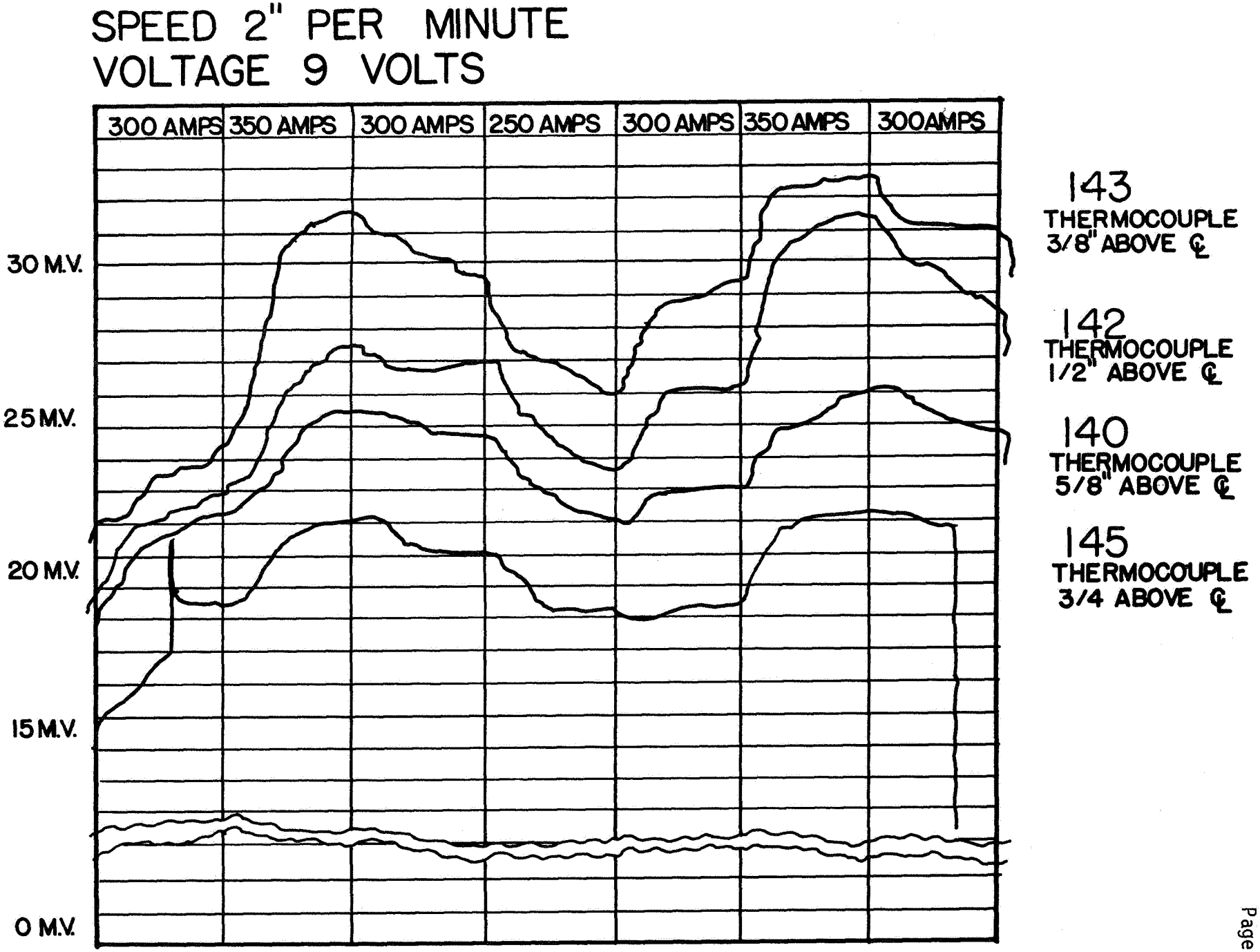


Figure 30: Thermocouple signal versus probe position.

3.1.3.3 WELD-REPEATABILITY TESTS WITH LARGE SPECIMEN SIZE

3.1.3.3.1 In order to determine the ability to repeat welds under laboratory conditions a series of tests were conducted. These tests were run with 2219 aluminum panels 3/8" X 5" X 23". The voltage was held constant at 9.0 volts and the speed was held constant at 3"/min. The distance between the thermocouple and the center line of the electrode was set at 3/8".

3.1.3.3.2 The first series of tests were run with six uncleaned plates, number 122, 123, 124, 125, 126 and 127. The amperage was varied in 50 ampere increments. The thermocouple output voltage in millivolts versus amperage increment is shown in Figure 31 and 32. The average change in thermocouple output versus amperage increment for the six panels is shown in Figure 33. The standard deviation about the mean is indicated with cross-hatching.

3.1.3.3.3 In the second series of tests, five plates, number 128, 129, 130, 131, and 132 were used. Each plate was thoroughly wire brushed just prior to testing, and the constantan thermocouple tip was cleaned with emery cloth before each test. The resulting thermocouple output voltage versus amperage increment is shown in Figure 34 and 35; and the standard deviation for these five plates is shown in Figure 36.

3.1.3.3.4 In order to observe the effect of a large sample, the results for the six plates of Section 3.1.3.3.2 and the five plates of Section 3.1.3.3.3 were combined and a plot of average change in thermocouple output versus amperage increment was made. This plot is shown in Figure 37. As in Figures 33 and 36, the standard deviation about the mean is shown with cross-hatching.

3.1.3.3.5 The conclusions drawn from these test were as follows:

(1). No appreciable improvement in repeatability was observed with the cleaned plates.

(2). In both series of tests the standard deviation was highest for the second incremental amperage change after initiating the test weld. This result emphasizes the difficulty of starting a weld under identical conditions of penetration, heat sink considerations, etc.

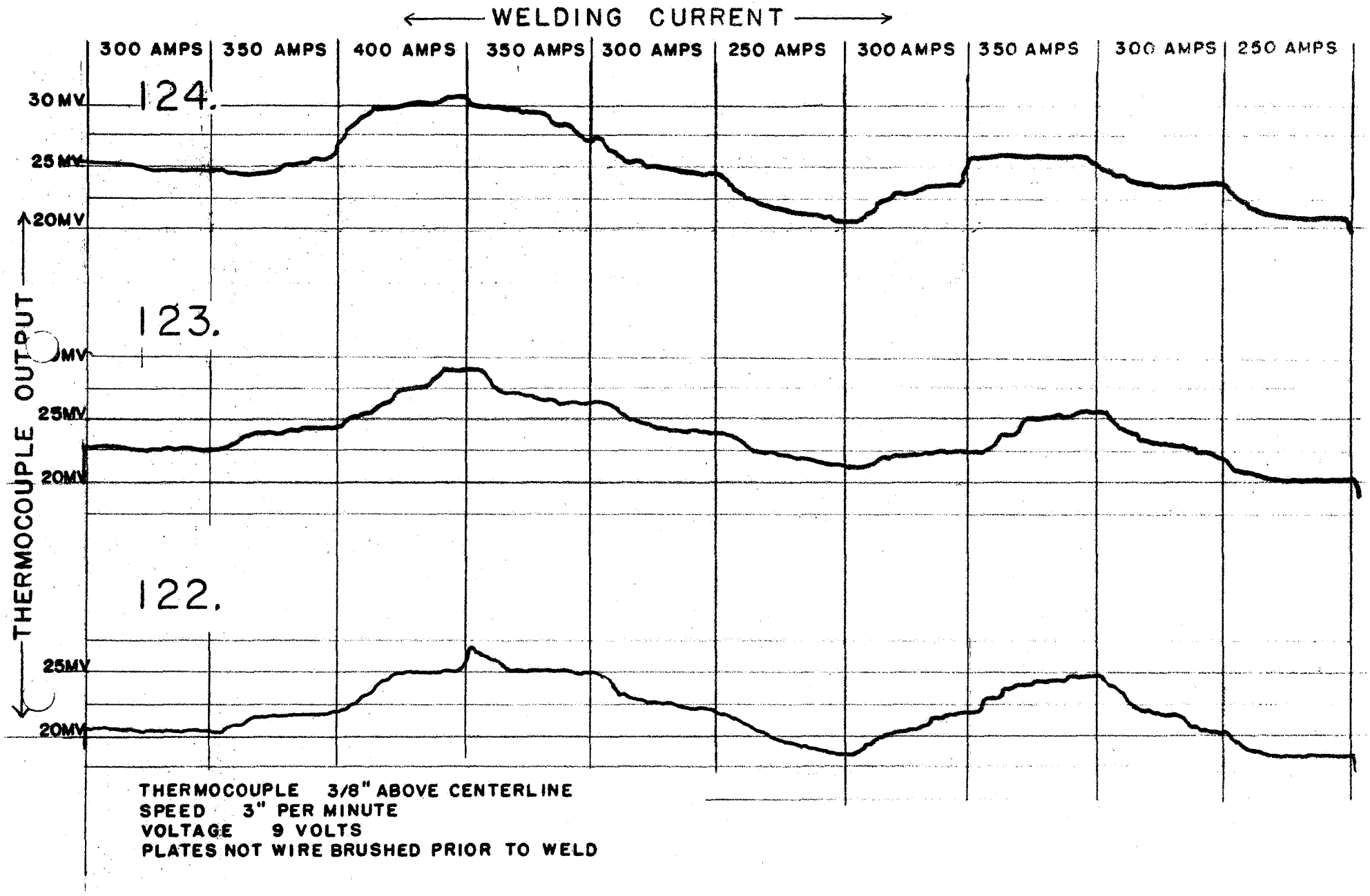


Figure 31: Thermocouple output versus current variation, uncleaned plates.

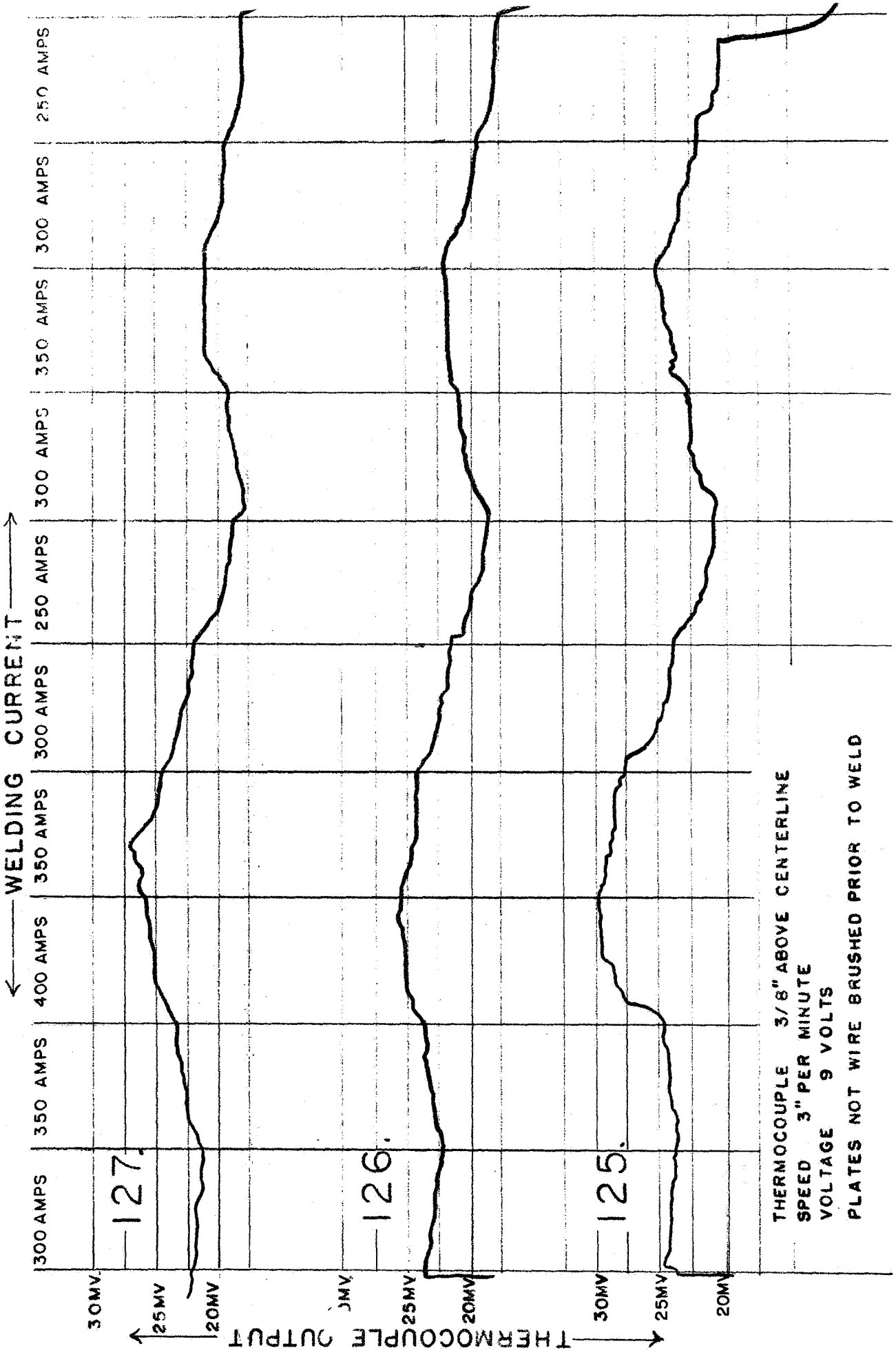


Figure 32: Thermocouple output versus current variation, uncleaned plates.

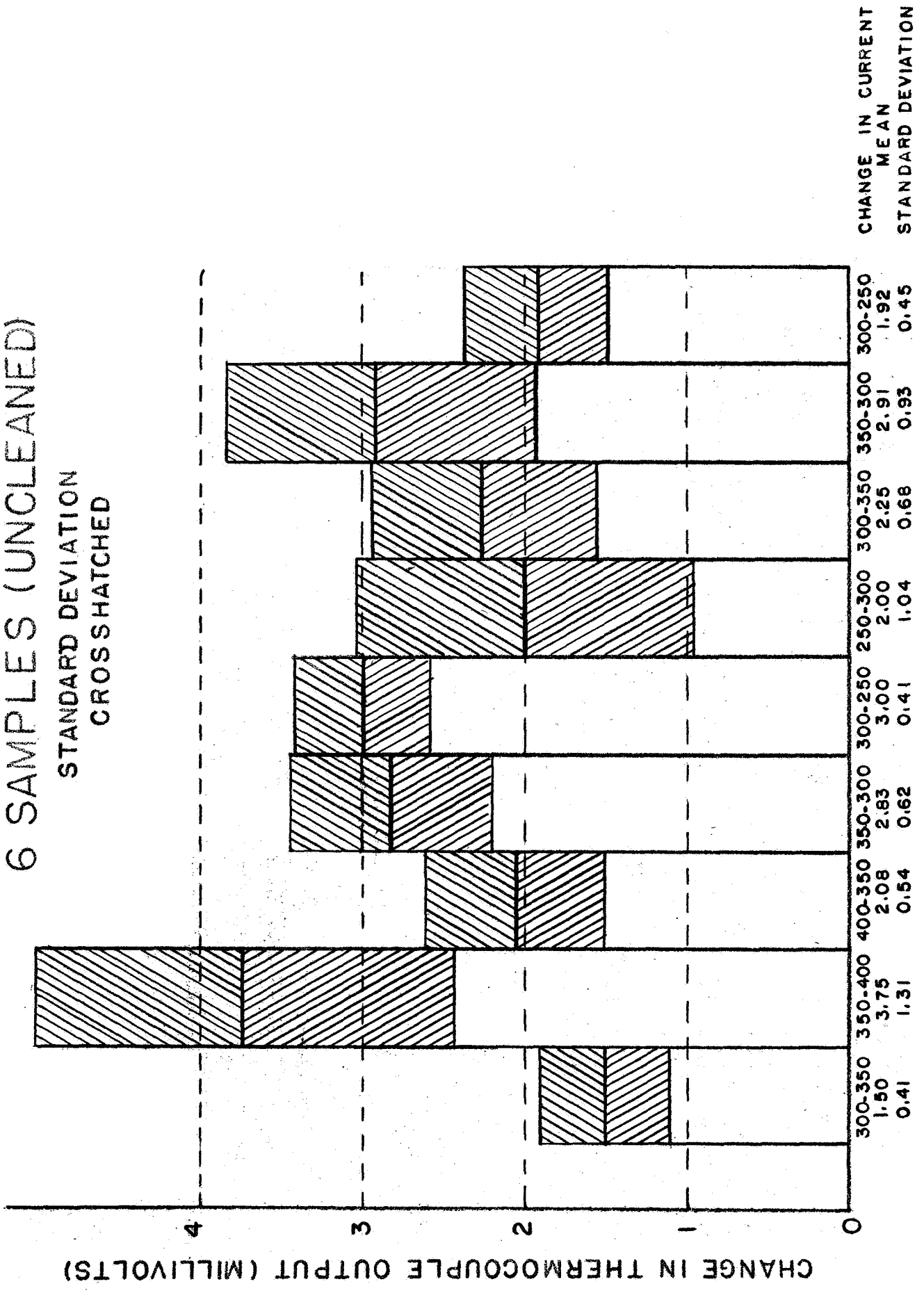


Figure 33: Average change in thermocouple output versus current variation, uncleaned plates.

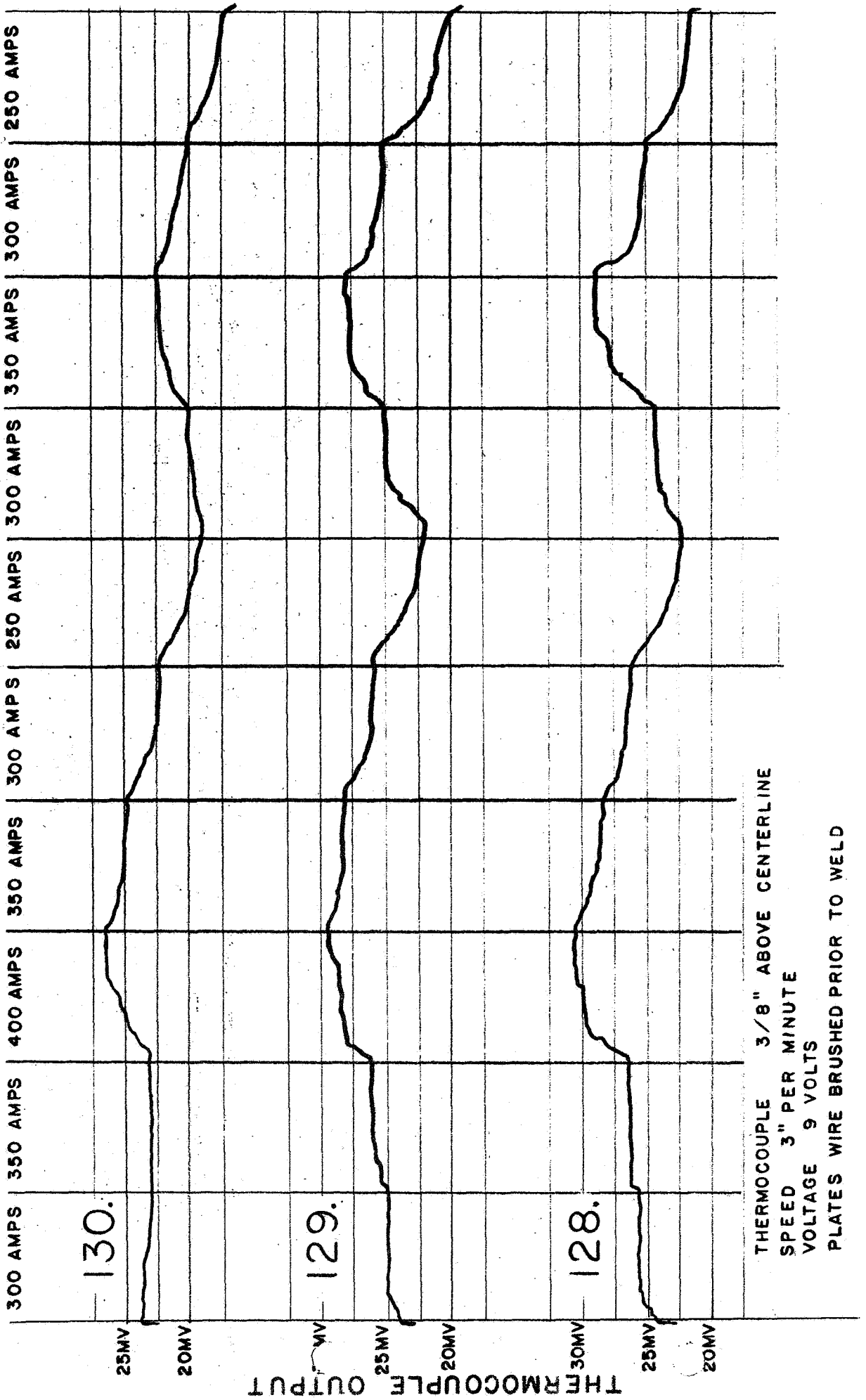


Figure 34: Thermocouple output versus current variation, plates wire brushed prior to weld.

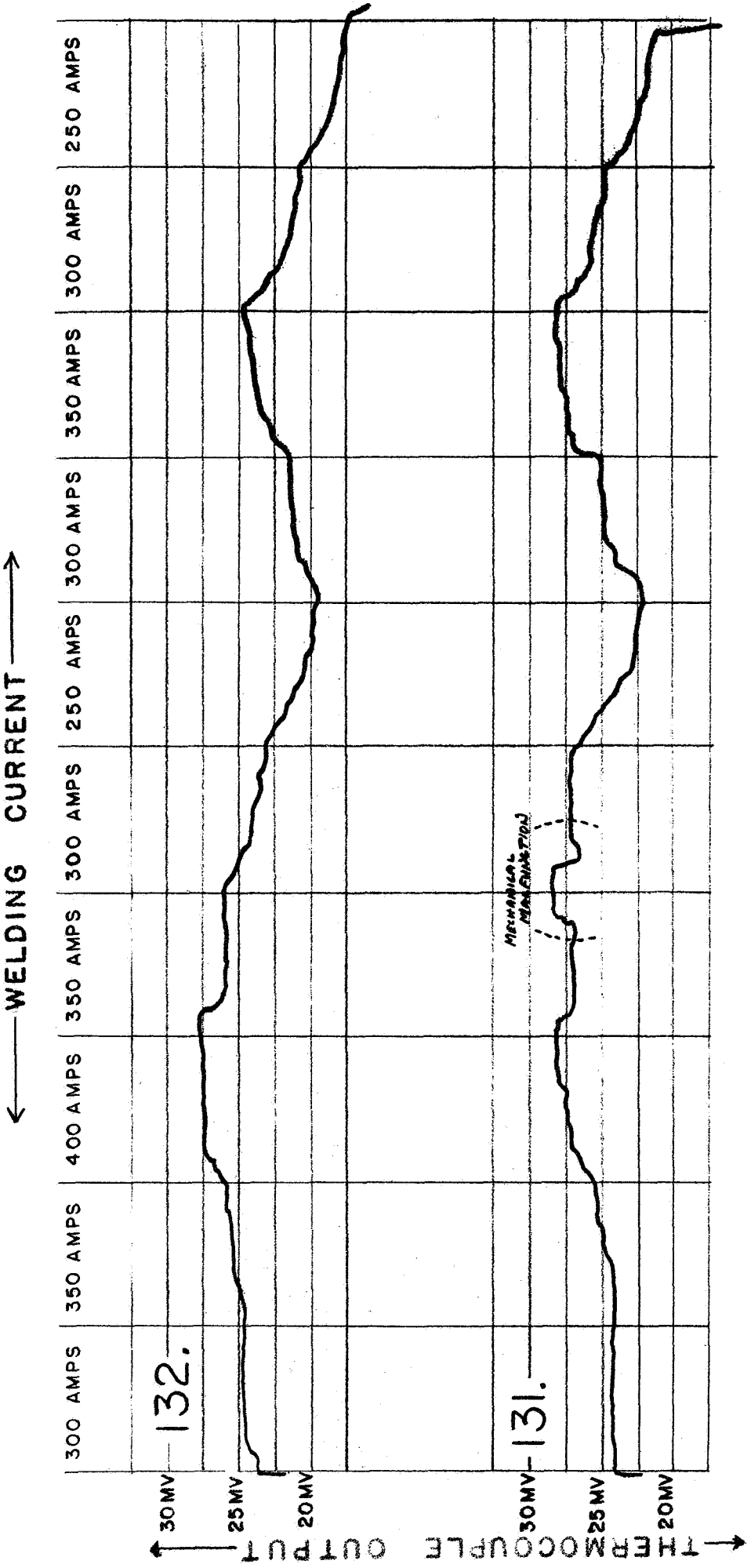


Figure 35: Thermocouple output versus current variation, plates wire brushed prior to weld.

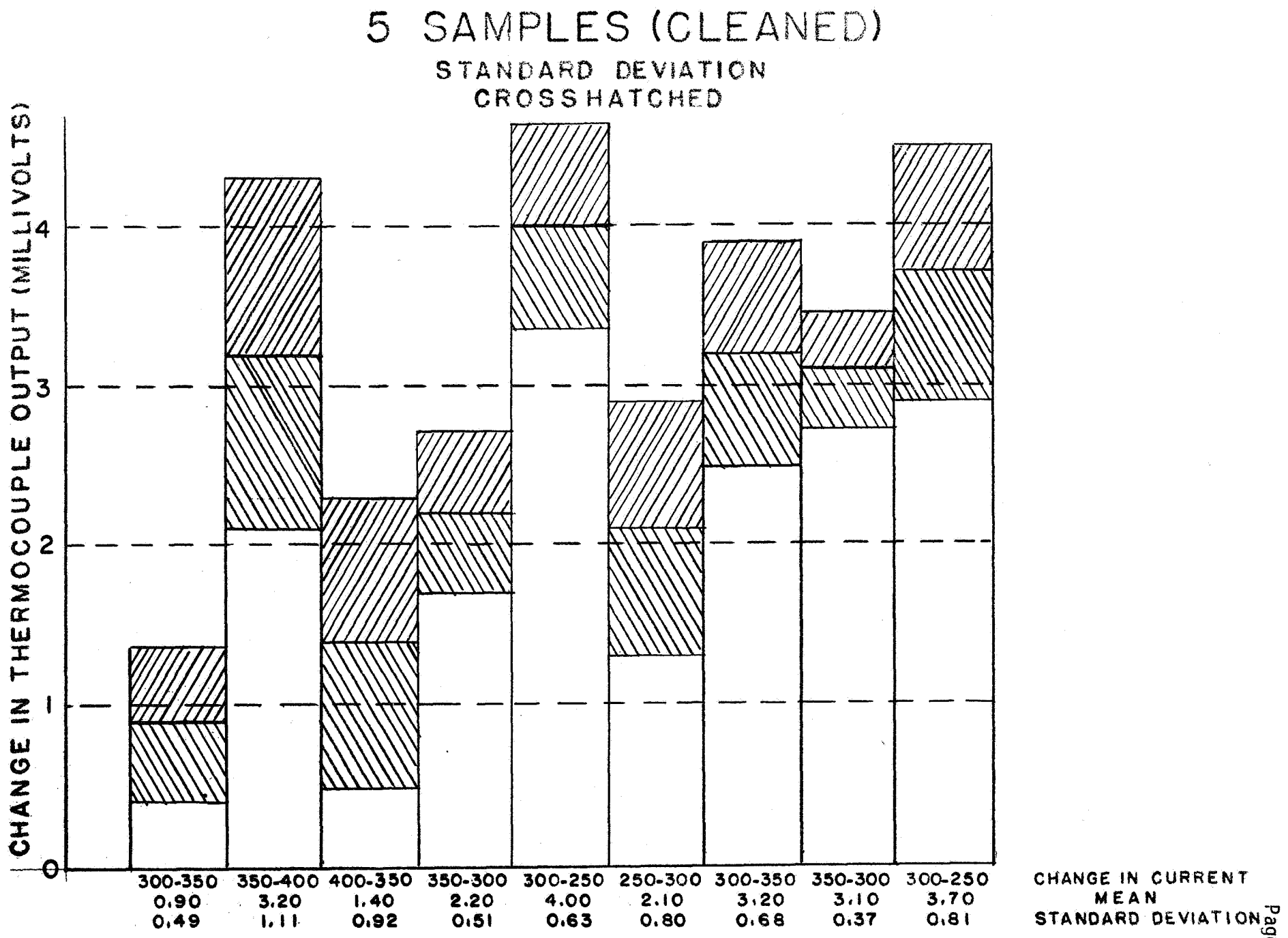


Figure 36: Average change in thermocouple output versus current variation, plates wire brushed prior to weld.

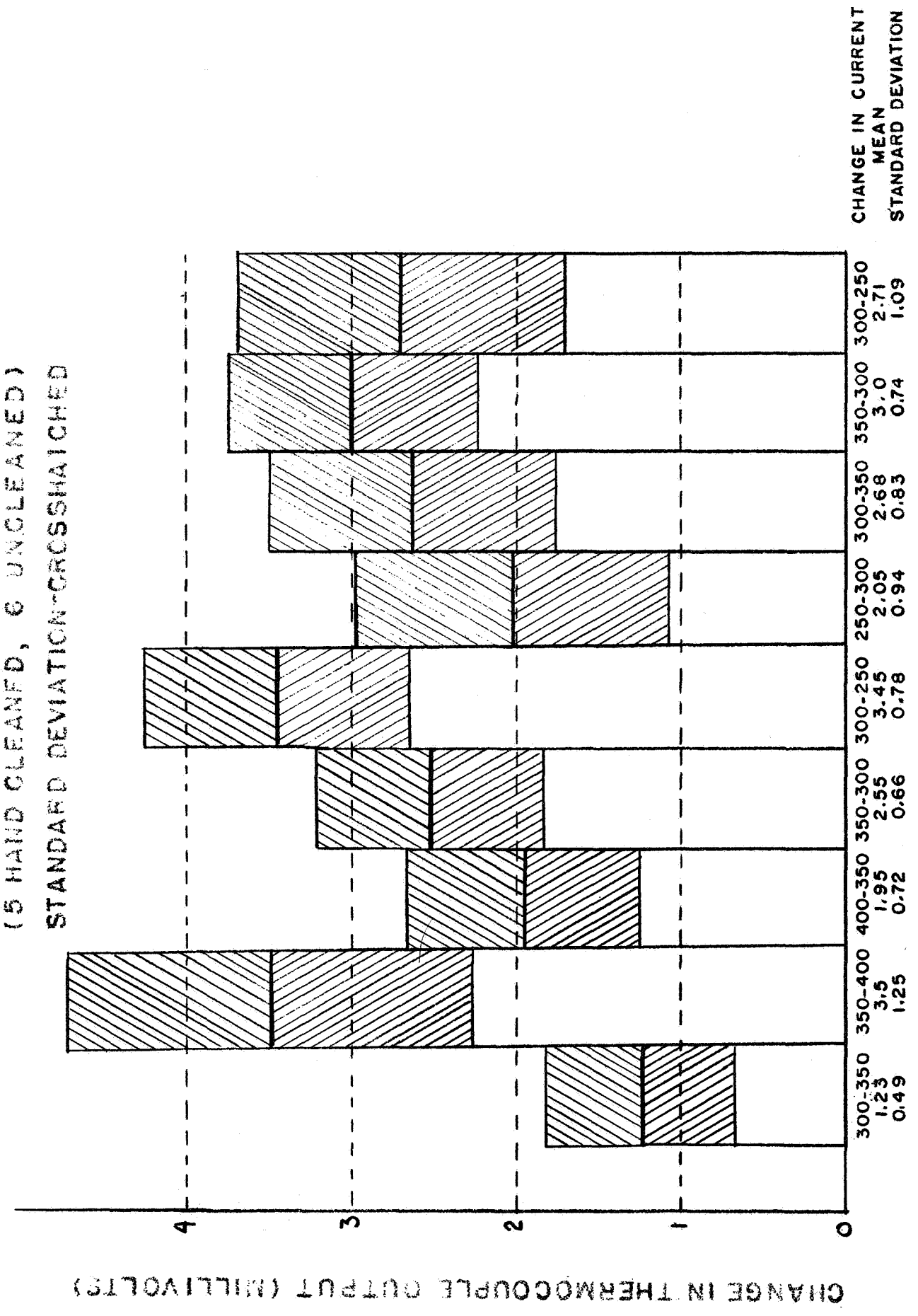


Figure 37: Average change in thermocouple output versus current variation, cleaned and uncleaned plates.

(3). The standard deviation about the mean for eleven samples was not appreciably different than that for five or six samples. This indicates that the number of samples taken was adequate, and that it is very difficult to repeat welds because of the many varying conditions.

3.1.3.4 HEAT GRADIENT FROM FRONT TO BACK SIDE OF TEST PANEL

3.1.3.4.1 In this series of tests three thermocouples were stationed at fixed locations on the back side of the test weld. The thermocouples were placed 4 inches apart with the first one 4 inchest from the weld start. The first thermocouples was positioned 3/8" above the centerline of the torch, the second 1/4" above, and the third on the centerline of the torch. The results of these tests are given in the table below. The recording of the thermocouple outputs for this test is given in Figure 38.

Thermocouple output in mv.

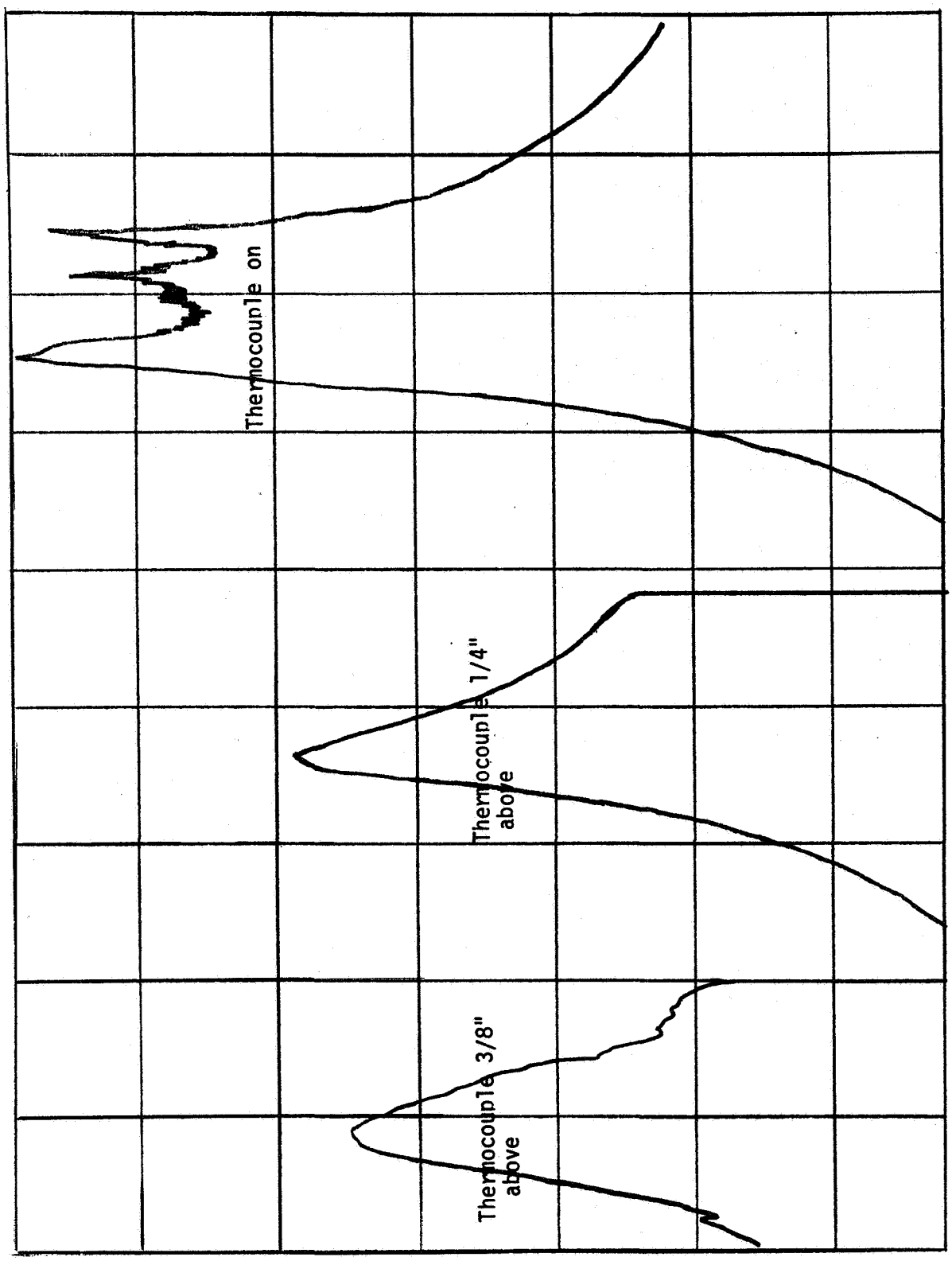
Thermocouple Position	Ahead	2"	1"	1/4"	Arc	1/4"	1"	2"	Behind
3/8" Above Centerline		12.0	19.0	28.5	30.0	28.7	24.5	--	
1/4" Above Centerline		8.5	15.0	29.0	31.7	29.3	24.0	--	
On Centerline		9.0	17.5	X	X	X	X	X	

"X" - Thermocouple in Puddle.

3.1.3.4.2 The above test was repeated with the three stationary thermocouples positioned in the front side of the test panel. The results are summarized in the table below, and the thermocouple recordings are given in Figure 39.

Thermocouple Output in mv.

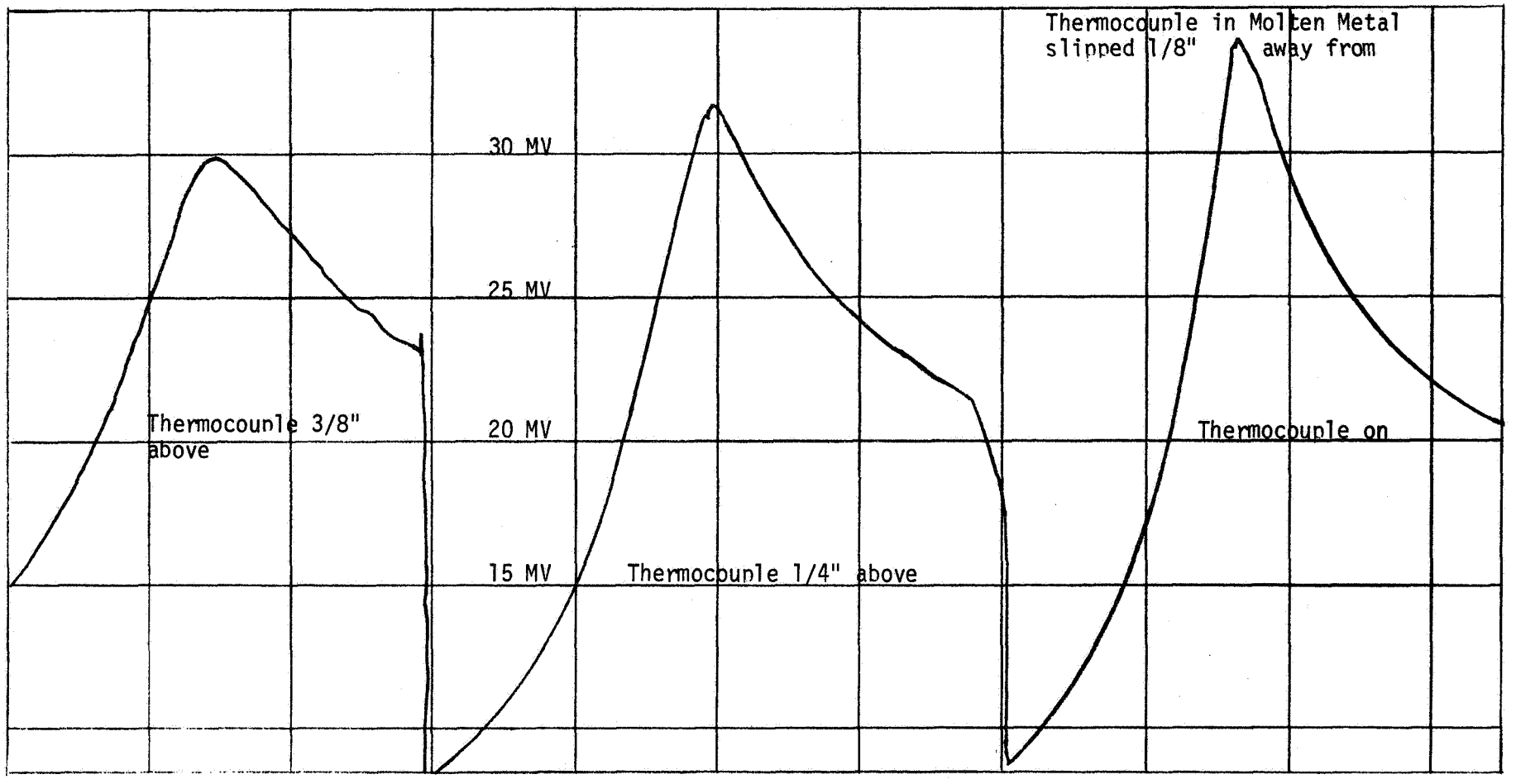
Thermocouple Position	Ahead	2"	1"	1/4"	Arc	1/4"	1"	2"	Behind
3/8" Above Centerline		--	17.0	31.5	32.0	28.0	20.0	X	
1/4" Above Centerline		7.0	13.0	28.0	34.5	30.5	23.0	-	
On Centerline		6.5	13.0	X	X	X	-	-	



SAMPLE #232

Voltage 9 1/2 volts
Amperage 320 amps
Speed 3 ipm

Thermocounles were snaced 4" anart from each other and on the front of the nlate. Chart sneed was 3 ipm.
Figure 38: Heat Gradient Test



SAMPLE #231

Voltage 9 volts
Current 320 amps
Speed 3 ipm

Thermocouples were on the back side of the plate. Chart speed was 3 ipm. Thermocouples were 4 inches apart.

Figure 39: Heat Gradient Test

3.1.3.5 INSULATION OF TEST PANELS

With the fixturing system described previously, pronounced heat sink differences occurred along the length of the test panel. In addition these heat sink conditions varied as a function of the eccentricity of the test panel, the pressure of the clamps, the physical positioning of the panel, etc. Since these varying heat sinks made it difficult to evaluate the stability of the thermocouple output, fibe glass strips were used to insulate the test panel from the fixture.

When the test panels were insulated from the workpiece it was possible to maintain relatively consistent penetration over the entire length of the panel with welding parameters maintained constant. With this condition established, it was then possible to add heat sinks or vary one or more weld parameters and be assured that the corresponding variation in thermocouple output was a result of the system parameter so changed.

3.1.3.6 STABILITY OF THERMOCOUPLE OUTPUT

Several tests were run with all parameters maintained constant, as follows: welding current = 185 amperes, voltage= 10 volts, travel speed = 4.5 inches/minute, and speciman dimension = 6" X 24" X 1/4". The difference between the thermocouple output voltage and a highly stable reference voltage was recorded on a fast response Sanborn recorder for each test-run (see Figure 40). The reason for recording this difference signal rather than the thermocouple output directly was that by recording the difference between the thermocouple output voltage and a voltage equal to its average value, only the deviation in thermocouple output would be plotted. This allowed the recorder scale to be expanded so that even slight deviation in thermocouple output would be detected.

The procedure for running each test was as follows: The arc was initiated and after full penetration was developed, the travel was begun. After approximately 1 1/2 inches of weld had been made, the reference source (see Figure 40) was adjusted until the digital voltmeter read zero. At this time the strip chart

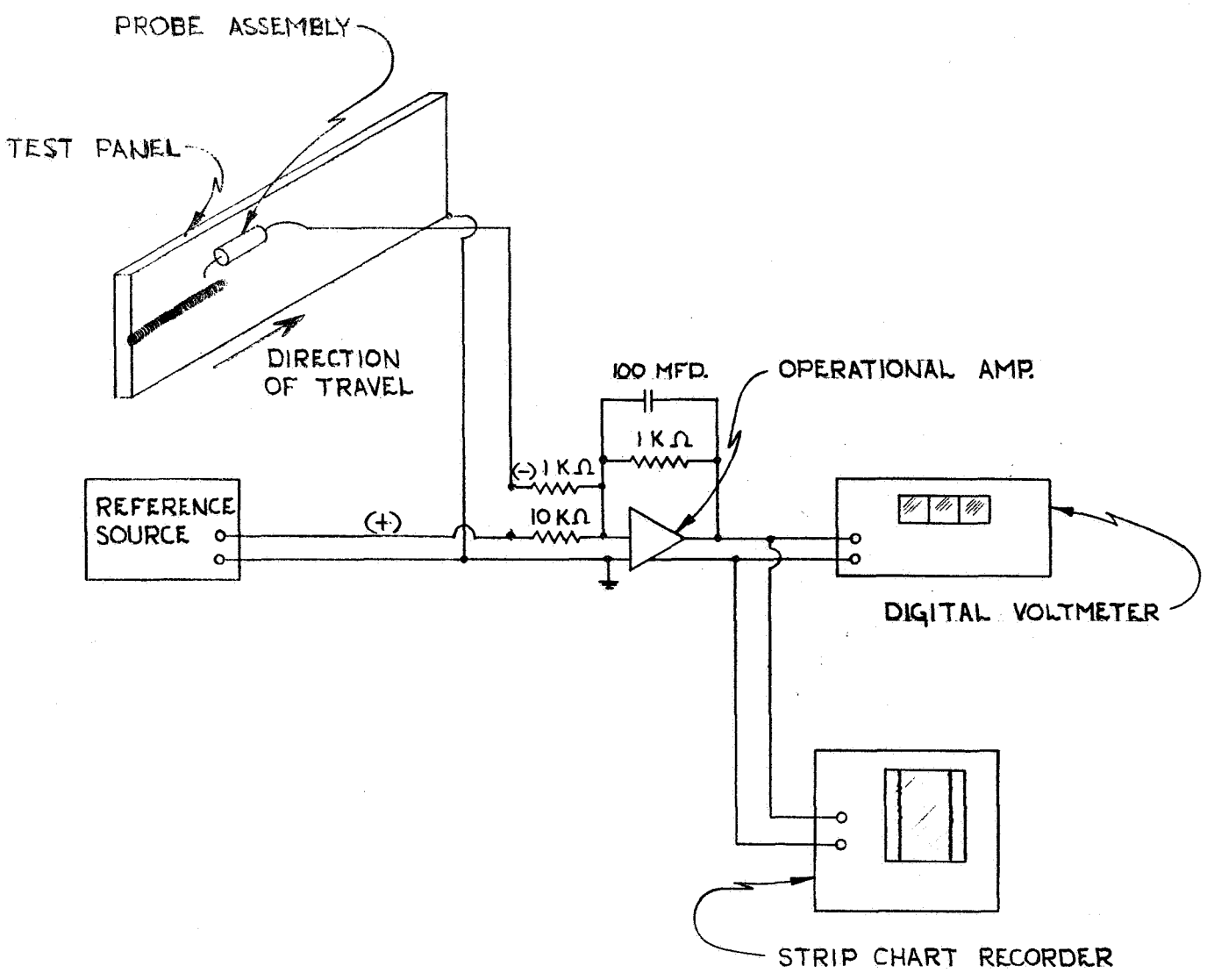


Figure 40: Instrumentation for thermocouple stability tests.

recorder was switched-in. After this, any deviation of the thermocouple output voltage from the set reference source value was recorded. Referring to Figure 40, it is seen that a 100 mfd. capacitor was connected across the feedback capacitor of the operational difference-amplifier. The purpose of this capacitor was to partially reduce the noise inherent in the thermocouple output signal. The capacitor introduces a time constant in the amplifier of 0.1 seconds, which was assumed negligible in the speed of response measurements (See section 3.1.3.7).

Test plates were run with the probe positioned at three different points with respect to the electrode. A discussion of the results for each location follows:

3.1.3.6.1 Probe Position Number One

In the first series of tests the probe was positioned 5/16 inches above the centerline of the electrode and 3/32 inch in front of the electrode. On each test panel welded under these conditions, penetration was visually consistent over the entire length of the panel. The thermocouple output, however, varied approximately 3.0 millivolts peak-to-peak, and was highly irregular and unpredictable.

3.1.3.6.2 Probe Position Number Two

In the second series of tests the probe was positioned exactly 5/16 inches above the centerline of the electrode. On these tests the penetration was again visually consistent. The thermocouple output varied approximately 2.5 millivolts peak-to-peak.

3.1.3.6.3 Probe Position Number Three

In the third series of tests the probe was positioned 5/16 inches above the centerline of the electrode and 3/32 inches behind the electrode. Penetration was consistent, and the thermocouple output voltage varied by only about 0.5 millivolts peak-to-peak.

3.1.3.6.4 Discussion of Results

An explanation of the above results can be hypothesized by studying a typical set of isotherms that exist around a moving

puddle. A set of isotherms are shown in Figure 41 for the conditions: travel speed = 33 inches per minute, voltage = 14 volts, weld current = 165 amperes, and plate thickness = 1/8 inch (See "Infrared Temperature Sensing Systems for Automatic Fusion Welding", Welding Journal, May, 1958, page s210). This set of isotherms was determined for different conditions than those tests discussed above, however, the general configuration is typical of any moving molten puddle.

As can be seen, the isotherms are extremely close together either directly above the electrode or above and offset toward the front of the electrode. Thus if the probe is positioned in either of these two positions, the thermocouple output will change appreciably if even a slight change occurs in the physical position of the probe. Small deviations in the physical position of the probe can occue due to tolerances in the mechanical probe assembly or due to voltage changes.

Again referring to Figure 41, it can be seen that the isotherms are more spead out above the electrode and offset toward the rear. This explains why the third set of tests discussed in section 3.1.3.6.3 resulted in less deviation in the thermocouple output than the previous two.

3.1.3.6.5 Conclusions

It was concluded that some limitations may be imposed on the position of the probe with respect to the very steep temperature gradient regions. The results of the three positions discussed in section 3.1.3.6.4 show that for best stability the probe should be offset behind the electrode. However, this location is not desirable if excessive lag time occurs in the correction of changingheat sink conditions.

All three sets of experiments discussed in section 3.1.3.6.4 were conducted with the probe positioned 5/16 inches above the electrode and offset either to the front or rear. The isotherms in Figure 41 indicate that if the probe were positioned higher above the electrode it might be possible to offset it toward the front

and still be in a relatively stable region of the isotherm pattern. However, with the probe positioned higher above the electrode, it becomes less sensitive to heat sink variations beneath the weld bead. Conversely, the further the probe is positioned above the electrode the more likely it is to give false indication of heat sink conditions above the weld bead. For instance, it could conceivably indicate a heat sink variation that would not be indicative of the weld bead area.

For correction of heat sink variations, the most desirable location of the thermocouple probe would be directly in front of the molten puddle and as close to it as possible. From the standpoint of stability, however, the isotherm pattern immediately in front of the molten puddle (See Figure 41) is very closely spaced which is the condition that leads to poor stability. It should be noted, however, that for slower travel speeds and thicker materials, the isotherm pattern will be more spread out around the molten puddle than that shown in Figure 41.

Summarizing, the optimum location of the probe for most stable output is in the more gradual steeping gradient regions about the puddle, while the most optimum location for correction of varying heat sink conditions is as close to the molten puddle as possible. Thus two conflicting objectives exist and a compromise is necessary.

3.1.3.7 RESPONSE SPEED OF HEAT TRANSFER IN ALUMINUM PANEL

Several tests were run to determine the speed of response of the heat transfer in the aluminum test panel. The welding parameters were set as follows: starting value of weld current = 180 amperes, voltage = 10 volts, travel speed = 4.5 inches per minute, and specimen dimensions = 6" X 24" X 1/4". The setup was identical to that shown in Figure 40 however, in these tests the current was varied in steps so that the speed of thermocouple correction could be measured. The probe positioning was identical to that in section 3.1.3.6.3.

A representative sample of these tests is shown in Figure 42. The chart speed was set at 1 mm per second as indicated by the

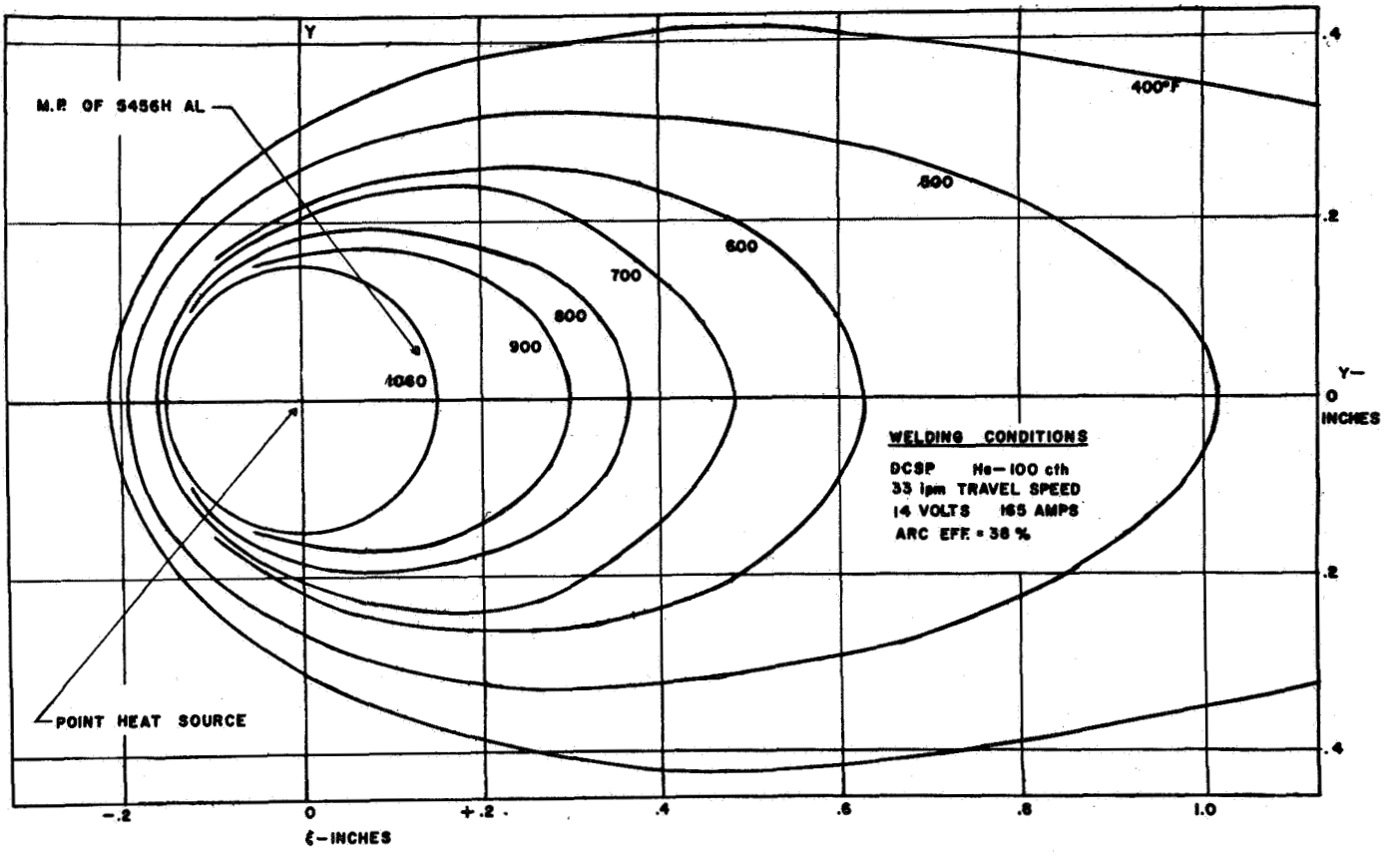


Figure 41: Typical set of welding isotherms.

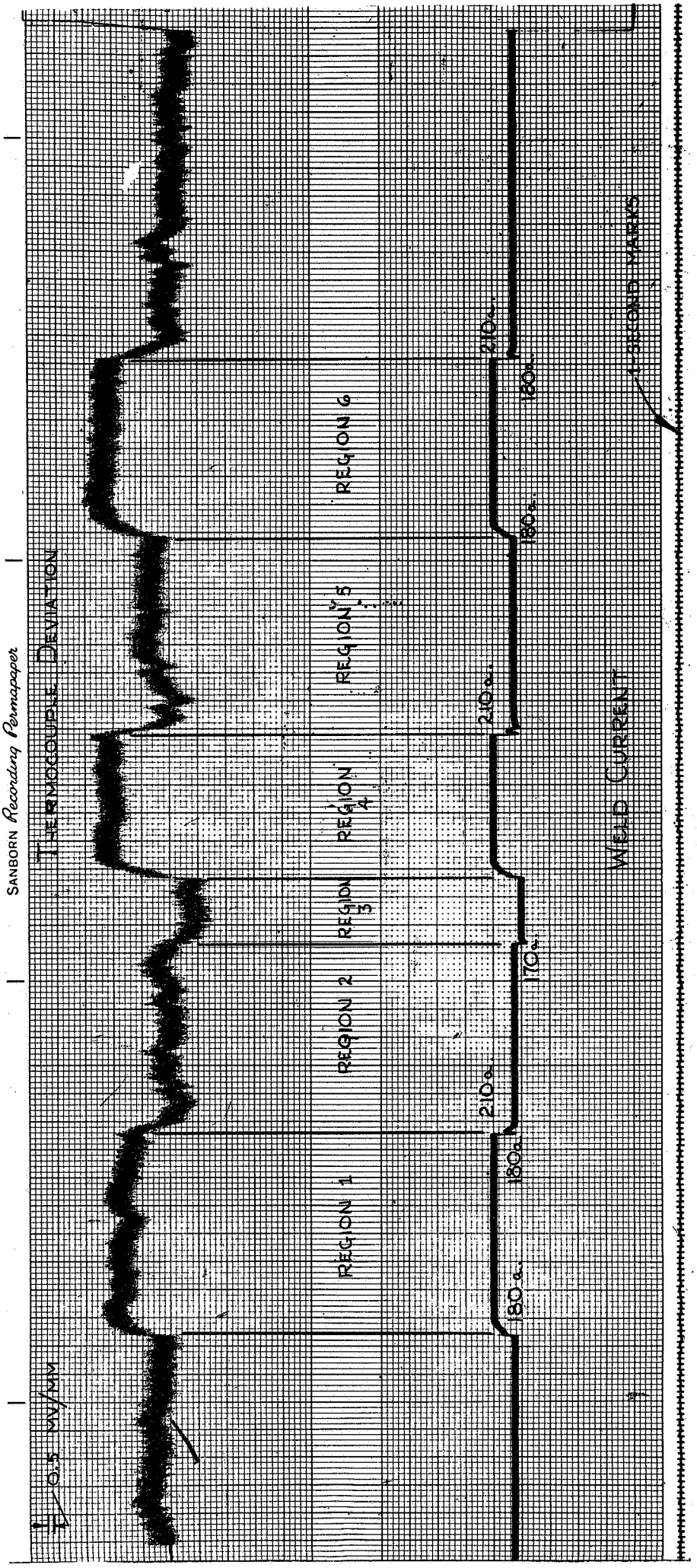


Figure 42: Response speed tests.

1-second marks on the recording. The recorder sensitivity for the channel recording the thermocouple deviation was set at 0.5 mv/mm. The weld current was varied by manually adjusting the 10-turn weld current dial on the power source from one value to another. Except for region 3, the weld current was varied between 180 and 210 amperes in all cases.

Referring to Figure 42, it can be seen that in all cases when the current was increased from 180 amperes to 210 amperes, the corresponding response in thermocouple output was almost instantaneous. However, when the weld current was decreased from 210 amperes down to 180 amperes, the thermocouple deviation lagged by approximately 1.0 to 2.0 seconds.

3.1.3.7.1 Discussion of Results

Since the thermocouple deviation was almost instantaneous for current increase from 180 to 210 amperes, it can be concluded that the speed of response of heat transfer through the aluminum panels is very fast. The reason that the thermocouple deviation lagged behind changes in current from a high value to a low value can be explained as follows: In all of the tests that were conducted, the aluminum test panels were insulated from the fixture by fiber glass strips. Thus the panel was very nearly "floating" as far as thermal conduction to other material was concerned (metal clamps were still contacting the panel; however, the point of contact was very small). Thus heat added to the panel (increase in current) resulted in a nearly instantaneous thermocouple output deviation due to the fast thermal response of the aluminum, however, when the heat input was reduced the thermocouple output response was slow due to the fact that the heat already in the panel had no convenient place to go. Heat conduction from the plate through the fiber glass insulation was small due to the low thermal conductivity of the fiber glass; conduction through the metal clamps was small due to the small contact area; and conduction of heat away from the plate by radiation was small due to the low thermal emissivity of

the aluminum panels.

It should be emphasized that the thermal lag in going from a high value of current to a low value of current is not necessarily detrimental. If the penetration has the same time lag as the thermocouple output then we would conclude that the system is responding exactly as desired; i.e., a direct relationship between penetration and thermocouple output. It is difficult to determine if the penetration was, in fact, lagging also since for a welding speed of 4.5 inches per minute, one second corresponds to only 0.075 inches of travel.

3.2 BACKSIDE SENSING

3.2.1 MODIFIED, INTRINSIC THERMOCOUPLE CONTROL FROM BACK SIDE OF WELD PLATE

3.2.1.1 In Memo No. R-ME-ME-198-64, the possibility of using one thermocouple wire placed in an insulated backup bar to produce a signal by contacting the molten metal was suggested. The paragraphs including this suggestion from Mr. Wm. McCampbell of NASA and Detail A which shows the emplementation of this suggestion are shown in Figure 14, section 2.2.2.

3.2.1.2 The first experiments run to determine the feasibility of the above method were to see if the thermocouple wire would adhere to the molten metal. Three thermocouples were affixed to the back of the plate which was to be welded. The setup is shown in Figure 43. None of the thermocouples stuck to the molten aluminum, although they did get red hot and mark the weld. Thermocouple No. 2 was forced against the plate with a screwdriver and still it did not stick to the weld puddle.

3.2.1.3 This experiment was to determine the effect of parallel thermocouples. A thermocouple of iron-constantan was made and affixed to one end of an aluminum plate. Using the same thermocouple wires, another thermocouple was made and affixed to the center of the aluminum plate. This test setup is shown in Figure 44.

TEST SAMPLE X271

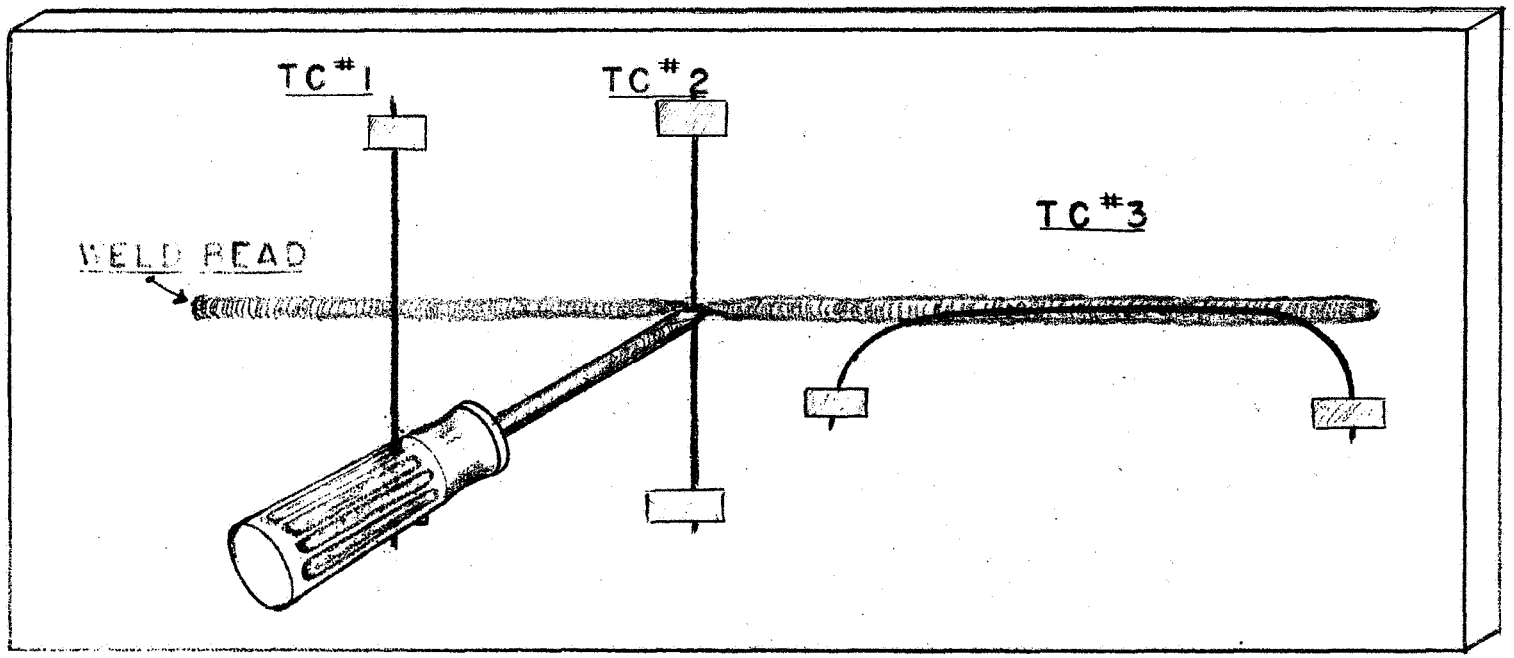
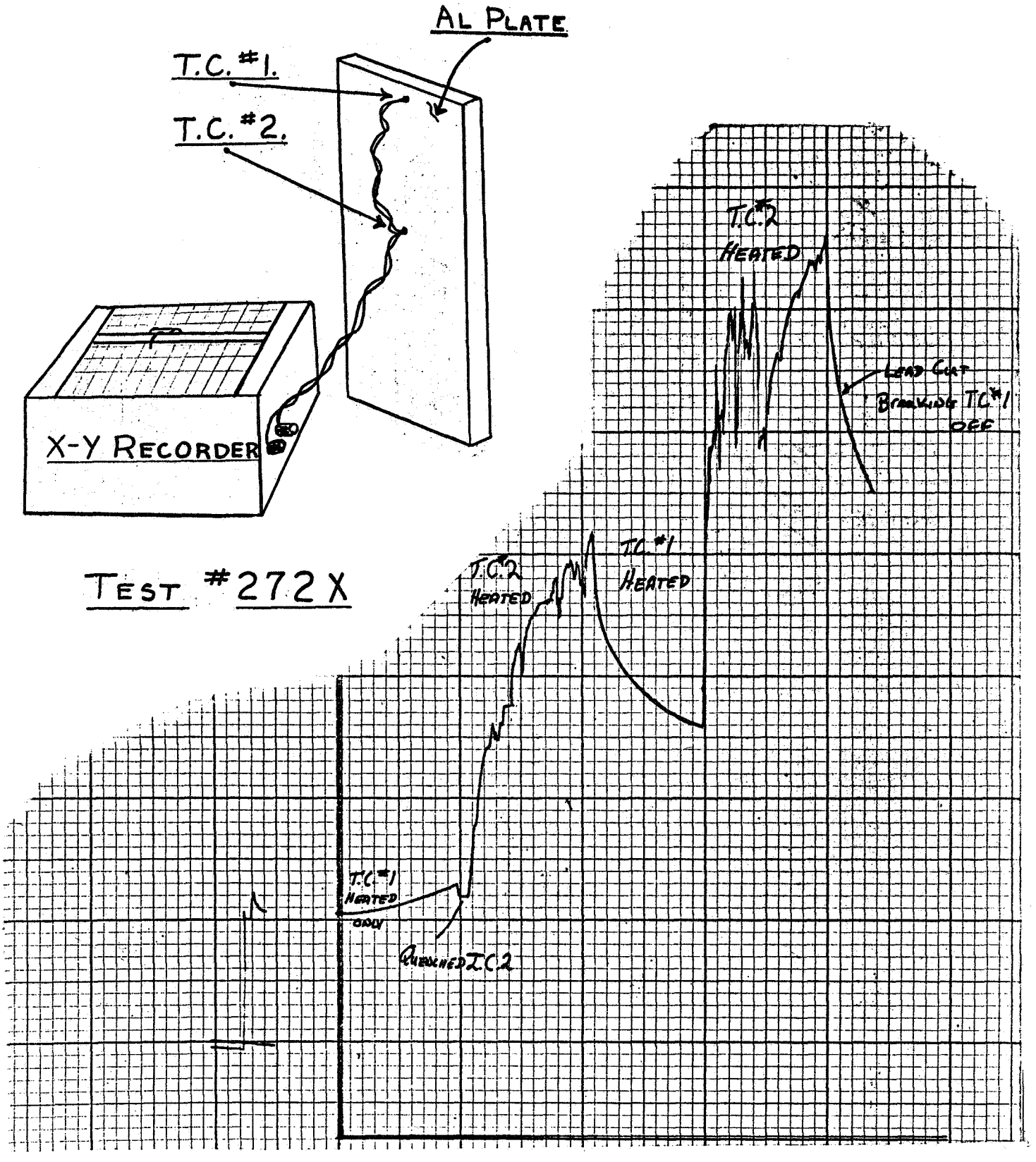


Figure 43: Experiment to determine if intrinsic thermocouple would adhere to molten aluminum.



TEST NO. 272X

Test Consisting of Two Thermocouples Swagged In An Aluminum Plate And Alternately Heated With An Acetylene Torch

FIGURE 44

Figure 44: Parallel thermocouples.

3.2.1.3.1 The two thermocouples were alternately heated and the output was monitored on the Moseley X-Y Recorder.

3.2.1.3.2 The first thermocouple had no effect on the output. The only thermocouple which actually gave an output was the one closest to the recording instrument.

3.2.1.4 The experimental setup of the second test run is shown in Figure 45. The distance from the hot junction to cold junction is "d". This distance was varied to simulate different loading effects on the hot junction. The hot junction was formed by twisting the iron and constantan thermocouple wires together. Two series of tests were run; one in which a single twisted turn was used to form the hot junction and a second in which a multiple turn twist was used, providing more contact area. With both series of tests, for a fixed distance d, readings were taken on the digital voltmeter with the cold junction open circuited and then closed. The results are listed below:

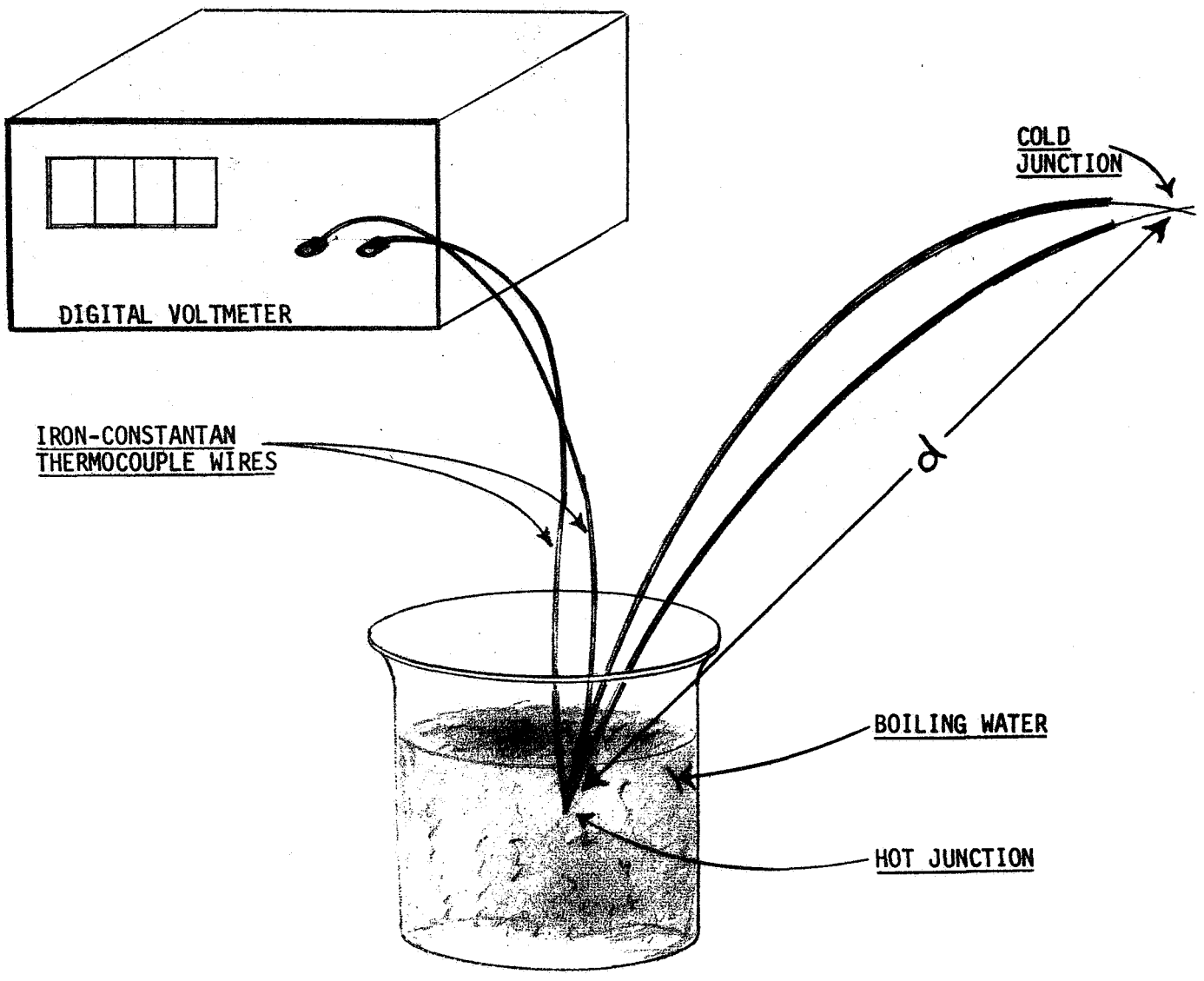
HOT JUNCTION FORMED WITH SINGLE TWISTED TURN

	Distance d		
	31"	8"	4"
Cold Junction Open	3.95 mv	3.85 mv	3.85 mv
Cold Junction Closed	3.85 mv	2.85 mv	2.65 mv

HOT JUNCTION FORMED WITH MULTIPLE-TURN TWIST

	Distance d		
	31"	8"	4"
Cold Junction Open	3.85 mv	3.90 mv	3.87 mv
Cold Junction Closed	3.84 mv	3.90 mv	3.87 mv

FIGURE 45: EXPERIMENT TO DETERMINE THE EFFECT OF LOADING ON THERMOCOUPLE JUNCTION



The second set of data listed above indicates that in an actual weld setup, where the thermocouple junction is continuous, the thermocouple output will be indicative only of the temperature at, and very close to, a point at the molten puddle.

3.2.1.5 In order to simulate more closely the actual weld setup, a third experiment was run. In this experiment a constantan thermocouple wire was attached to one end of an aluminum test panel immersed in a container of boiling water. The test setup is shown in Figure 46. The thermocouple output was read continuously with the digital voltmeter as indicated. The electrically insulated rod shown in the figure was used to wedge the free end of the constantan wire firmly against the aluminum panel; it then being progressively moved from point A toward Point C. The digital voltmeter reading did not change until Point B moved out of the boiling water; at this point the reading dropped and progressively sloped downward as Point B moved toward the cool end at Point C.

These results indicate that the temperature at Point B was being measured and that this reading was independent of the varying junction between Points A and B.

This experiment was repeated, but with Point C immersed in the boiling water and Point A out of the water. With the insulating rod again moving progressively from Point A to Point C, the digital voltmeter reading gradually increased until Point B entered the Boiling water; at which point the reading remained constant until Point C was reached. Thus, these results also indicate that the temperature at Point B was being measured.

3.2.1.6 In conclusion the tests described above indicate that in an actual weld setup, as shown in Figure 47, the thermocouple output will be indicative of the temperature at Point B which moves progressively with the torch tip motion.

3.2.1.7 INVESTIGATION OF INSULATING MATERIALS TO INSULATE THERMOCOUPLE WIRE FROM GROOVE OF BACKUP BAR

3.2.1.7.1 Mr. William Moore of 3M Tape Division was contacted first. He stated that they did manufacture a plutonium tape

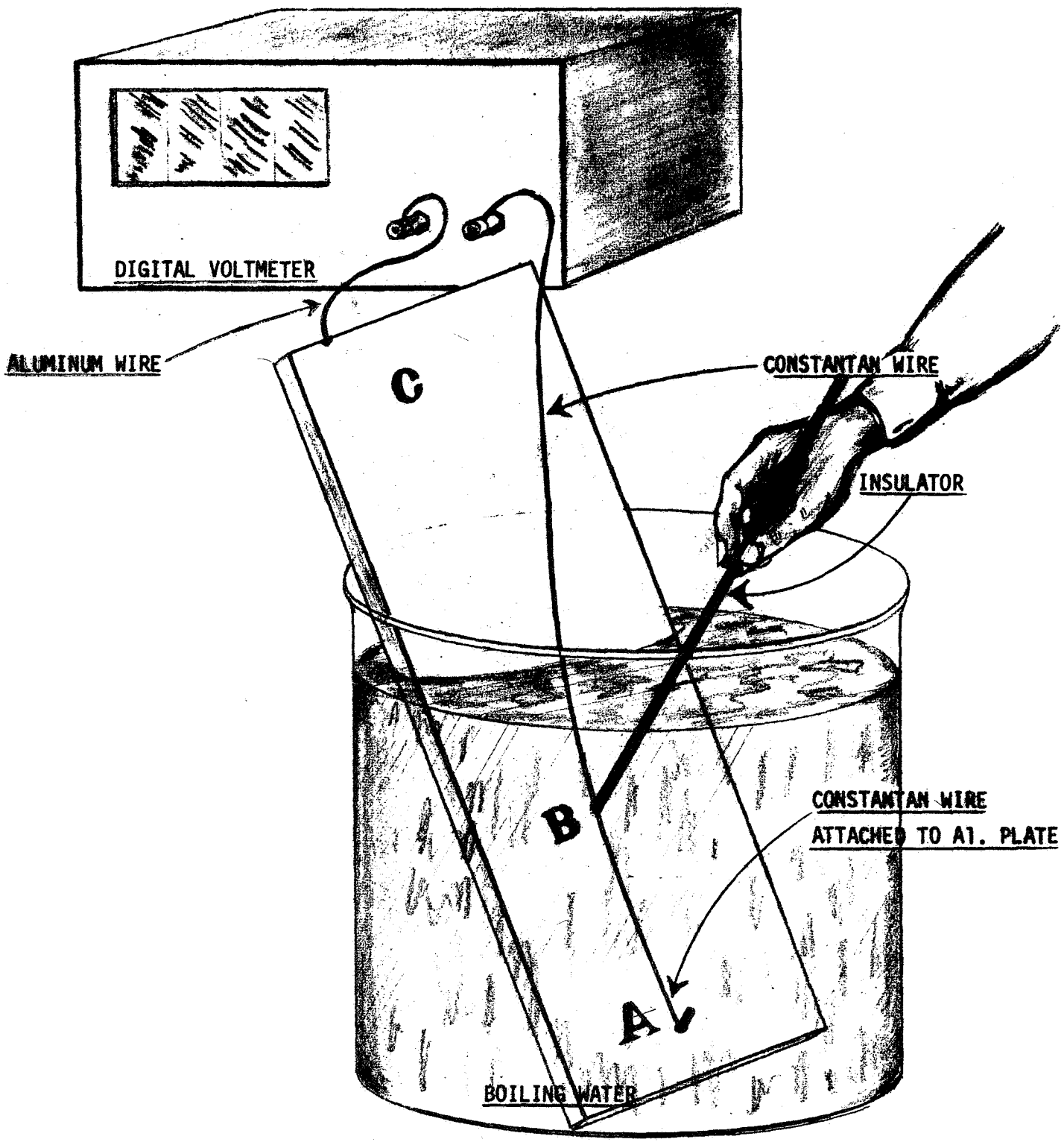


Figure 46: Simulation of backside intrinsic thermocouple method.

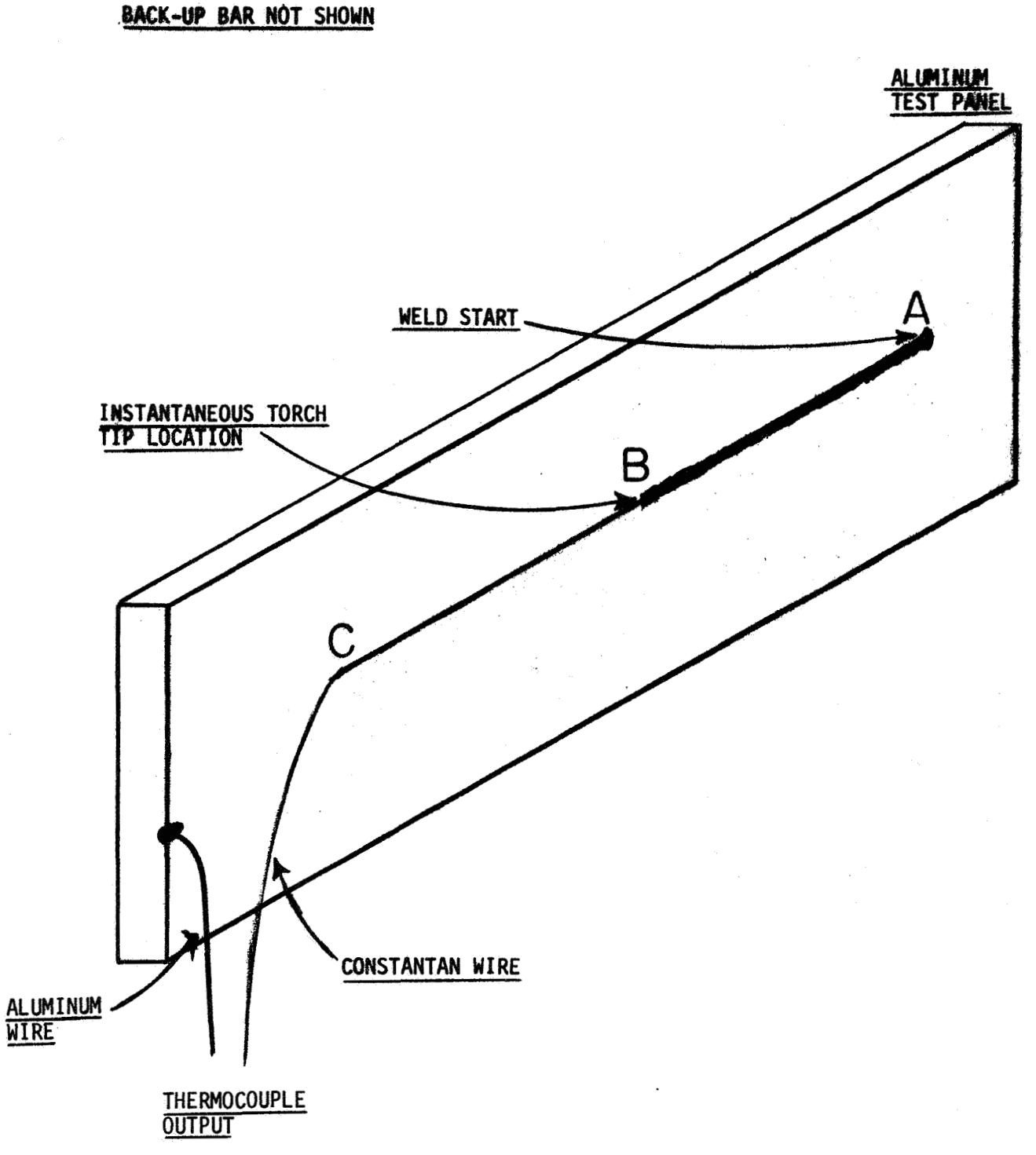


Figure 47: Backside sensing, intrinsic thermocouple.

which was covered with an aluminum reflective tape, but that they did not have anything else which would operate in a high temperature range.

3.2.1.7.2 The Dupont Company was contacted to determine the availability of teflon sprays. They stated that they did not manufacture a spray compound, and that teflon would not withstand temperature as high as needed.

3.2.1.7.3 A Sales Engineer for the Breeding Insulation Company was contacted and he stated that they had nothing available that operated above 1000^{o}F. The Breeding Insulation Company are local distributors for the Philip Carey Company, Owens-Corning Company, Aerocor, and Pittsburgh-Corning.

3.2.1.7.4 Mr. Goff of A. P. Green Firebrick Company was contacted, and he stated that he did have an adhesive that was used to secure firebrick and that this might be useable. One gallon of this adhesive was obtained and the V-groove in an aluminum backup bar was coated with it. When the test weld was performed, the adhesive decomposed, giving off a gas which blew the molten aluminum out the front of the plate.

3.2.1.7.5 In addition to the above adhesive insulation, and alumina-hydrate, sodium-silicate mixture was used in an experiment. Again, however, the mixture decomposed, producing a gas which blew through the weld from the backside.

3.2.2 EXPERIMENTS WITH MAGIC WIRE SENSING

3.2.2.1 The purpose of the first experiments conducted was to determine the relationship between temperature and magic wire output voltage, and to determine whether the output of the magic wire indicated temperature at the closest point to the output leads or the hottest point in the line.

3.2.2.2 Two aluminum blocks were used with iron-constantan thermocouples imbedded in them. The magic wire was clamped to each block, allowing about 3.5 feet of wire between the blocks. The blocks were labeled A and B for identification. The block at the extreme end of the magic wire was designated A, and the block nearest the output end was designated B (see Figure 48).

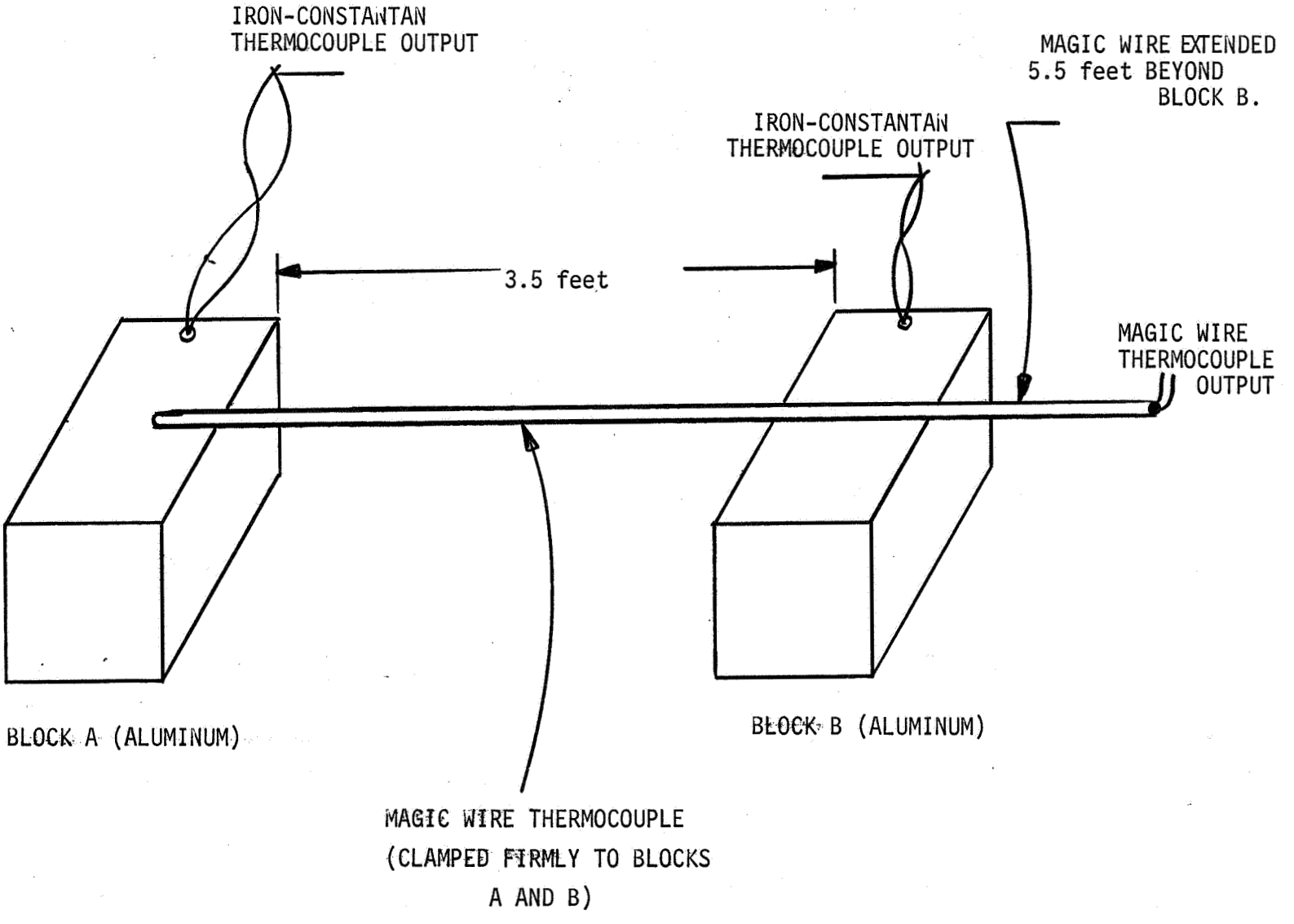


Figure 48: Magic Wire Thermocouple Experiment

3.2.2.3 Before the experiment was begun, both blocks were placed in the same heating area and allowed to heat until they reached equilibrium. At that point, each iron-constantan thermocouple was approximately 12.0 millivots (400^{o} F). This indicated that an accurate reading was being obtained from both of the iron-constantan thermocouples.

3.2.2.4 For the magic wire experiment, block B was heated until equilibrium was reached with an iron-constantan thermocouple output of 12 millivolts (400^{o} F). At this point a reading of 8.5 millivolts was recorded on the output of the magic wire. This reading intermittently dropped to 4.5 millivolt. This drop was attributed to a partial short in the magic wire. The 8.5 millivolt reading was translated on a thermocouple calibration chart to be equivalent to 400^{o} F. At this point a reading of 0.05 millivolts was recorded on the iron-constantan thermocouple output at block A. Block A was then heated until its output (via the iron-constantan thermocouple) was 31.0 millivolts. The heat was then removed, and recordings were made of : (1) the magic wire output, (2) the iron-constantan thermocouple at block A, and (3) the iron-constantan thermocouple at block B. The readings taken are listed below. A plot of magic wire output versus block A output is shown in Figure 49. Block B output remained at 12.0 millivolts for the entire series of tests.

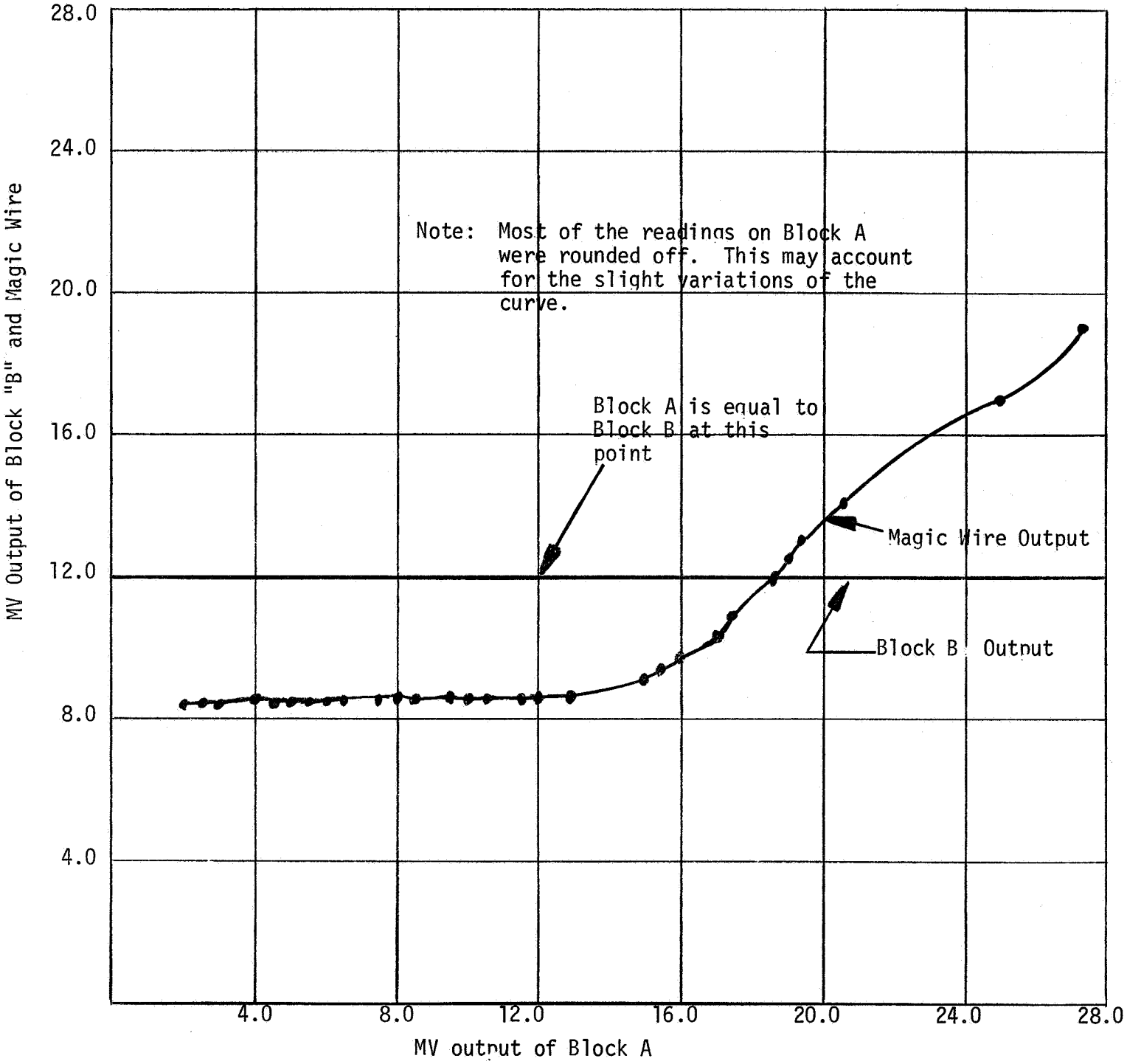


Figure 49: Magic wire temperature response.

Block A (Iron-Constantan Thermocouple Output)	Magic Wire Output
27.0 millivolts	19.0 millivolts
25.0	17.0
20.5	14.0
19.5	13.0
19.0	12.5
18.5	12.0
17.5	11.0
17.0	10.5
16.0	10.0
15.5	9.6
15.0	9.4
13.0	8.8
12.0	8.5
11.6	8.6
10.5	8.6
10.0	8.5
9.5	8.5
9.0	8.6
8.5	8.5
8.0	8.5
7.5	8.5
6.5	8.4
6.0	8.3
5.5	8.4
5.0	8.5
4.5	8.4
4.0	8.6

3.2.2.5 Based on the results presented in Figure 49, it was concluded that the thermocouple output of the magic wire indicates the temperature of the hottest point along its length. This indicated the favorability of using magic wire as a sensing device on the backside of the weld.

The drawback to this experiment was that at various times the output of the magic wire was 4 millivolts lower than it should have been. The reading would return to normal, if allowed to set. The return to normal was not gradual, but instantaneous. This indicated a temporary short circuit in the magic wire.

3.2.2.6 Response time experiments were conducted by touching the magic wire to a preheated block and recording the output as a function of time. Results are shown in Figure 50.

4.0 PHASE III - IMPLEMENTATION OF ADAPTIVE FEEDBACK CONTROL

4.1 INTRODUCTION

Based on the results described in section 3.1, a prototype control system was designed and fabricated to utilize the hybrid thermocouple signal in such a manner that the mean temperature at the probe contact point could be maintained constant. The initial system was designed to vary the travel speed as needed to maintain the amplified thermocouple signal equal to a preset reference signal (see section 4.2). Later experiments were conducted in which current was made the slave variable of the adaptive feedback system (see section 4.14).

4.2 SERVOMECHANISM FOR SPEED CONTROL

4.2.1 A chassis layout of the servo control system is shown in Figure 51. A photograph of the servo chassis appears in Figure 52. The components used are listed below:

(1). Brown Electronik Amplifier, Model 359659-3.
(2). Philbrick Power Supply, Model SPR-30.
(3). Philbrick Amplifier, Model P45, or
(4). Philbrick Amplifier, Model SP656.
(5). Honeywell 20 Servo Motor, Model 362479-3.
(6). Design Corporation Magnetic Clutch, Model DX-1.

The preamplifier provided an additional variable gain to the overall system. It also allowed the used of more than one input

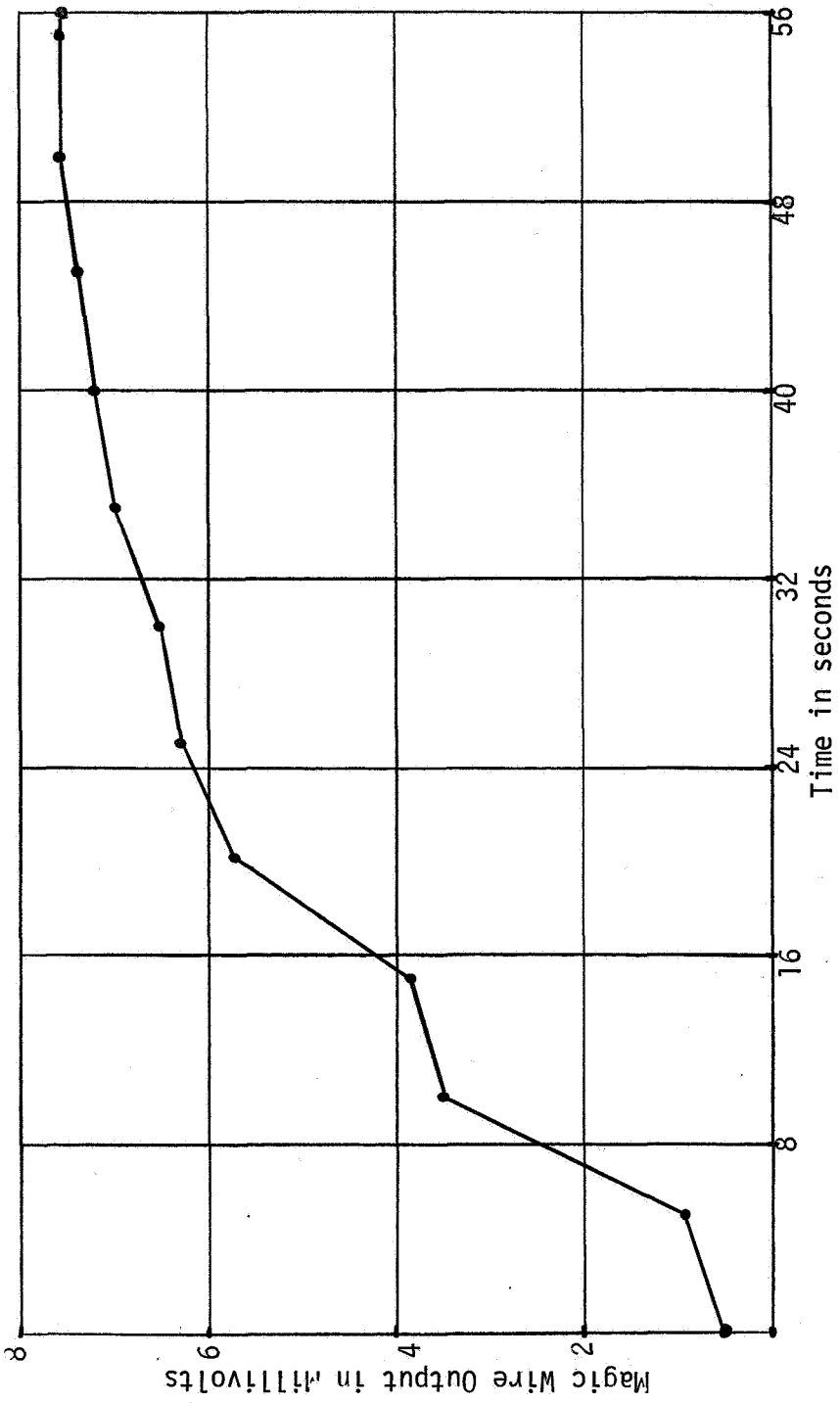


Figure 50: Magic wire response time characteristic.

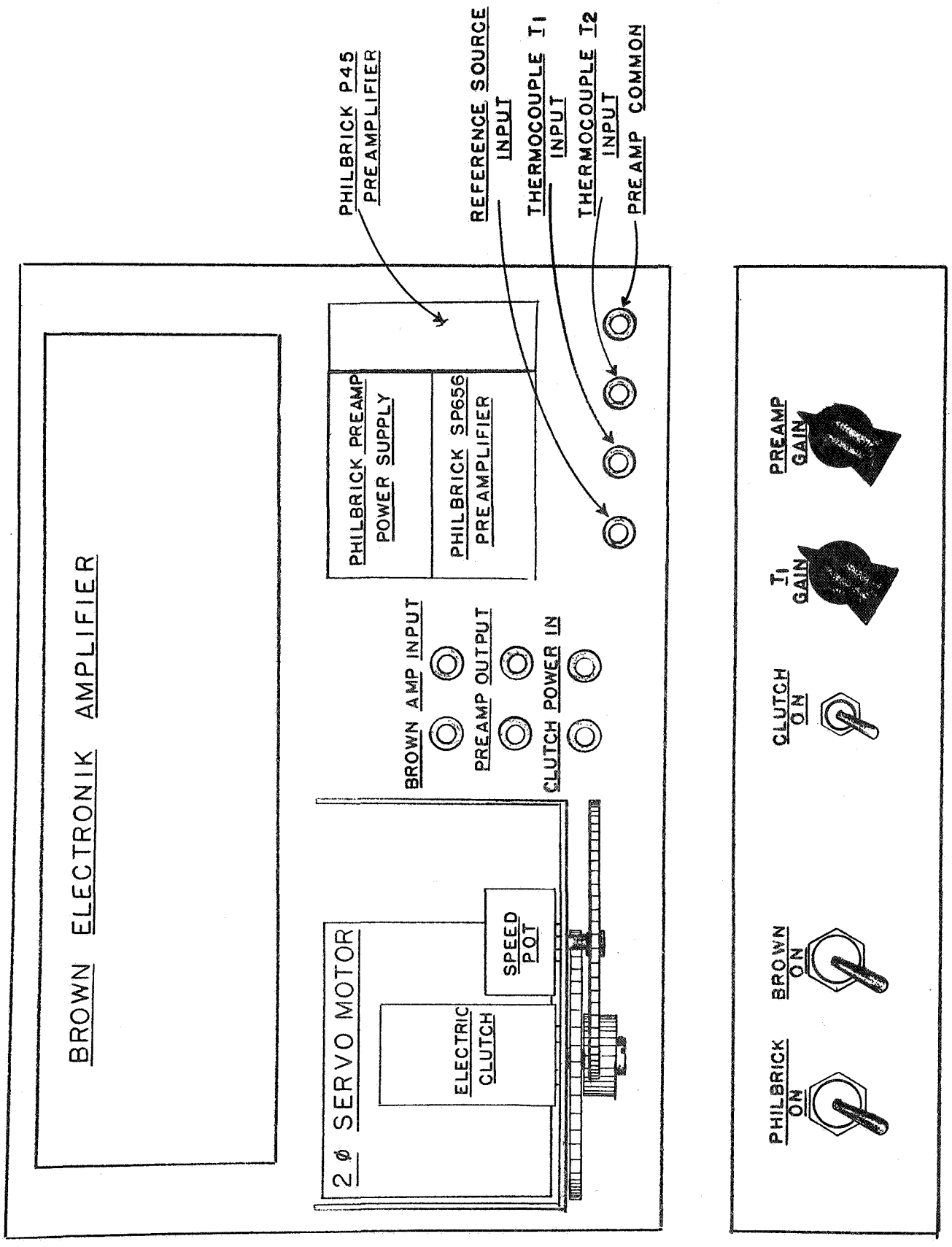


Figure 51: Chassis layout, prototype control system.

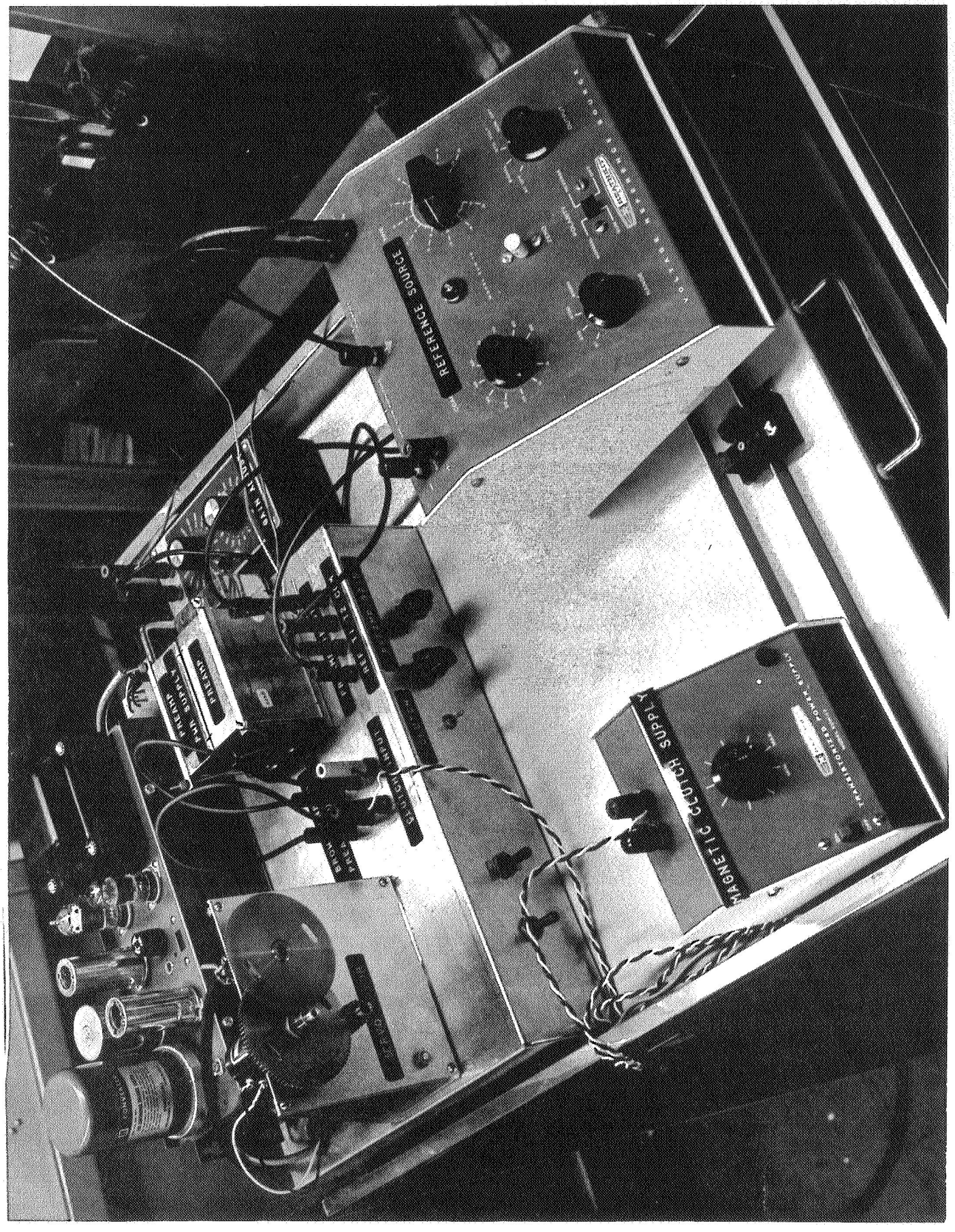


Figure 52: Prototype control system.

signal with the capability of individually adjusted gains for each. If it is desired to not use the preamplifier, jumper wires to the Brown amplifier input may be removed. The 20 motor was connected through a magnetic clutch to the travel speed potentiometer.

4.2.2 A schematic diagram of the preamplifier is shown in Figure 53. The output of the amplifier is given by,

$$\text{output} = K_1E_R - 10K_1E_{T1} - K_2E_{T2}$$

where K_1 = gain of range $33 \leq K_1 \leq 43$ (1)

K_2 = gain of range $K \leq 430$

E_R = reference voltage input

E_{T_2} = aluminum-constantan thermocouple input

E_{T1} = Auxiliary thermocouple input

When only one thermocouple is being used E_{T1} is equal zero in the above equation. The polarity of the reference source is made opposite to the polarity of the aluminum-constantan thermocouple input.

4.2.3 The operation of the servo control system can be explained by referring to the block diagram in Figure 54. When the output of the aluminum-constantan thermocouple equals the reference voltage, the output of the preamplifier is zero. It should also be noted that this explanation is based on one thermocouple input so that E_{T1} is equal zero. With zero output for the preamplifier no signal is fed to the Brown amplifier, and hence the 2-Ø motor, which is connected to the output of the Brown amplifier, is at null position. If the temperature of the aluminum plate at the point of contact with the constantan thermocouple wire increases, the thermocouple output voltage will increase and the output of the preamplifier will no longer be zero. An input signal is thus supplied to the Brown amplifier which, in turn, delivers a signal to the 2-Ø motor causing it to turn. The 2-Ø motor is connected through a magnetic clutch to either the travel speed potentiometer or weld current potentiometer. For the purpose of this explanation it is assumed that the travel speed is the slave variable. Thus when the 2-Ø motor begins to turn, it rotates the travel speed potentiometer

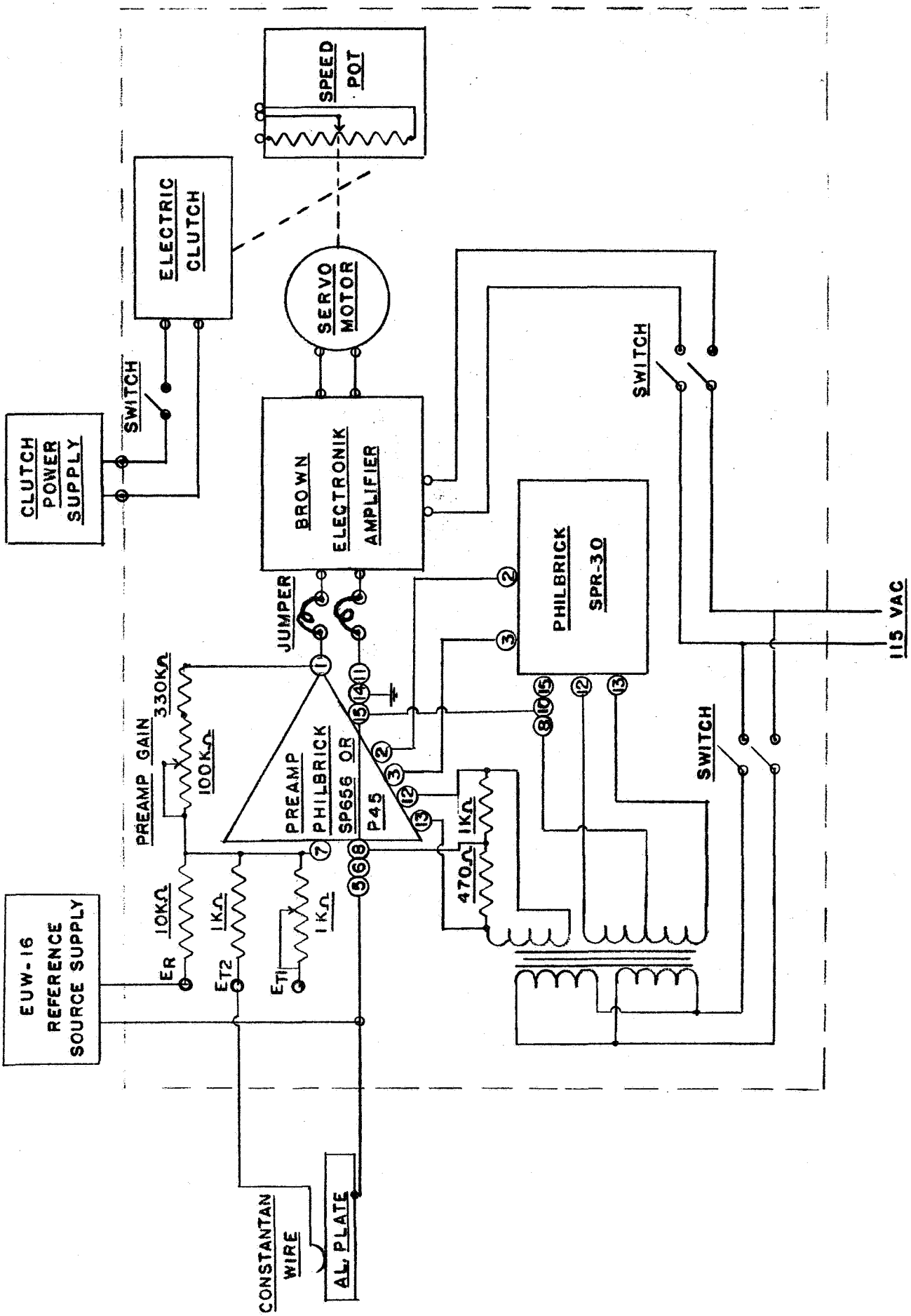


Figure 53: Schematic diagram, prototype control system.

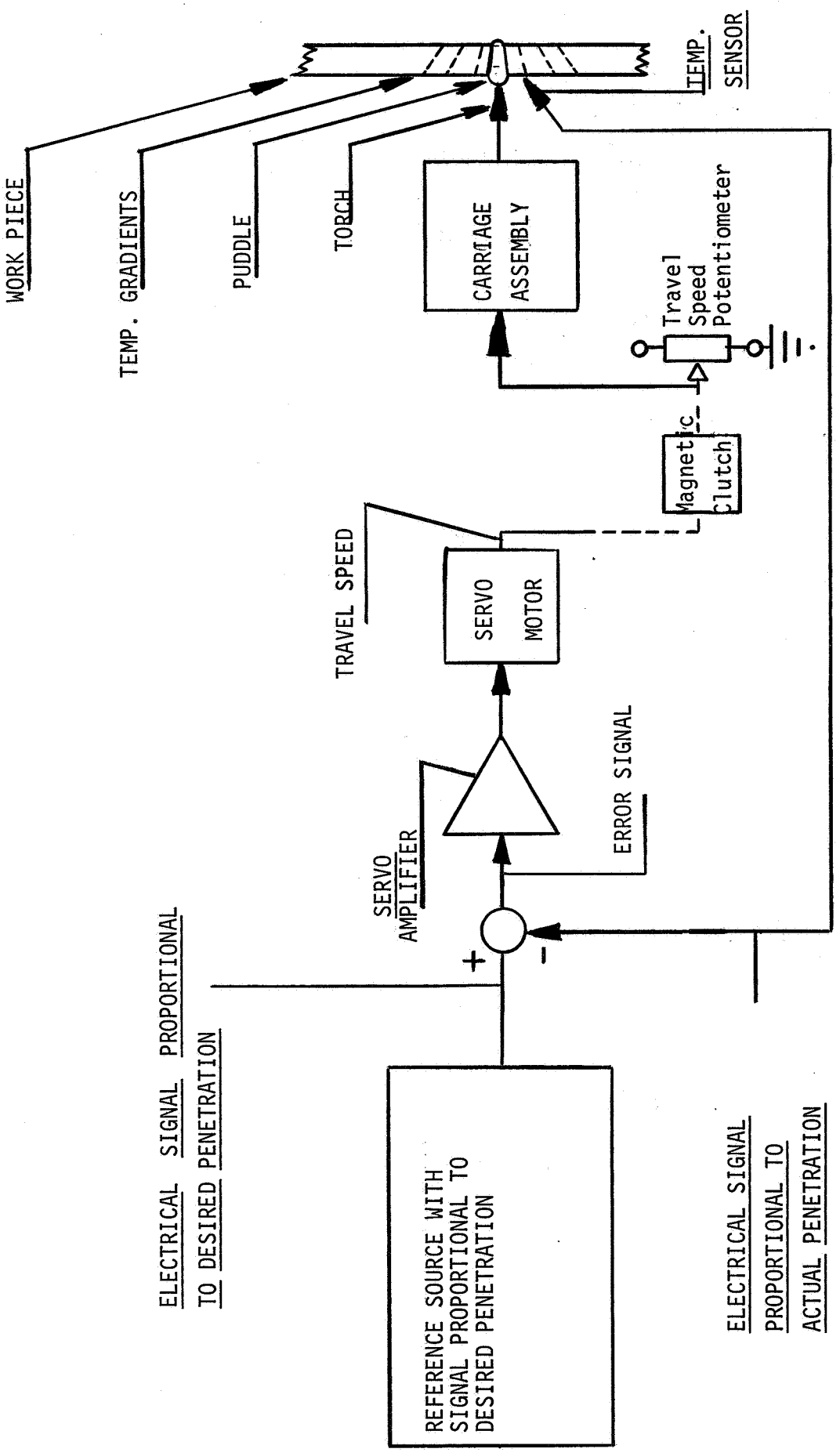


FIGURE 54: Block Diagram, Speed Control System

in such a direction as to increase the carriage speed. The increased carriage speed will result in a reduction in the temperature at the point of contact of the constantan wire and hence a reduction in the thermocouple output. The motor will continue to rotate the carriage speed potentiometer until equilibrium is re-established between reference voltage and thermocouple output. If the temperature at the point of contact of the constantan wire decreases, the 2-Ø motor will rotate the carriage speed potentiometer in the opposit direction until equilibrium is again established. In operation, the control system acts continuously to maintain constant temperature at the point of contact of the constantan wire with the aluminum plate.

4.2.4 On the initial tests the manner in which the servo compensating system was switched into operation was as follows:

With the magnetic clutch, that connects the 2-Ø servo motor to the travel speed potentiometer, unlatched, each weld was initiated and the travel speed and weld current were set for desired penetration. The reference source was then adjusted until the 2-Ø servo motor was nulled. The magnetic clutch between motor and travel speed potentiometer was then engaged and from that point on, automatic travel speed compensation was achieved.

4.3 PENETRATION CONTROL

Based on the results stated in section 3.1, it was concluded that for certain welding conditions a correlation existed between uniform penetration and the temperature gradients around the molten puddle. This assumption can be partially justified by examining the equation for heat flow from a line source of heat moving with constant velocity and direction in a flat plate, the line being perpendicular to the plane of the plate, and equal in length to the thickness of the plate. Assuming that the heat is generated uniformely and at a constant rate along the length of this short line, and no heat leaves either surface of the plate, then all heat flow will be two-dimensional, parallel to the plane of the plate, with a steady state temperature distribution given by [9]:

$$T' - T_o = \frac{q}{2\pi kt} \quad e^{m} K_o \left(\sqrt{m^2 + n^2} \right) , \quad (1)$$

where

T' = steady state temperature in the solid at the point (X,R) where the source is at the origin and the X direction is parallel to the direction of motion of the source. (Positive X is opposite the direction of motion of the source.) R is the distance to the point in question from the heat source path.

To = the initial temperature of plate.

α = thermal diffusivity.

q = rate of heat flow from source.

v = velocity of source.

m = $VX/2\alpha$

N = $VR/2\alpha$

$K_o\left(\sqrt{m^2 + n^2}\right)$ = modified Bessel Function of the second kind and zero order.

t = thickness of the plate.

Equation 1 shows that the temperature at a particular point is directly proportional to the rate of heat flow q from the source and inversely proportional to the plate thickness t. Thus, if the simplifying assumption is made that the required red heat flow from the source is directly proportional to the plate thickness t, i.e.,

$$q = K_1 T, \qquad (2)$$

then we can show that by substituting equation (2) into equation (1) the temperature at a set point referenced to the torch tip will be constant for a varying thickness workpiece, provided penetration is maintained. The resulting equation is given by the expression,

$$T' - T_o = \frac{K_1}{2\pi k} e^m K_o\left(\sqrt{m^2 + n^2}\right). \qquad (3)$$

Thus the servo system and single-wire thermocouple sensor developed under this program should theoretically maintain consistent penetration even for varying thicknesses of material.

4.4 INITIAL TESTS WITH SERVO COMPENSATION; SPEED CONTROL

4.4.1 On all of the initial experimentation, travel speed was made the slave variable of the servo compensation system.

4.4.2 The first series of tests were made on 2219 aluminum panels, measuring 3/8" X 5" X 23". The specific conditions under which each test was made are listed below in Table VIII.

Test Sample	Current	Voltage	Thermocouple Location	Initial Speed	Servo Compensation
#171	250 amp.	9 volts		2 ipm	Not present
#188	350	9	3/8" above C.L.	3.3	Present
#189	350	9	3/4" above C.L.	3.3	Present
#190	350	9	1.0" above C.L.	3.3	Present

Table VIII

Weld Parameters, Tests with Servo Compensation

Photographs of the above samples are shown in Figure 55. Travel speed charts are shown in Figure 56. Referring to the photographs, it can be seen that "burn-through" occurs at the end of panel No. 171 which did not have travel speed compensation. This is due to heat build-up at the end of the plate. Plates #188 through #190 do not have burn-through at the end of the plate because of the action of the servo compensation system to increase the travel speed. This can be seen on the travel speed charts shown in Figure 56.

Samples #188 through #190 were run with identical conditions except for changes in thermocouple location with respect to the torch. These tests were run as a preliminary attempt to find the optimum thermocouple location for temperature-penetration correlation. The point marked H.S. on the photographs corresponds to the location of a heavy aluminum block which acted as a heat sink.

4.4.3 The second set of tests were also run with panels measuring 5" wide and 23" long, however, the thickness was varied in four steps, with each step 10 thousandths of an inch more than the preceeding step. Photographs of these samples are shown in Figure 57. The purpose of "stepping"



Figure 55: Sample welds, speed control.

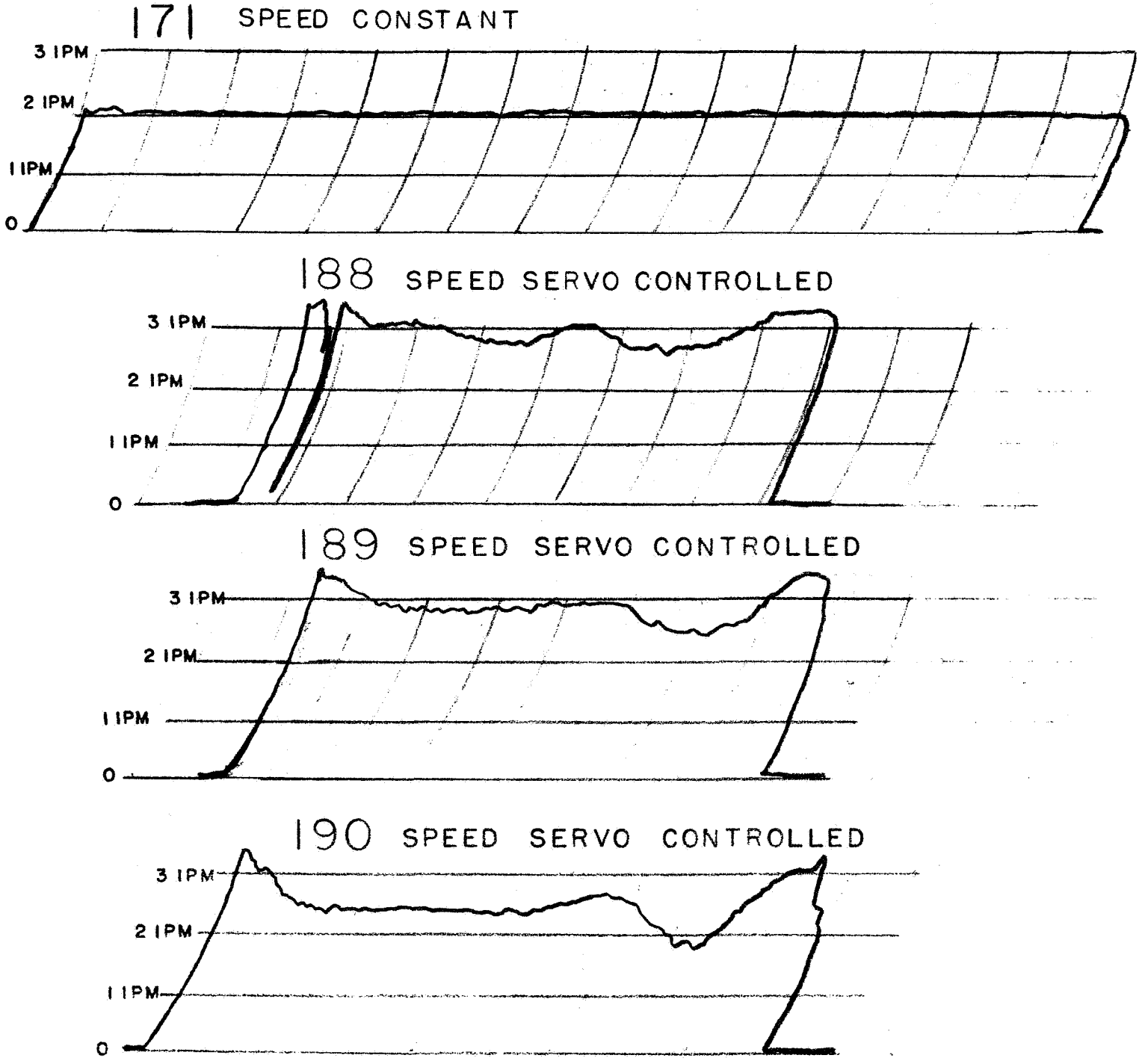


Figure 56: Travel speed charts, speed control.

the thickness of the aluminum panels was to test the ability of the servo compensating system to automatically adjust the speed in such a manner as to maintain even penetration over the stepped plate. The conditions under which these tests were made are listed below in Table IX.

Table IX
Weld Parameters, with Servo Compensation

Test Sample	Current	Voltage	Thermocouple Location	Initial Speed	Servo Compensation
#191	350 amp.	9 volts	3/4" above C.L.	3-1/4 ipm	Not Present
#192	300	9	3/4" above C.L.	4-1/4	Not Present
#193	300	9	3/4" above C.L.	4-1/4	Present
#194	300	9	1/2" above C.L.	4-1/4	Present
#195	300	9	1/2" above C.L.	3-1/2	Present

Travel speed charts for the above samples are shown in Figure 58. As can be seen from the photographs in Figure 57, penetration was definitely maintained better with the samples on which the servo compensation system was used. The point marked H.S. on the photographs again corresponds to the location of an aluminum block heat sink.

4.4.4 From the series of tests discussed in both sections 4.4.2 and 4.4.3 it appeared that the servo compensating system was actually overcompensating at the end of the plate where the heat sink builds up. In an attempt to circumvent this effect a series of tests were run in which a second thermocouple wire was positioned in front of the puddle. The second thermocouple wire was iron, forming an iron-aluminum thermocouple, with a polarity opposite to that of the constantan-aluminum thermocouple. The iron thermocouple lead was fed into the third input of the servo preamplifier. The idea of using the second thermocouple was based on the assumption that when excessive heat builds up in front of the puddle, as it does at the end of the test samples, the output of the iron-aluminum thermocouple would offset partially the output of the aluminum-constantan thermocouple and overcompensation would not occur. The conditions for these tests were as presented in Table X.



Figure 57: Stepped plate samples, speed control.

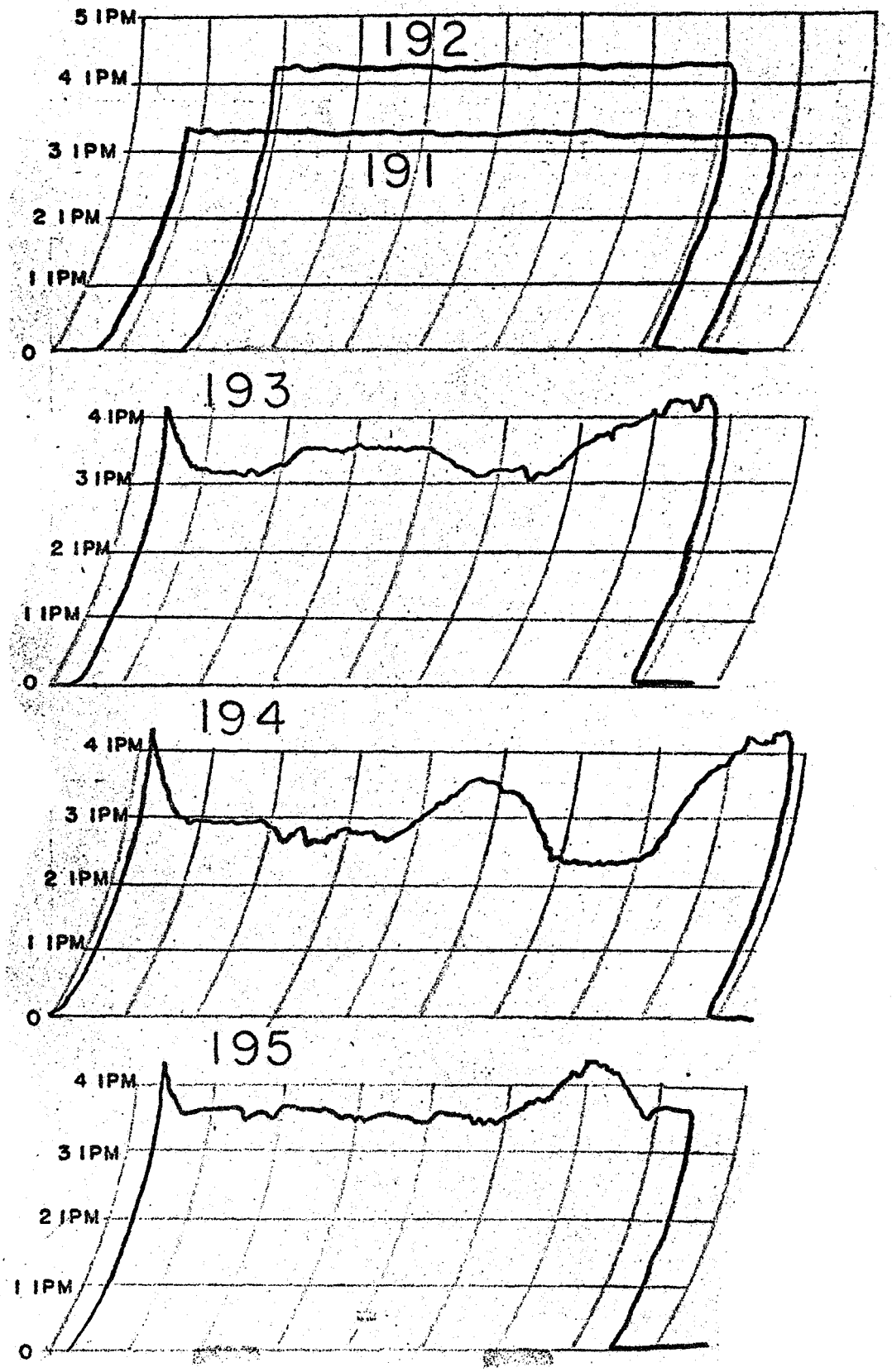


Figure 58: Travel speed charts for stepped plate welds with speed control.

Table X
Weld Parameters With Servo Compensation

Test Sample	Current	Voltage	Constantan Thermocouple Location	Iron Thermocouple Location	Initial Speed	Preamplifier gain for Second Thermocouple Input
#177	250 amp	9 volts	3/8" above C.L.	3/4" ahead of arc	1.91 ipm	62.5
#178	250	9	3/8"	3/4"	1.91	43.3
#179	250	9	3/8"	3/4"	1.91	9.15
#180	250	9	3/8"	3/4"	1.91	19.5

As can be seen from the above data, the gain for the iron-aluminum thermocouple input was varied in an attempt to find the proper balance between the two thermocouple inputs. Photographs of the above samples are shown in Figure 59 and speed charts are shown in Figure 60. As can be seen from the Photographs, penetration was maintained more consistently with Sample #179 corresponding to a preamplifier gain of 9.15 for the second thermocouple.

4.4.5 In conclusion, all three sets of experiments described above showed a definite improvement in weld consistency by use of the adaptive feedback system. However, none yielded perfect control indicating a need for: (1) more accurate information concerning the functional relationship between penetration and transducer signal, and (2) refinements in system operating characteristics.

4.5 EXPERIMENTS RUN TO DETERMINE FUNCTIONAL WELD PENETRATION.

4.5.1 These tests were run on 1/4" X 24" X 6" Aluminum plates, with heat sinks positioned at specified locations with respect to the weld start. The test setup is shown in Figure 61.

4.5.2 Servo compensation was not used, but penetration was maintained by visually monitoring the back of the weld plate and manually adjusting the speed potentiometer. The thermocouple output, for different positions of the pickup, with respect to the torch tip, was monitored on a Moseley X-Y Recorder.



Figure 59: Weld samples with speed control and two thermocouple sensors.

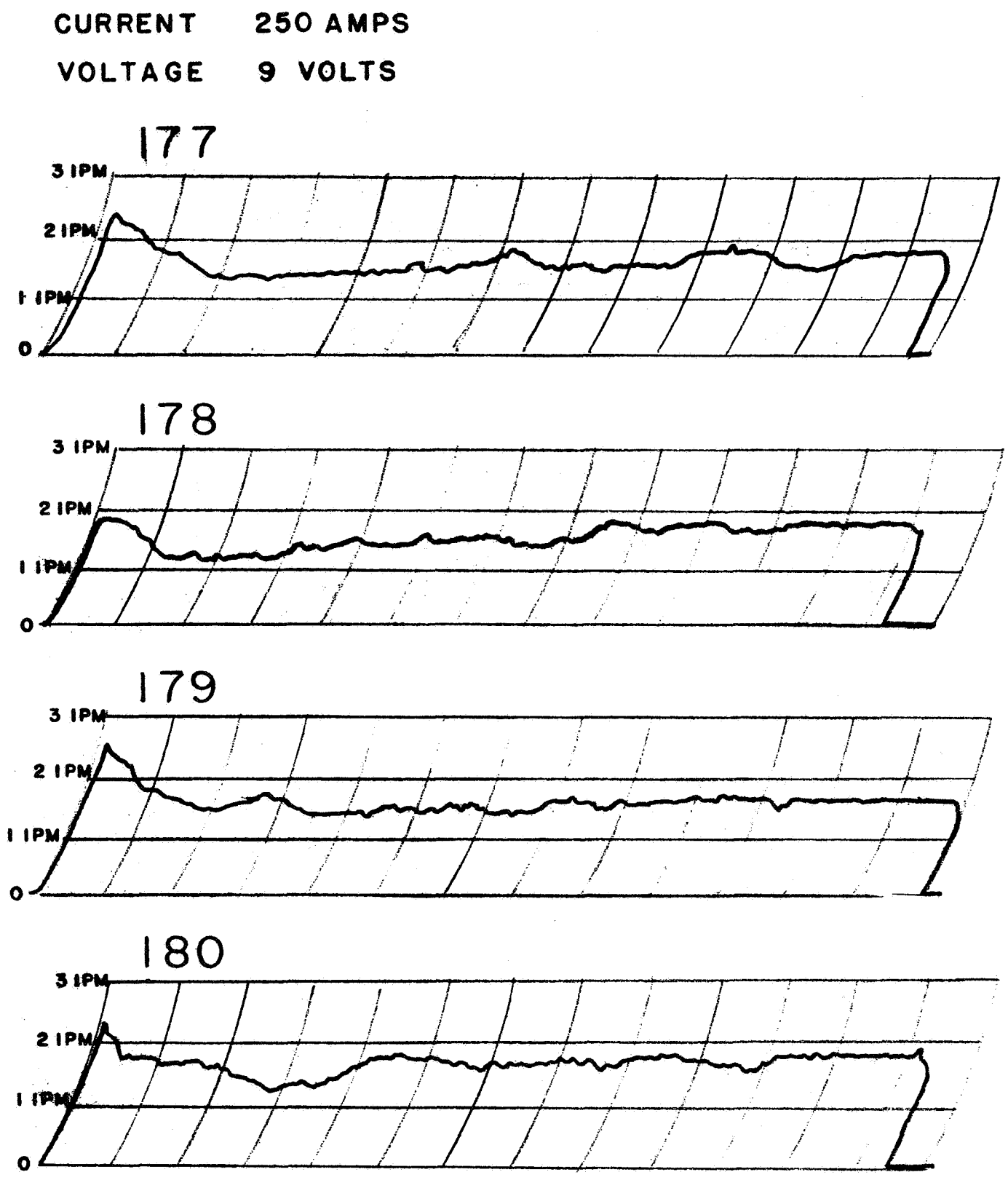


Figure 60: Speed charts for samples made using two thermocouple sensors.

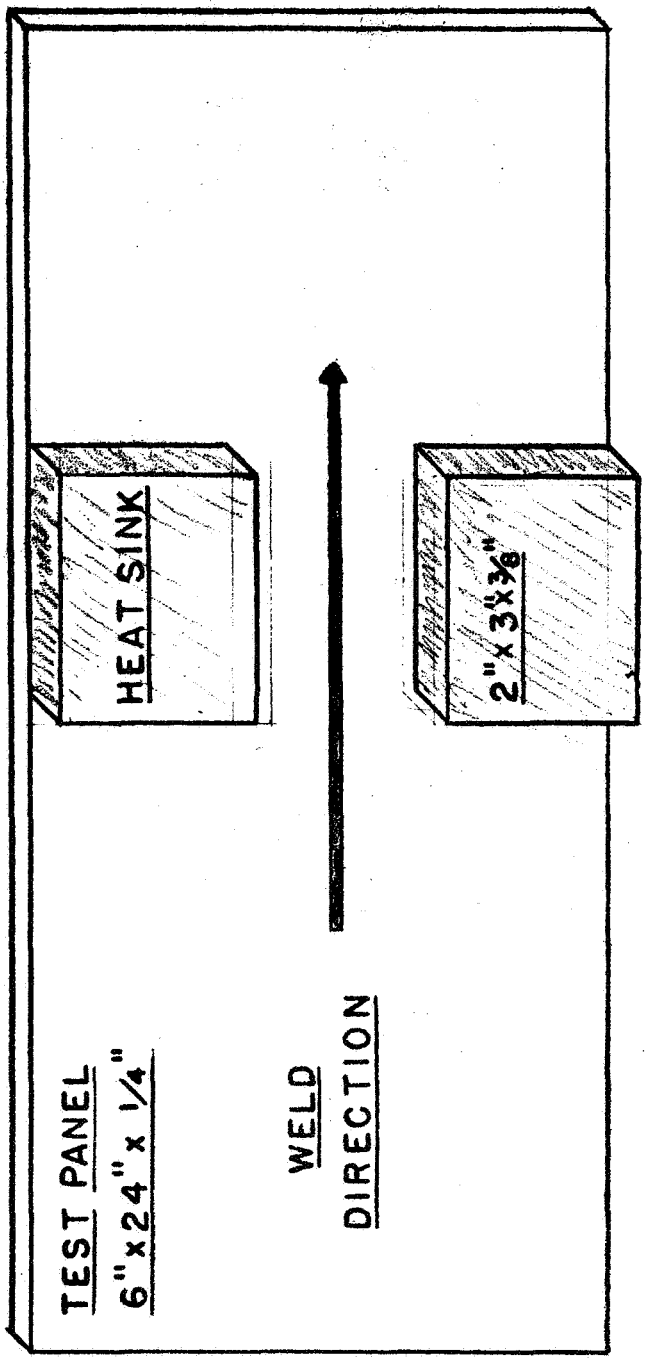


Figure 61: Test setup to detemine functional weld penetration.

4.5.3 The aim of these experiments was to collect a sufficient number of thermocouple output plots for different pickup location, to combine two or more of these in the proper functional relation to yield an overall transducer output that was constant for constant penetration.

4.5.4 It was found that it was difficult to maintain the same amount of penetration throughout a sample by manual means. Several samples were run by this method, and none of them were accurate enough to derive any useful relationships.

4.6 SERVO MECHANISM EVALUATION, SPEED CONTROL

4.6.1 This series of experiments were run to ascertain if the servo-mechanism was maintaining the temperature constant at the point of contact between the aluminum plate and thermocouple pickup.

4.6.2 These tests were run on 1/4" X 6" X 24" Aluminum plates with heat sinks positioned at specified locations in relation to the weld start. The test setup is shown in Figure 61.

4.6.3 The results of the first series of tests are given below in Table XI.

Table XI

Thermocouple Variation, Speed Control

TEST SAMPLE	MINIMUM T.C. OUTPUT	MAXIMUM T.C. OUTPUT	VARIATION	PERCENTAGE VARIATION
No. 250	24.9 mv	28.0 mv	3.1 mv	11.1%
No. 251	30.0 mv	32.0 mv	2.0 mv	6.25%

These tests show that the gain of the servo-mechanism was not high enough to maintain the temperature constant at the point of contact between the test panel and the thermocouple pickup.

4.6.4 The feedback resistor of the preamplifier was changed from 430 K. ohms to 1.1 Megohms, increasing the preamplifier gain by more than 130%. The results of the tests run with this preamplifier gain are listed below.

Table XII

Thermocouple Variation, Speed Control

TEST SAMPLE	MINIMUM T.C. OUTPUT	MAXIMUM T.C. OUTPUT	VARIATION	PERCENTAGE VARIATION
No. 255	26.5 mv	28.6 mv	2.1 mv	7.5%
No. 256	22.7 mv	23.7 mv	1.0 mv	4.2%
No. 257	23.3 mv	24.6 mv	1.3 mv	5.3%

As can be seen, these tests showed much better results.

4.6.5 The feedback resistance of the preamplifier was again increased. A value of 3.6 megohms was put in the circuit and again the servo-system functioned more accurately than before, as can be seen below.

Table XIII

Thermocouple Variation, Speed Control

TEST SAMPLE	MINIMUM T.C. OUTPUT	MAXIMUM T.C. OUTPUT	VARIATION	PERCENTAGE VARIATION
No. 258	22.3 mv	23.0 mv	.7 mv	3.1%
No. 259	20.5 mv	21.5 mv	1.0 mv	4.65%

4.6.6 It can readily be observed that the increased gain of the pre-amplifier greatly improved the response of the system. However, it was still not sufficient as the .7 mv. change in Sample No. 258 represents a temperature difference of 28^{o} F. and the 1. mv. change in Sample No. 259 represents a temperature change of 37^{o} F.

4.6.7 Based on the above tests it was concluded that the overall system gain was being impaired by input loading and/or ac pickup. Experiments conducted to determine these effects are described below.

4.7 EQUIVALENT RESISTANCE OF ALUMINUM-CONSTANTAN HYBRID THERMOCOUPLE PROBE

In order to determine the impedance looking back from the servo pre-amplifier into the thermocouple probe, the equipment shown in Figure 62 was used. The Thevenin equivalent circuit of the system is shown in Figure 63,

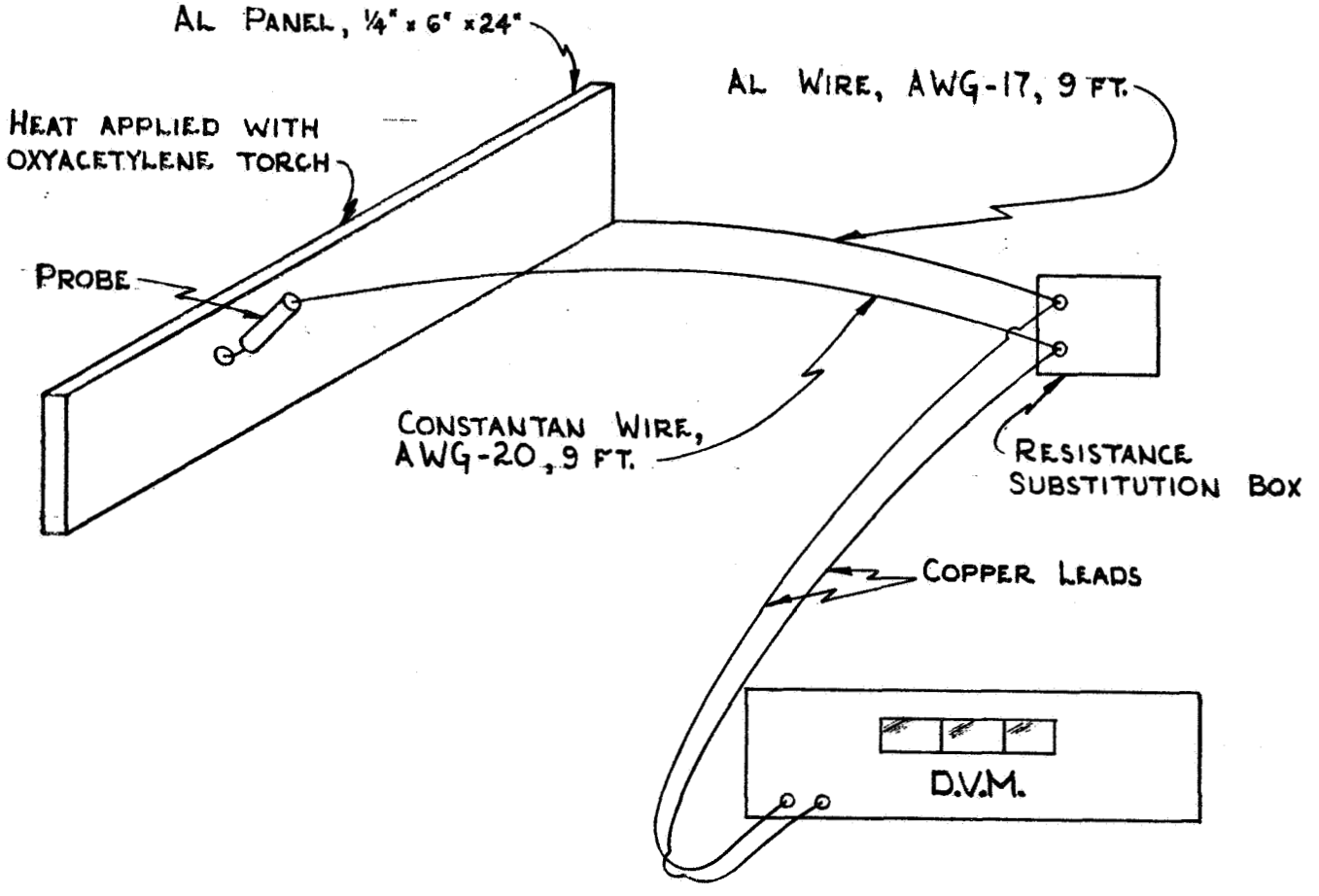


Figure 62: Instrumentation to determine equivalent resistance of aluminum-constantan hybrid thermocouple probe.

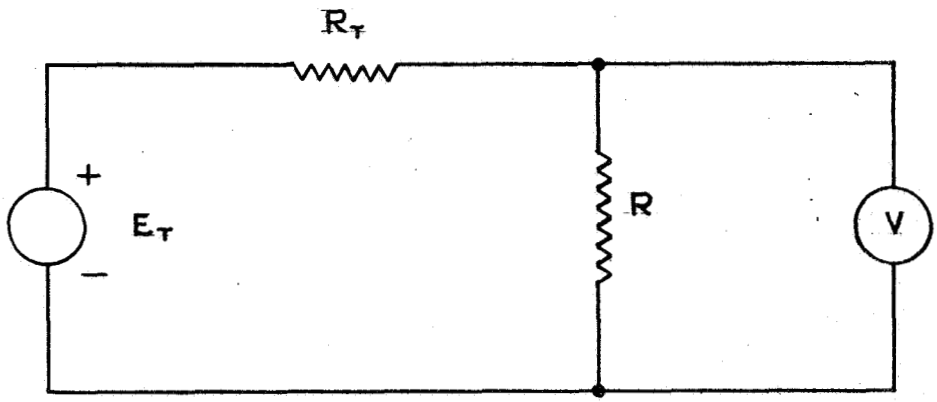


Figure 63: Thevenin equivalent circuit.

where E_t = Thevenin equivalent voltage of hybrid thermocouple,

R_t = Thevenin equivalent resistance of hybrid thermocouple.

R = Resistance of the Resistance Substitution box.

V = Voltage read by high input impedance, digital voltmeter.

With the resistance of the substitution box set at 10 megohms (essentially open-circuit), the Thevenin equivalent voltage E_t is read by the digital voltmeter, since the Thevenin equivalent voltage is by definition the open-circuit voltage.
With R of the resistance substitution box set to a known lower value R_L, R_t can be determined from the equation

$$V = \frac{R_t}{R_L + R_t} E_t$$

or

$$R_t = \frac{R_L (E_t - V)}{V} \qquad (1)$$

The following data was taken:

R of Resistance Substitution Box	Digital Voltmeter Reading
10 megohms	17.45 mv = E_t
16 ohms = R_L	15 mv = V

Substituting the above values into equation (1), we get

$$R_t = \frac{16\ (17.45-15)}{15}$$

$$R_t = 2.61\Omega$$

It would be expected that the above value for R_t would equal the sum of the resistance per foot of the aluminum and constantan leads multiplied by their respective lengths. As indicated in Figure 62, the wire size of the constantan lead is AWG-20, and the wire size of the aluminum lead is AWG-17. The length of both leads was 9.0 feet.

The resistance per foot of constantan wire AWG-20 is

0.289 ohms/foot,

and the resistance per foot of aluminum wire, AWG-17 is

0.0083 ohms/foot.

Thus we have

R = (Resistance per foot of Constantan) X length +
(Resistance per foot of Aluminum) X length

R = 0.289 (9) + 0.0083 (9)

R = 2.67 Ω

The above value for R agrees rather closely with the experimental value for R_t, therefore we can conclude that the Thevenin equivalent resistance of the Hybrid Thermocouple probe can be taken as the dc resistance per foot of the constantan plus the dc resistance per foot of the aluminum. Since the input impedance of the servo preamplifier is 1000 ohms, we can further conclude that it will not appreciably load the Hybrid Thermocouple for lead lengths of 30 feet or less.

4.8 SENSITIVITY OF SERVO AMPLIFIER-MOTOR COMBINATION

By using a precision, continuously adjustable, reference voltage source, it was found that an input of 0.6 mv to the Brown power amplifier was sufficient to rotate the servo motor at maximum rpm. Thus with a gain of 100 for the servo preamplifier, a change of 0.006 mv at the servo input produces maximum change in the motor rotation. Typically the output of the hybrid-thermocouple probe is approximately 25 mv. This, therefore, represents a (0.006/25) X 100% = 0.024% change in probe output for maximum motor rotation change.

4.9 TEST SAMPLES WITH PRE POSITIONED HEAT SINKS, SPEED CONTROL

4.9.1 DISCUSSION OF EXPERIMENTS WITH SMALL HEAT SINK

In this series of tests an aluminum block, measuring 1 7/8" X 3" X 3/8", was used as the heat sink. The heat sink was located 10 inches from the start of the weld and 1/2" above the center line of the weld bead, as shown in Figure 64. The test panel dimensions were, 6" X 24" X 1/4".

4.9.1.1 In the first series of tests, servo compensation was not operative. The parameters were set as follows: current-185 amperes, voltage-11.5 volts, travel speed-4.5 inches/minute.

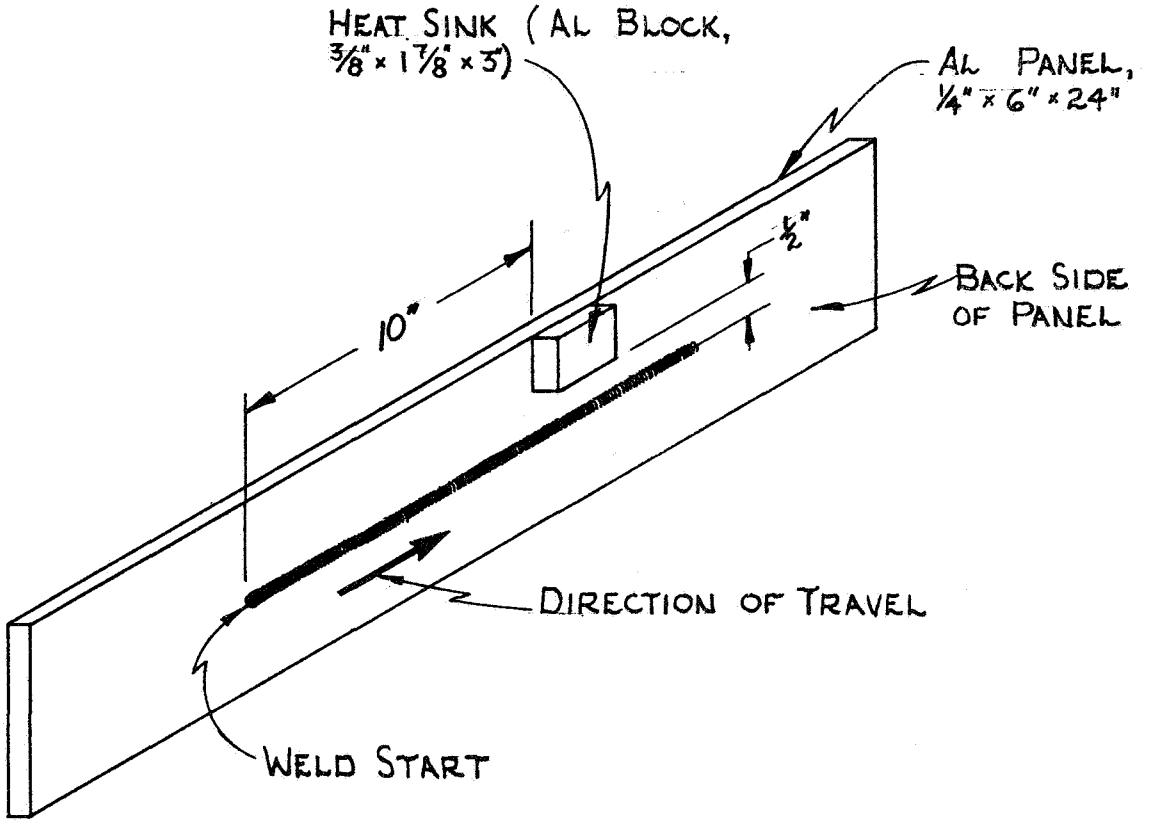


Figure 64: Test setup, experiments with speed control.

In this series of tests the penetration was maintained relatively consistent past the heat sink even though the servo compensation system was not in operation.

4.9.1.2 In the second series of tests the servo compensation system was made operative with the hybrid thermocouple probe positioned 1/2" above the centerline of the tungsten electrode. The parameters were set identical to the series of tests described in 4.9.1.1 with the starting travel speed set at 4.5 inches/minute.

With the speed compensating system in operation, penetration was maintained more consistent in the area of the heat sink. However, when the travel speed slowed down to correct for the heat sink, the system went into oscillation that took approximately 4 inches of travel to settle out. The oscillation produced a peak-to-peak change in travel speed of approximately 3 inches per minute to 6 inches per minute. The damped resonant frequency of the oscillation was approximately 0.3 cycles per second. While penetration was more consistent with servo compensation operative, a ripple could visually be detected in the region of oscillation.

4.9.1.3 Several conclusion were made from the experiments discribed under 4.9.1.1 and 4.9.1.2. These conclusions were as follows:

4.9.1.3.1 The travel speed compensation system was apparently excessively sensitive, since a heat sink that produced very little Visual change in penetration without compensation was sufficient to drive the system with compensation into wide oscillation.

4.9.1.3.2 The conclusions described in 4.9.1.3.1 indicate that either tachometer feedback or other compensation techniques or both would possibly be necessary to stabilize the system while still maintaining the high degree of sensitivity.

4.9.1.3.3 Similar experiments needed to be run with the heat sink positioned beneath the weld bead. (See 4.10)

4.9.1.3.4 Experiments needed to be run with a larger heat sink to provide a complete loss of penetration when servo compensation was not operative (See 4.10)

4.10 EXPERIMENTS WITH LARGE HEAT SINKS, SPEED CONTROL

In this series of tests a larger aluminum block was used as the heat sink. Its dimensions were 1" X 1 1/2" X 6". The heat sink was again located 10 inches from the start of the weld and 1/2" above or below the center line of the weld as shown in Figure 65. The test panel dimensions were again, 6" X 24" X 1/4".

4.10.1 In the first series of tests with the larger heat sink, no servo compensation was used. The heat sink was located above the weld bead, and the parameters were identical to those described under 4.9.1.1. With the larger aluminum block, penetration was completely lost in the vicinity of the heat sink.

4.10.2 In the next series of tests, using the larger heat sink, the speed compensation system was made operative with the parameter settings and probe location identical to those described under 4.9.1.2. Penetration was maintained throughout the weld, however, over-compensation occurred in the region of the heat sink, i.e., the penetration was excessive in this region. Again the system went into oscillation as the torch passed the heat sink area.

4.10.3 In the third series of tests with the large heat sink, the compensation system was made inoperative, and the heat sink was located beneath the weld bead. The parameter settings were identical to those described under 4.9.1.1.
With the large heat sink located beneath the weld bead, penetration was again lost in the vicinity of the heat sink.

4.10.4 In the final series of tests with the large heat sink, the compensation system was made operative, and the heat sink was located beneath the weld bead. The parameter settings and probe location were identical to those described under 4.9.1.2.
Penetration was relatively consistent, however, the system again went into oscillation, as the torch passed the heat sink, and remained in oscillation for approximately 4 inches of travel.

4.11 OVERALL CLOSED-LOOP STABILITY OF SYSTEM, SPEED CONTROL

A simplified block diagram of the overall closed-loop feedback system used in sections 4.9 and 4.10 is shown in Figure 66. In these experiments, tachometer feedback (shown in dotted lines) around the servo amplifier-motor

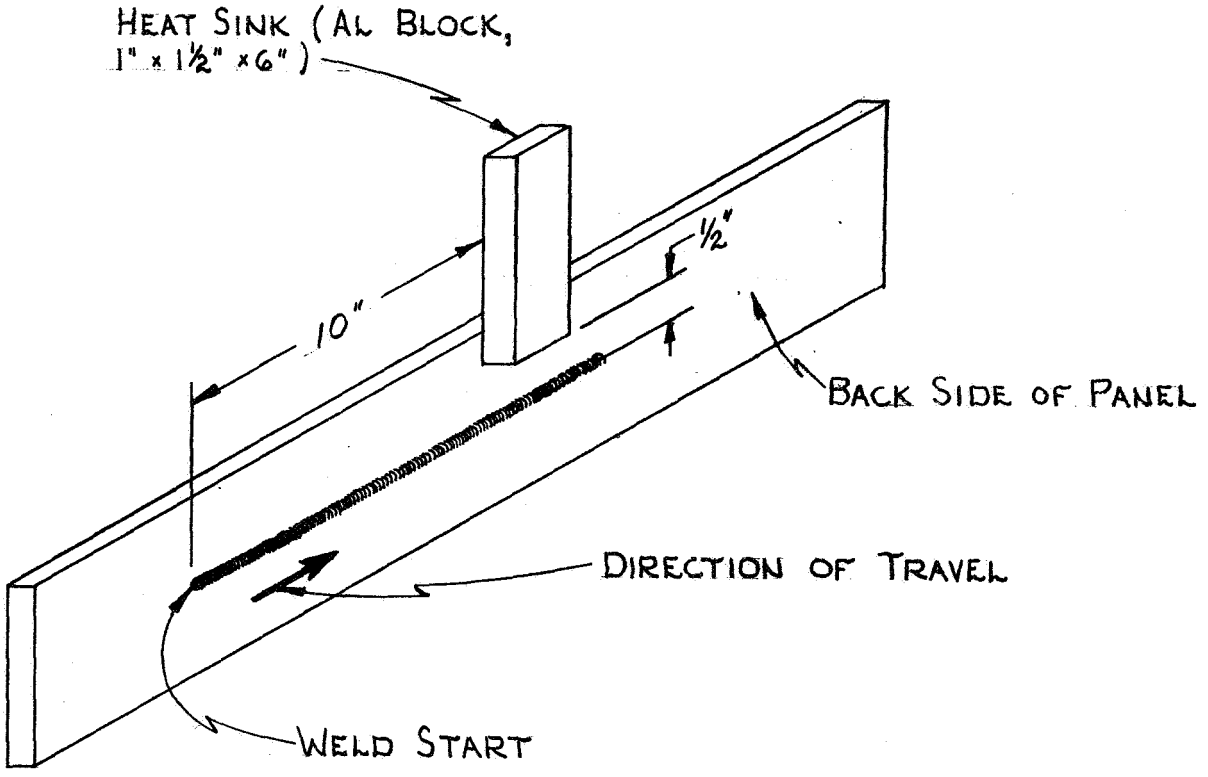


Figure 65: Test setup, experiments with speed control.

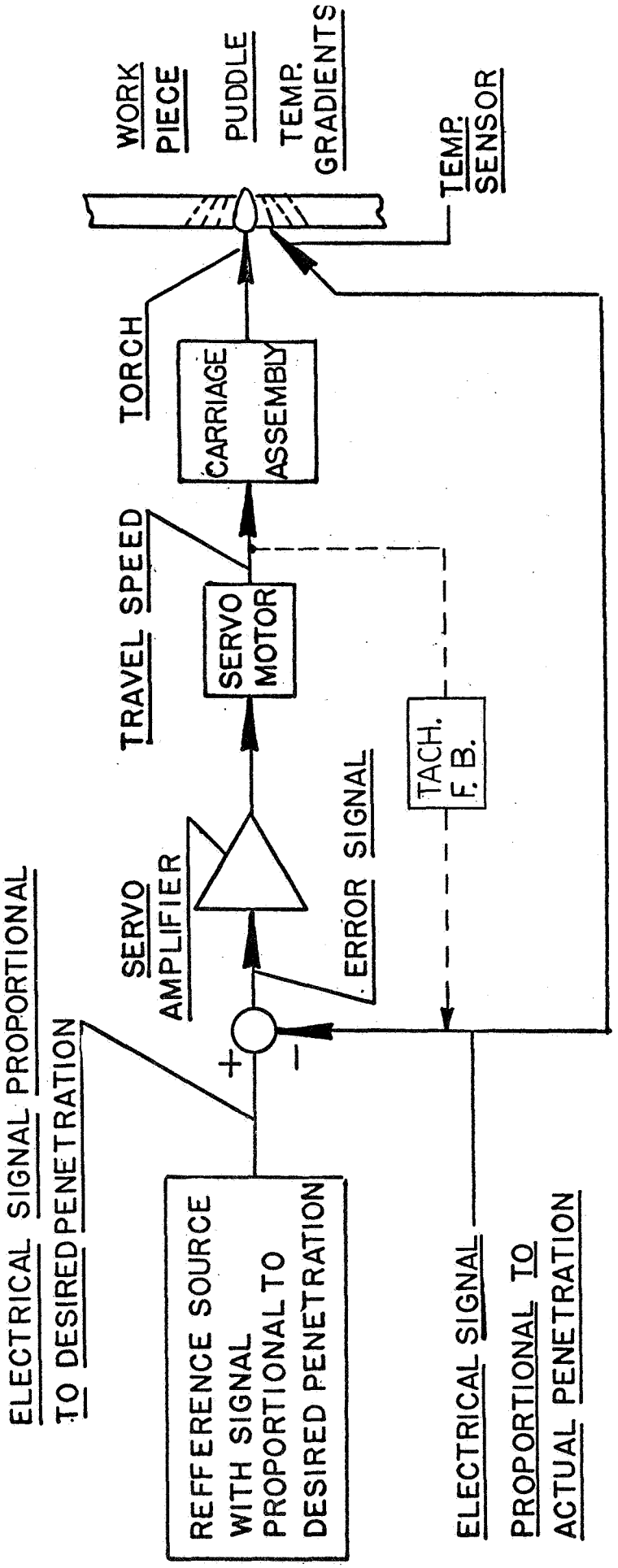


FIGURE 66: FEEDBACK CONTROL SYSTEM BLOCK DIAGRAM, SPEED CONTROL

combination was not included. Hence, without the tachometer feedback included, the servo amplifier-motor combination operated open-loop in the forward path of the overall closed-loop system.

A stability analysis, however, of the overall system showed that the addition of the inner feedback loop would greatly improve the stability of the system. Later experiments were conducted in which tachometer feedback was included.

4.12 REDUCTION OF NOISE EFFECTS

Subsequent experiments indicated that considerable AC was being picked up by the thermocouple leads due to close proximity to the welding cables. This, in turn, was found to be saturating the preamplifier, reducing its effective gain. This problem was eliminated by use of shielded leads for the transducer return.

4.13 EXPERIMENTAL SETUPS TO APPROXIMATE IDEAL CONDITIONS

4.13.1 USE OF ALUMINUM STRIPS

In order to improve the heat sink characteristics of the 6" X 24" X 1/4" test panels, several aluminum strips were sheared to the dimensions of 2" X 24" X 1/4". These strips were then positioned on the backside of the aluminum workpiece as shown in Figure 67. Several tests were run with the parameters set as follows: welding current= 185 amperes, voltage= 10 volts, travel speed= 4.5 inches/minute. The hybrid thermocouple probe was positioned 5/16 inches above the centerline of the torch and offset3/32 inches to the rear. With all parameters maintained constant, the thermocouple output deviation was recorded.

On all of the tests run, the penetration and thermocouple output varied considerably. The variation was, in fact, greater than that for similar tests not using the aluminum-strip heat sinks. The variation in penetration and thermocouple output was attributed to nonuniform contact between the aluminum strips and the test panel.

4.13.2 INCREASE OF TEST PANEL EMISSIVITY

The second method used in an attempt to improve the heat sink characteristics of the test panels was to coat the panels with black paint, leaving a bare two-inch strip on the front side for the weld

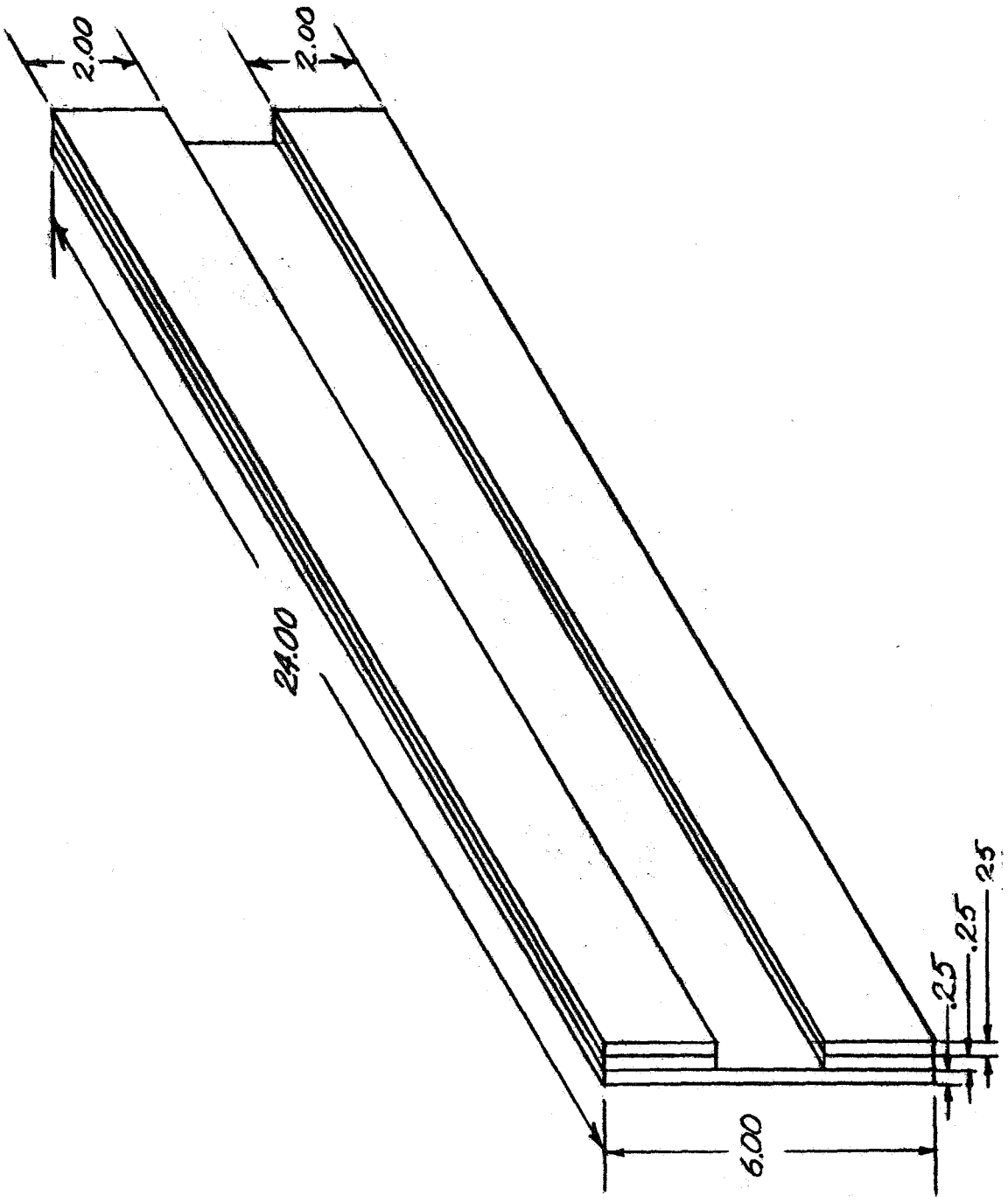


Figure 67: Test setup, experiments to approximate ideal conditions.

bead. It was anticipated that the black coating would increase the emissivity, and hence the heat radiation, by a factor of nearly ten.

Several tests were run with the parameters initially set identical to those in section 4.13.1. The thermocouple output, however, still indicated a distinct build-up of heat in the plate as the molten puddle progressed toward the end of the plate. It was found that approximately 10% more current was needed to achieve penetration on the blacked plate than on panels that had not been coated.

4.13.3 TESTS WITH STEPPED PLATES

A set of tests were run with panels again measuring 6" wide and 24" long, however the thickness was varied in four steps, with each step 10 thousandths of an inch less than the preceeding step. The arc voltage was set at 10 volts, the speed was set at 4.5 inches/minute, and the current was manually varied to maintain consistent penetration. The thermocouple output was recorded. After the first step in plate thickness had been reached and after the current had been readjusted to give the initial penetration pattern, the thermocouple output returned to its initial value. This, of course indicates a direct relationship between constant penetration on the backside of the plate and temperature at the point of contact on the front side of the plate. However, as the molten puddle progressed to the succeeding steps in the test panel, the voltage control head became oscillatory thereby preventing any intelligent information to be obtained. These tests were later repeated using an Airco HMH-D automatic voltage control head.

4.14 SYSTEM MODIFICATIONS FOR CURRENT CONTROL

4.14.1 GEAR TRAIN ASSEMBLY

Using a set of gears and breadboard purchased from the PIC Company, a new gear train assembly was constructed for the servo control unit (see Figure 68). Provisions were made to control current rather than travel speed, and a tachometer was added to the system so that stabilizing feedback could be used if necessary.

4.14.2 MILLER ESR400 POWER SUPPLY

A Miller ESR400 power source (provided by Merrick Engineering) was used for all later tests. The servo-controlled, constant-current characteristics and the remote current capabilities of the ESR400 made it extremely well suited for this program. A photograph of the power supply, instrumentation, and test fixture is shown in Figure 69.

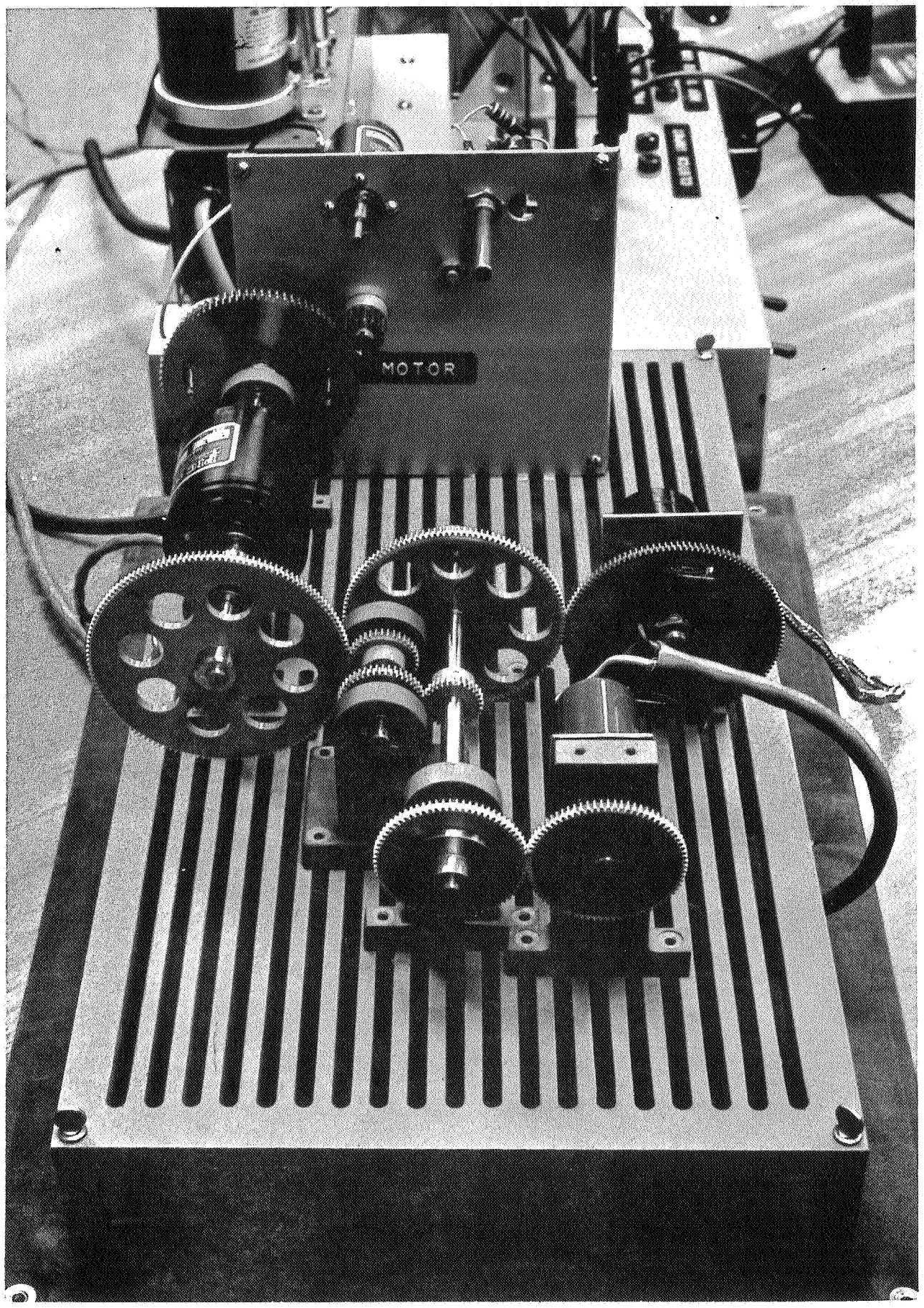


Figure 68: Gear train assembly, prototype control system.

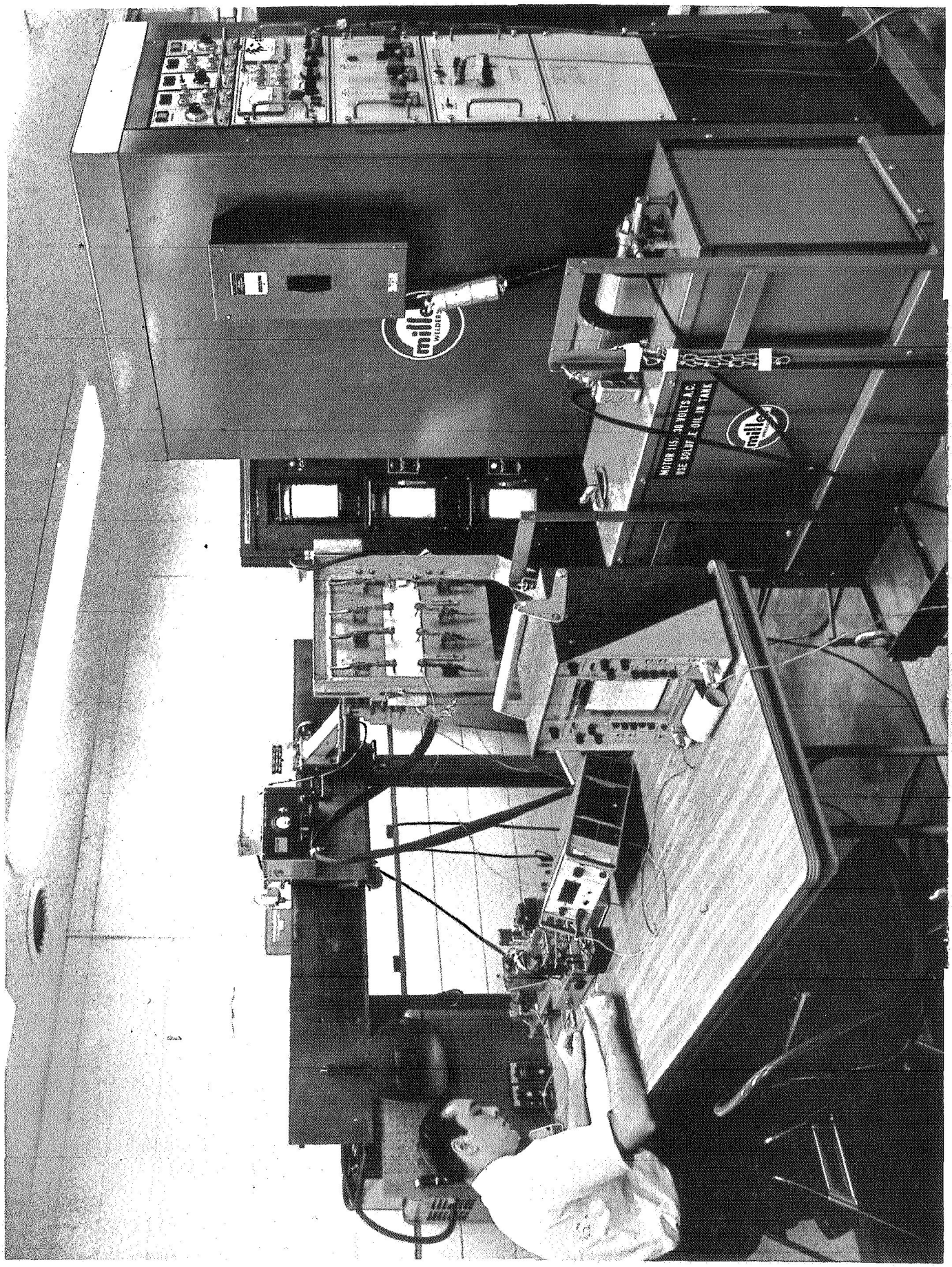


Figure 69: Power supply, instrumentation, and test fixture.

4.14.3 INSTALLATION OF AIRCO HMH-D HEAD

After current was made the slave variable of the control system, it was found that the Airco HMH-F voltage control head was incapable of maintaining a constant stable voltage as the system automatically varied the current to maintain constant penetration. An Airco HMH-D head was therefore purchased and installed. The new, larger head was able to maintain a stable voltage even for large and rapid transitions in current.

4.14.4 THERMOCOUPLE PROBE ASSEMBLY

A new probe assembly, compatible with the Airco HMH-D head was designed and fabricated. The assembly was also designed to be spring-loaded in a line parallel to the electrode. With this design, any variation in voltage that might occur would not result in a displacement of the thermocouple tip from its normal position with respect to the electrode centerline.

4.14.5 MODIFICATION OF FIXTURE

When the HMH-D head was installed, it was found that vibrations were present in the fixture when the head was in the process of correcting for voltage variations. A mechanical structure was fabricated and installed to eliminate this instability.

4.15 RESPONSE TO FORCED CHANGES IN CURRENT, CURRENT CONTROL

Bead-on-plate welds were made on test samples, 6" X 24" X 1/4", with the parameters set as follows: welding current = 150 amperes initially, voltage = 10 volts, and travel speed = 4.5 inches/minute. The thermocouple tip was positioned 0.35 inches above and 0.25 inches behind the centerline of the torch.

When the puddle had been established and the control system locked-in, several forced variations in current (overriding the normal control level) were introduced. The system automatically sensed these current variations, via corresponding change in heat input, and brought the current back to the normal level necessary for consistent penetration.

4.16 STEPPED - PLATE WELD (INCREASING THICKNESS, CURRENT CONTROL)

As a result of the success achieved with the tests explained in section 4.15 a test was run on a sample plate stepped in four steps, each step being 0.010 inches greater than the preceeding thickness. The system automatically varied the current as necessary to maintain extremely consistent penetration.

The response time, as the electrode moved pass each step in thickness was sufficiently rapid to avoid loss of penetration prior to correction.

4.17 STEPPED - PLATE WELD (DECREASING THICKNESS, CURRENT CONTROL)

A test similar to that described above was run except that the plate was oriented such that the weld progressed from the thicker to the thinner end. The system attempted to decrease the current as each succeeding step in thickness was reached, however, due to excessive heat buildup in the plate, the thermal time constant was too long and the servo sensitivity was too low to prevent excessive penetration prior to correction.

4.18 SYSTEM RESPONSE TIME,CURRENT CONTROL

After the system gain had been adjusted for optimum response, a test was run to determine the time required for the system to respond to simulated variation in heat sink conditions. The recording of thermocouple deviation and current are shown in Figure 70. In order to simulate variations in heat sink, the current was manually forced to override the normal control level by plus or minus approximately 30 amperes. As can be seen, the system corrected for positive variations in current (simulates reduced heat sink) in approximately 10 seconds and it corrected for negative deviations in current (simulates increased heat sink) in approximately 6 seconds.

4.19 OUT-OF-POSITION WELDING, CURRENT CONTROL

It was found that penetration could be maintained accurate and stable for bead-on-plate welds where the preset penetration was less than 100%. However, on all attempts to maintain 100% penetration it was found that control settings became extremely critical. This was attributed to the "digging-in" of the tungsten, as full penetration was reached, and the corresponding non-linear relation of puddle edge-to-probe tip distance.

5.0 PHASE IV - COMPLETE SYSTEM EXPERIMENTATION

5.1 EQUIPMENT

A list of equipment used in the final phase of this program is presented below. Figure 71 shows the complete welding station for all Phase IV expementation.

5.1.1 POWER SOURCE

A Miller ESR400 power supply was used for all testing in the final phase of this program. The Miller ESR400 power source is rated at 100%

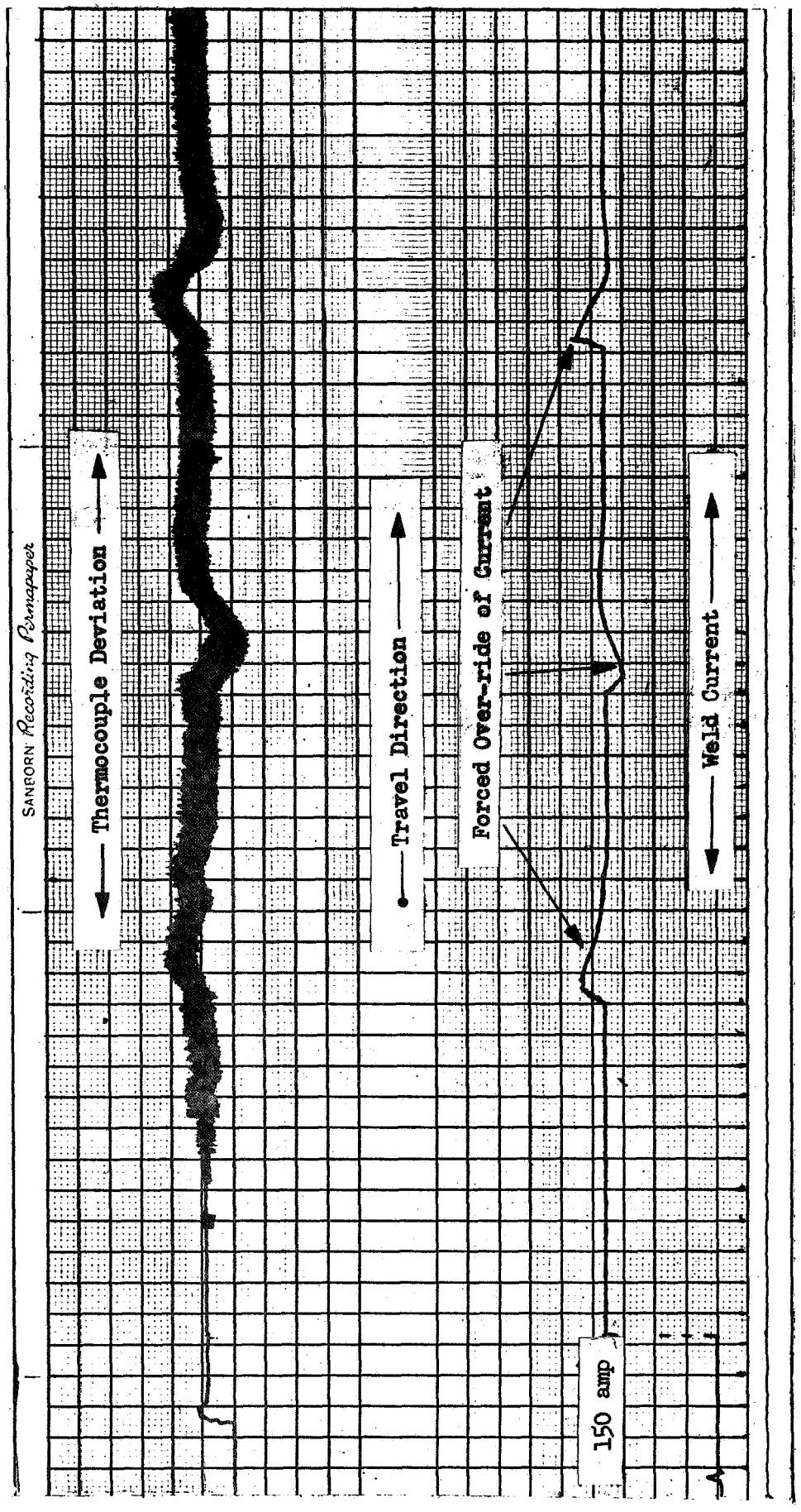


Figure 70: System response time, current control.

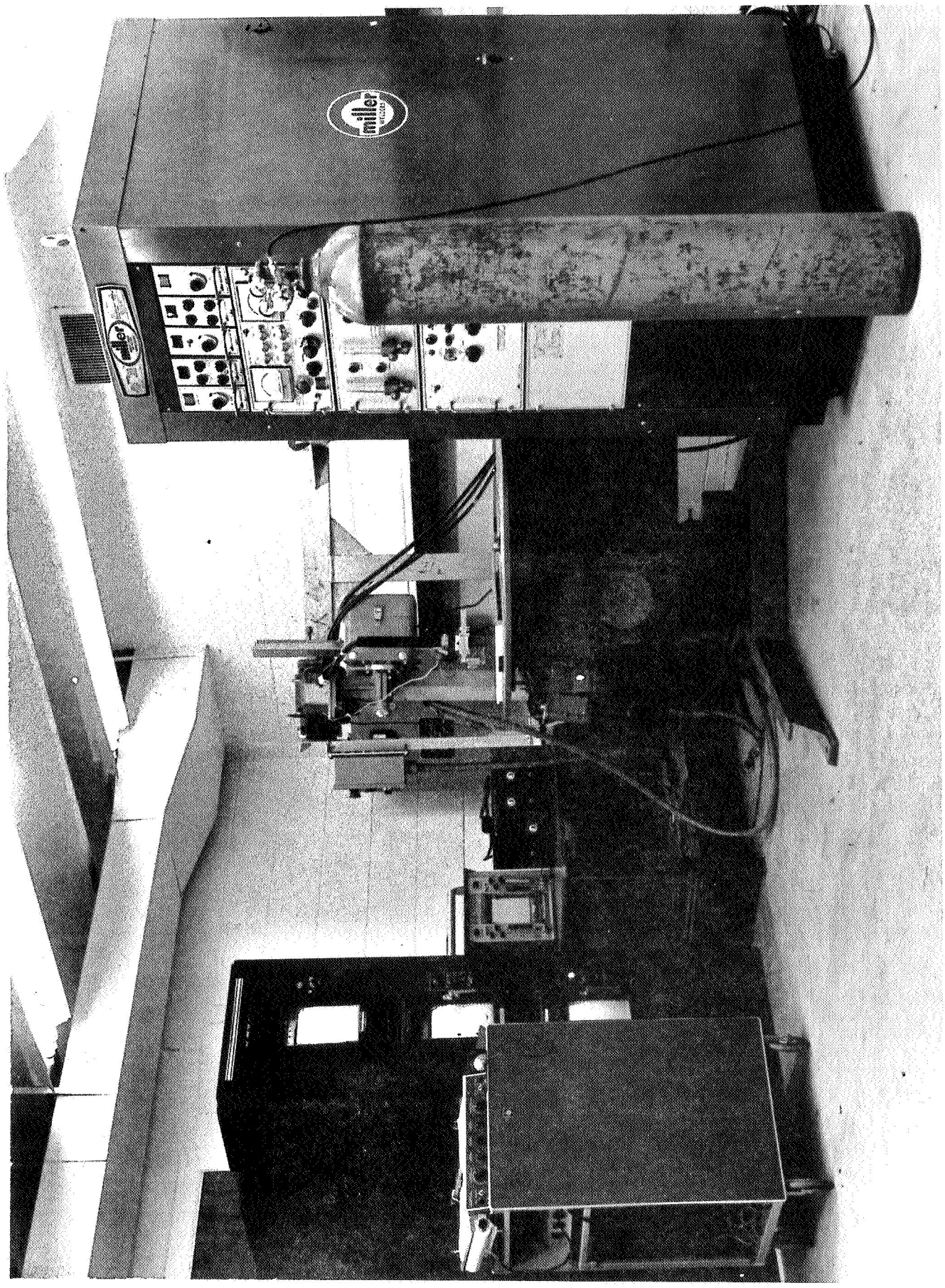


Figure 71: Welding station for complete system experimentation.

duty cycle for a current range of 4 to 400 amperes in a singular wide range. The weld current is set by a direct-reading 3 digit dial on a 10 turn potentiometer. True constant-current, vertical volt-ampere curves, which absolutely compensates for arc length and voltage changes, is achieved by the incorporation of a servo feedback control system in which the output current is continuously checked against a stable reference voltage.

An overall view of the ESR400 is shown in Figure 72. The programming modules and control panel are shown in Figure 73, and the gas and impulse started panels are shown in Figure 74.

5.1.2 VOLTAGE CONTROL HEAD

An Airco model HMH-D voltage control head was used on all final phase experimentation. The complete assembly consisted of the HMH-D head, with barrel and 3" and 12" offset arms, Model M50A Holder and Model HMC-B Control with push button station. The HMH-D head is shown in Figure 71.

5.1.3 TRAVEL SPEED RECORDER - Esterline Angus Microammeter (See Figure 71).

5.1.4 WELD CURRENT RECORDER - Esterline Angus Ammeter (See Figure 71).

5.1.5 ARC VOLTAGE RECORDER - Esterline Angus Voltmeter (See Figure 71).

5.1.6 THERMOCOUPLE RECORDER - Moseley Model 7000 A, X-Y recorder (See Figure 71).

5.1.7 MISCELLANEOUS RECORDING - Sanborn Model 320 strip chart recorder (See Figure 71).

5.1.8 ROTARY POSITIONER - Ransome Model 25P, heavy duty precision positioner (See Figure 71).

5.1.9 FIXTURE

The test fixture, used with the Ransome positioner, is shown in Figure 75 (Drawing number NA 00305-0). A view of the fixture with clamping arms extended is shown in Figure 76. Additional views are shown in Figures 77 through 80.

5.1.10 HYBRID PROBE ASSEMBLY

Experiments conducted during the early phases of this program indicated the following requirements for the probe mechanism.

5.1.10.1 The constantan probe had to be held against the work with a constant pressure regardless of vertical torch movement or surface irregularities.

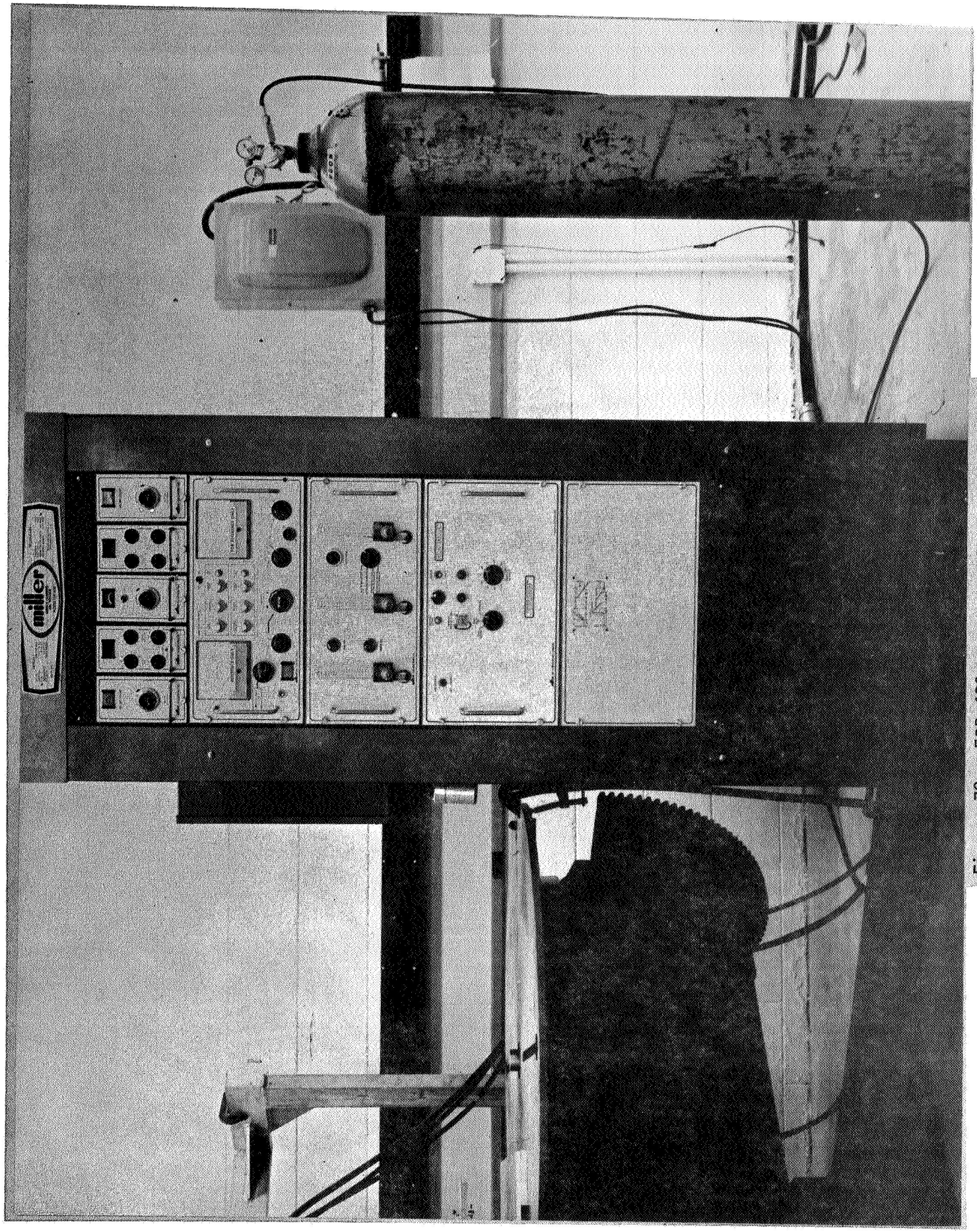


Figure 72: ESR 400 programmable power source.

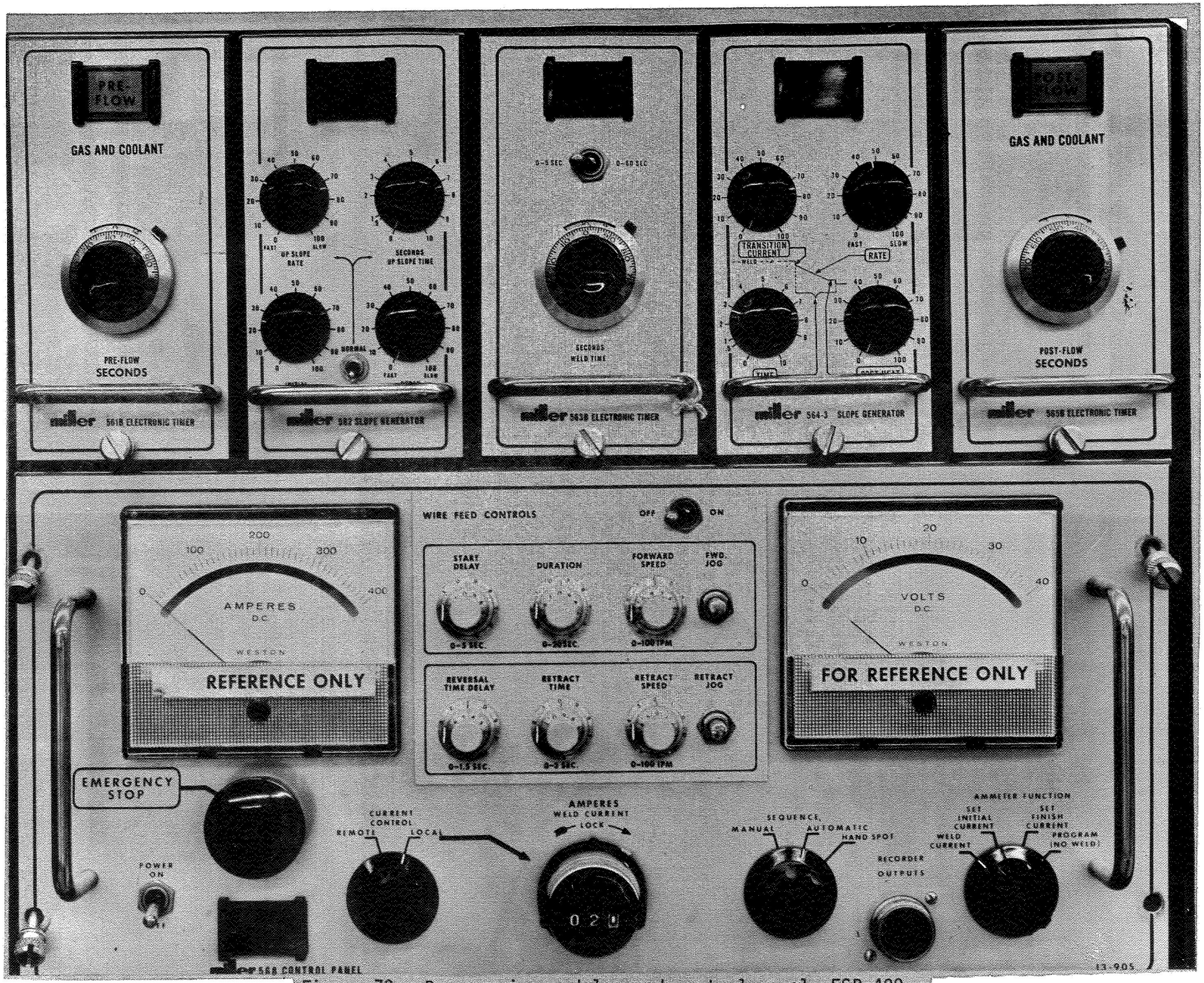


Figure 73: Programming modules and control panel, ESR 400.

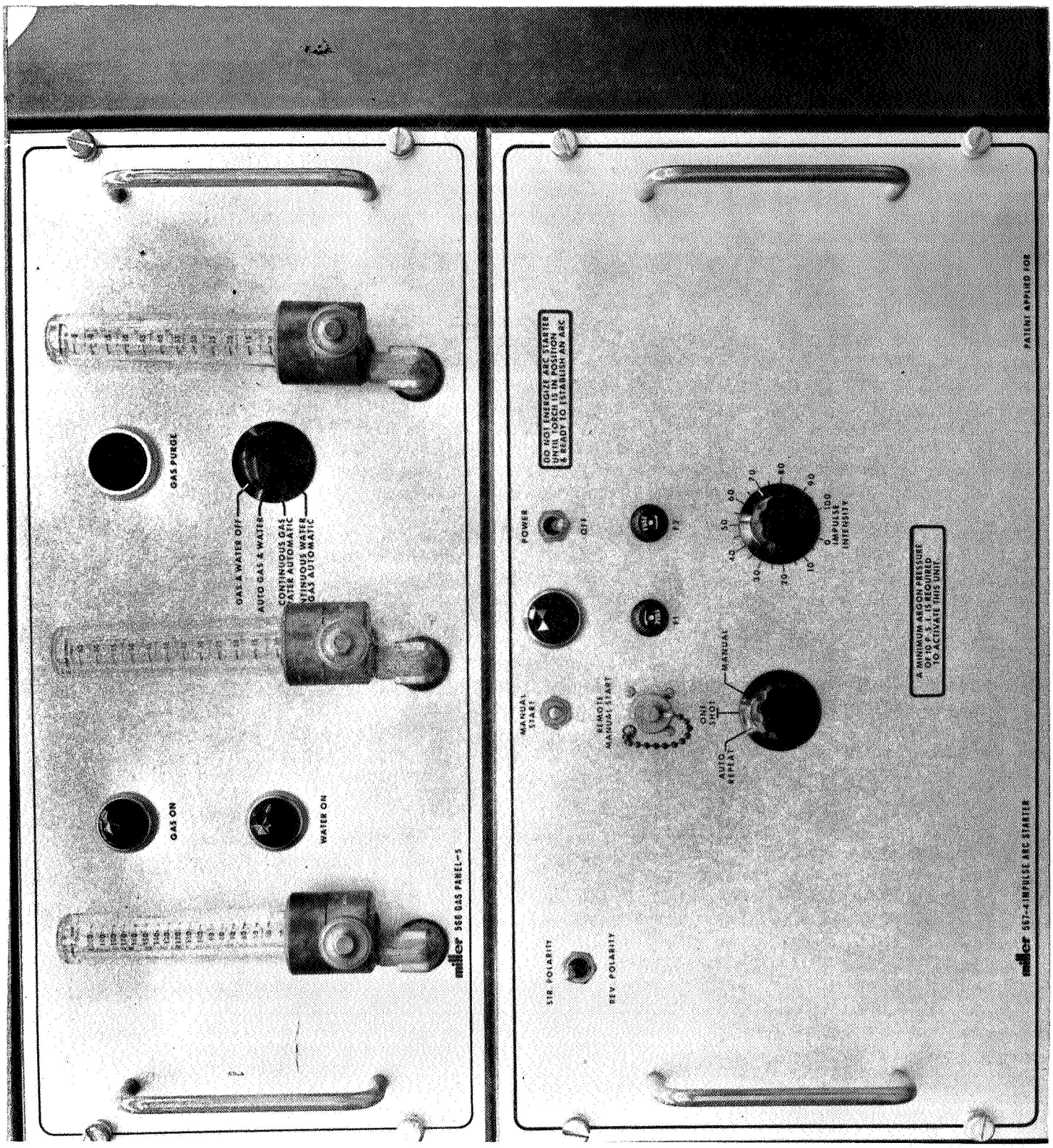
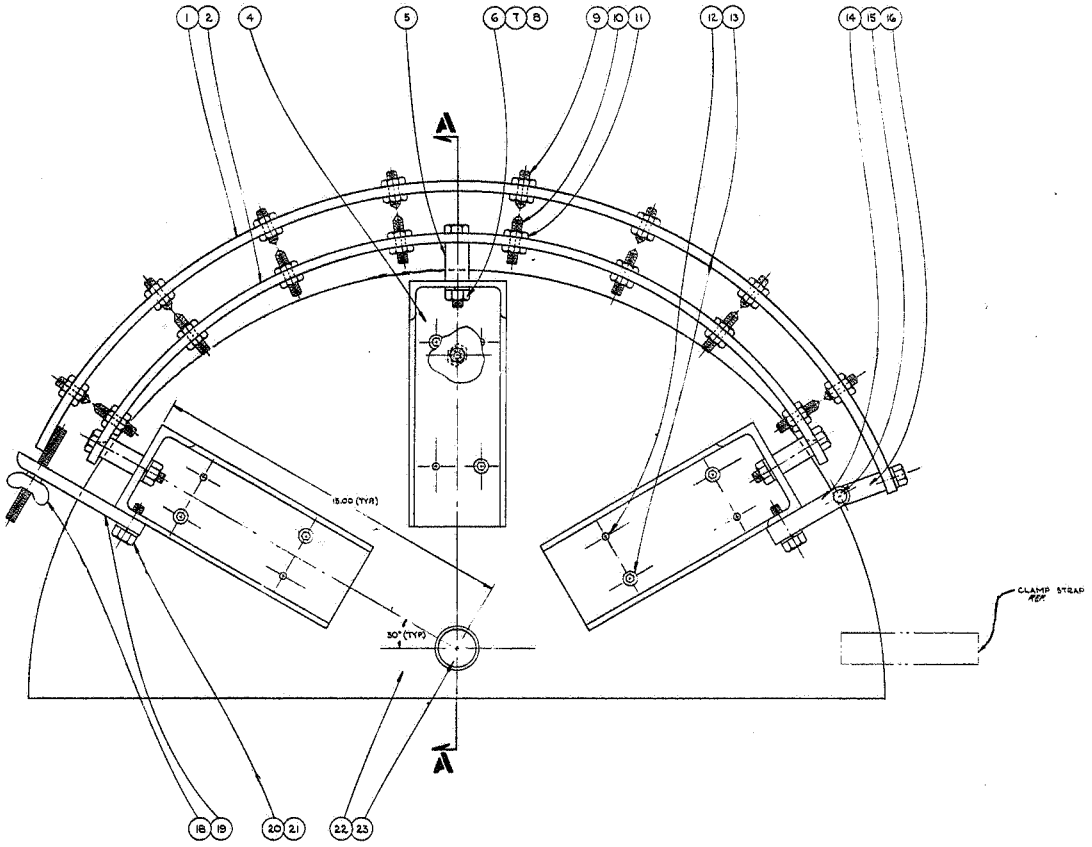
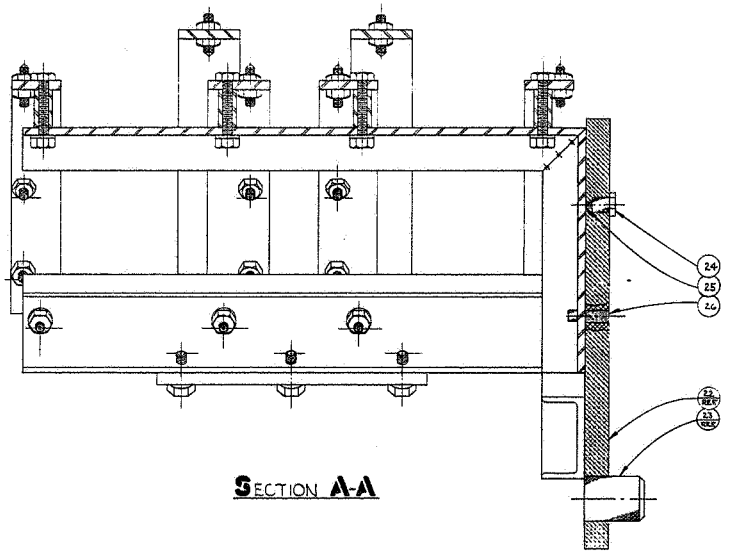


Figure 74: Gas panel and impulse starter panel, ESR 400.



WELD FIXTURE (1) REQ'D
1. DO NOT SCALE DWG



SECTION A-A

DETAIL	NO. REQD	NOMENCLATURE	MATERIAL	SIZE	SPECIFICATION	DWG SIZE
		DESCRIPTION				
26	6	KEENSERT	KNS 516 (FOR 5/16 STUDS)			—
25	1	SCREW	S.H.C.S. ¼-20 × ⅞			—
24	1	FIXTURE KEY, REAMED HOLE			VLIER E-90	—
23	1	LOCATOR				B
22	1	BASE PLATE				C
21	6	LOCK WASHER	⅜ I.D. TO SUIT			—
20	6	SCREW	H.H.M.S. ⅜-16 × 1¼			—
19	1	STRAP				A
18	2	WING NUT	⅜-16			—
17	2	THREADED STUD	⅜-16 × 6½			—
16	2	HINGE				B
15	2	DOWEL PIN	⅛ DIA. × 4			—
14	1	HINGE				B
13	6	SCREW	S.H.C.S. ⅜-16 × 1"			—
12	6	DOWEL PIN	⅛ DIA. × 1⅛			—
11	86	JAM NUT	⅜-16			—
10	32	SCREW, SET	S.H.S.S. ⅜-16 × 2		CONE POINT CONE POINT	—
9	16	SCREW, SET	S.H.S.S. ⅜-16 × 1¼			—
8	12	BOLT, HEX. HD.	⅜-16 × 3			—
7	12	HEX. NUT	⅜-16			—
6	12	LOCK WASHER	⅜ I.D. TO SUIT			—
5	12	SPACER	STL. TUBING ⅝ OD × TGA. × 1¾ (LG)			—
4	3	CHANNEL				C
3						
2	1	STRAP				C
1	2	STRAP				C

BILL OF MATERIAL OR PARTS LIST

UNLESS OTHERWISE SPECIFIED
DIMENSIONS ARE IN INCHES
TOLERANCES ON
DECIMALS .X ± .06, .XX ± .03, .XXX ± .010
ANGLES ± 0° 30'
FRACTIONS ± 1/32
SURFACE ROUGHNESS
DO NOT SCALE THIS DRAWING
RELEASE DATE

DRAWN R.G.J. 12 APR 68
CHECK Van Clarke 17 Feb 68
ENGR
STRESS
WEIGHT

APPROVED
CUSTOMER APPROVES

MERRICK ENGINEERING INC.
AFFILIATED WITH
MID-SOUTH TOOL & DIE INC.
2401-C 12th AVE. SO. NASHVILLE, TENN. 37212

WELD FIXTURE

PROJECT NO. 003 | SIZE E | NA 00305-C
SCALE ½ | FINISH | SHEET ___ OF ___

NEXT ASSY	USED ON	NEXT ASSY	FINAL ASSY
APPLICATION		QTY REQD	

FIGURE 75: Test Fixture

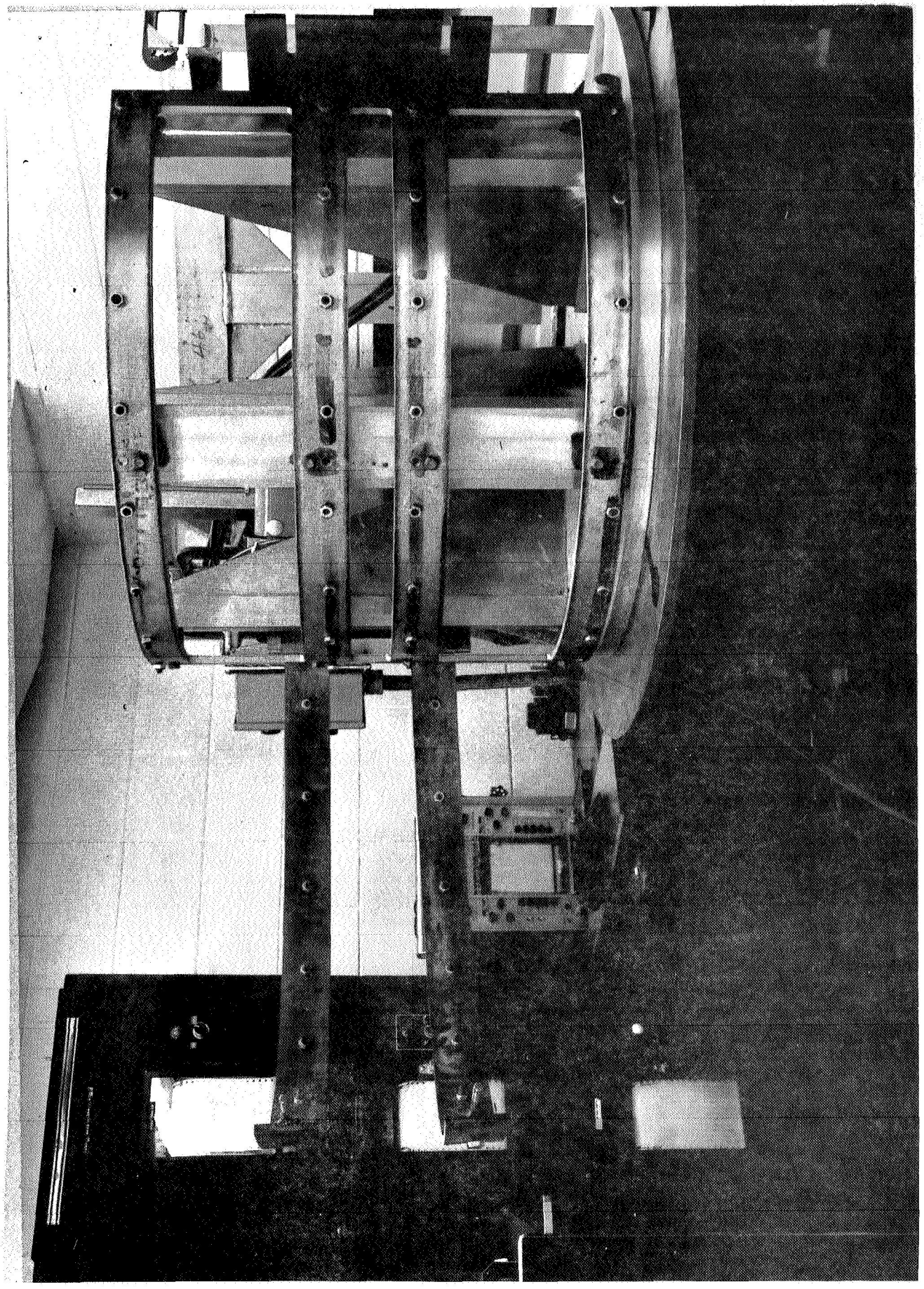


Figure 76: Cylindrical fixture with clamping arms extended.

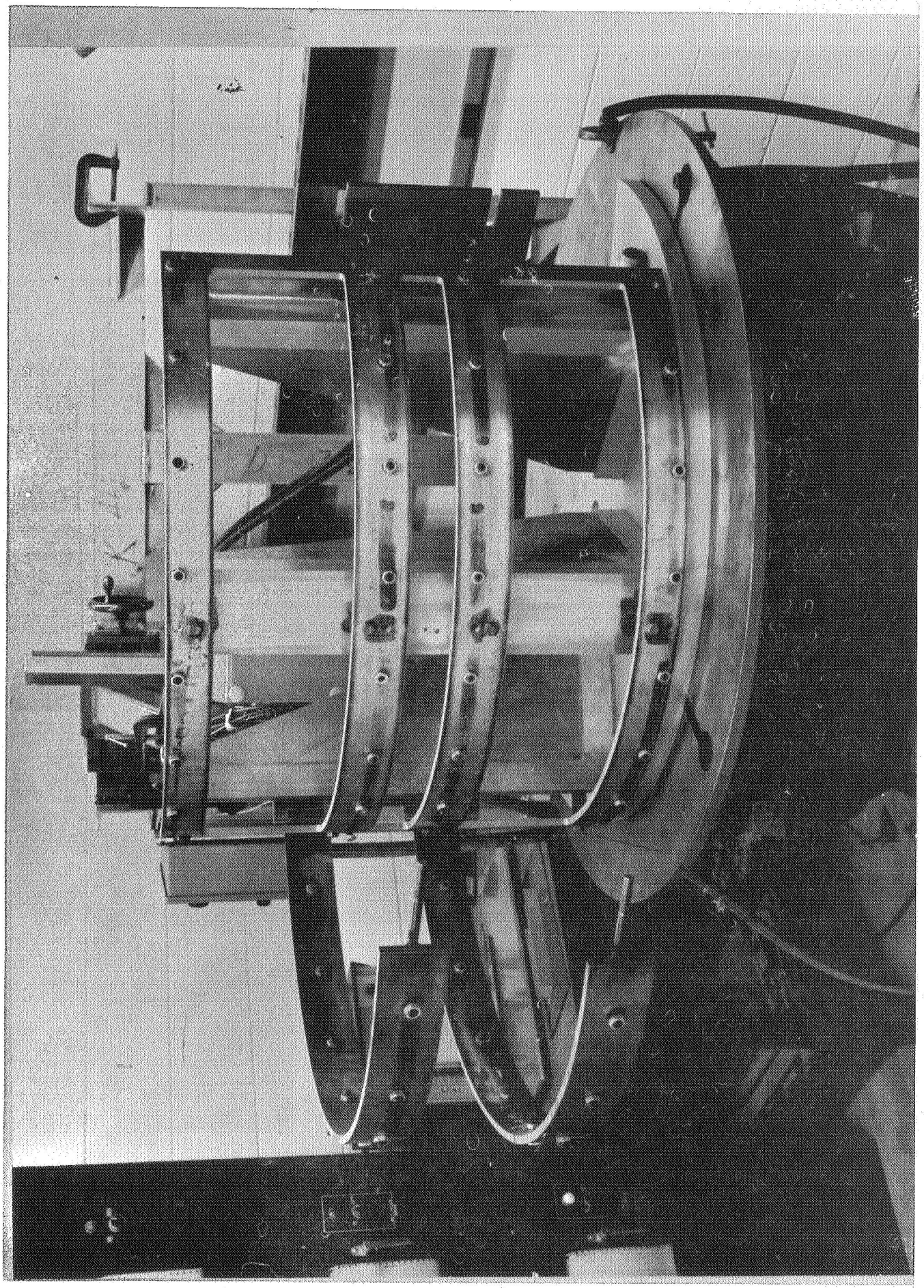


Figure 77: Cylindrical fixture and recording equipment.

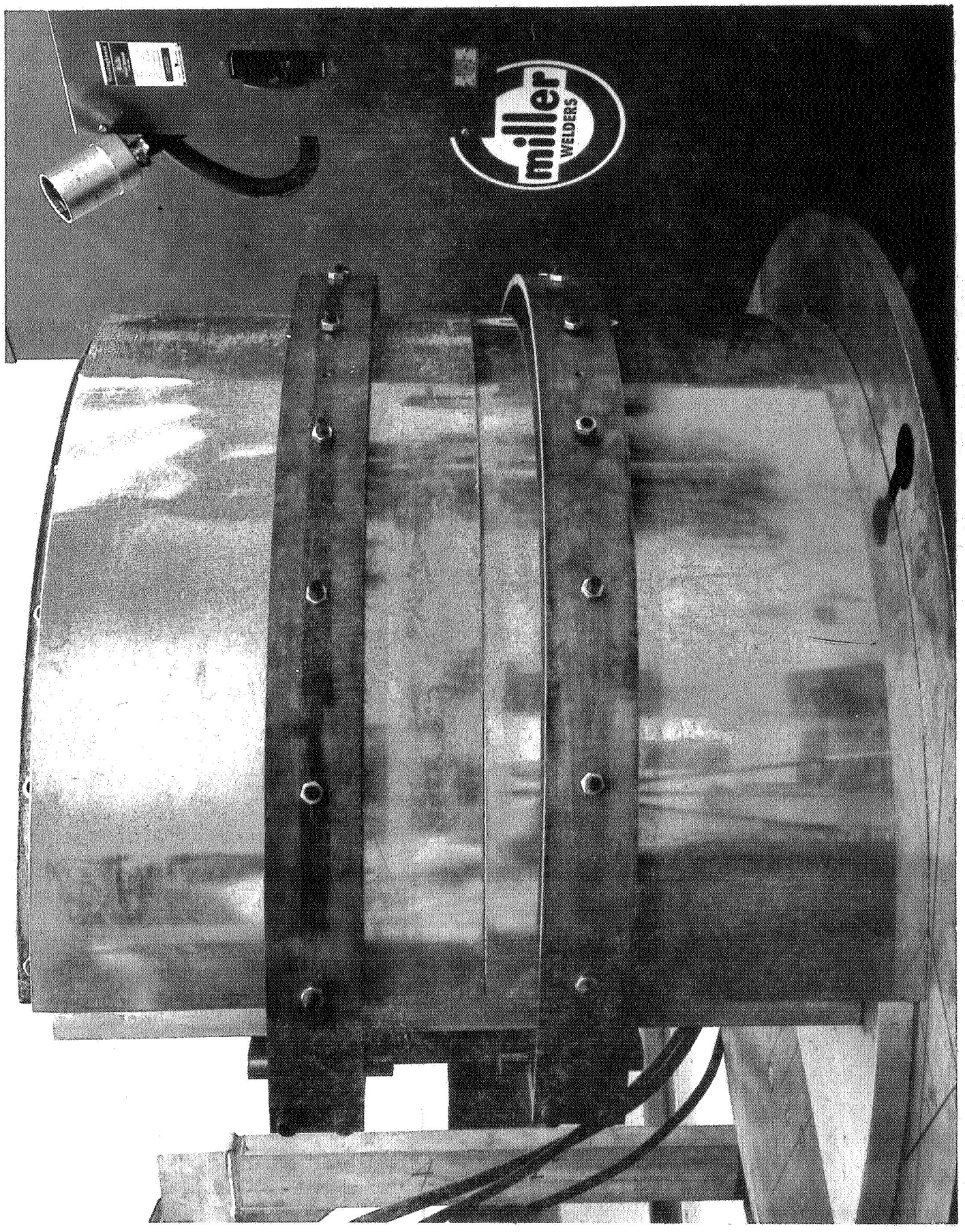


Figure 78: Cylindrical fixture with parts clamped in place.

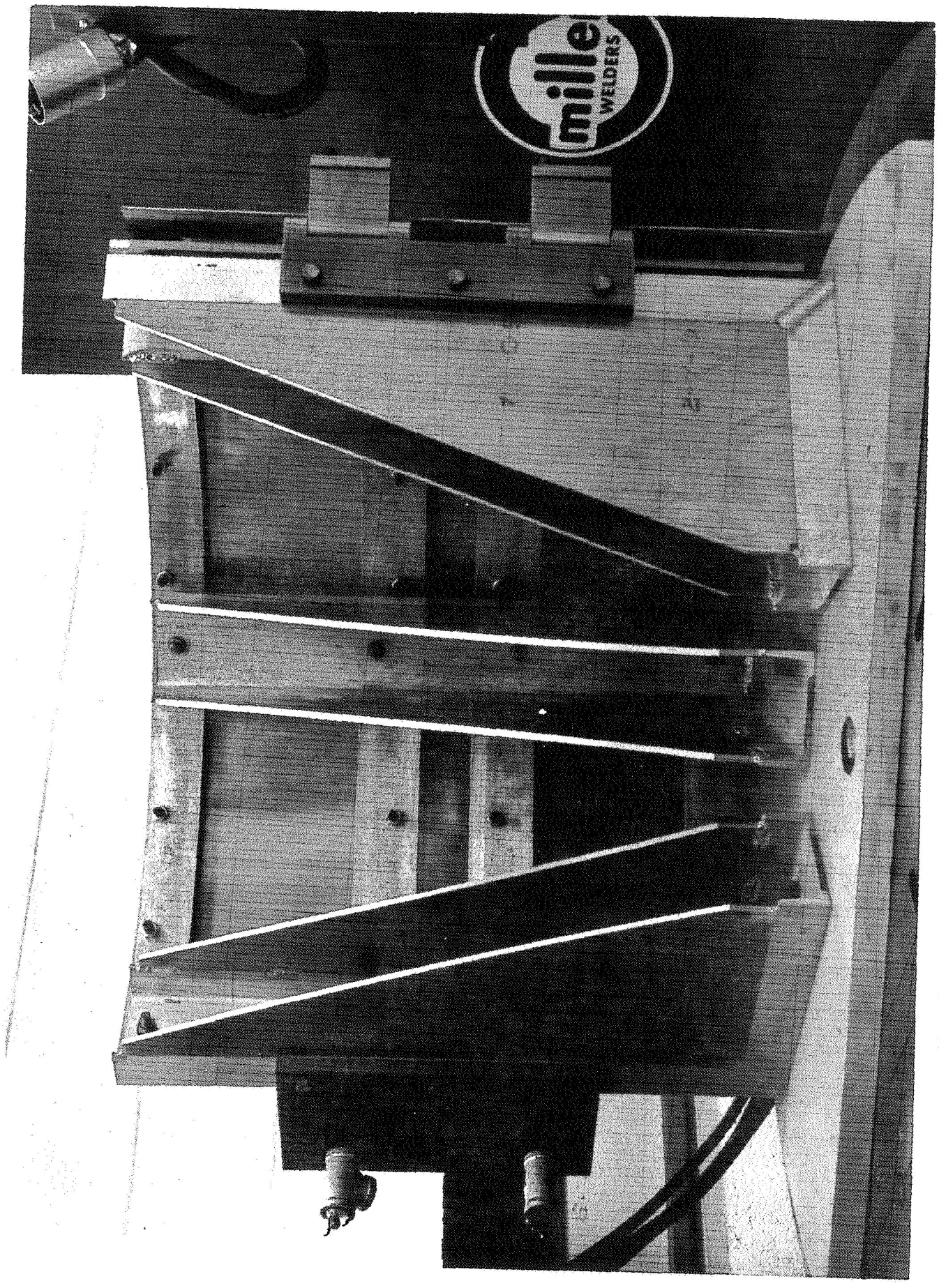


Figure 79: Rear view of cylindrical fixture with parts clamped in place.

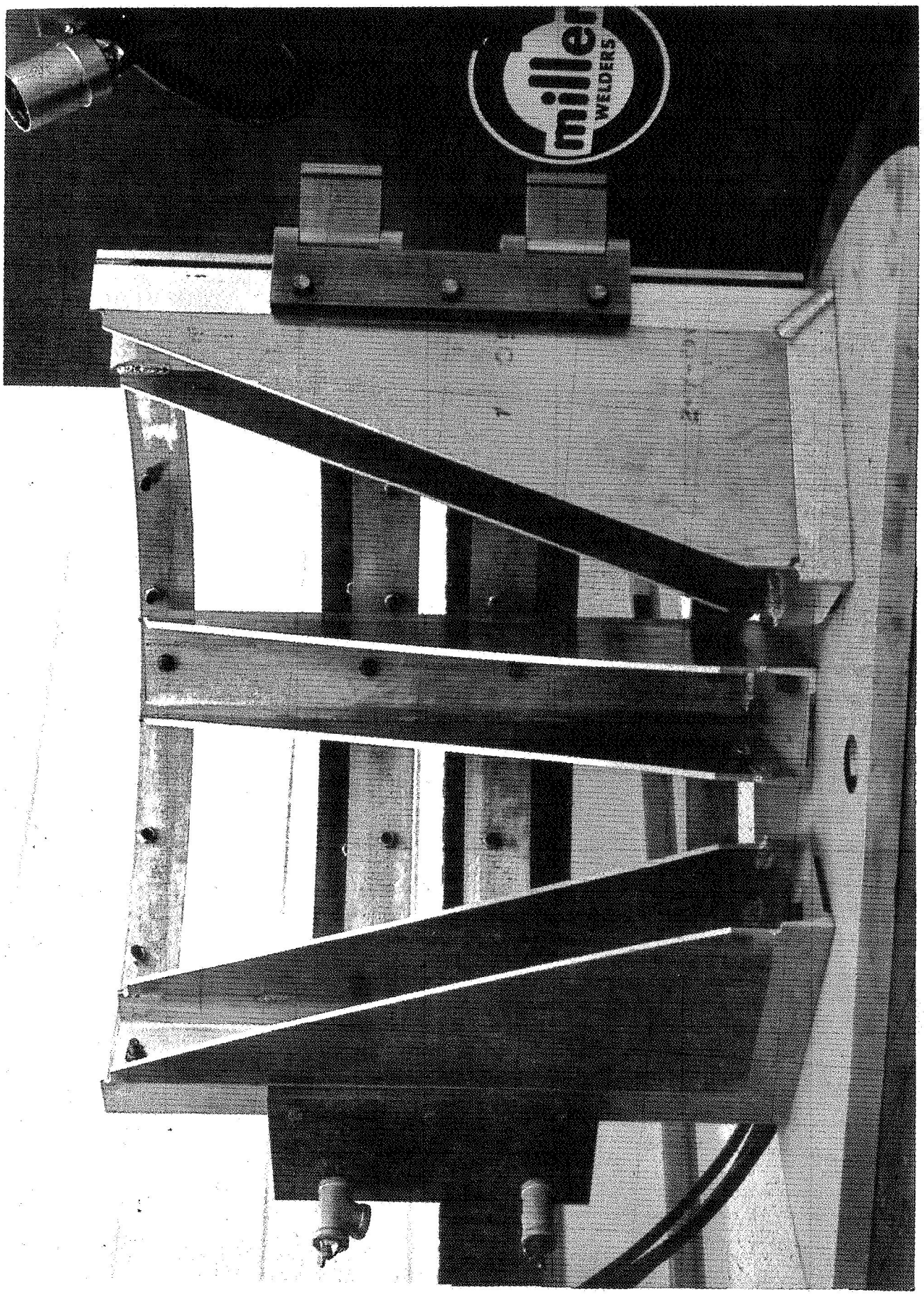


Figure 80: Cylindrical fixture, rear view.

5.1.10.2 The position of the probe relative to the puddle center could not change during movement of the torch.

5.1.10.3 A means had to be provided for adjusting and measuring the probe position relative to the puddle center.

5.1.10.4 The entire mechanism had to be rigid enough to avoid fluctuations in location during a weld program.

The hybrid probe and torch assembly are shown in Figure 81. A spring loaded Smith-Russell linkage assures that vertical movement of the probe is parallel to the vertical movement of the voltage control mechanism, thus maintaining a constant relative position between the probe and electrode. Longitudinal and cross seam adjustments are made through the use of vernier scales. The longitudinal adjustment is shown in Figure 82, and the cross seam adjustment is shown in Figure 83. The proper position of the probe with respect to the electrode is shown in Figure 84. The probe and torch assembly are shown during a test weld in Figures 85 and 86.

5.1.11 ADAPTIVE CONTROLLER

Electrically, the adaptive controller was the same as used in the prototype system (see the schematic diagram, Figure 53). The finalized mechanical layout is shown in Figure 87. Views of the front panel, top, botton, and rear of the controller are shown in Figures 88 through 92.

5.2 THICK-PLATE EXPERIMENTS

5.2.1 THERMOCOUPLE OUTPUT VERSUS PENETRATION

A series of experiments were conducted on 0.375 inch thick samples, 10 inches wide and 24 inches long, to determine under what conditions a functional relationship existed between thermocouple output and penetration.

5.2.1.1 On test specimen number 40, the weld current was varied in 10 ampere increments from 150 ampere to 210 amperes as shown in Figure 94. The weld conditions were: arc voltage, 12 volts; travel speed, 8 ipm; shielding gas, Helium at 100 CFH; thermocouple probe location, 18/64 inch abeam and 15/64 inch behind center of puddle; and Moseley strip chart settings, 2 ipm chart speed and 5 mv/inch sensitivity. The thermocouple recording is shown in Figure 93;

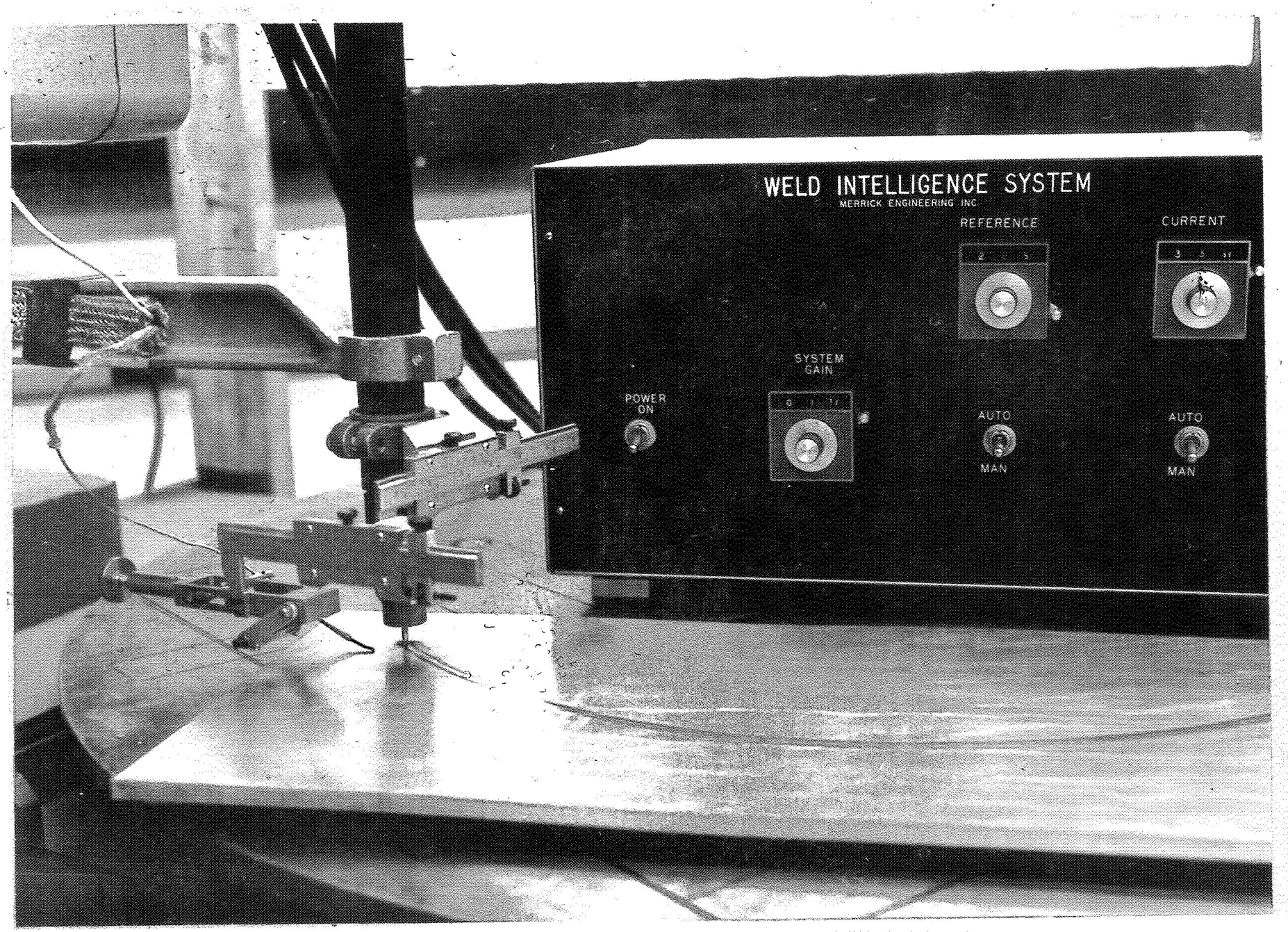


Figure 81: Torch, hybrid probe, and adaptive feedback controller.

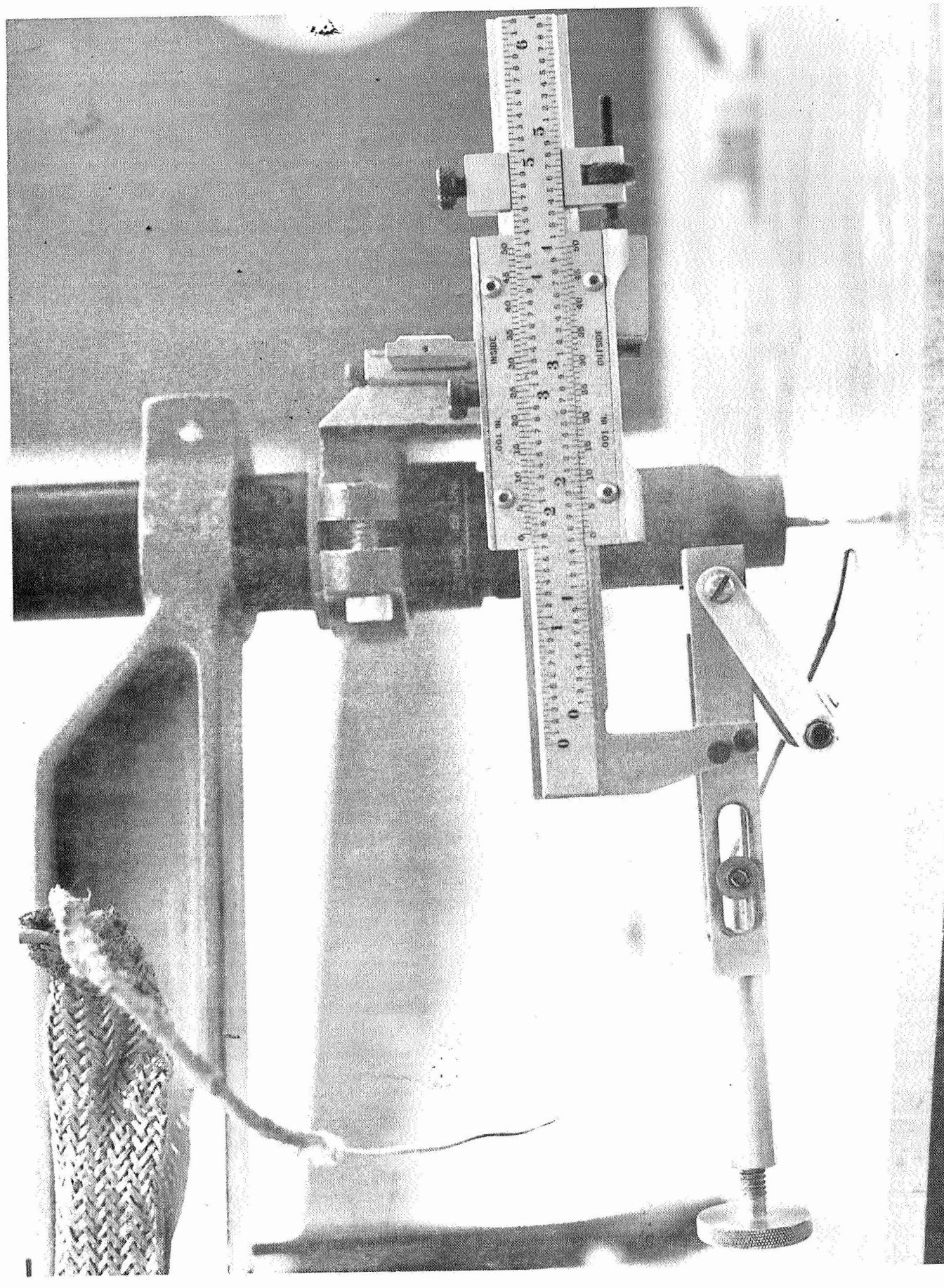


Figure 82: Hybrid probe assembly, vernier scale adjustment.

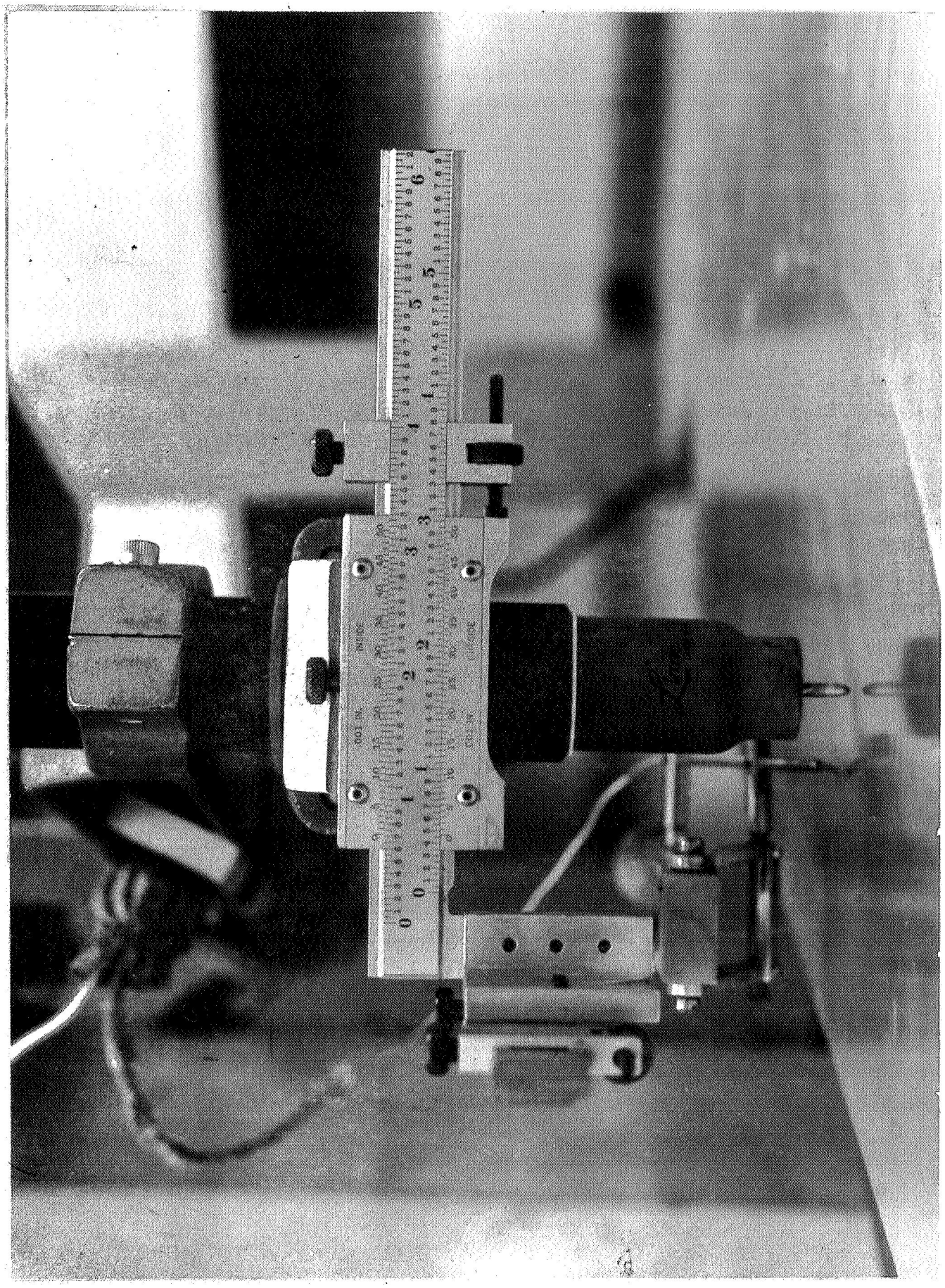


Figure 83: Hybrid probe assembly, vernier scale adjustment.

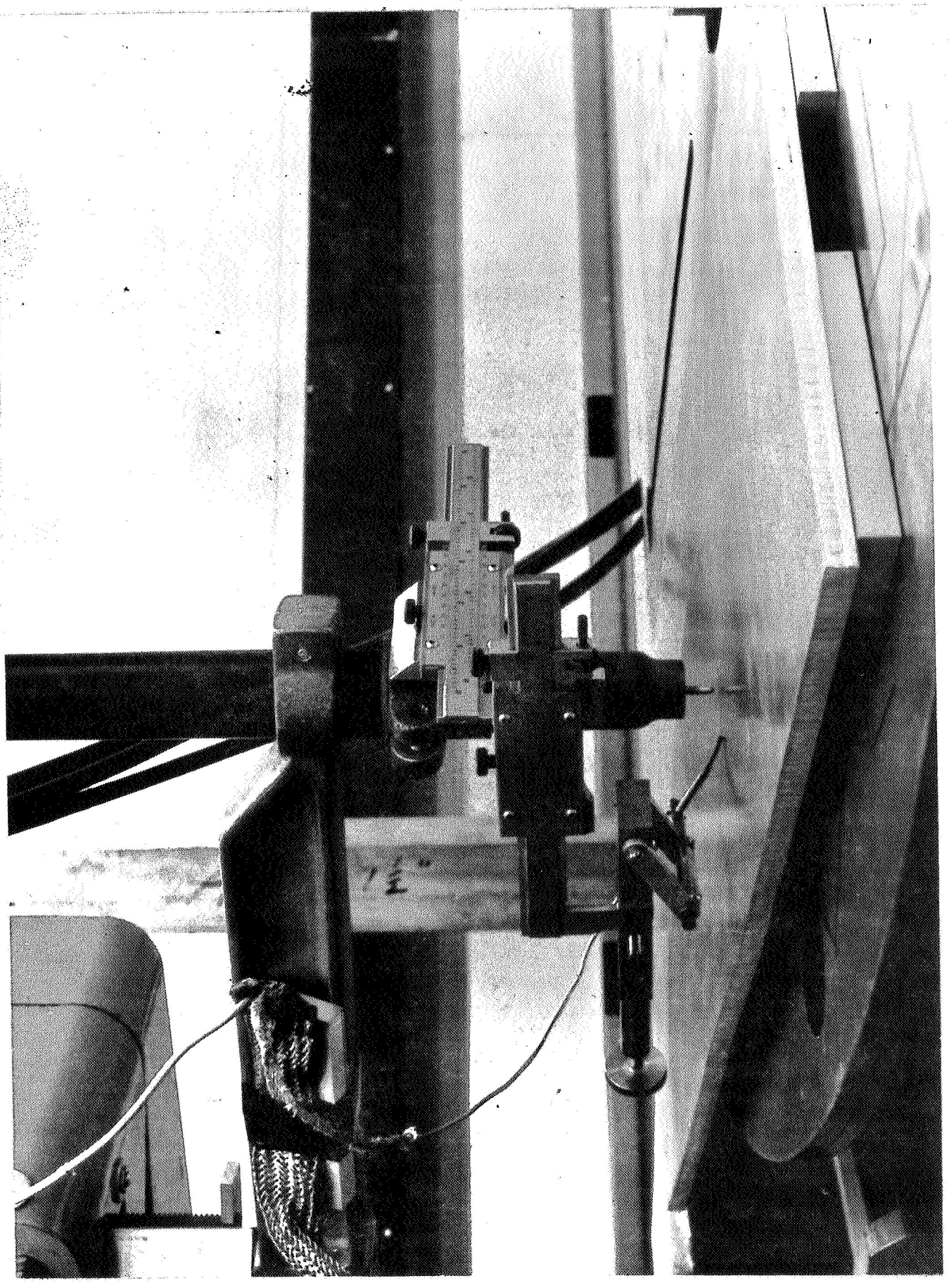


Figure 84: Position of hybrid probe with respect to electrode.

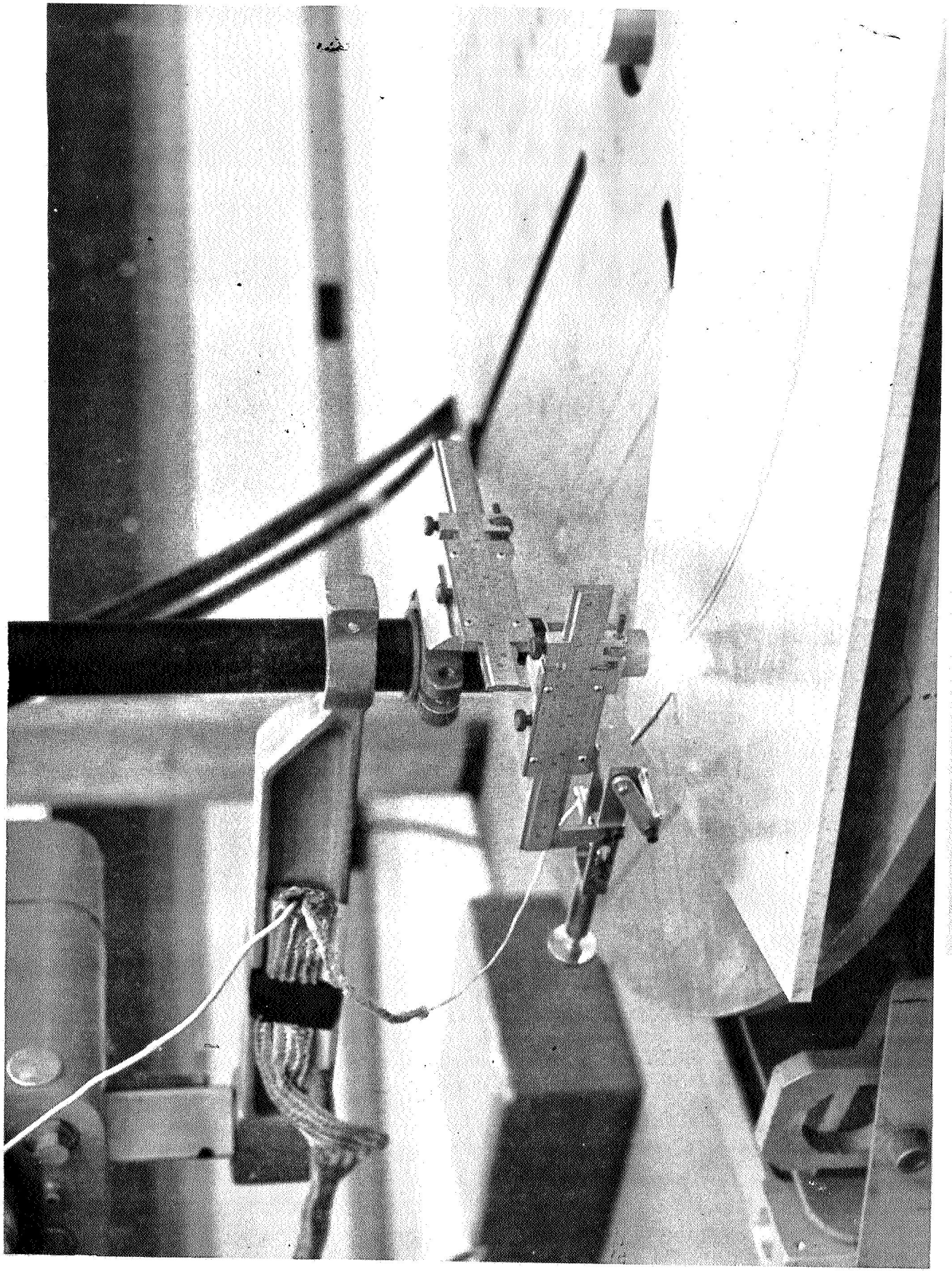


Figure 85: Hybrid probe and torch assembly during weld.

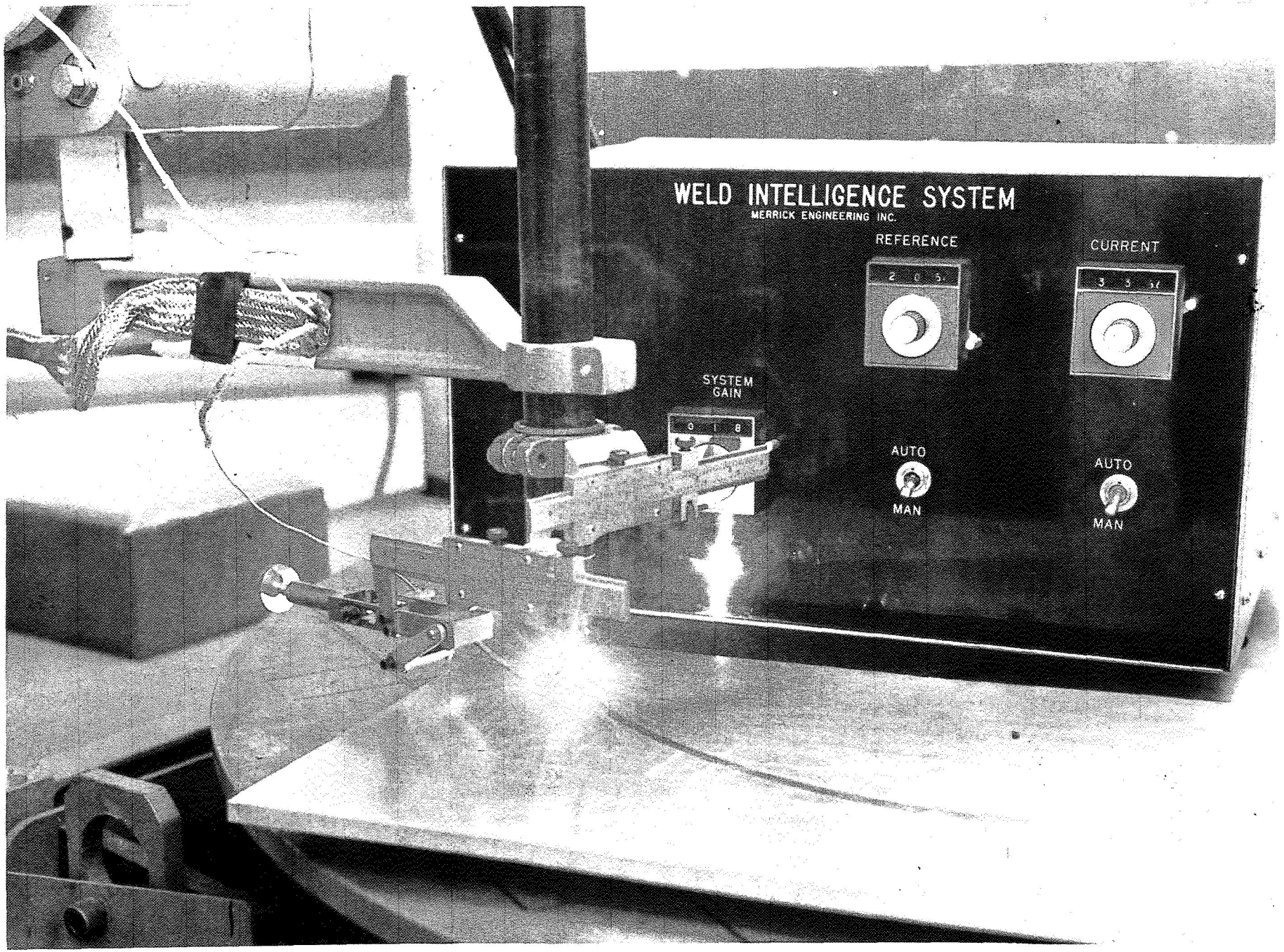


Figure 86: Hybrid probe, torch, and adaptive controller during weld.

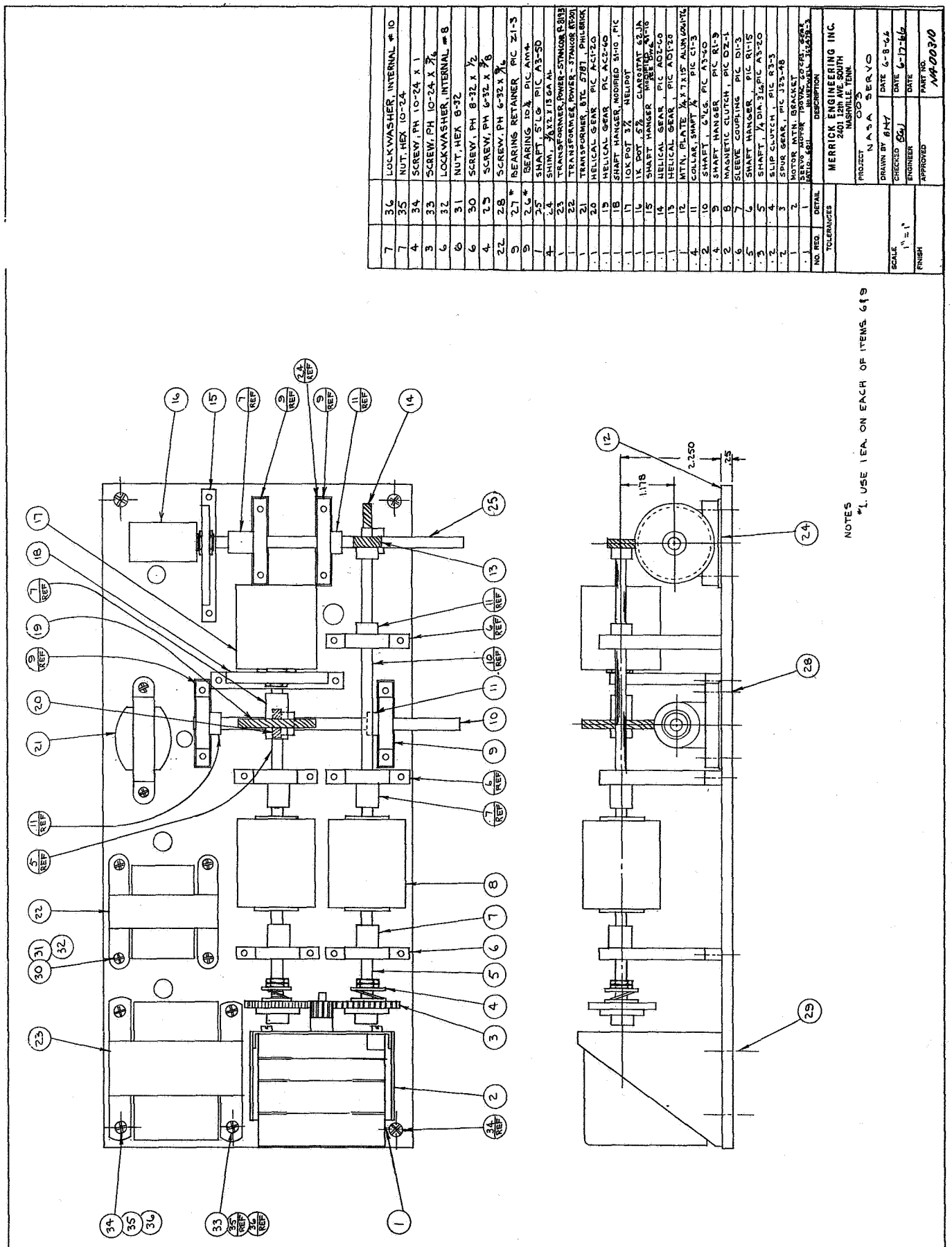


FIGURE 87: Adaptive Controller Layout

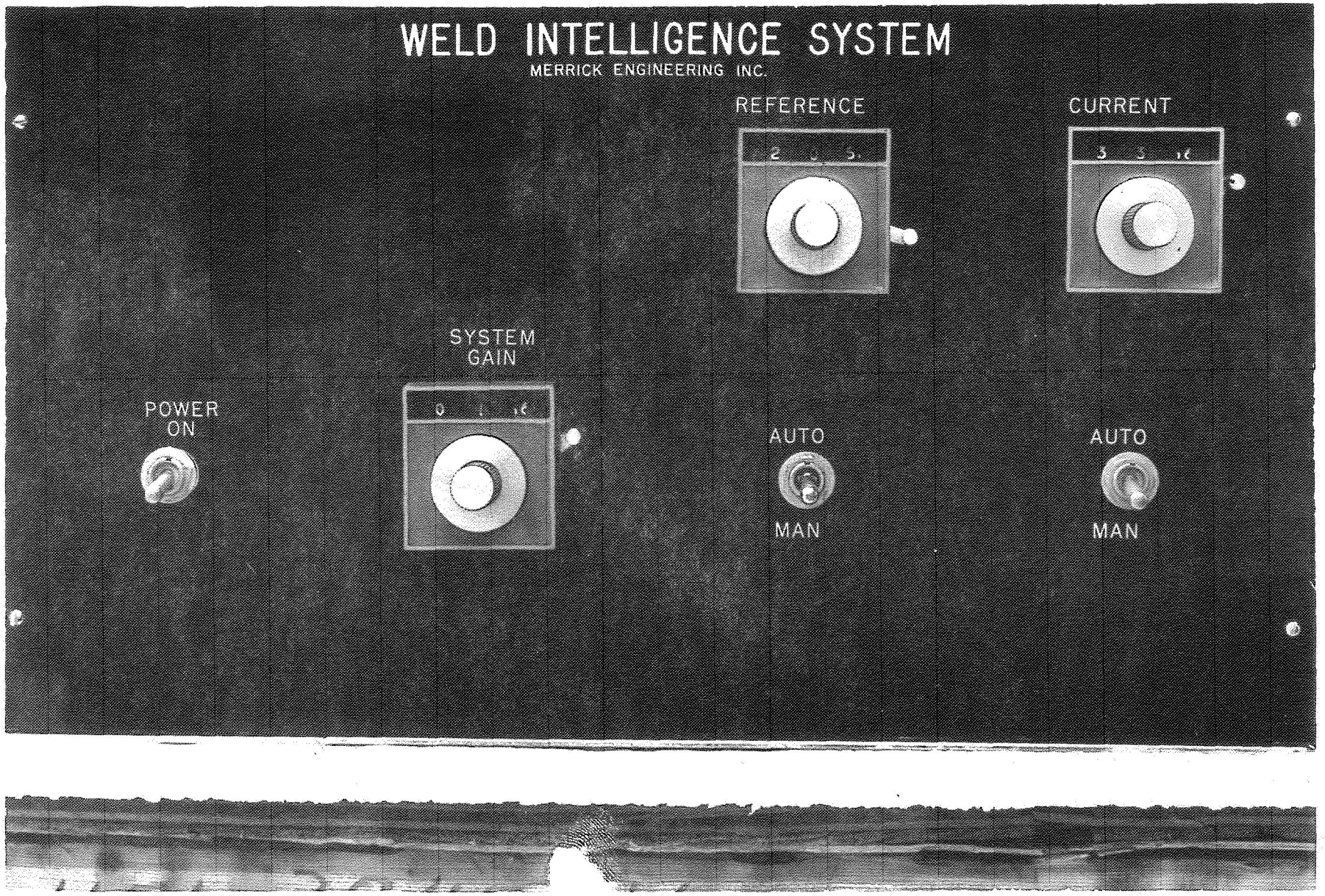


Figure 88: Front panel, adaptive controller

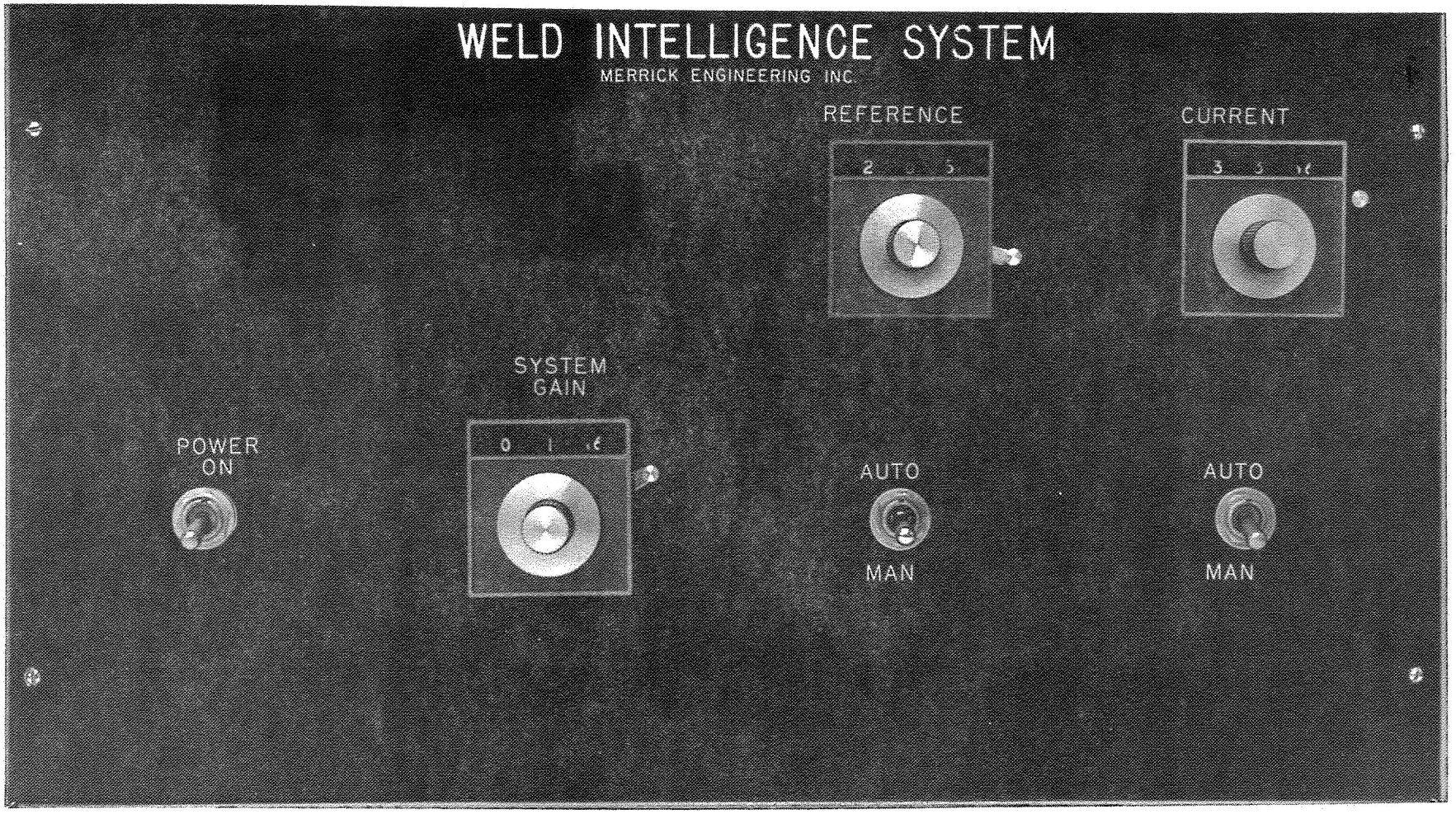


Figure 89: Front Panel, adaptive controller.

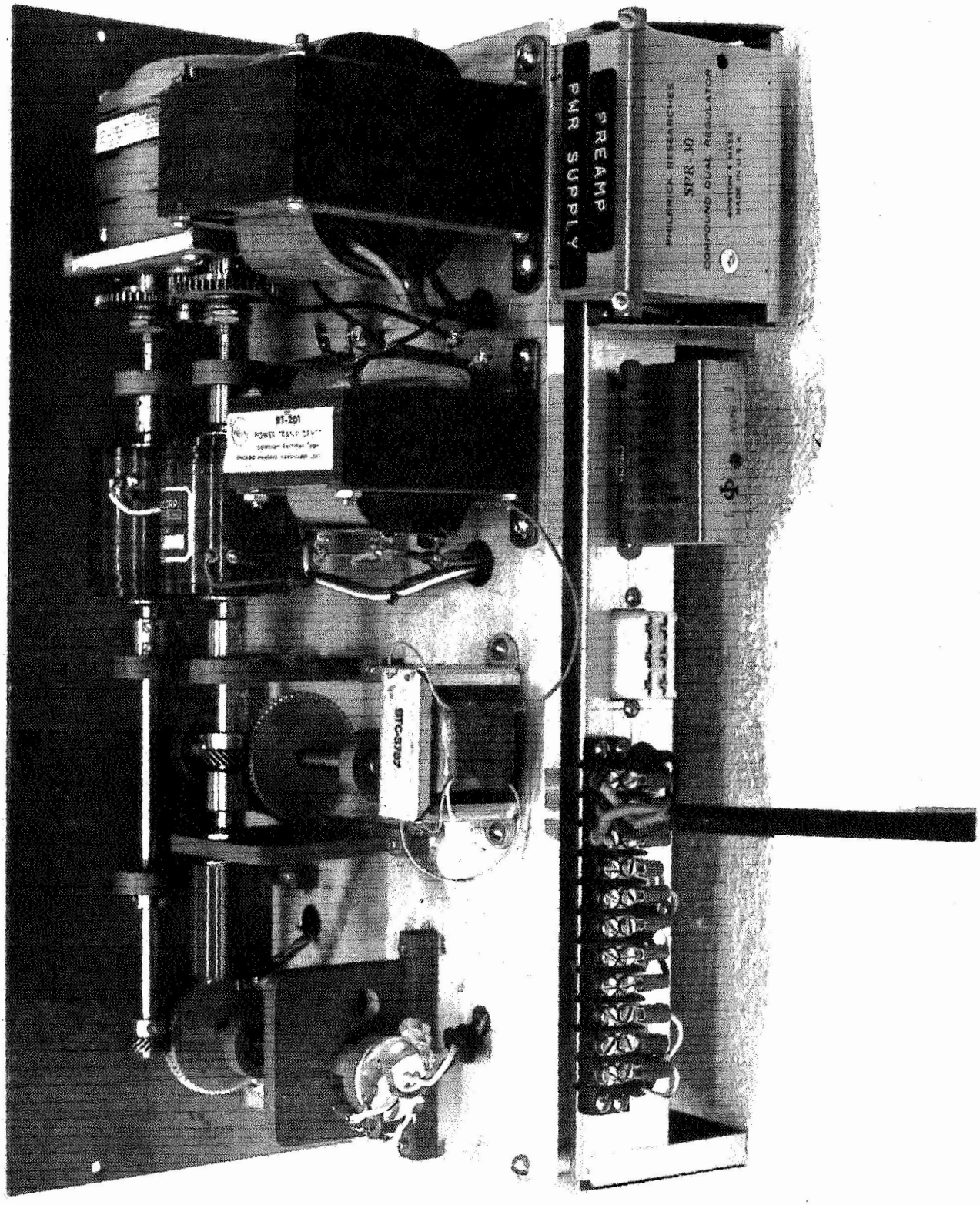


Figure 90: Top view, adaptive controller.

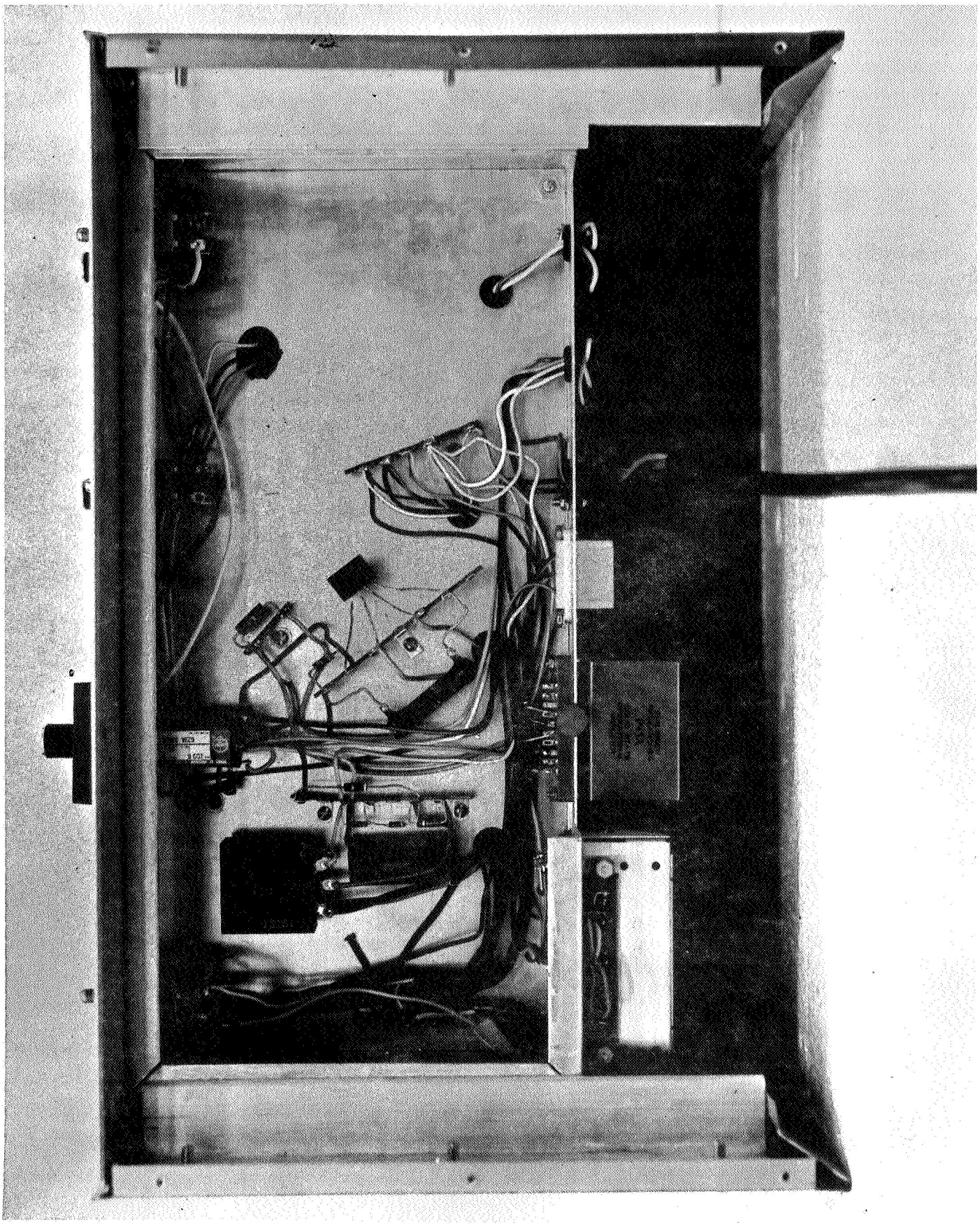


Figure 91: Bottom view, adaptive controller.

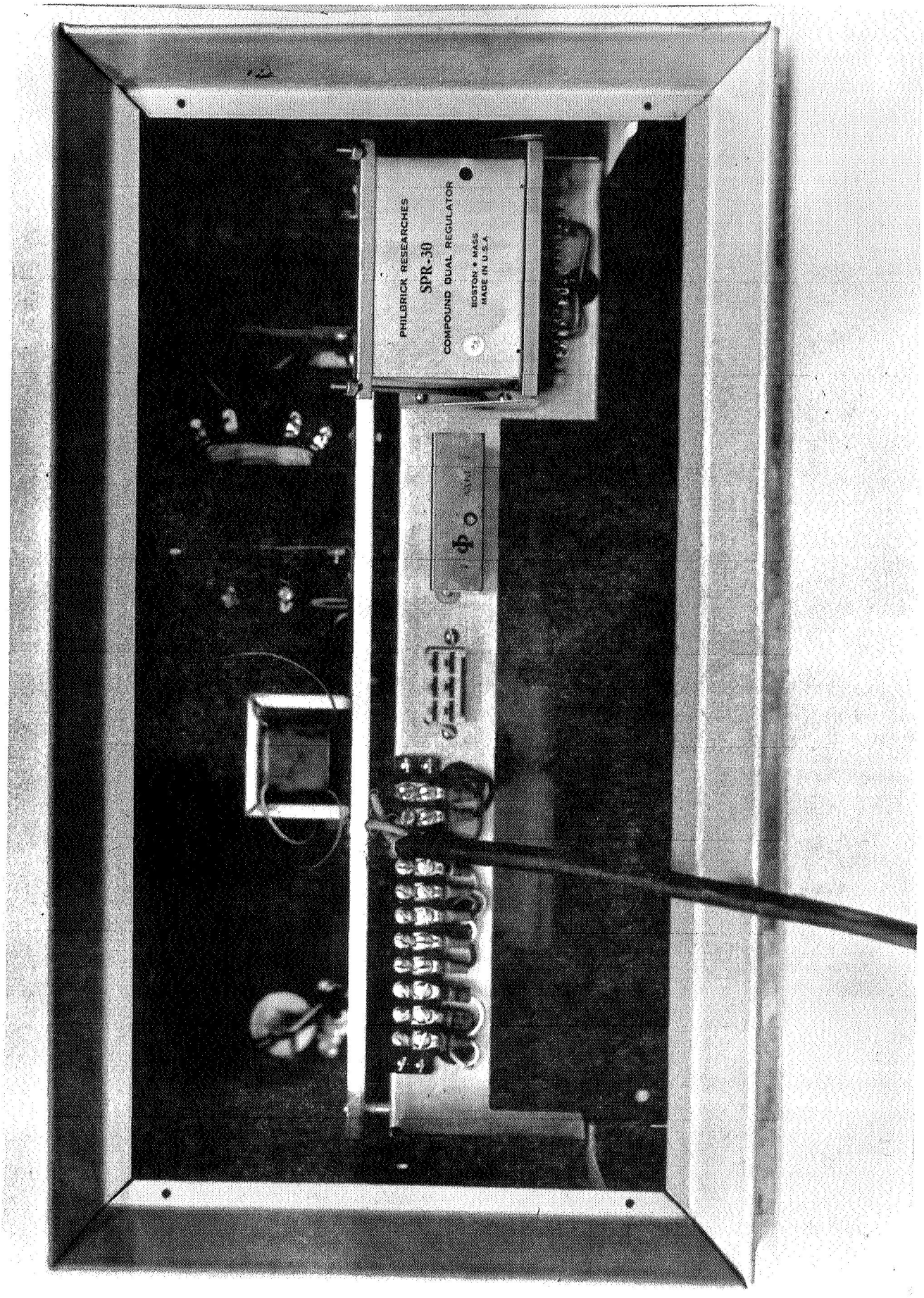


Figure 92: Rear view, adaptive controller.

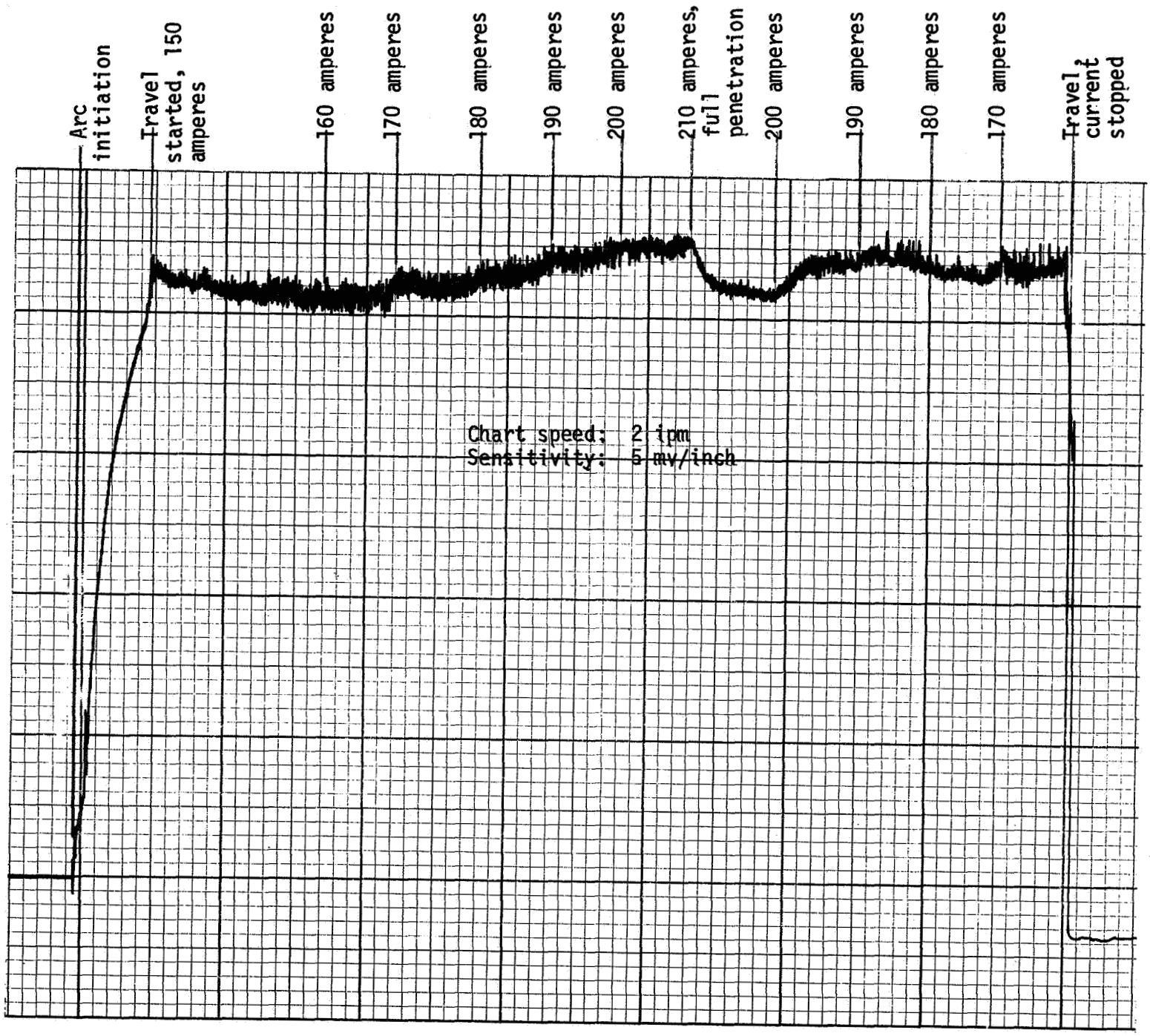


Figure 93: Hybrid thermocouple output, test number 40.

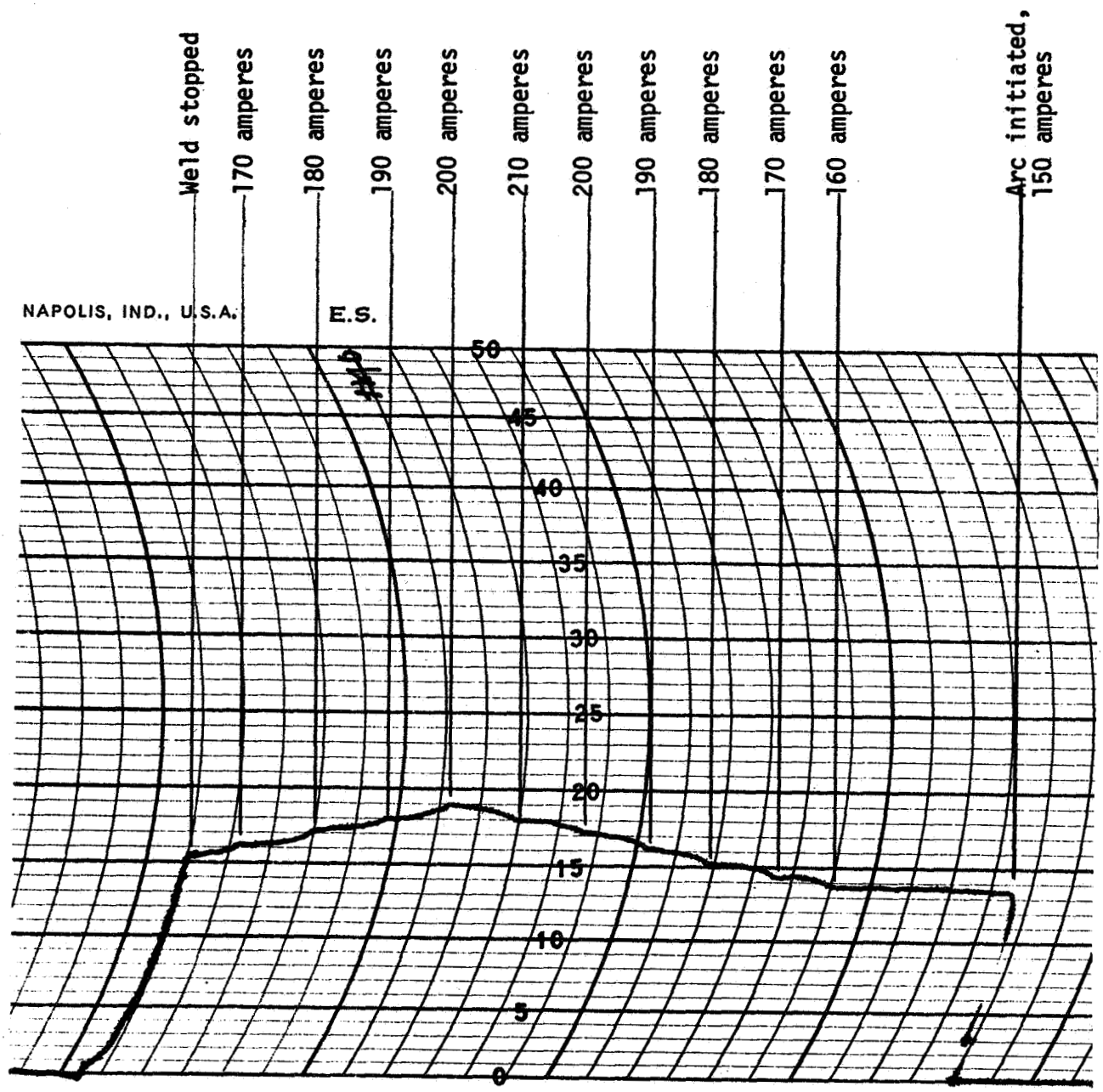


Figure 94: Welding current, test number 40.

the front and back sides of the weldment are shown in Figures 95 and 96; and cross sections of the weldment are shown in Figure 97. As can be seen in Figures 96 and 97, full penetration occurred at 210 amperes. Referring to Figure 93, the thermocouple output decreased when the current was changed from 200 to 210 amperes and increased for increasing current for all other values corresponding to partial penetration. The conclusion drawn from this experiment was that it would be difficult to control full penetration welds on thick plates. See section 2.1.1.2.3 for further discussion.

5.2.1.2 Tests numbers 41 and 42 were run to illustrate the relationship that does exist between penetration and thermocouple output on partial penetration welds. On both welds the parameters were: arc voltage, 12 volts; travel speed, 8 ipm; shielding gas, Helium at 100 CFH; Moseley strip chart settings, 2 ipm chart speed and 5 mv/inch sensitivity; and thermocouple probe location, 18/64 inch abeam and 15/64 inch behind center of puddle. The thermocouple recordings, front and back side views, current recordings and cross sections of these two specimens are shown in Figures 98 through 107. As can be seen, in both cases the thermocouple output was proportional to penetration.

5.2.2 PENETRATION CONTROL, PARTIAL PENETRATION WELDS

5.2.2.1 Tests number 27, 28, and 29 were run on 6" X 24" X 0.375" Al plates to test the adaptive control system's ability to maintain penetration on partial penetration welds. Tests numbers 28 and 29 were run without control and tests number 27 was run with the adaptive loop closed.

The weld parameters on these welds were: base current, 150 amperes; arc voltage, 12 volts; travel speed, 8 ipm; shielding gas, Helium at 100 CFH; thermocouple location, 11/32 inch abeam and 6/32 inch behind center of puddle; and Moseley strip chart recorder settings, 2 ipm chart speed and 5 mv/inch sensitivity. The thermocouple recordings, weld current recordings, and cross sections for these three tests are shown in Figures 108 through 113. The thermocouple recording for test number 27 was not obtained due to a malfunction in the Moseley recorder. As can

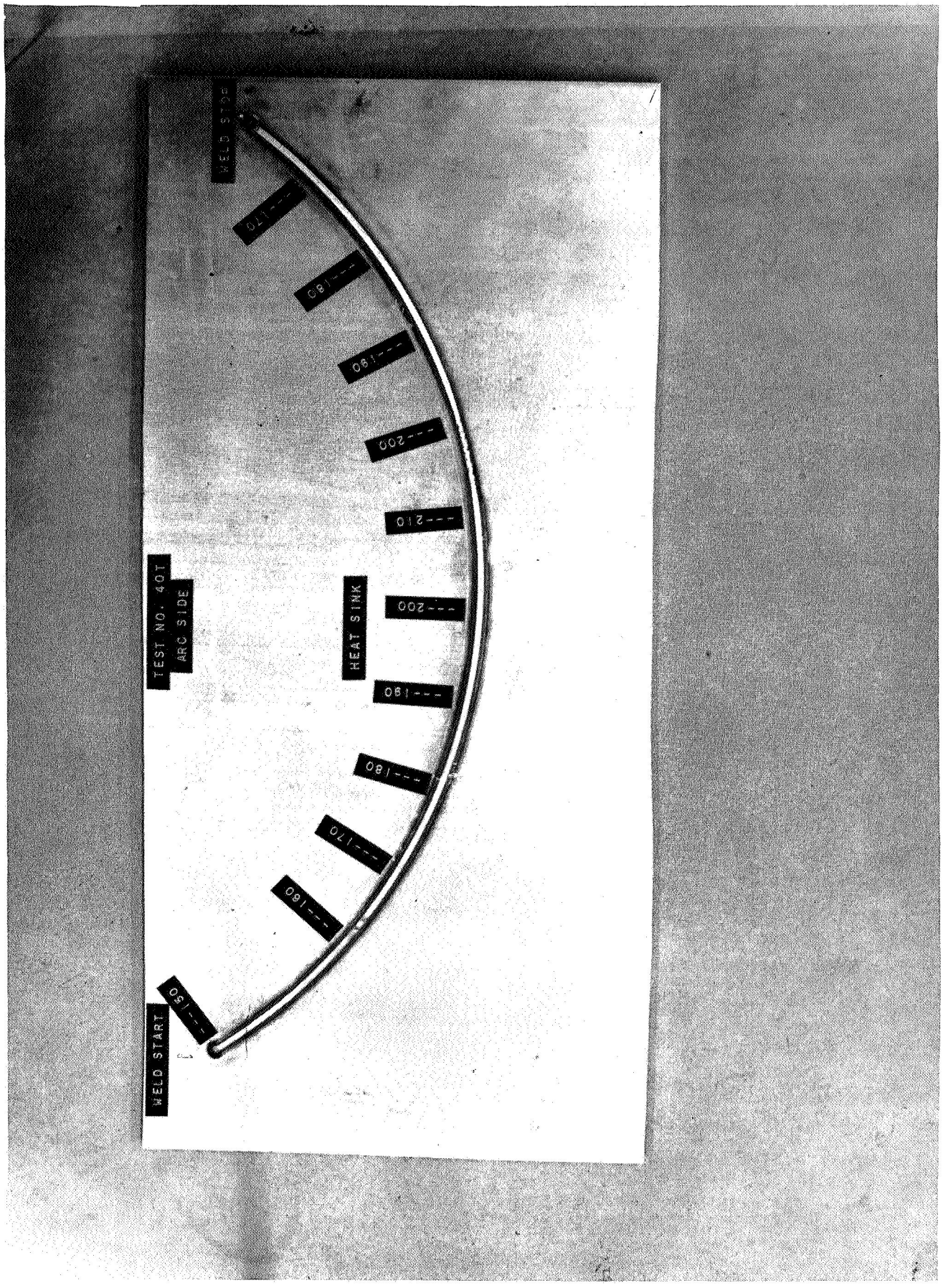


Figure 95: Weld bead, Arc-side, test number 40.

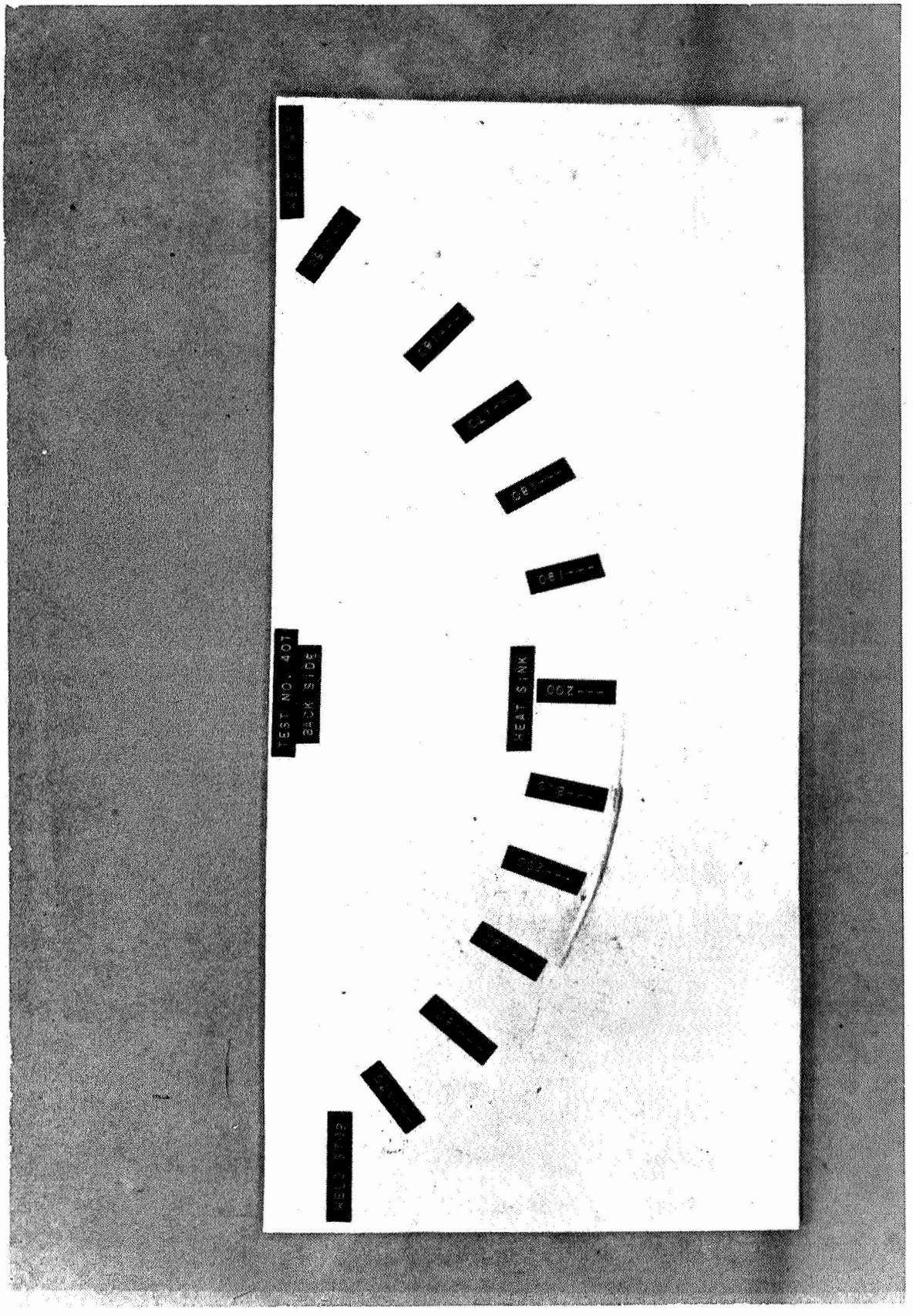


Figure 96: Backside of test number 40.

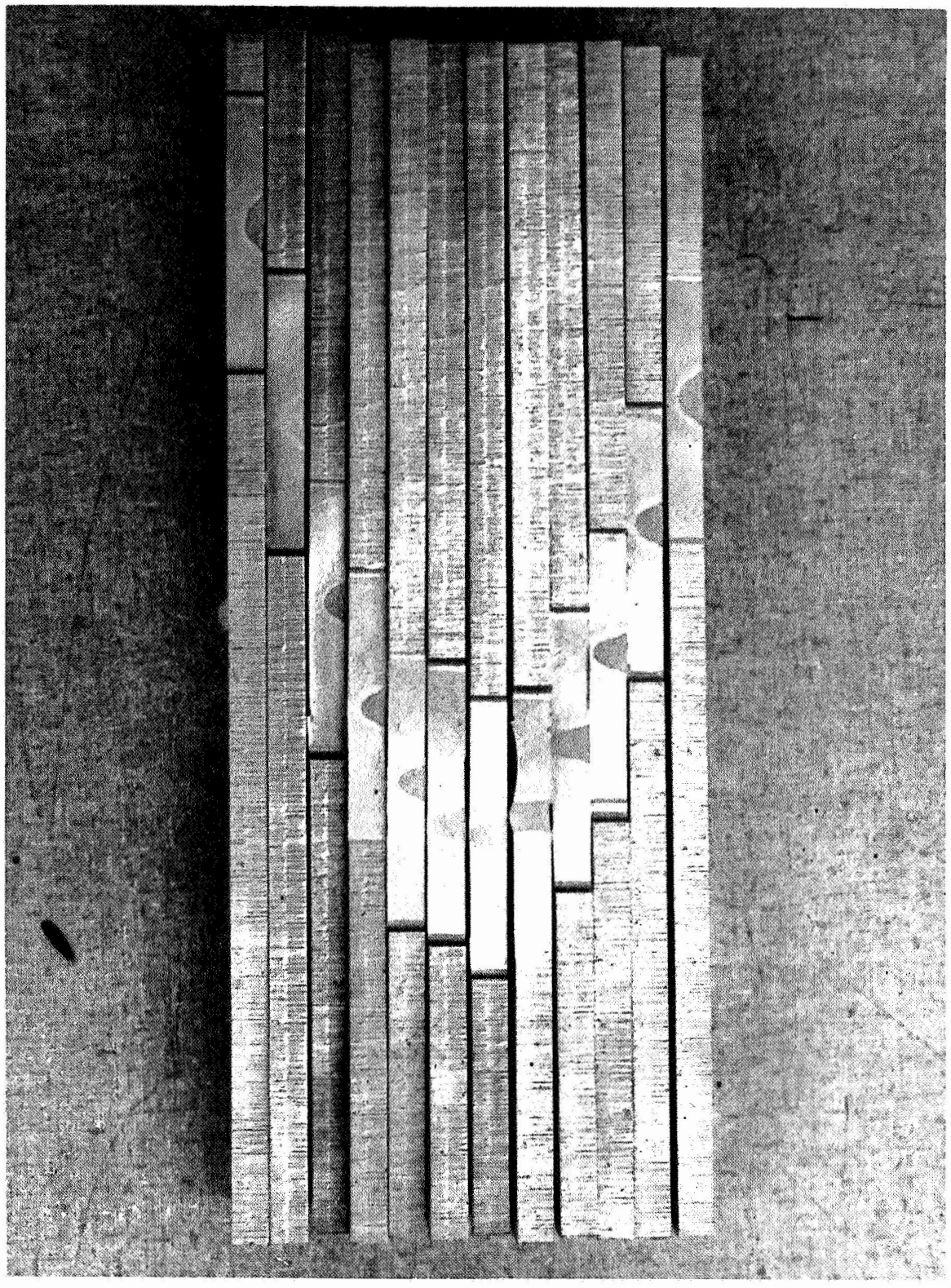


Figure 97: Cross Sections of test Number 40.

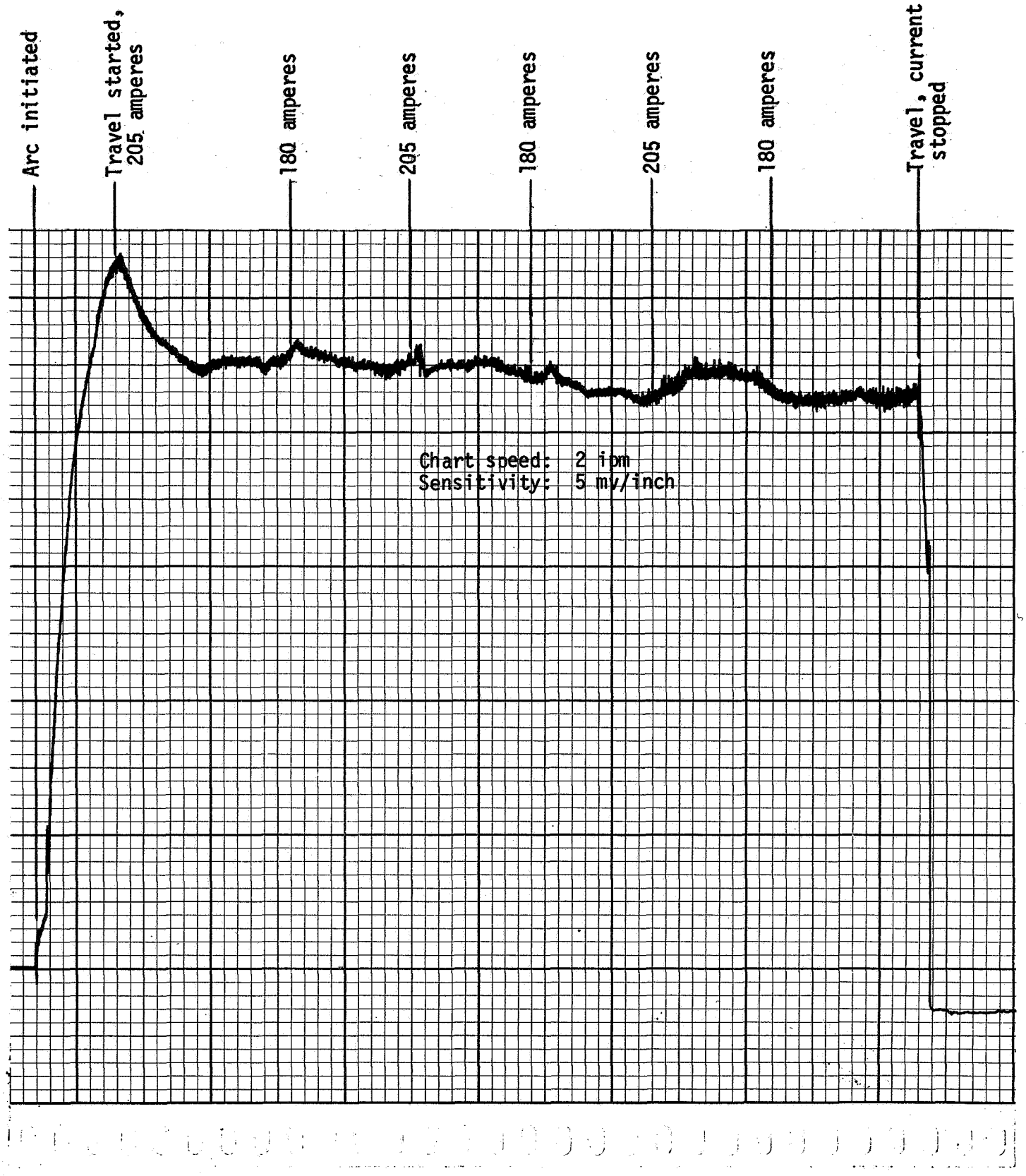


Figure 98: Hybrid thermocouple output, test number 41.

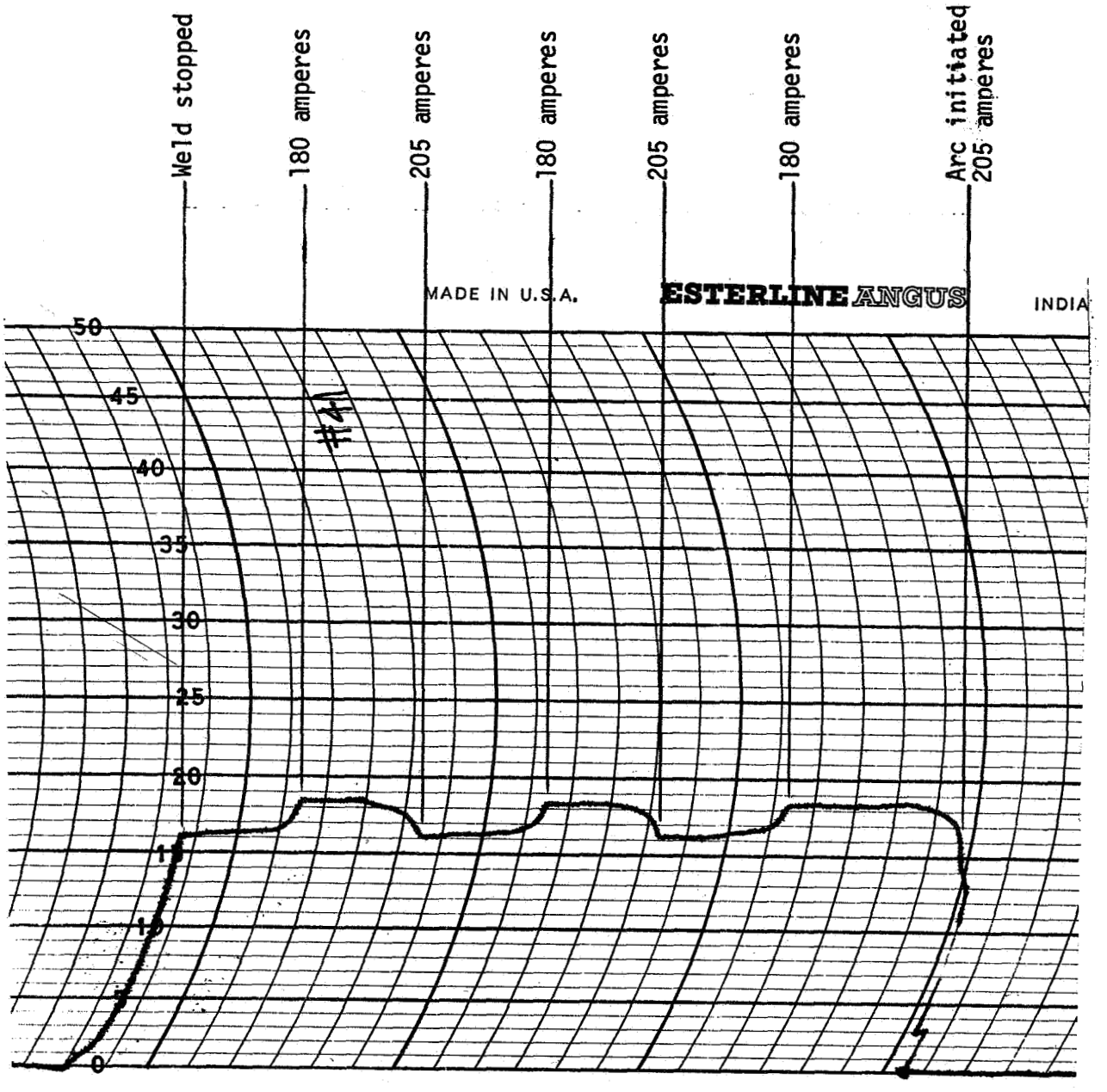


Figure 99: Welding current, test number 41.

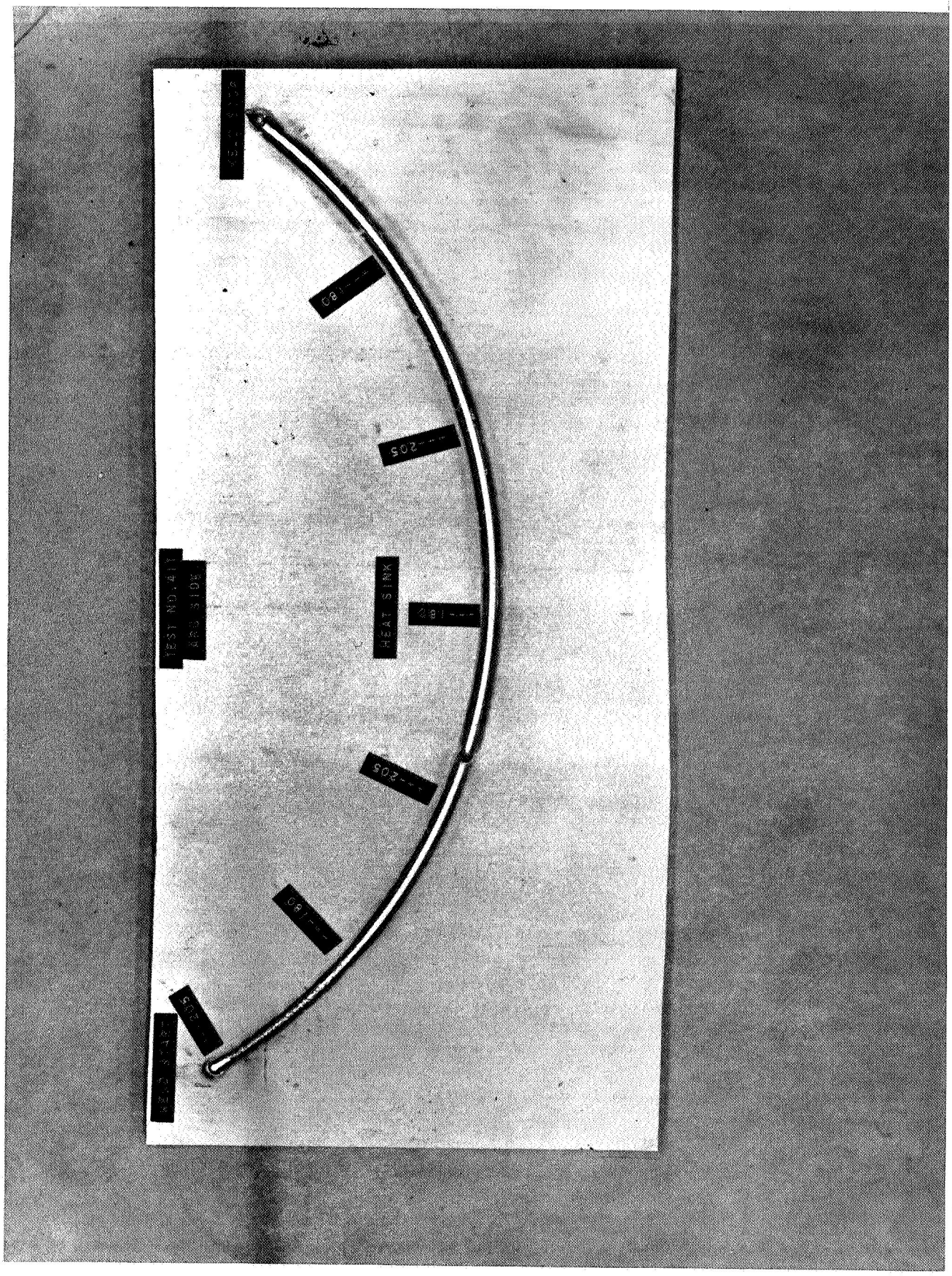


Figure 100: Weld bead, arc-side, test number 41.

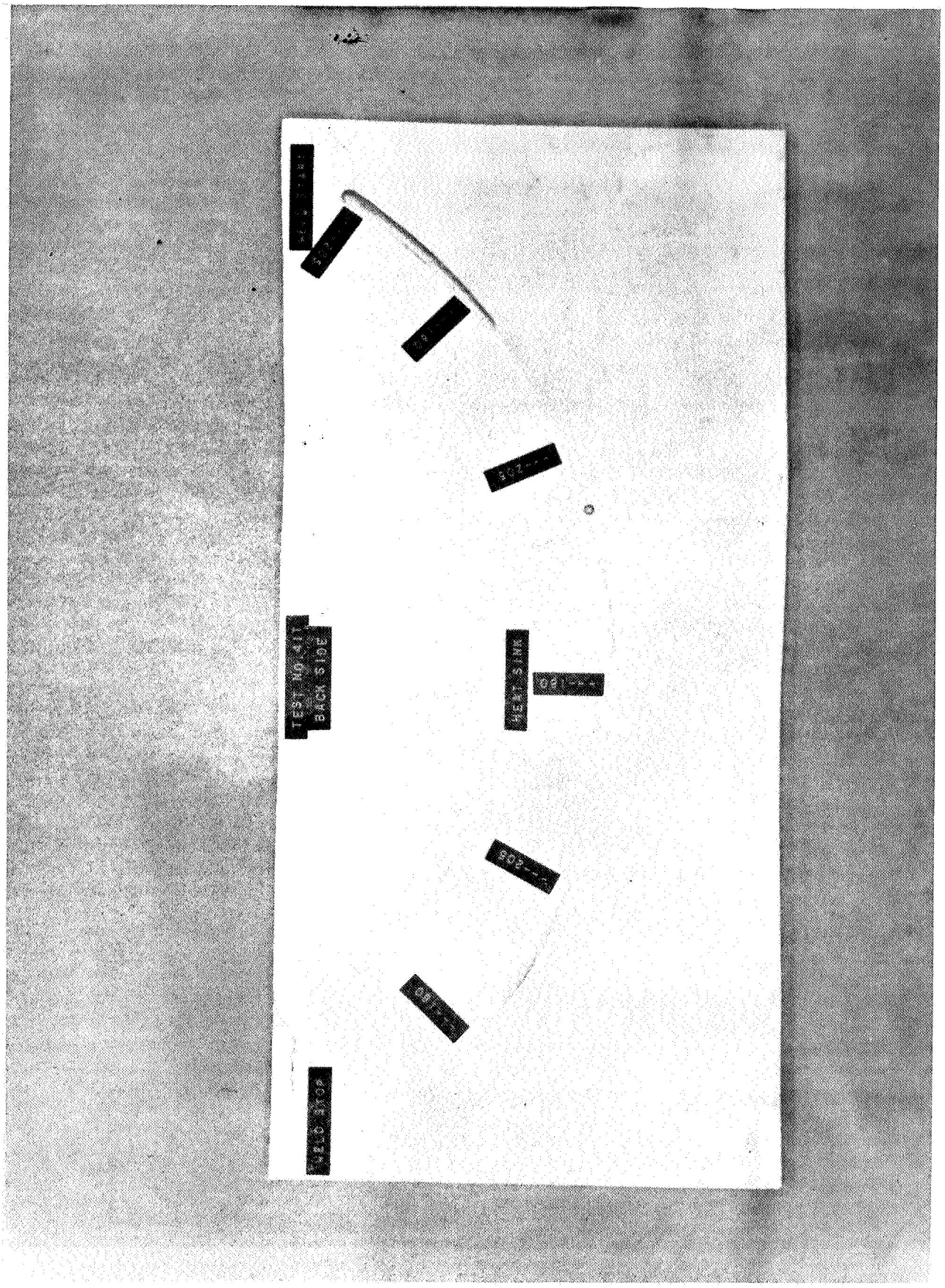


Figure 101: Backside of test number 41.

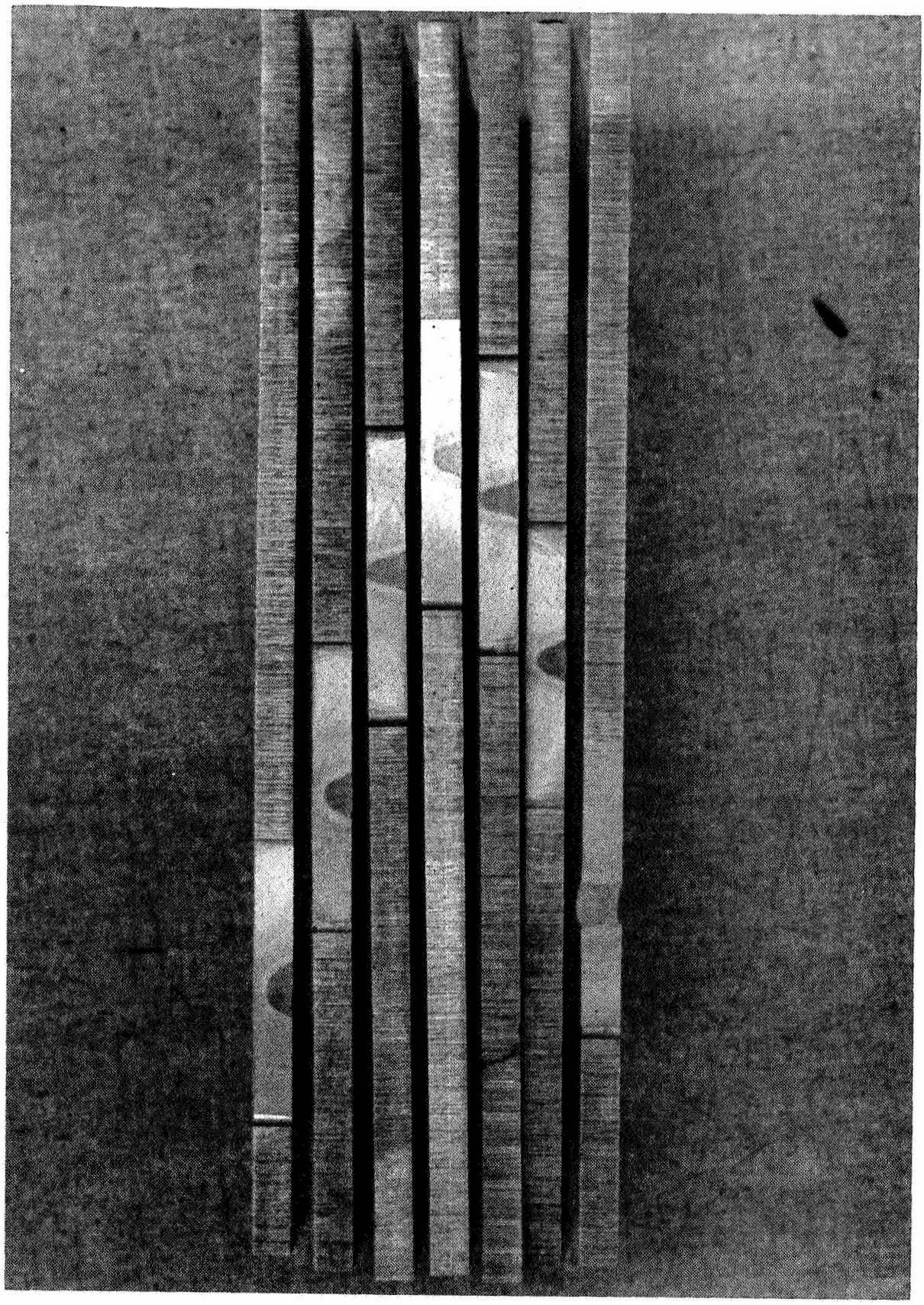


Figure 102: Cross Sections of Test Number 41.

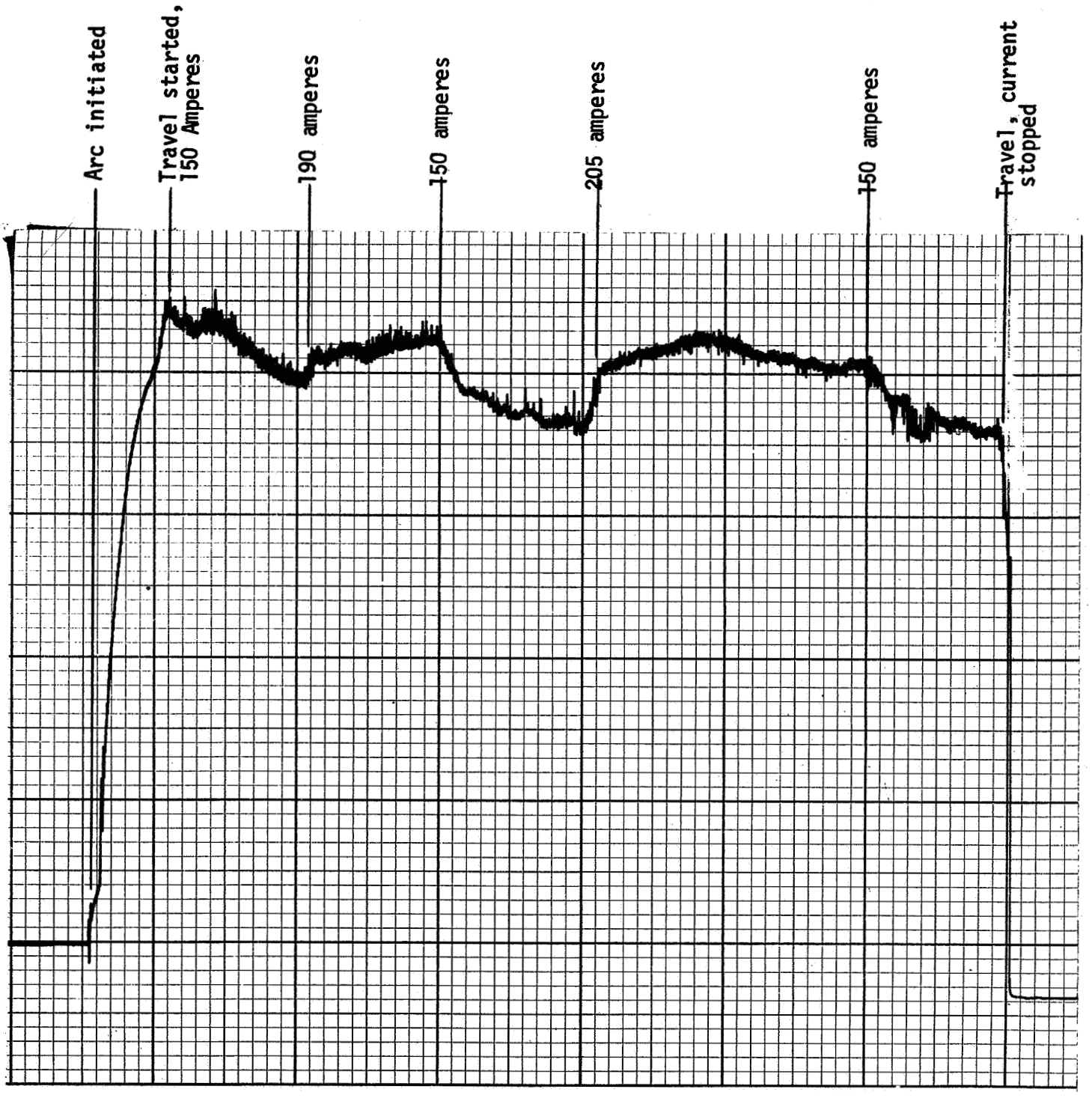


Figure 103: Hybrid thermocouple output, test number 42.

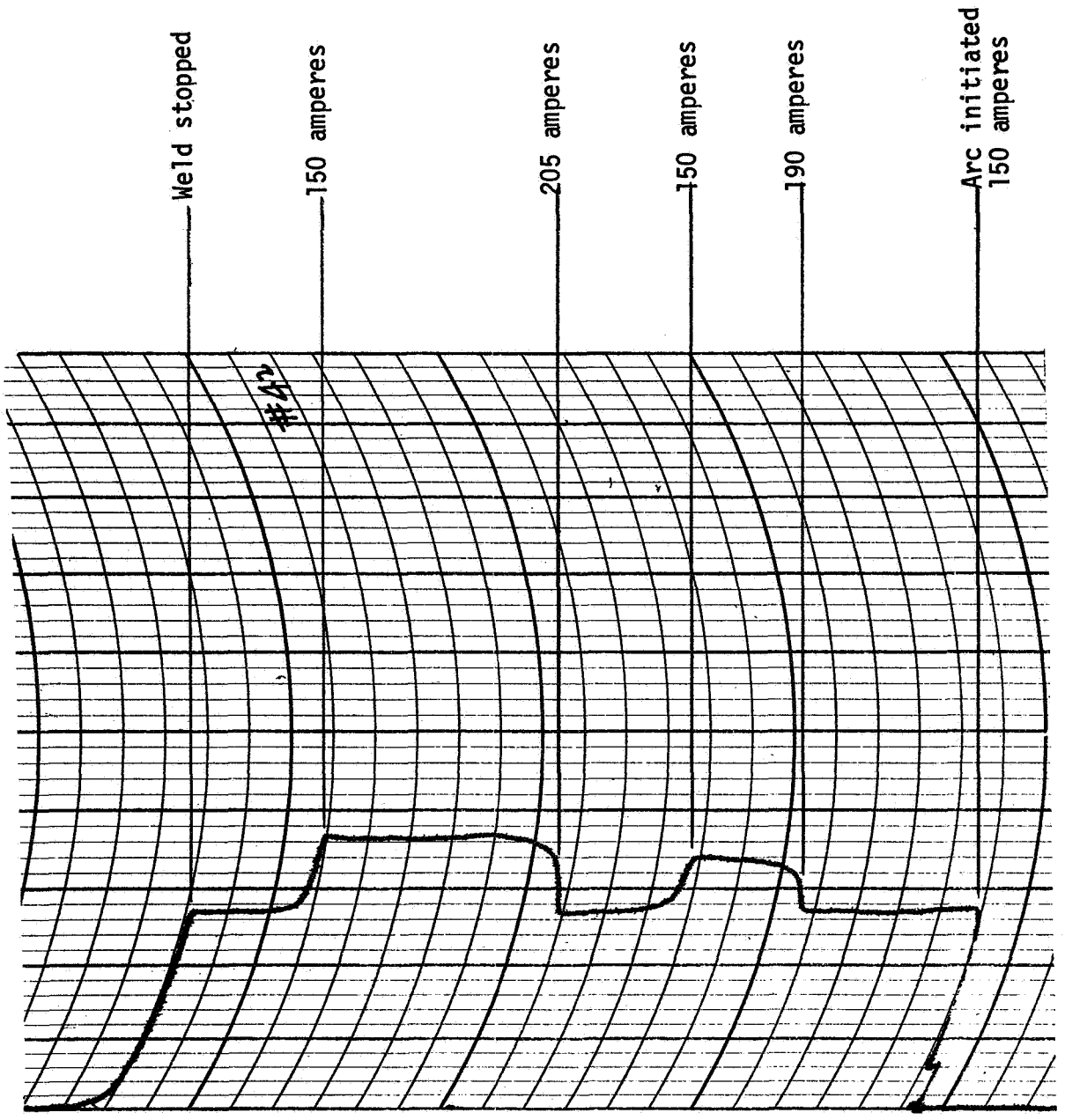


Figure 104: Welding current, test number 42.

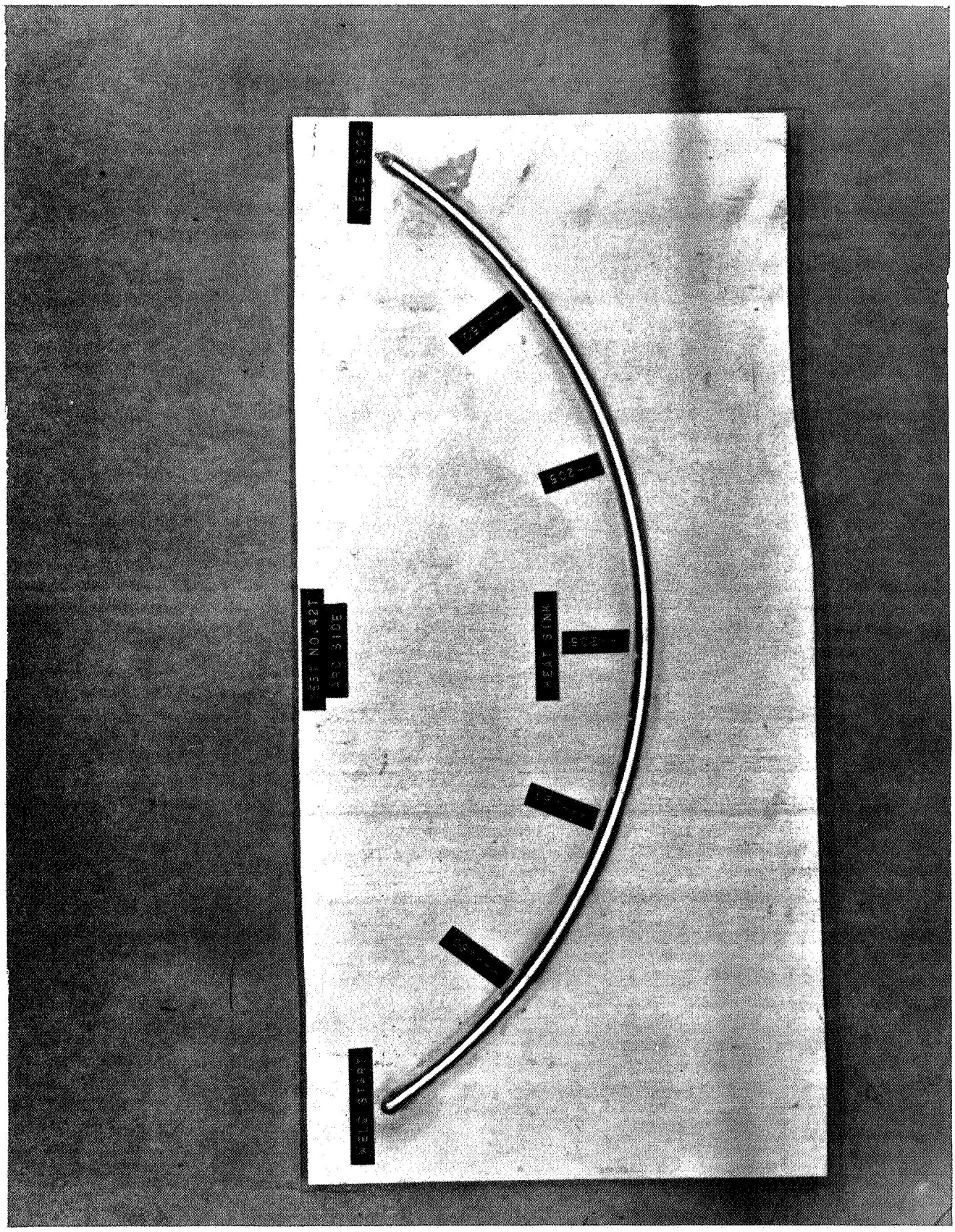


Figure 105: Weld bead, arc-side, test number 42.

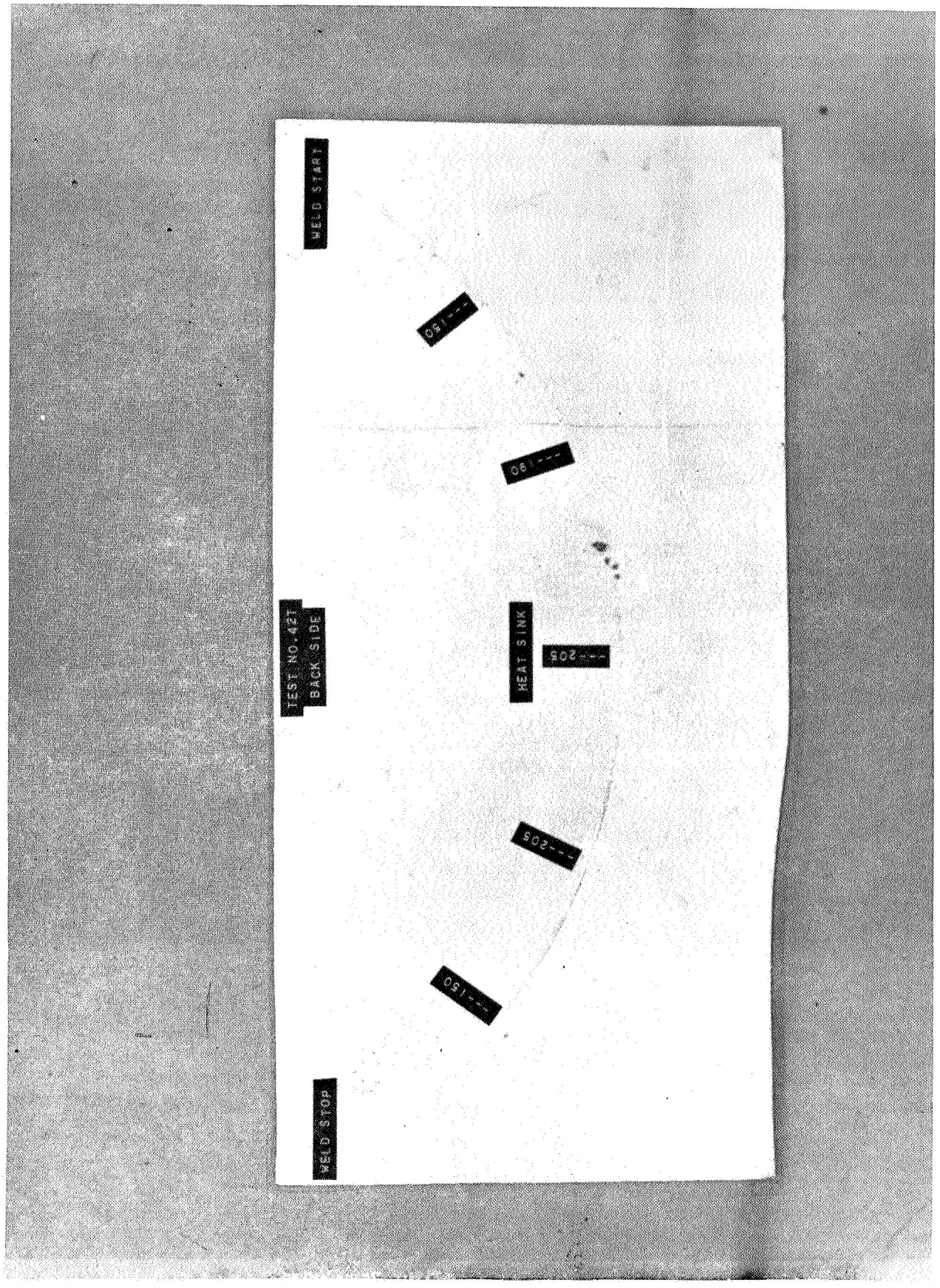


Figure 106: Backside of test number 42.

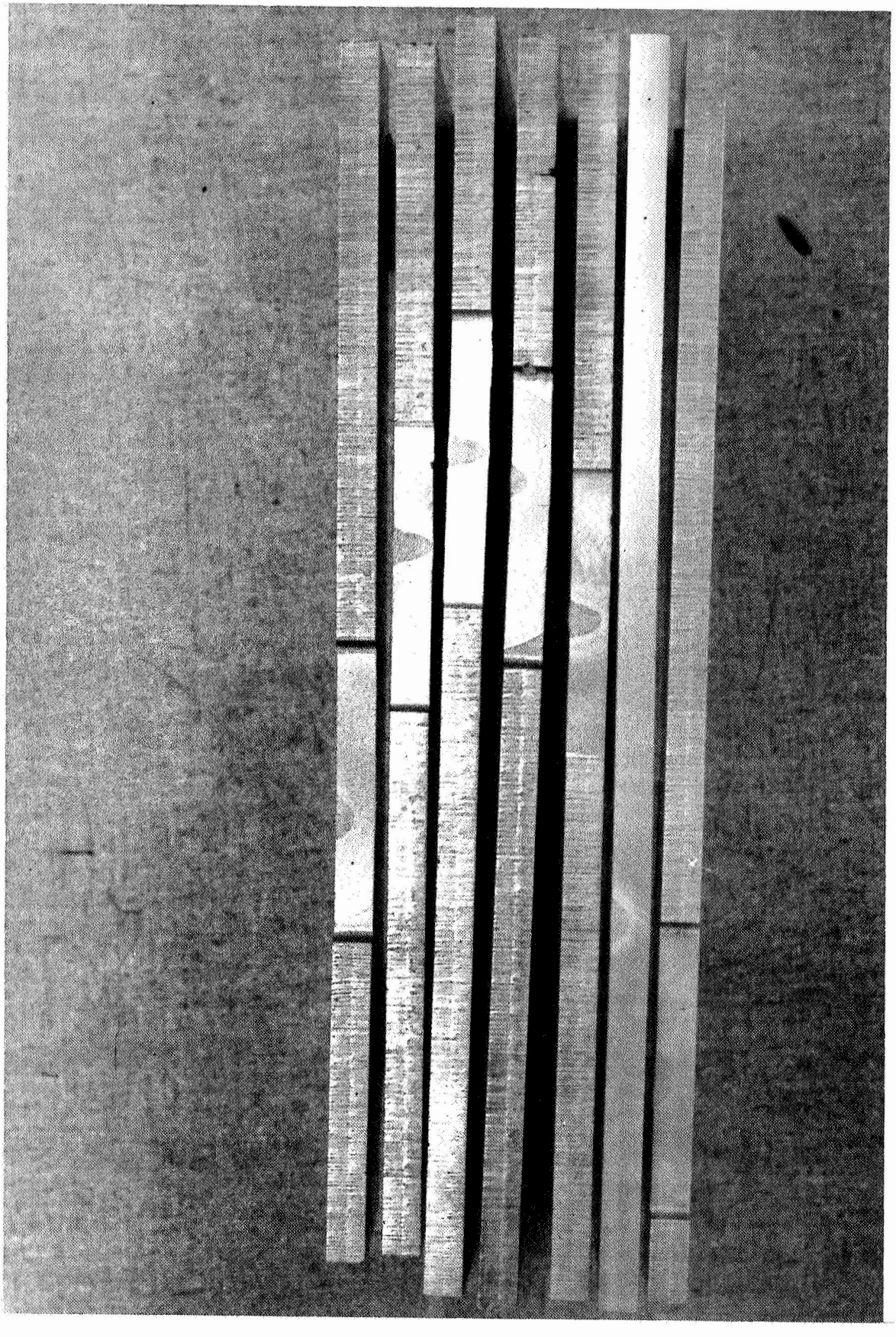


Figure 107: Cross Sections of Test Number 42.

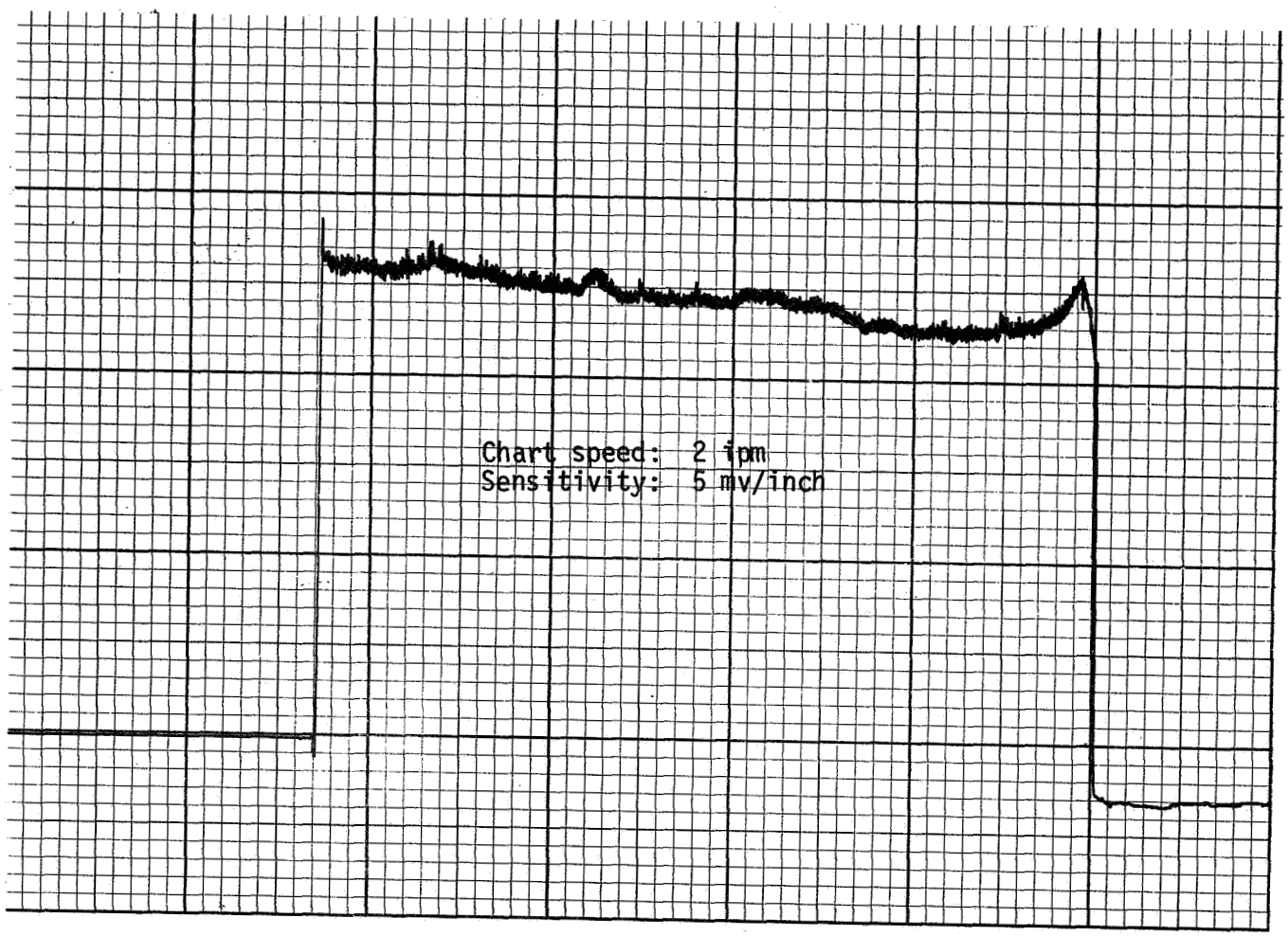


Figure 108: Hybrid thermocouple output, test number 28.

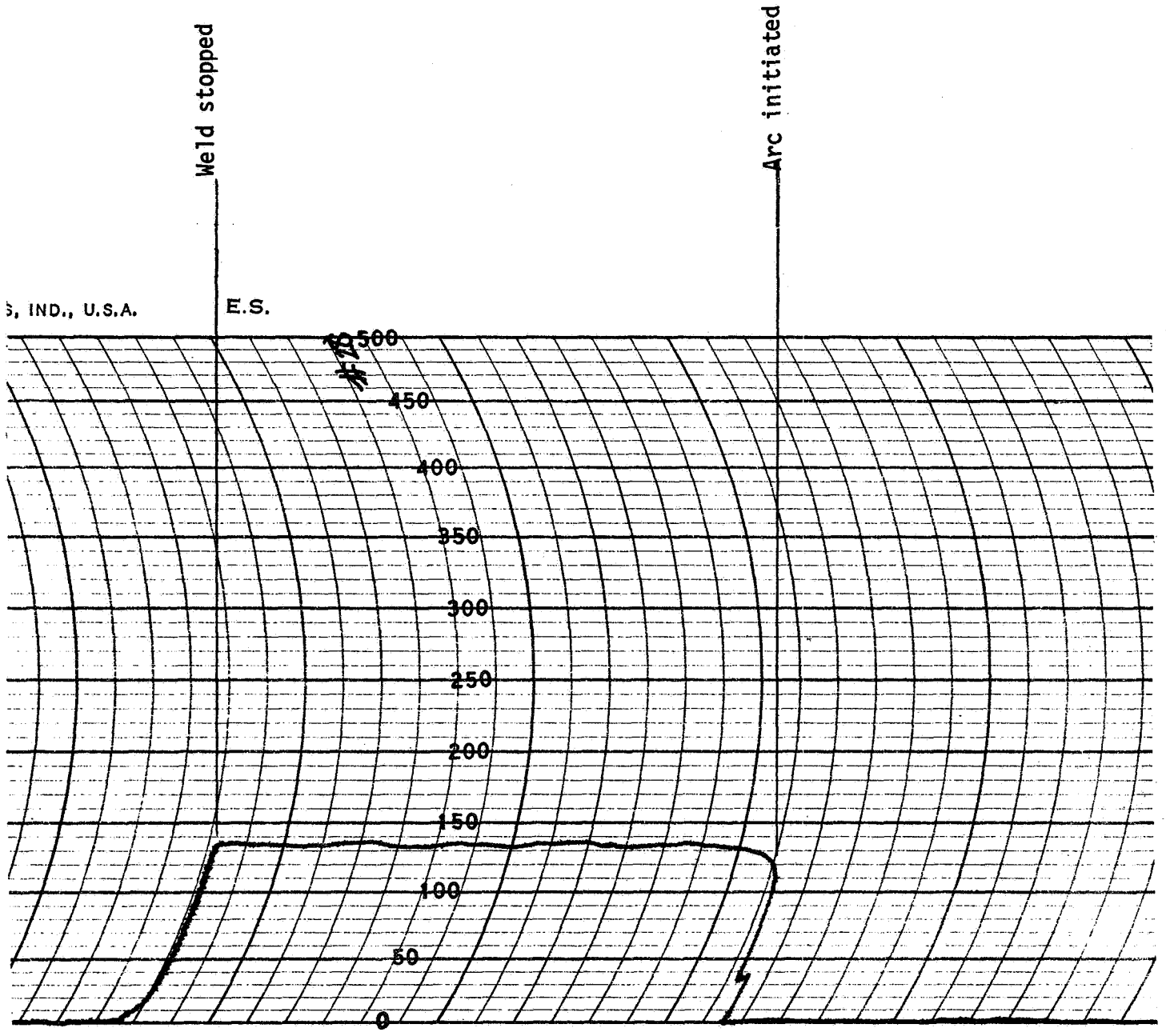


Figure 109: Welding current, test number 28.

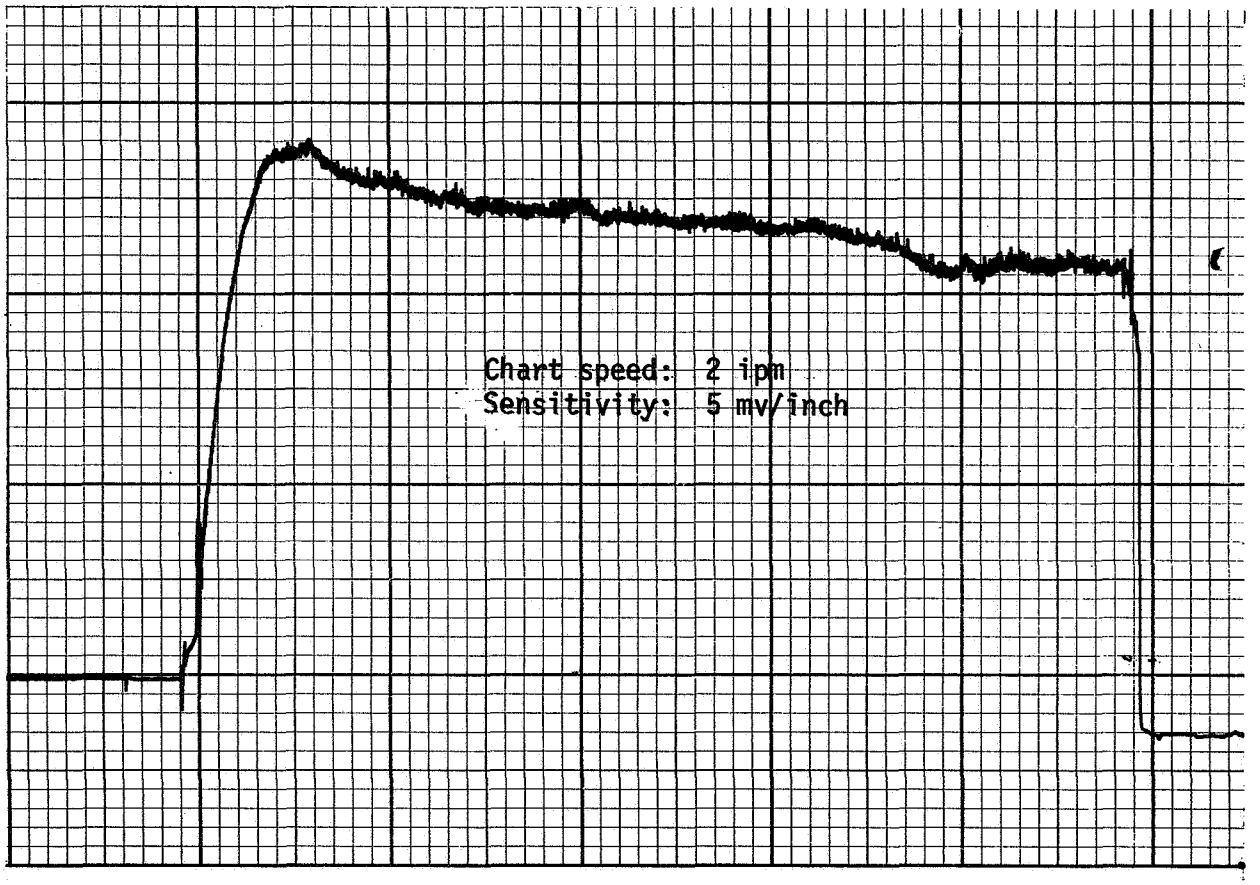


Figure 110: Hybrid thermocouple output, test number 29.

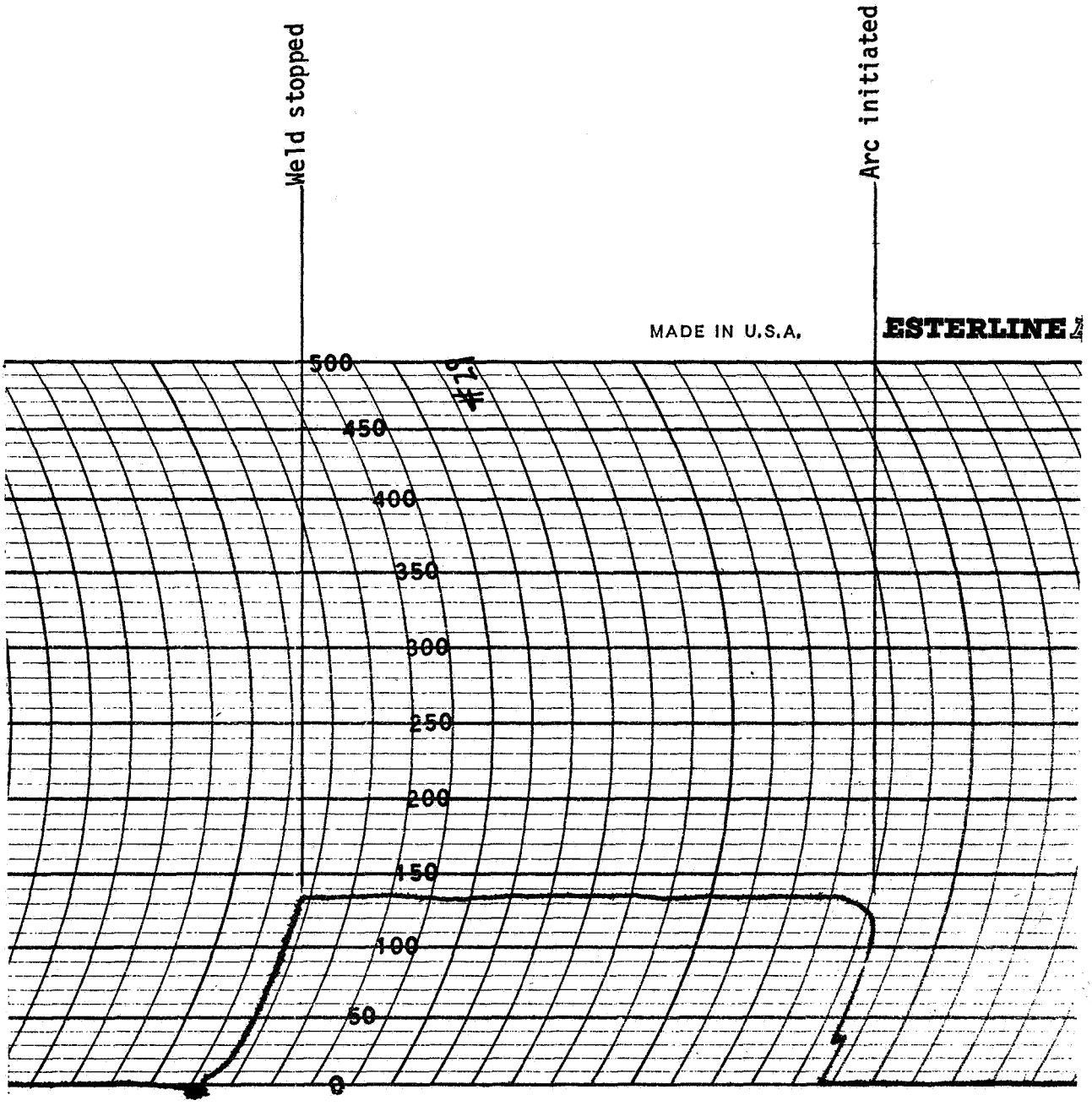


Figure 111: Welding current, test number 29.

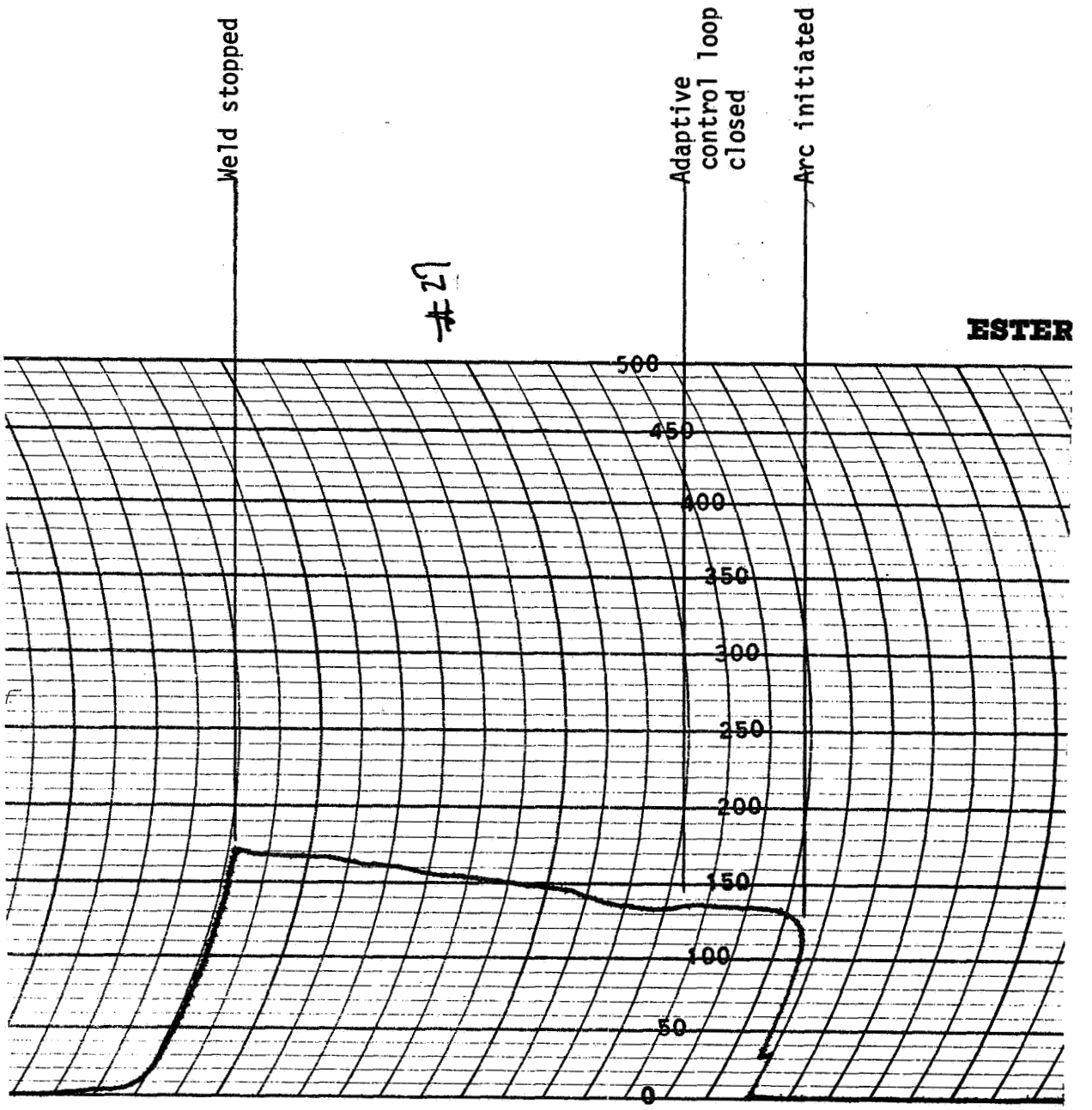


Figure 112: Welding current, test number 27.

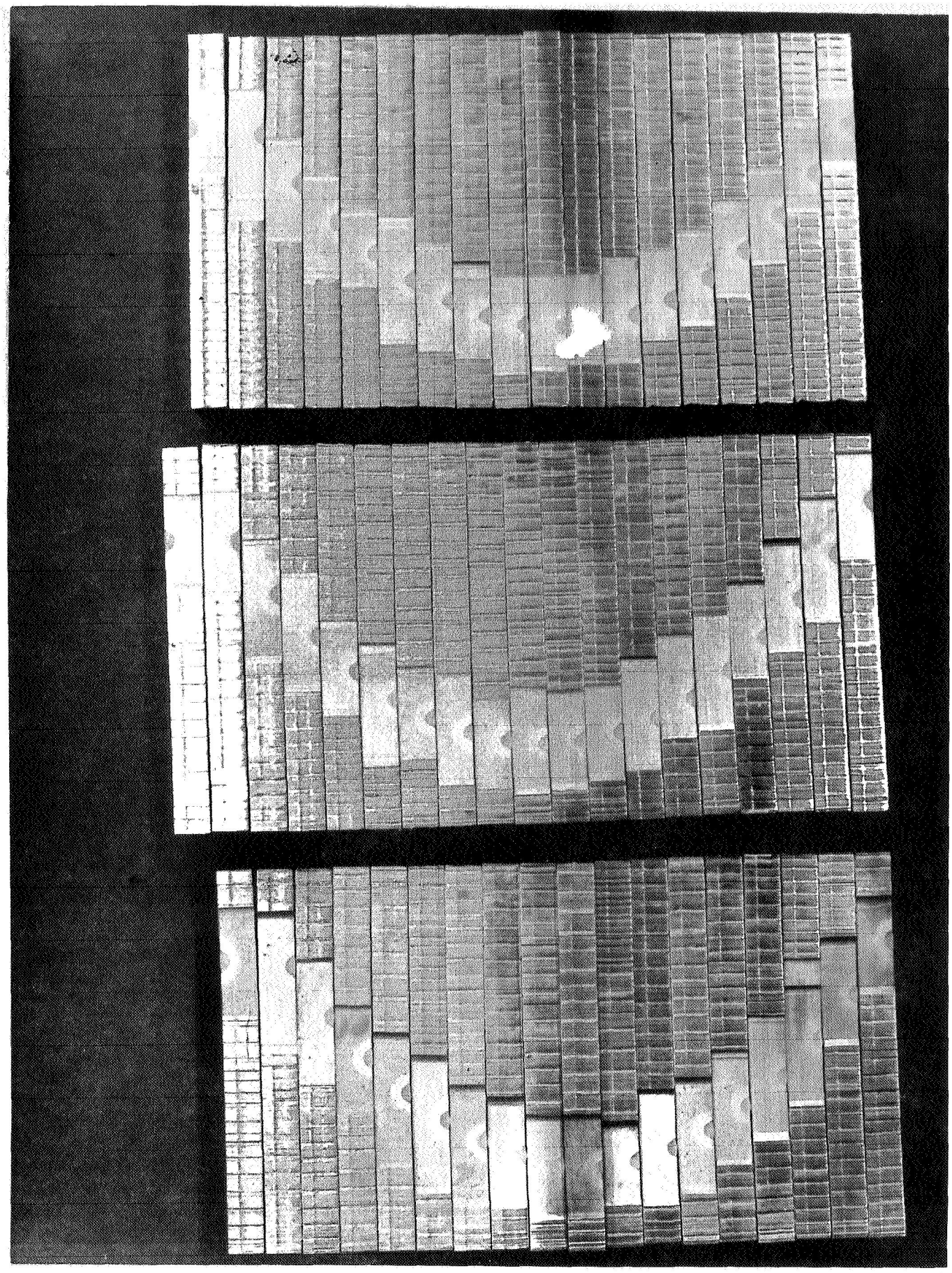


Figure 113: Cross sections, tests numbers 27, 28, 29.

be seen in Figure 113, no appreciable variation in thermocouple output occurred in tests numbers 28 and 29 where no adaptive control was used. It was therefore concluded that these tests should be repeated with external heat sinks added to produce penetration variations when adaptive control was not used. This was done in the experiments reported in the next section.

5.2.2.2 Tests number 30, 31, 33, 34, 35, and 36 were conducted to determine the ability of the adaptive system to maintain penetration on partial penetration welds made under varying heat sink conditions. All of these tests were conducted on 10" X 24" X 0.375" Al samples with an aluminum block heat sink positioned mid-way of the weld. The weld parameters were: weld current, 150 amperes on all tests except number 36 where the current was increased to 170 amperes; travel speed, 8 ipm; shielding gas, Helium at 100 CFH; thermocouple location, 22/64 inch abeam and 14/64 inch behind the center of the puddle; Moseley strip chart recorder settings, 2 ipm chart speed and 5 mv/inch sensitivity. The adaptive control loop was not used on tests number 30, 33, and 34. The adaptive loop was closed on tests number 31, 35 and 36. The thermocouple recordings, current recordings, and cross sections for these welds are shown in Figures 114 through 130. The current recording for test number 31 was not obtained due to a malfunction in the Esterline-Angus recorder. As can be seen in Figures 117, 125, and 128, the themocouple output (proportional to temperature at probe position) was held relatively constant by the adaptive loop action. As can be seen by comparing the penetration patterns (Figures 116, 118, 121, 124, 127 and 130) of the welds made with control to those made without control, penetration was more consistent when the adaptive control loop was closed.

5.3 THIN-PLATE EXPERIMENTS

Tests numbers 1T through 15T were conducted on 10" X 24" X .090" aluminum plates. The purpose of these experiments was to determine the adaptive control loop's ability to maintain full penetration on thin plates

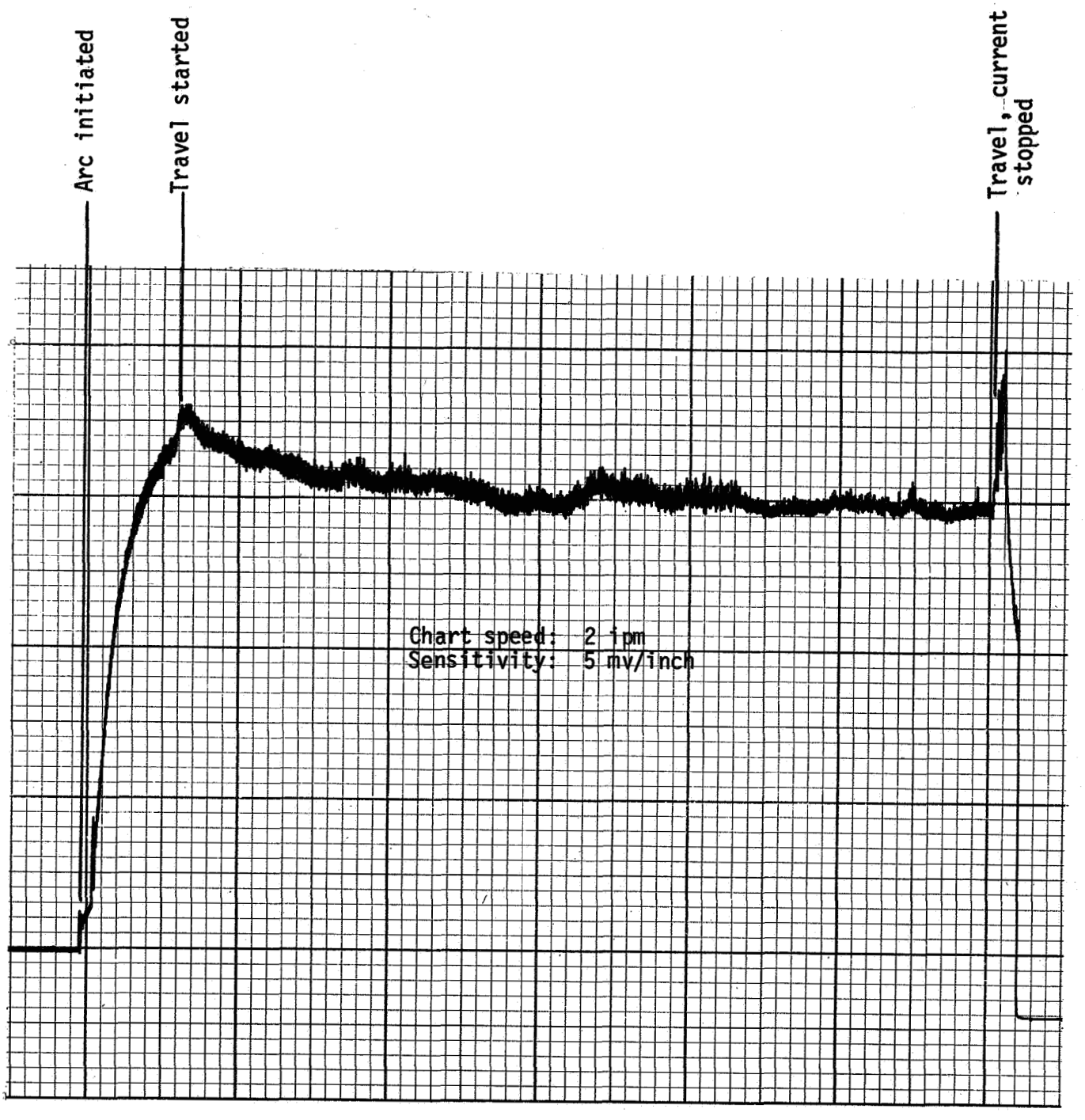


Figure 114: Hybrid thermocouple output, test number 30.

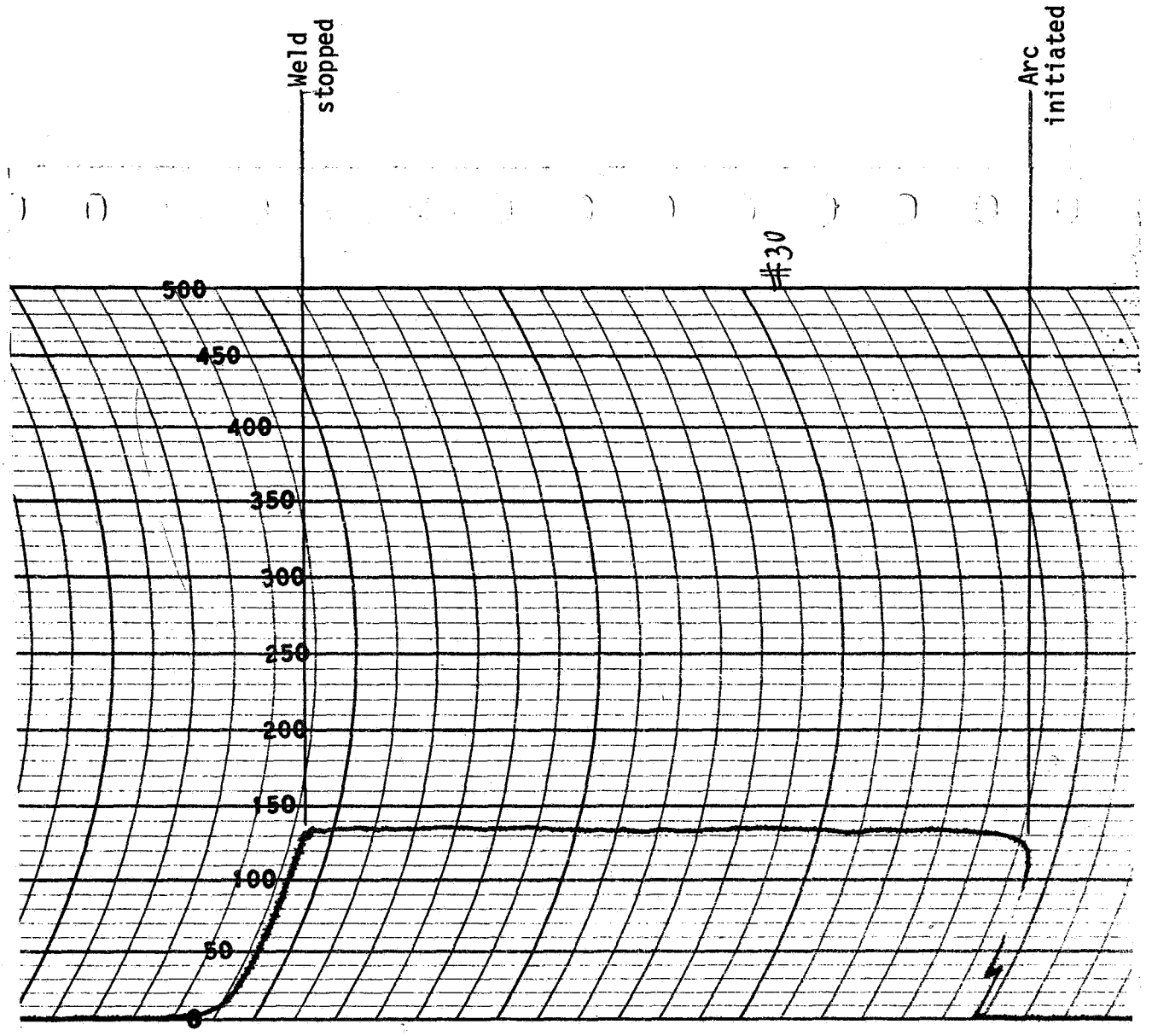


Figure 115: Welding current, test number 30.

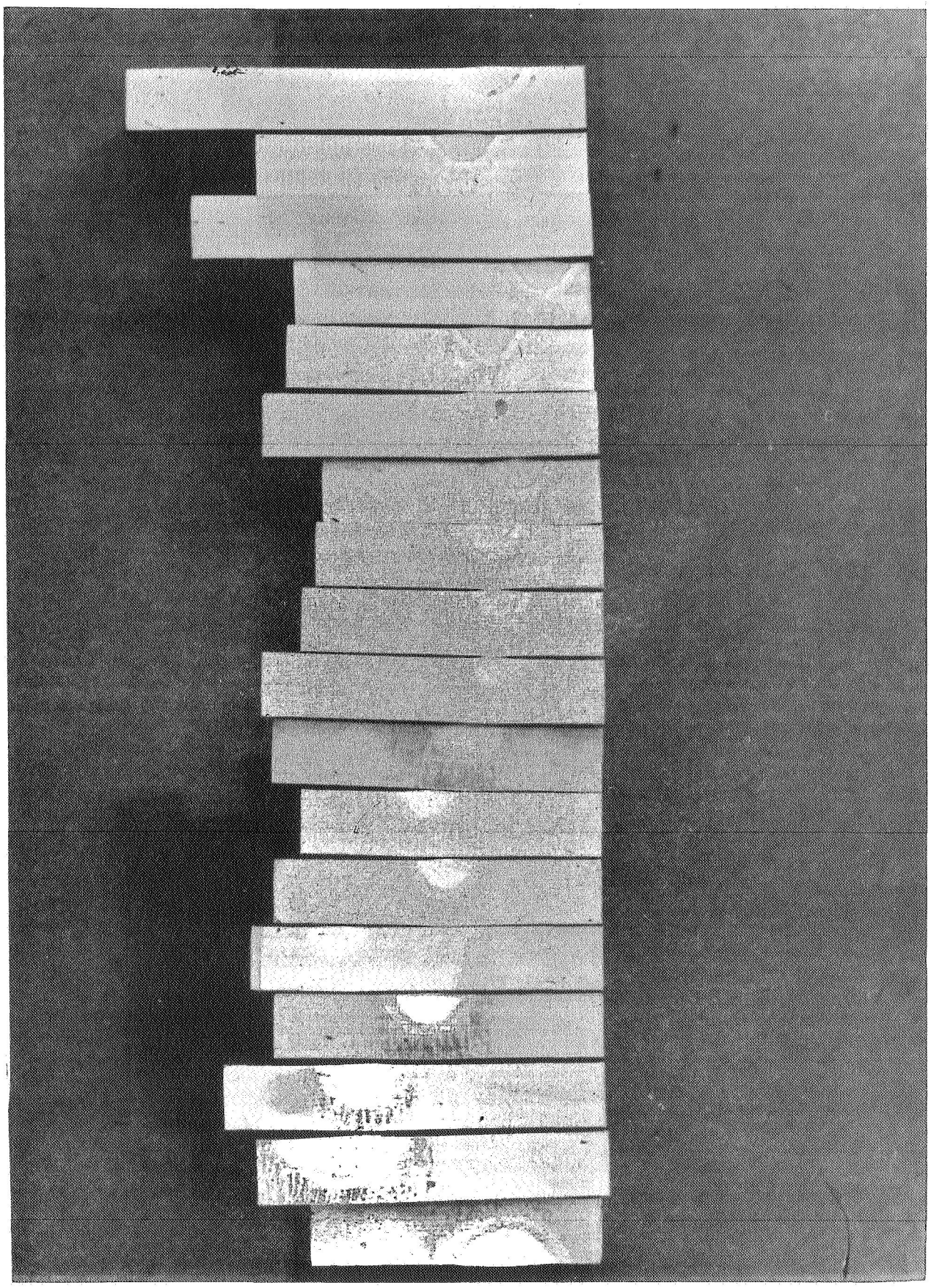


Figure 116: Cross sections, test number 30.

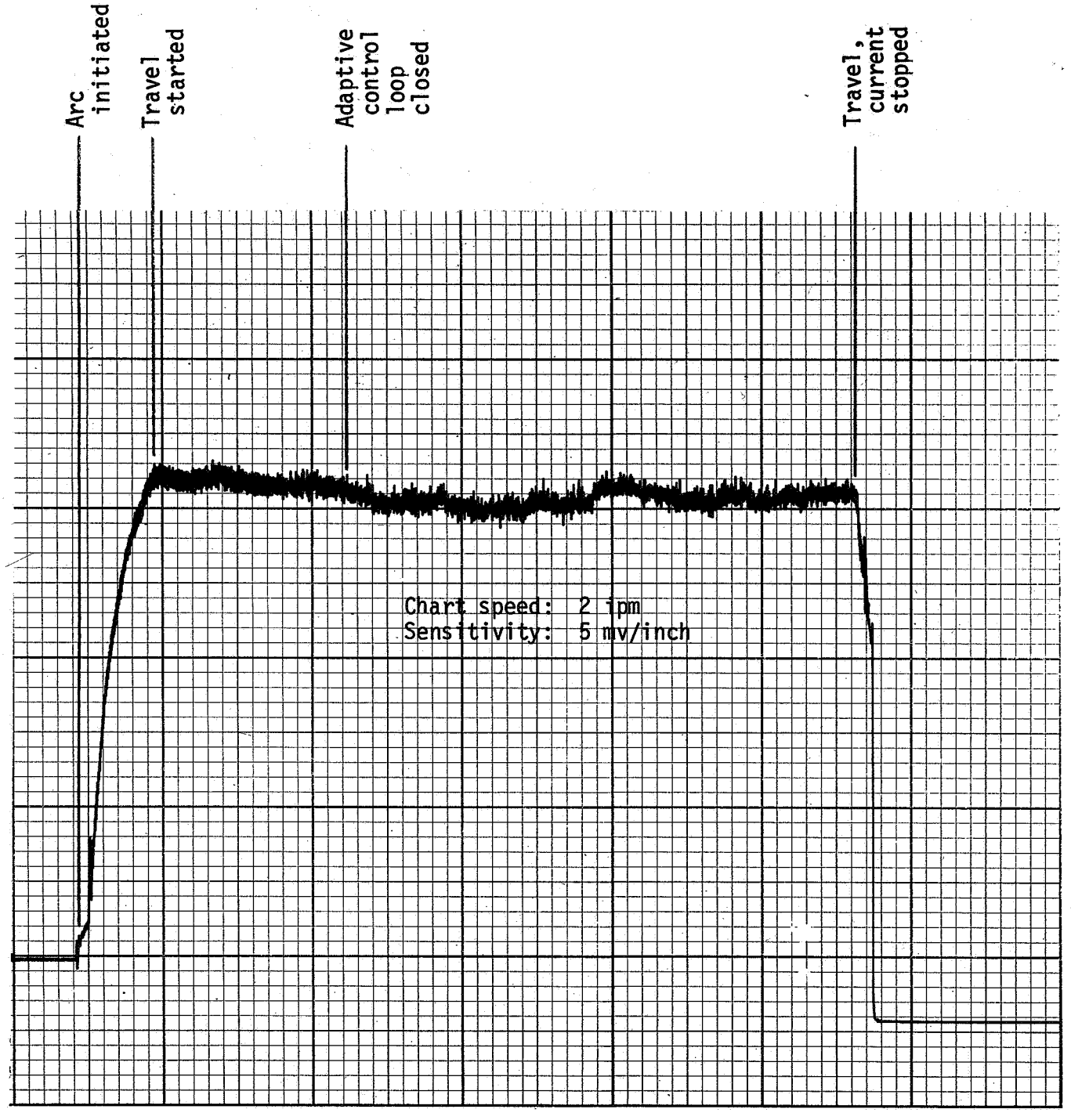


Figure 117: Hybrid thermocouple output, test number 31.

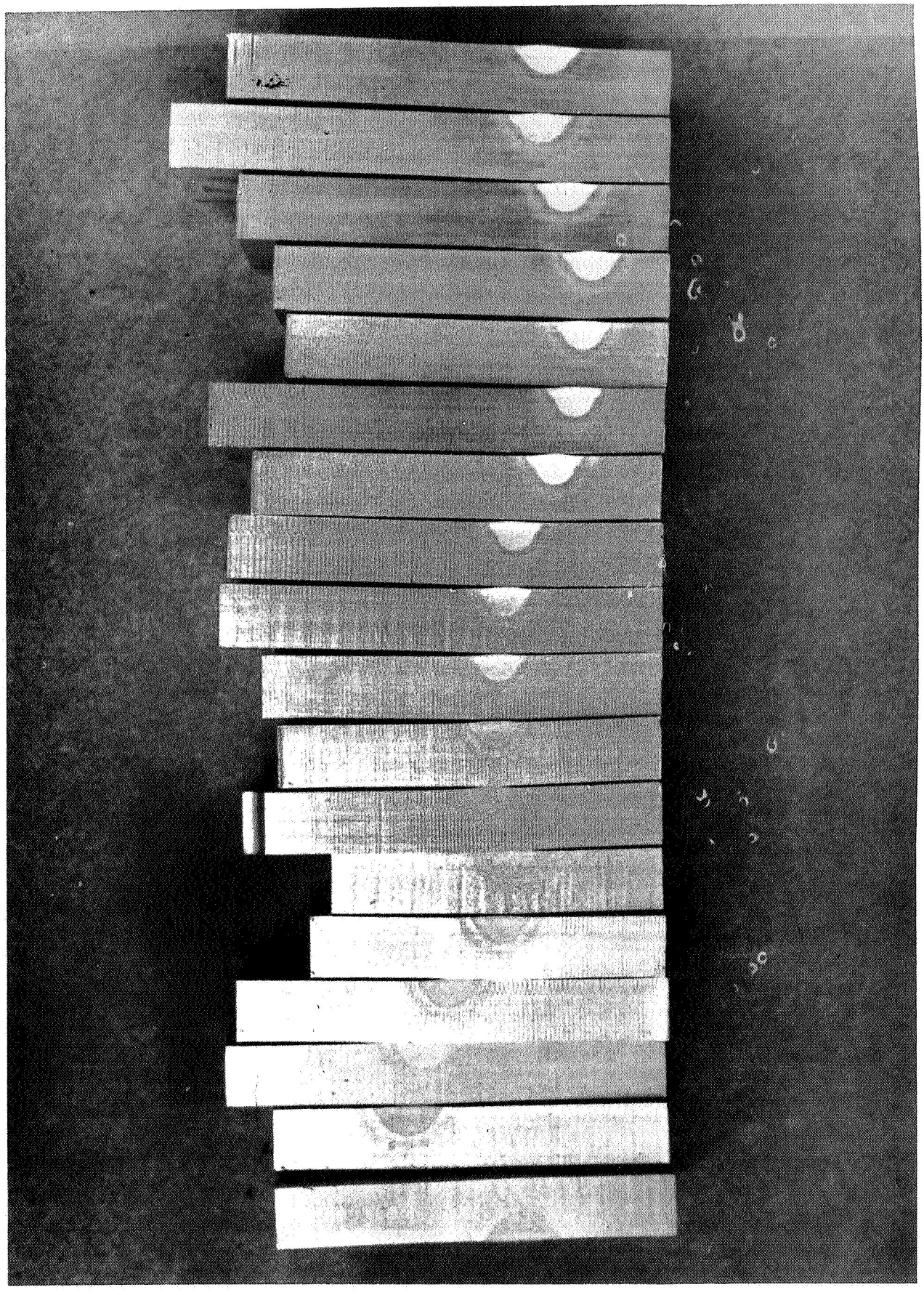


Figure 118: Cross sections, test number 31.

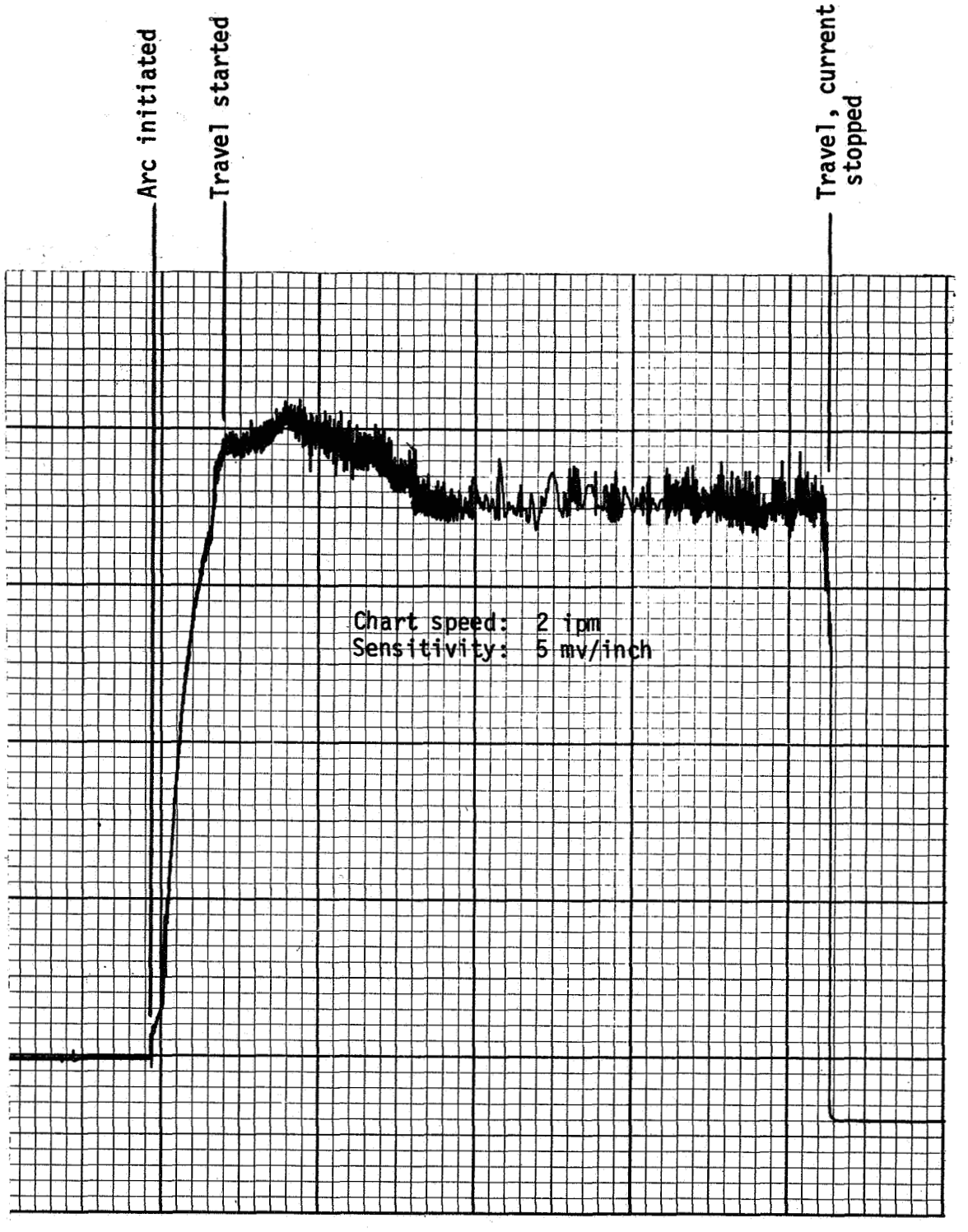


Figure 119: Hybrid thermocouple output, test number 33.

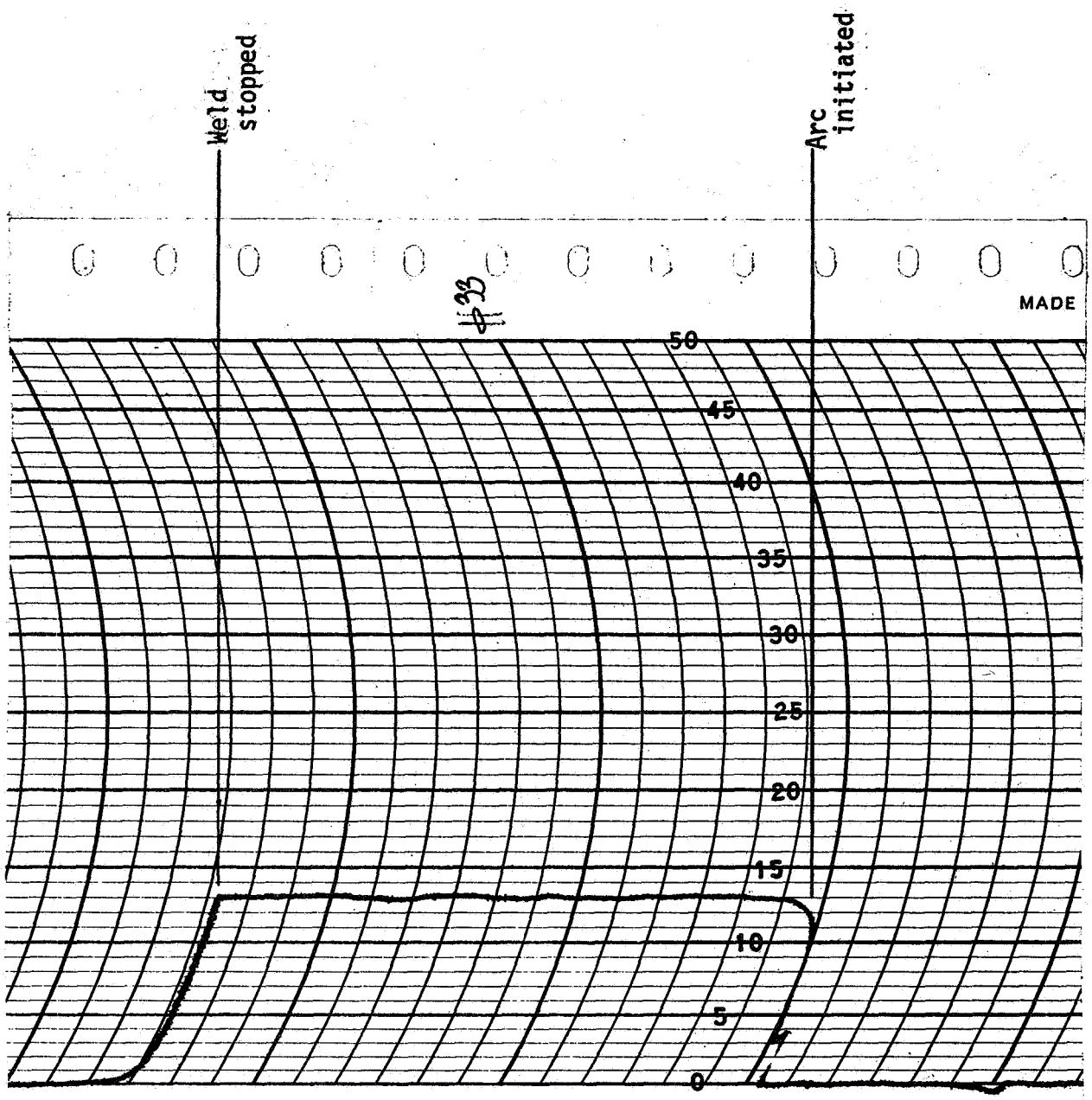


Figure 120: Welding current, test number 33.

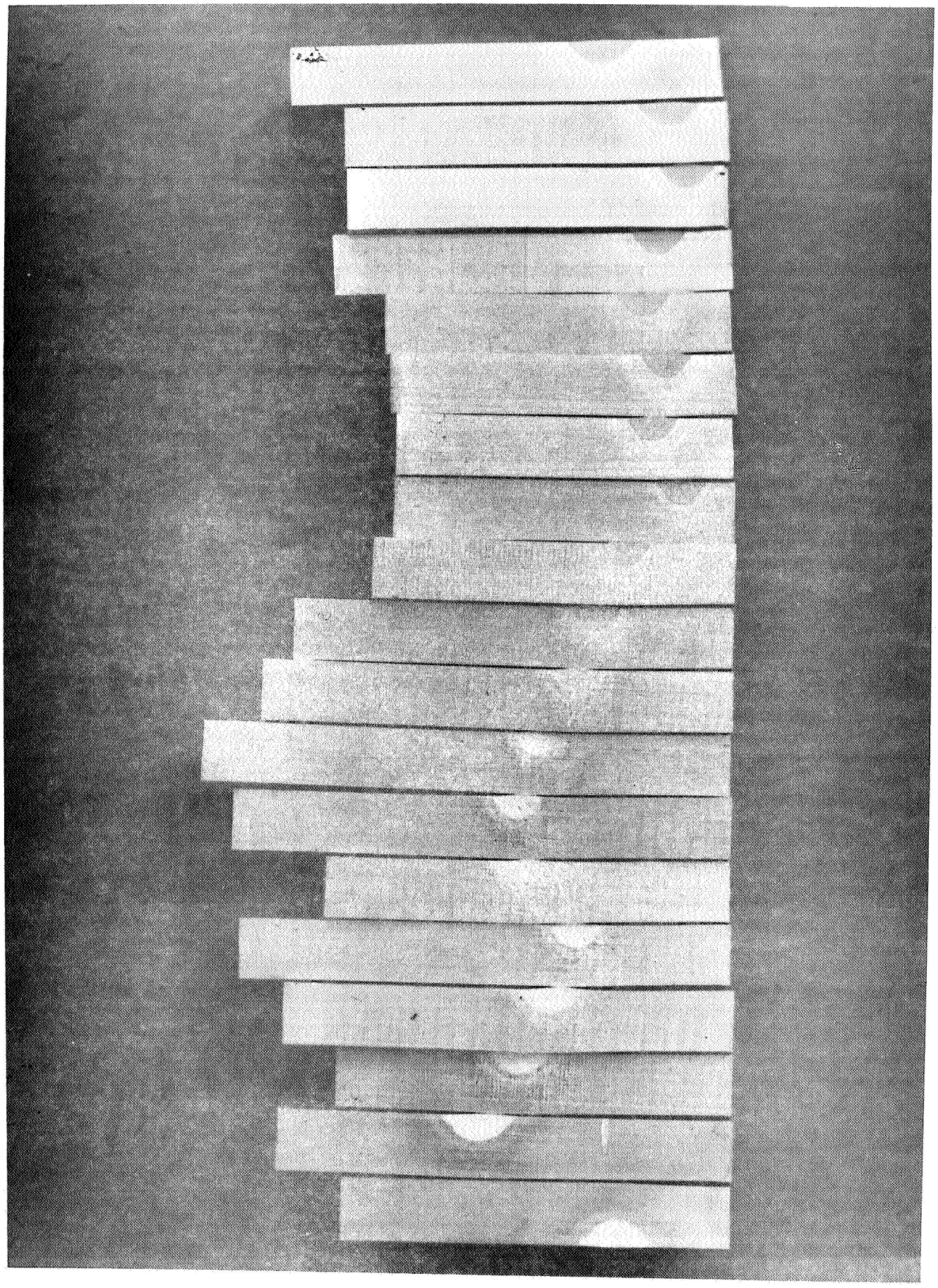


Figure 121: Cross sections, test number 33.

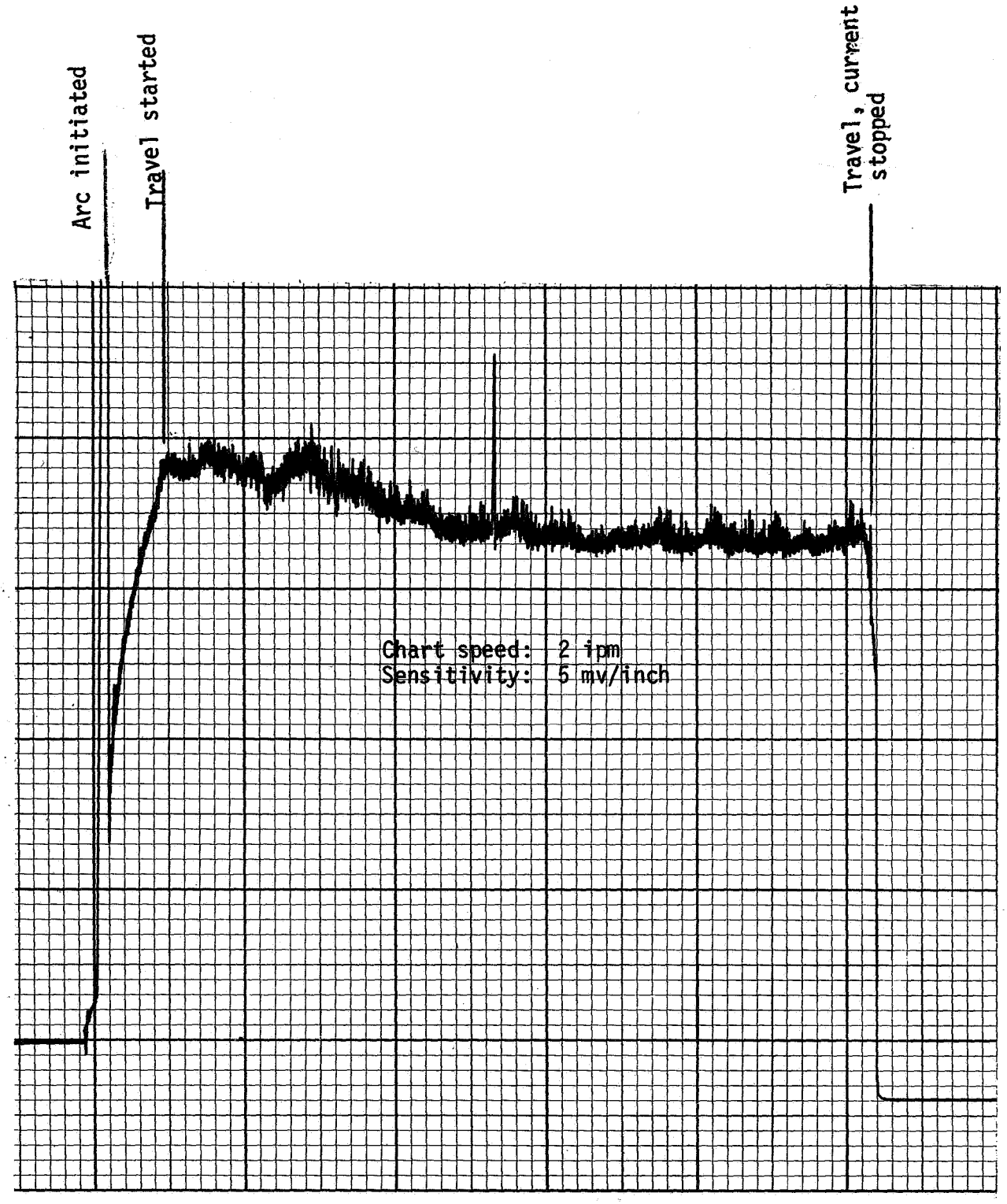


Figure 122: Hybrid thermocouple output, test number 34.

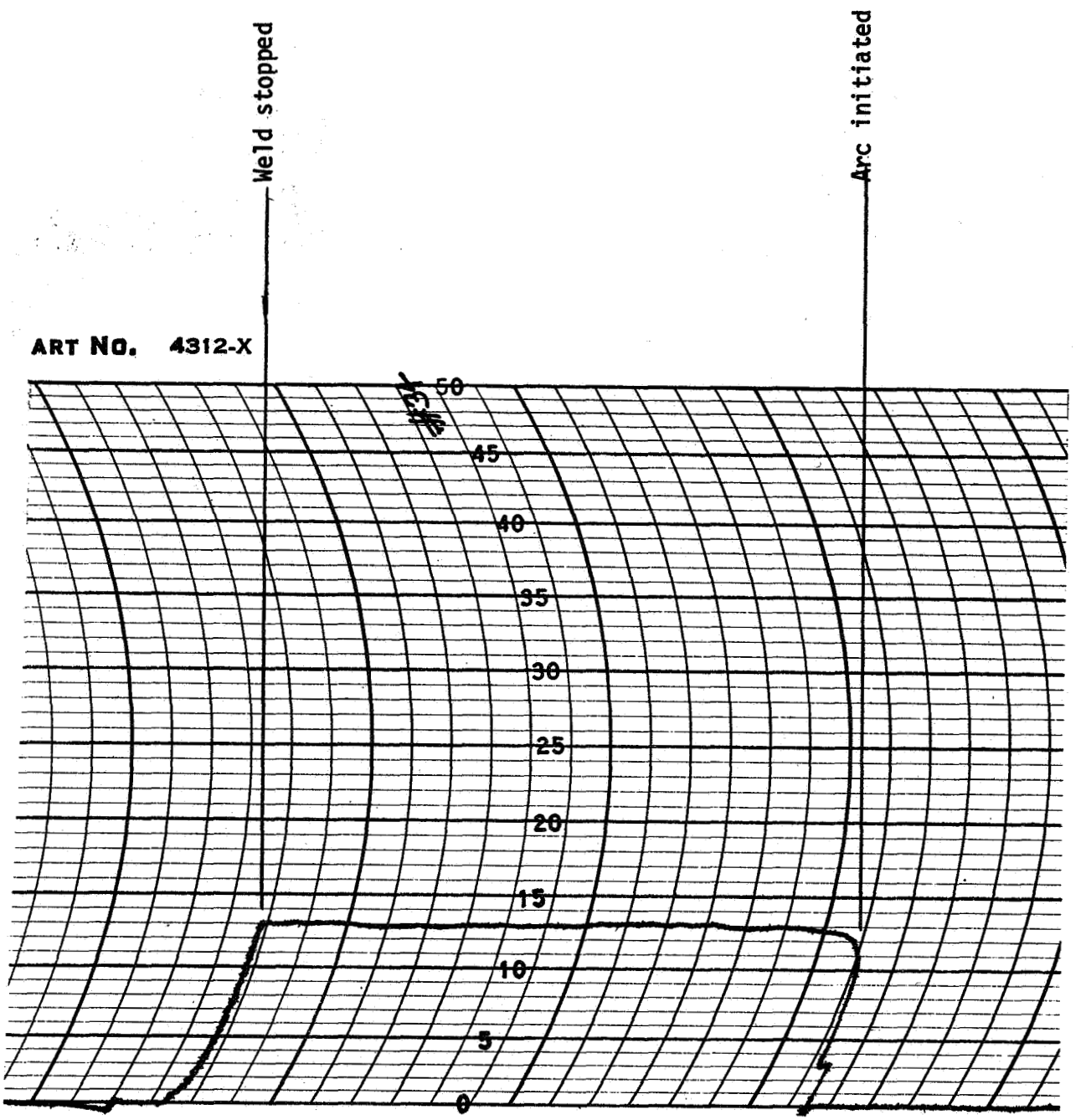


Figure 123: Welding current, test number 34.

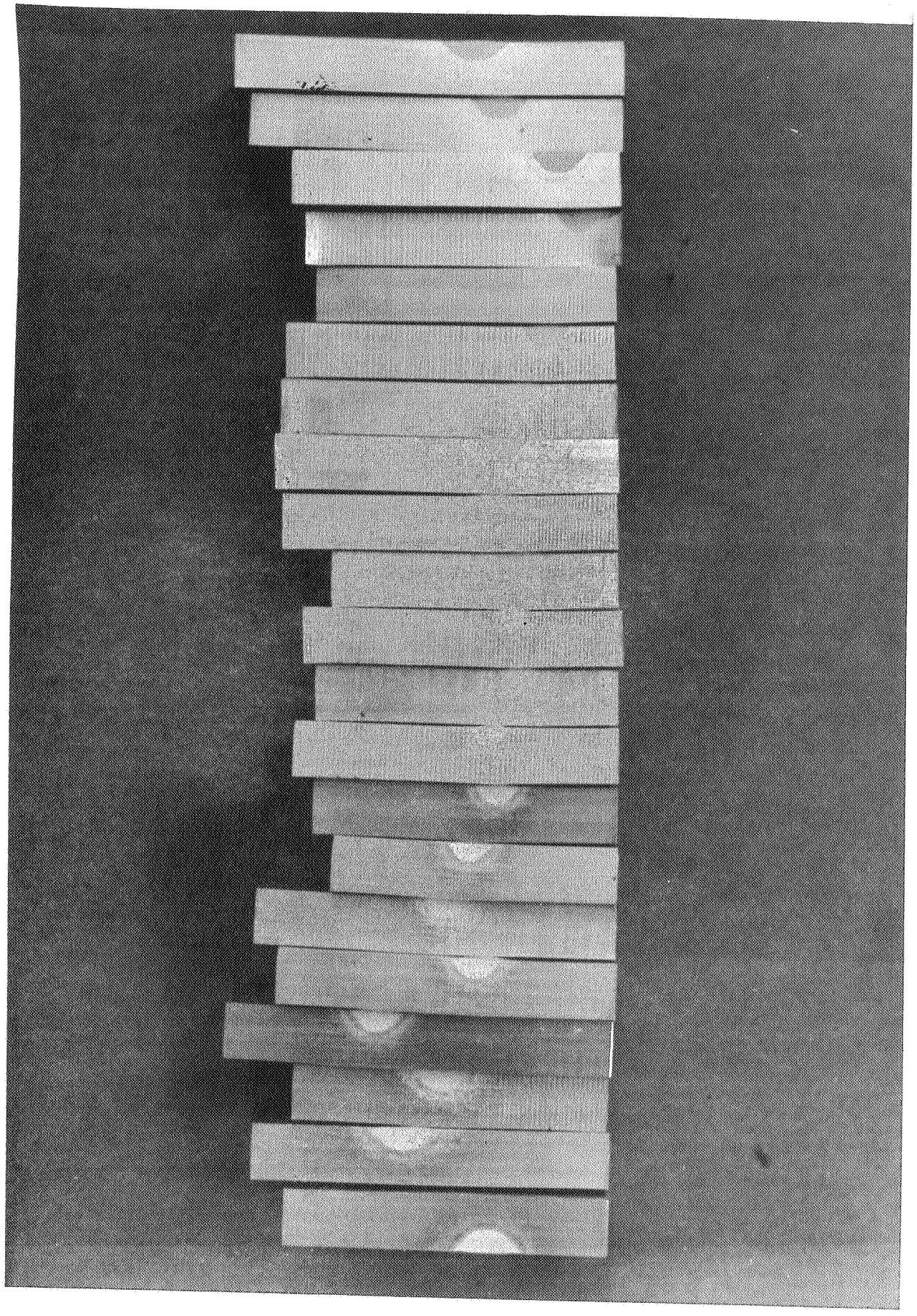


Figure 124.: Cross sections, test number 34.

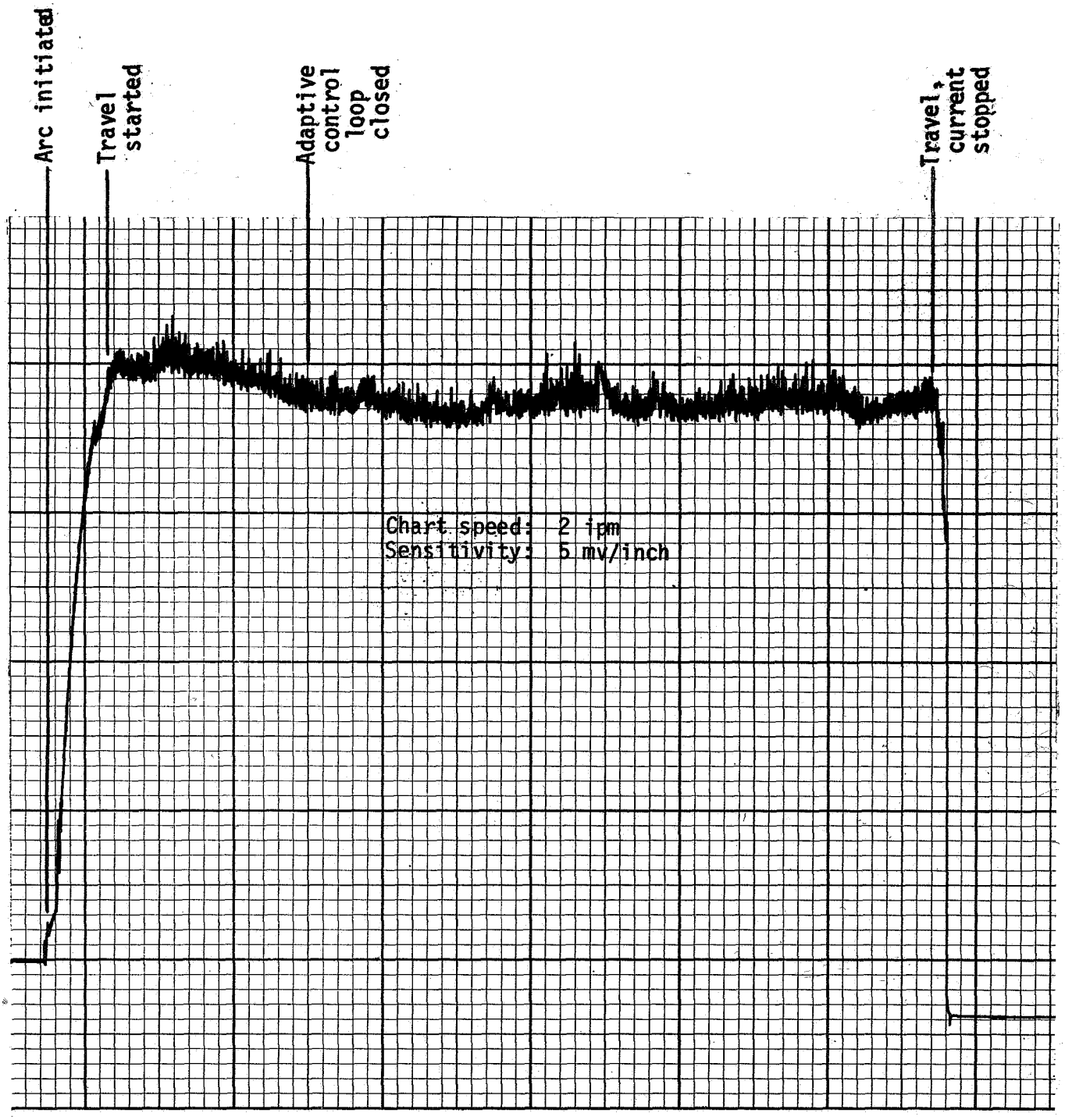


Figure 125: Hybrid thermocouple output, test number 35.

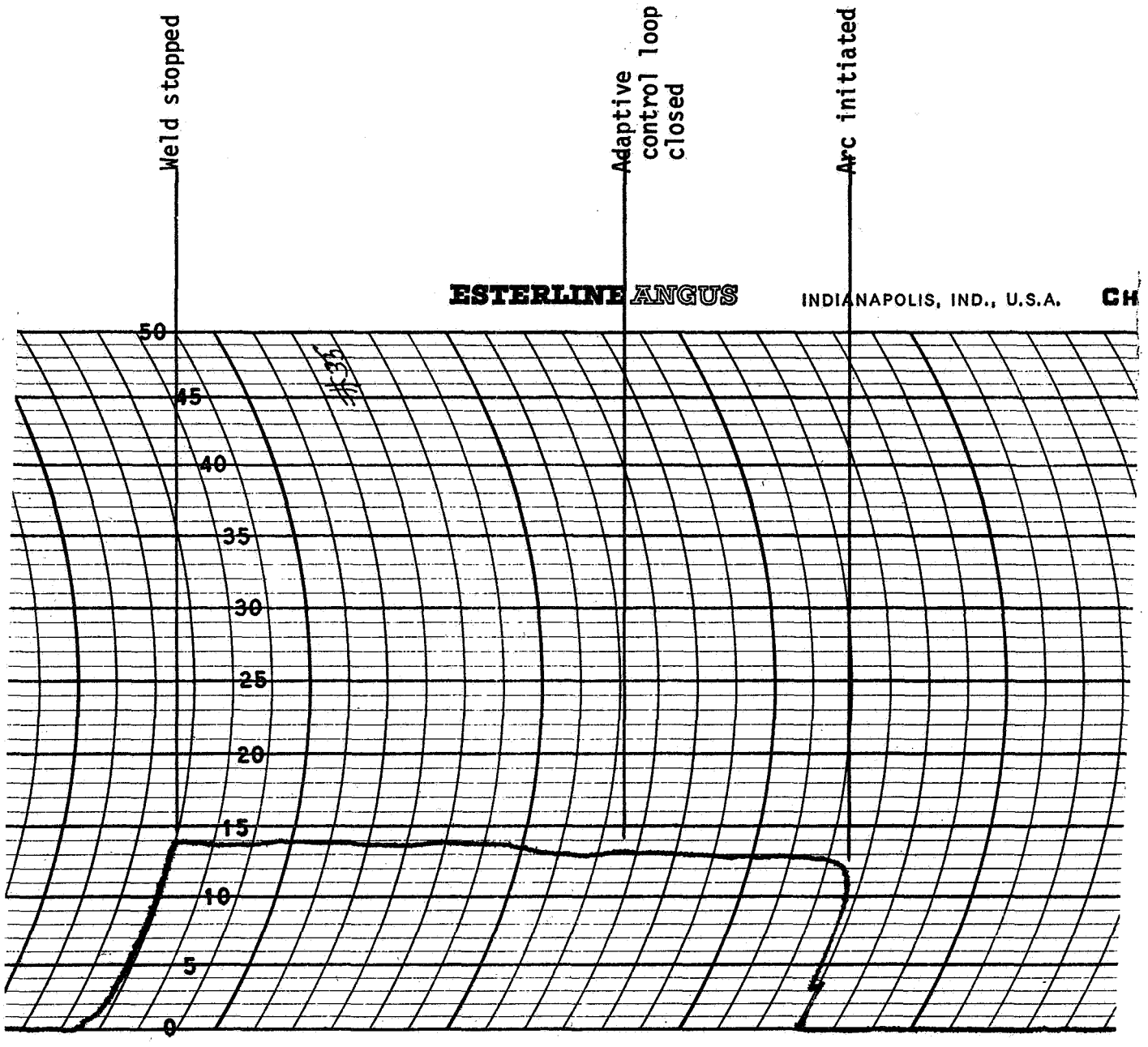


Figure 126: Welding current, test number 35.

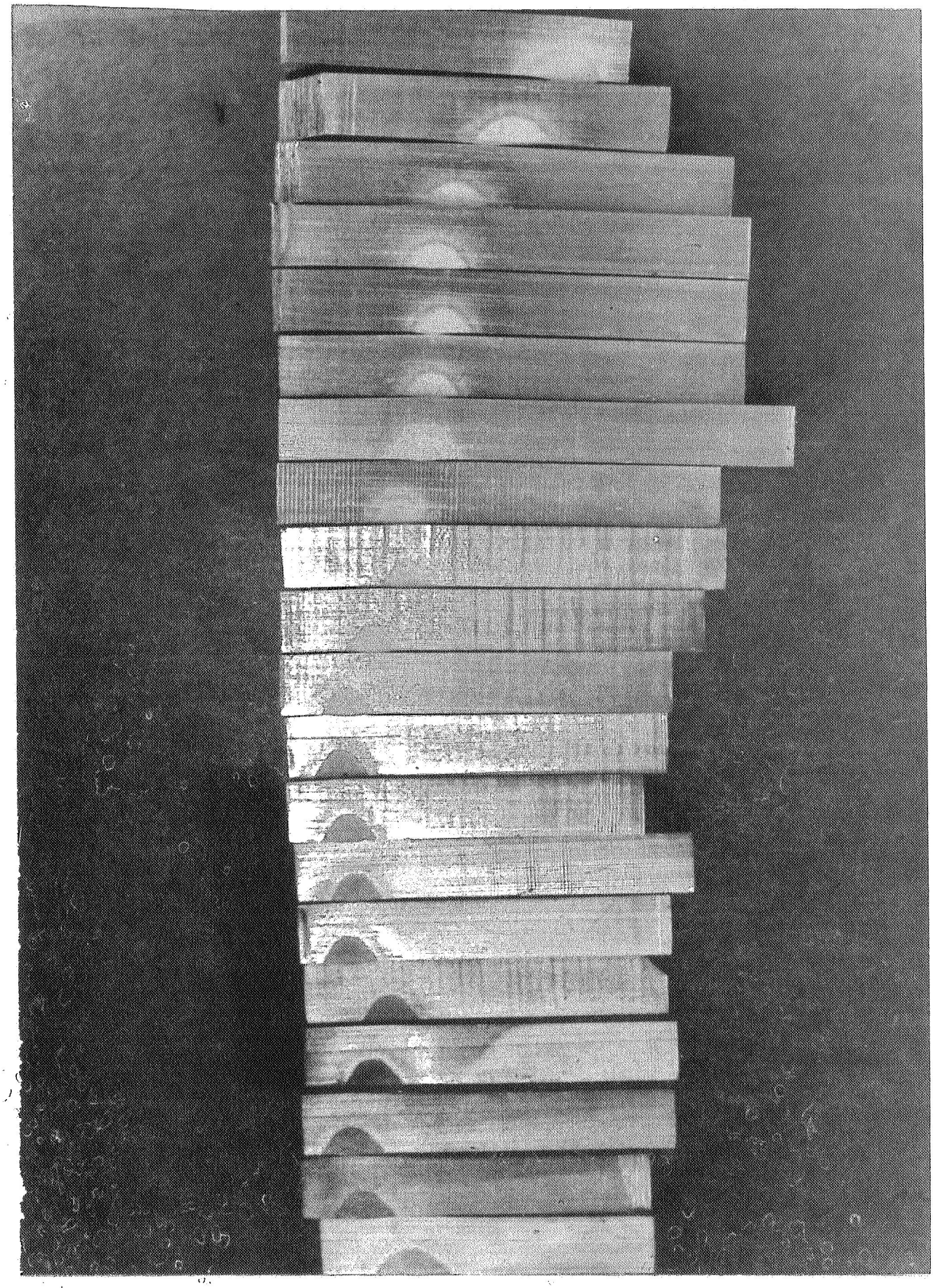


Figure 127: Cross sections, test number 35.

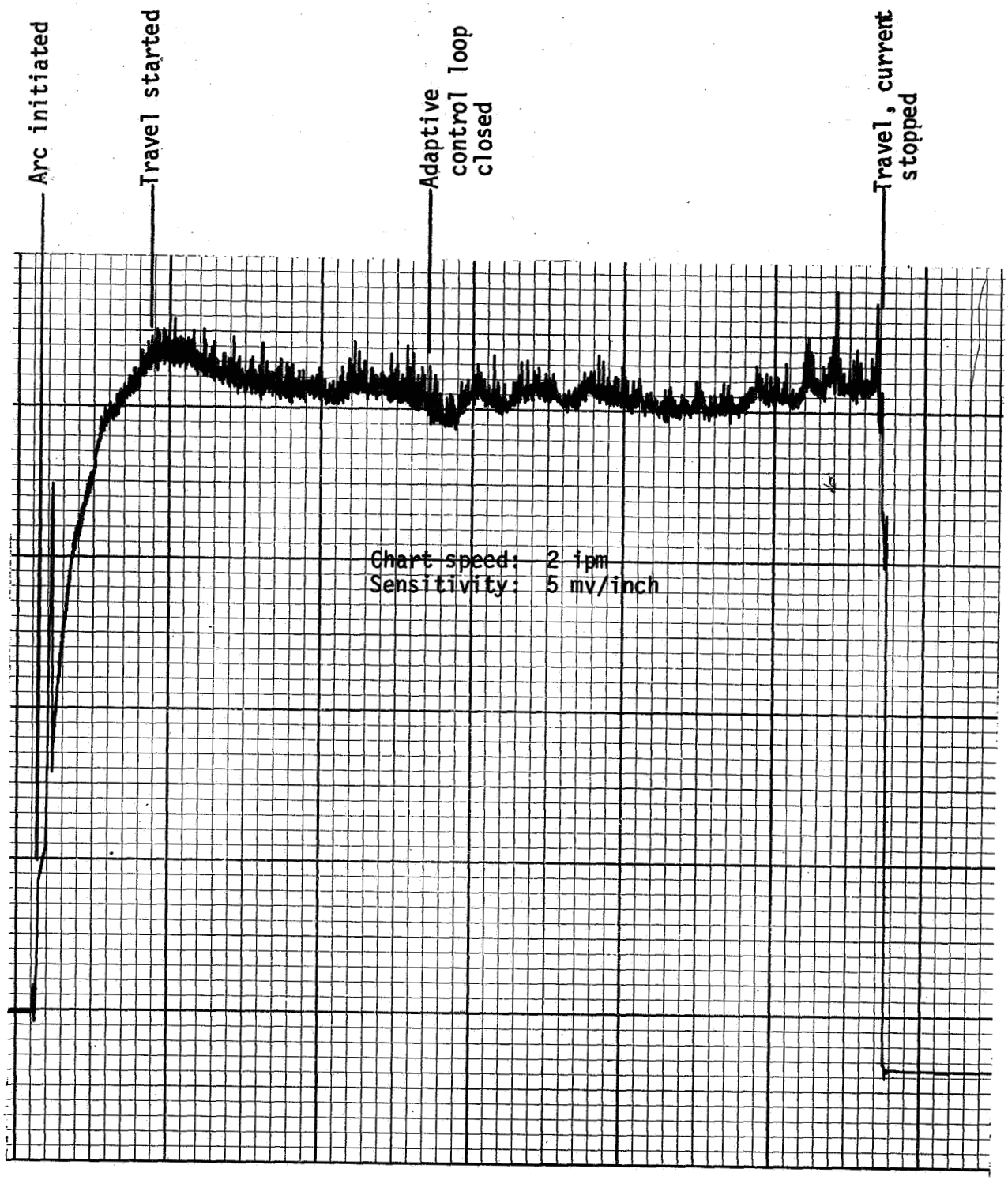


Figure 128: Hybrid thermocouple output, test number 36.

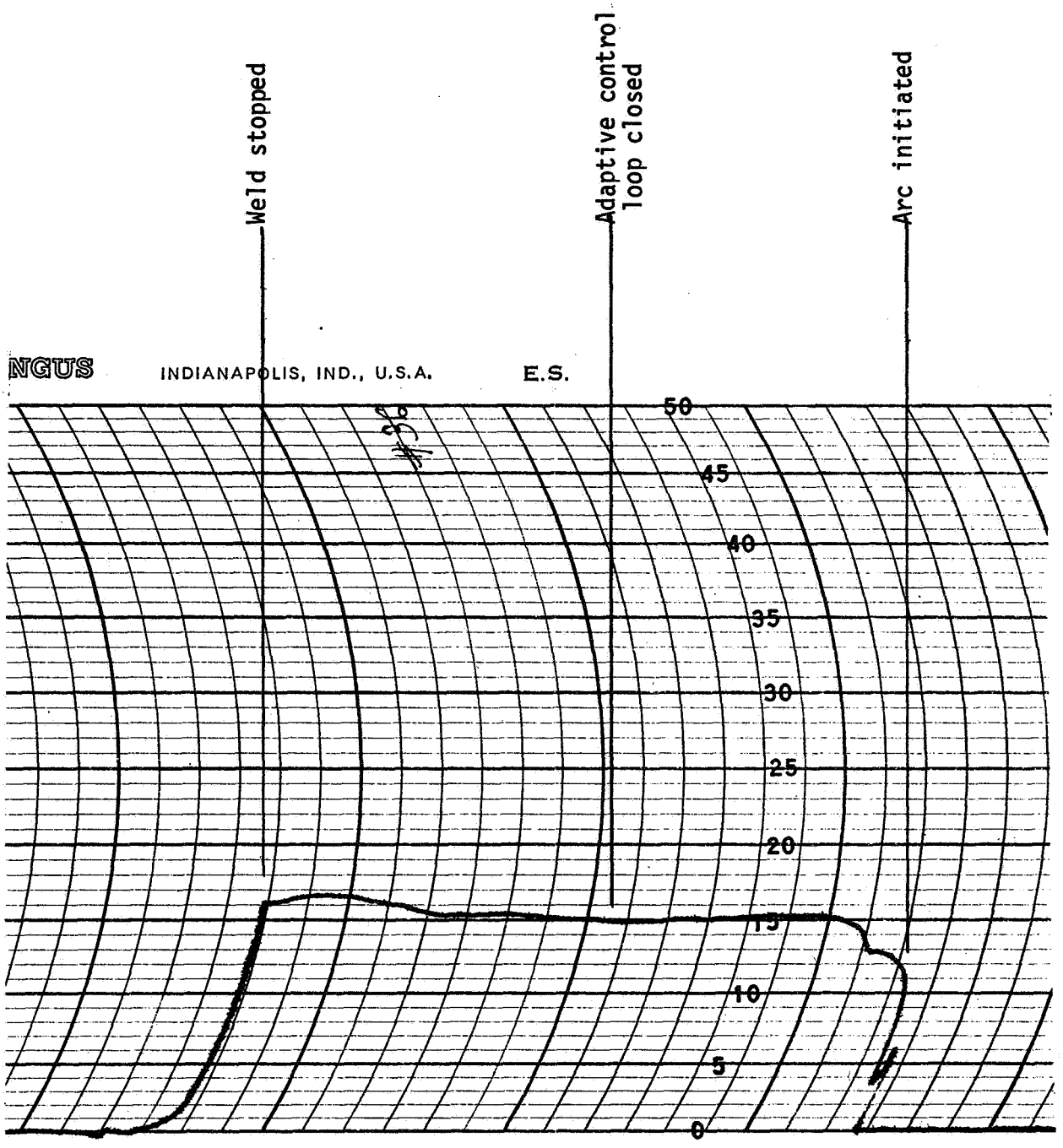


Figure 129: Welding current, test number 36.

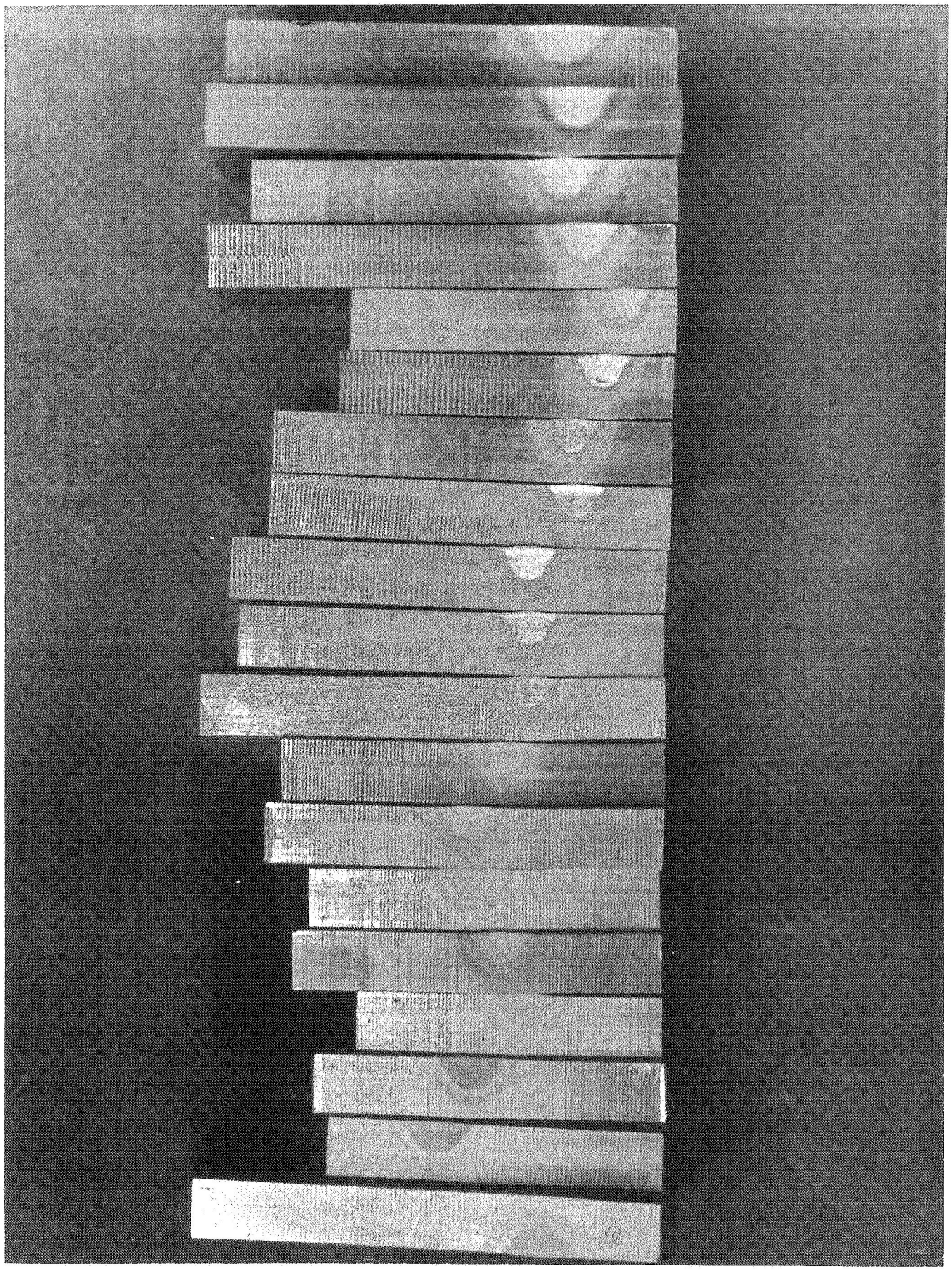


Figure 130: Cross sections, test number 36.

in the presence of external and varying heat sink conditions. The heat sink was simulated by positioning an aluminum block midway of the weld, firmly in contact with the test speciman. The heat sink was positioned immediately adjacent the weld bead trajectory. The heat sink dimensions were 1.5" X 3" X 2". The weld parameters on these tests were: arc voltage, 13 volts; travel speed, 8 ipm; shielding gas, Helium at 100 CFH; thermocouple probe location, 0.250 inch abeam and 0.250 inch behind center of puddle; Moseley recorder settings, 2 ipm chart speed and 5 mv/inch sensitivity.

5.3.1 TEST NUMBERS 1T, 2T, 3T, 4T

The first four tests were conducted with the adaptive control loop open. The thermocouple recordings, front and backside views, and cross sections for these tests are shown in Figures 131 through 146. As can be seen, in all cases the penetration was lost in the region of the heat sink. Also, in all cases the thermocouple output decreased in the region of the heat sink indicating the need for an increase in weld current.

5.3.2 TEST NUMBERS 5T and 6T

Tests number 5T and 6T were conducted with the adaptive control loop closed. In both cases the adaptive controller gain was set at 30 (dial setting). The thermocouple recordings, front and backside views, and cross sections for these tests are shown in Figures 147 through 154. In Figures 149 and 150 it can be seen that the penetration became more narrow in the region of the heat sink but was never lost. This is also pointed out by the dip in the thermocouple signal, as shown in Figure 147. In test number 6T the adaptive controller reference potentiometer was set slightly high and as a result penetration was somewhat excessive after the adaptive loop was closed. The reason that this occurred can be seen by referring to Figure 151. As can be seen the adaptive control loop was closed prior to steady state conditions being established after travel initiation.

5.3.3 TEST NUMBER 7T, 8T, 9T

On tests number 7T, 8T, and 9T the gain of the adaptive controller was increased from 30 to 60 (dial setting). The thermocouple recordings, front and backside views, and cross sections of these tests are shown in

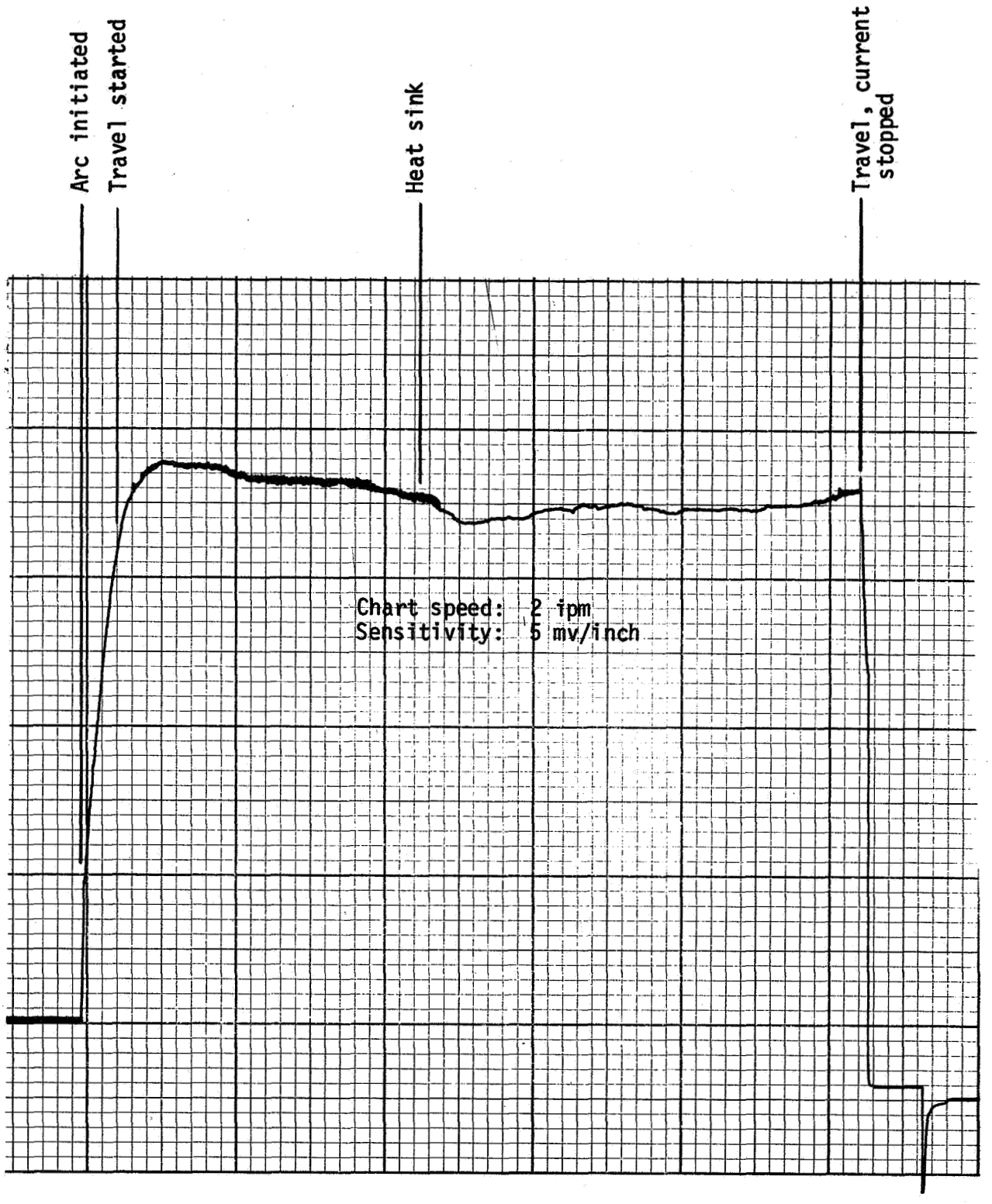


Figure 131: Hybrid thermocouple output, test number 1T.

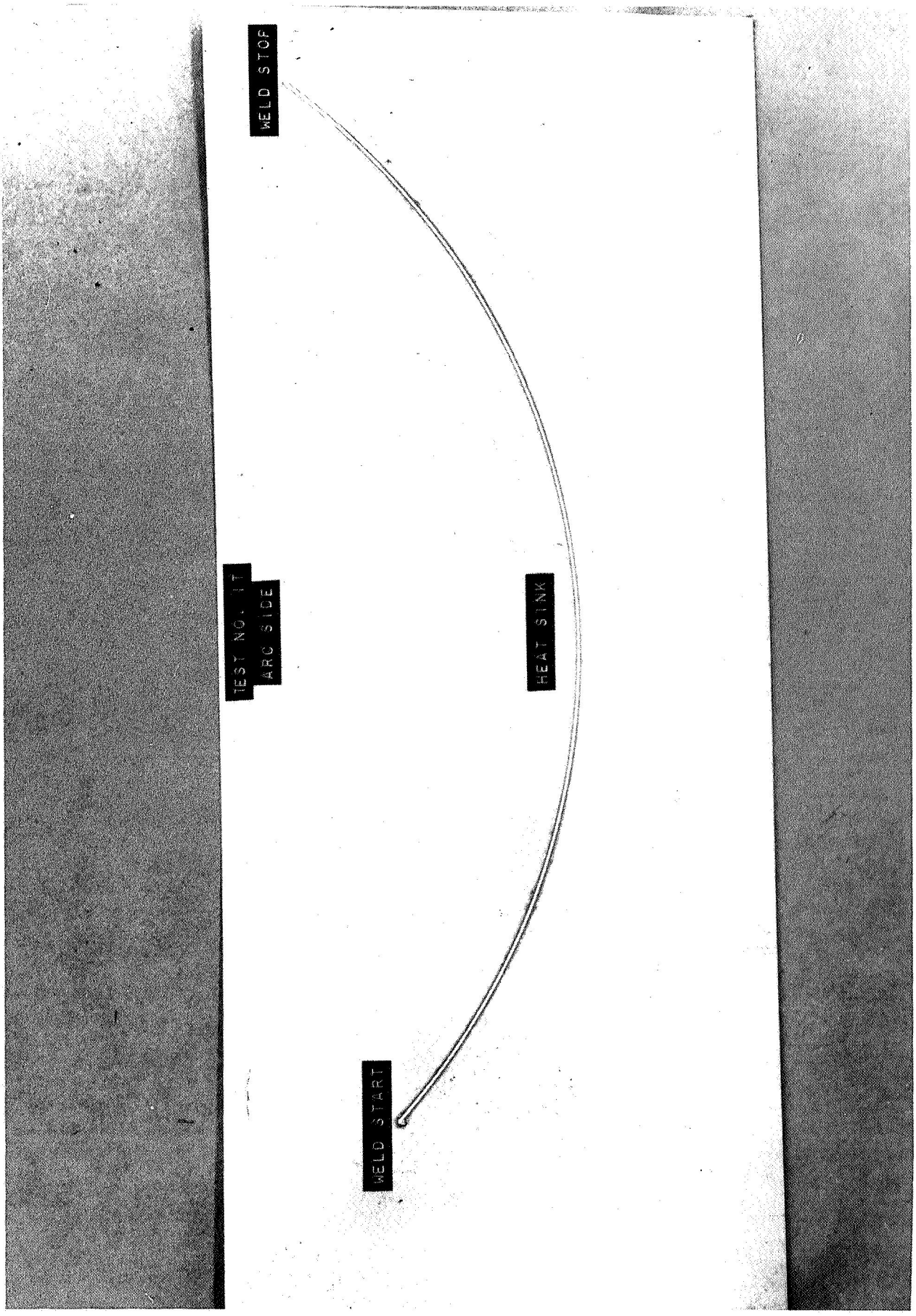


Figure 132: Weld bead, arc side, test number 1T.

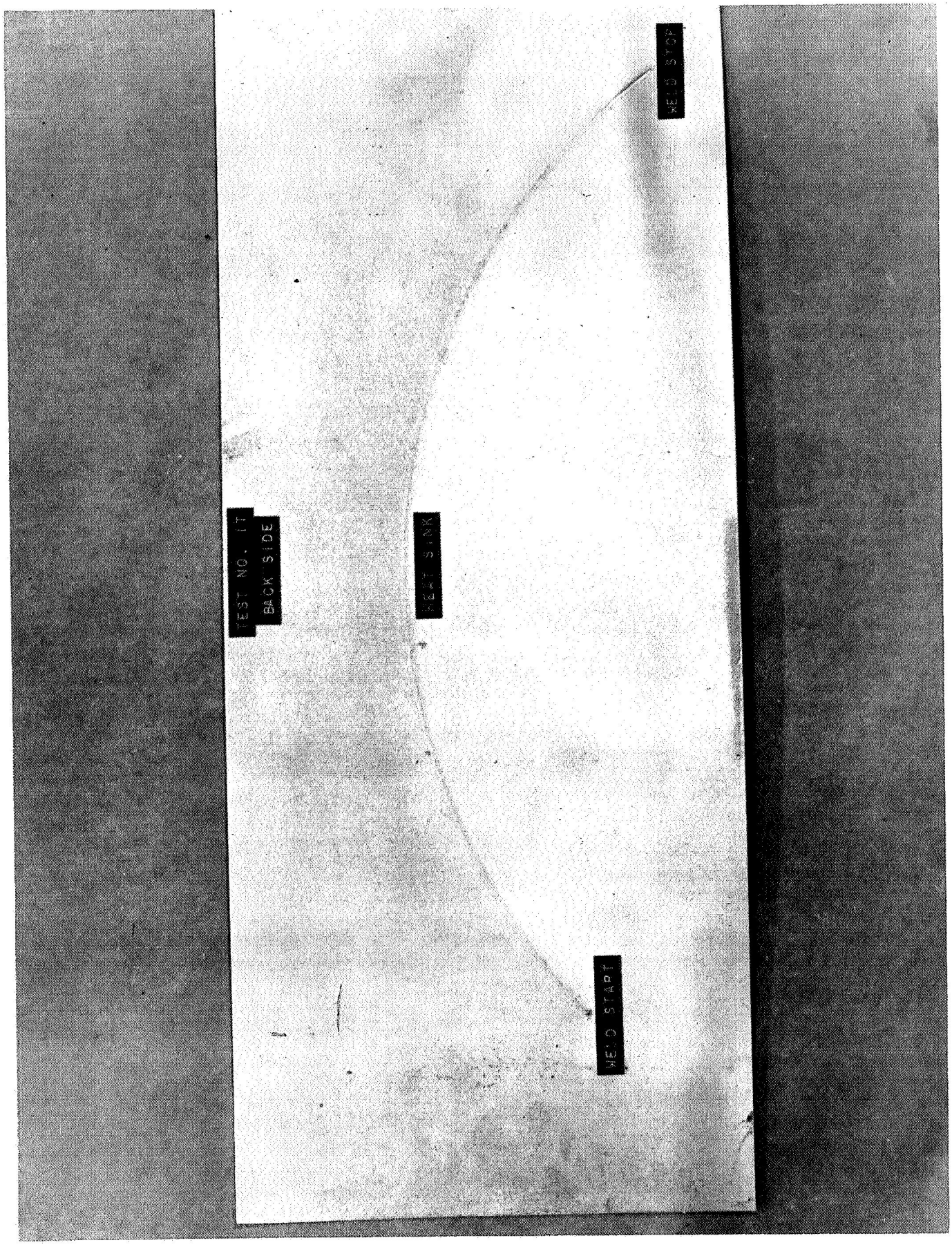


Figure 133: Weld bead, backside, test number 1T.

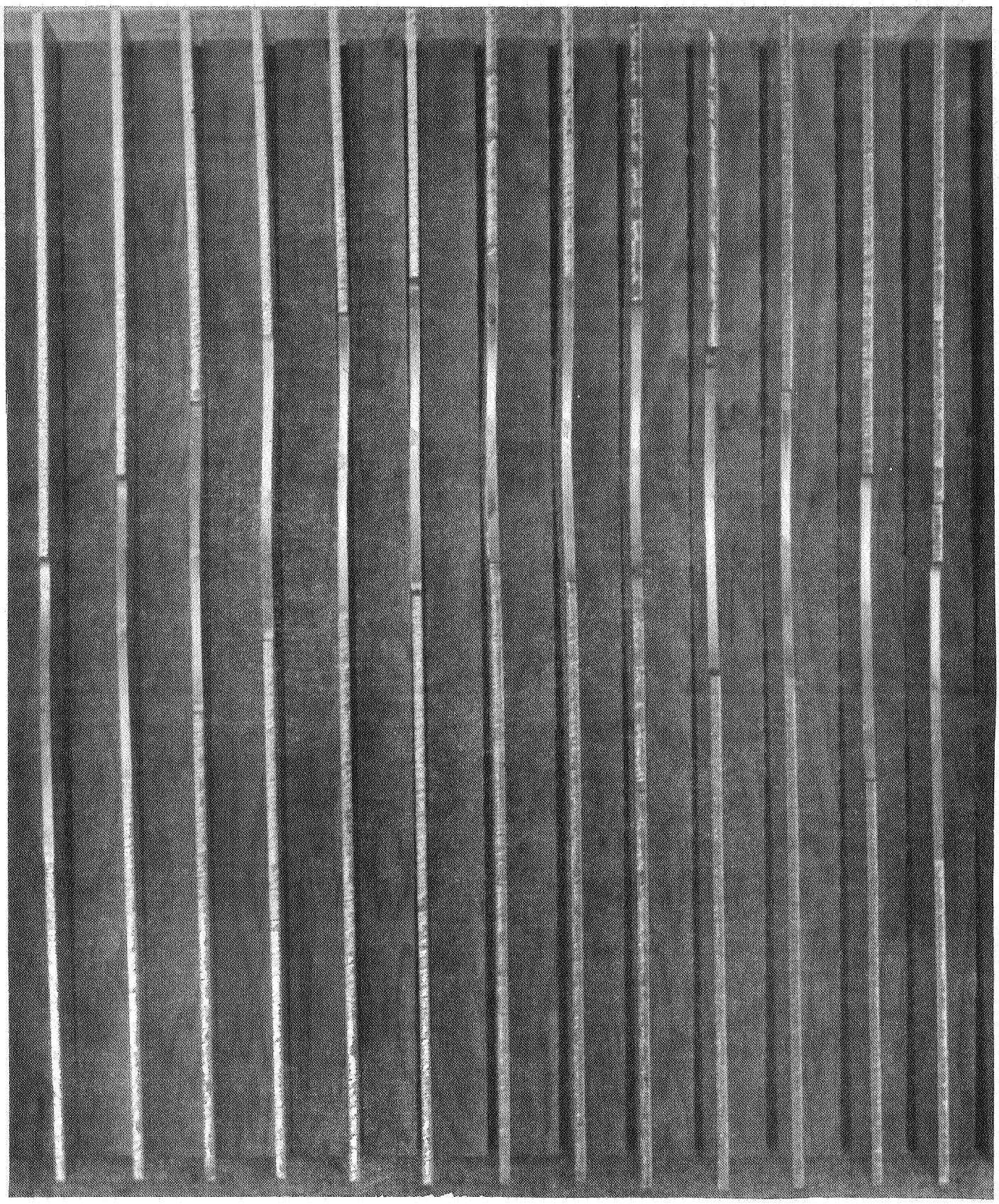


Figure 134: Cross Sections, Test Number 1T.

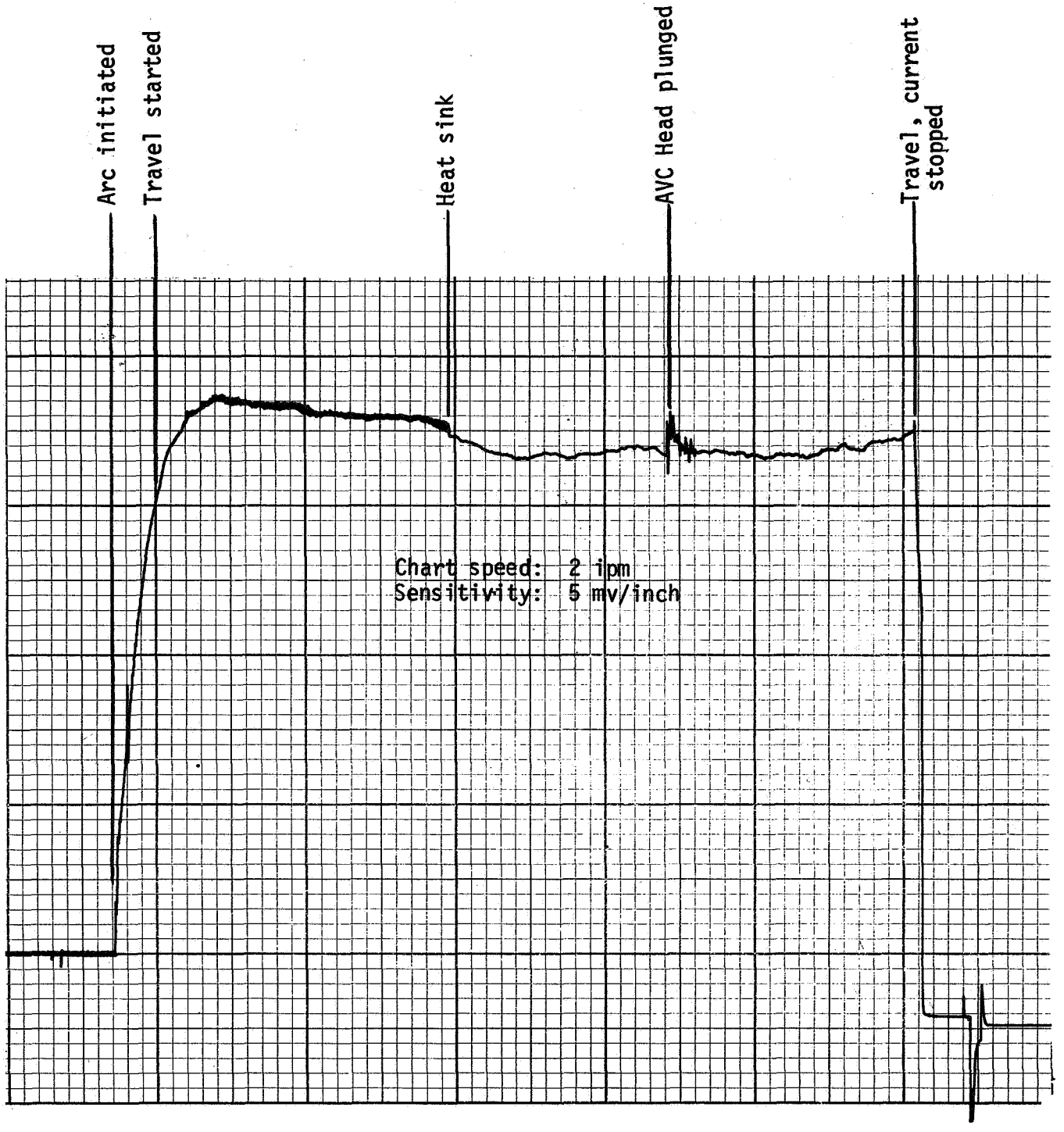


Figure 135: Hybrid thermocouple output, test number 2T.

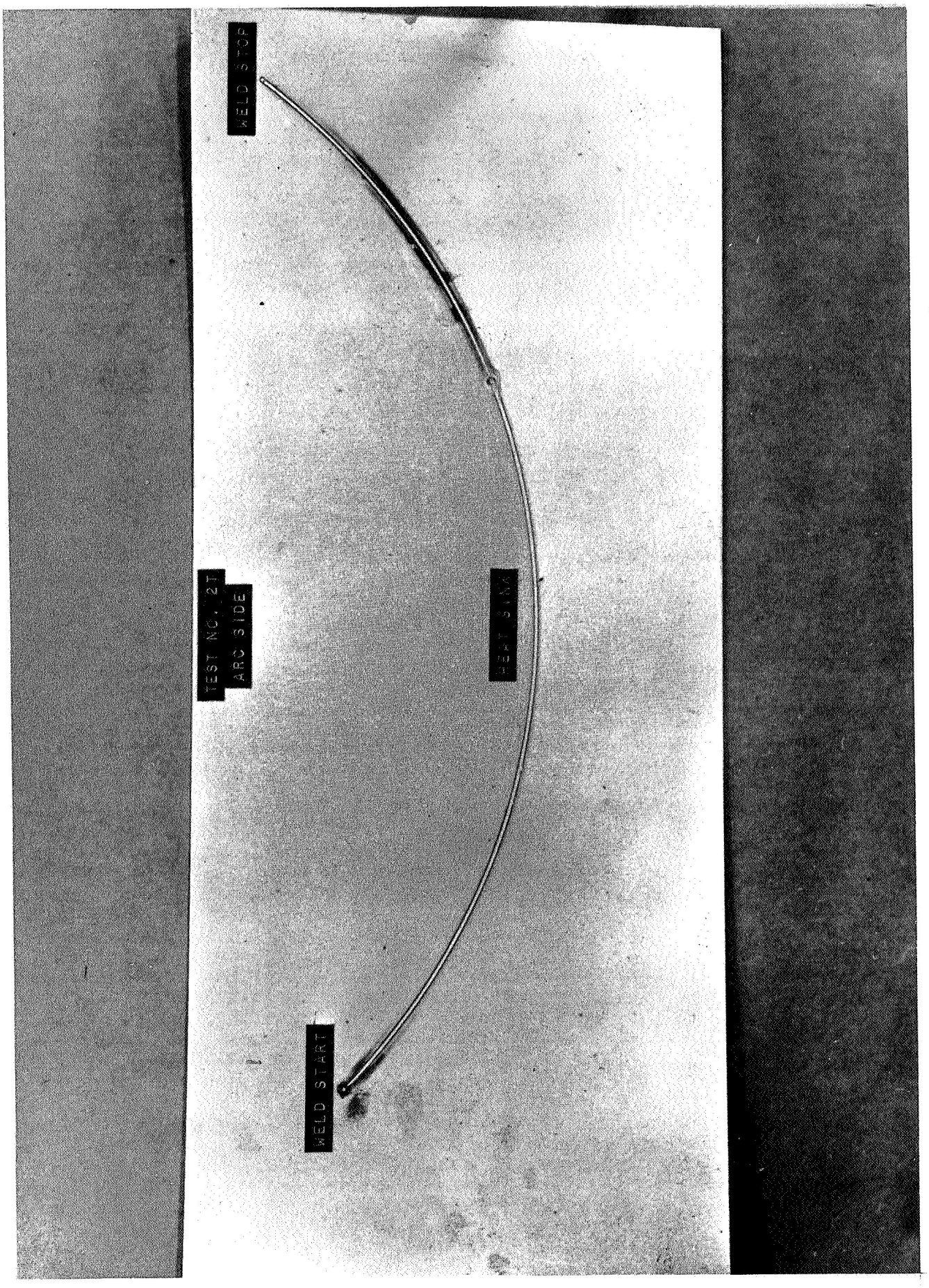


Figure 136: Weld bead, arc side, test number 2T

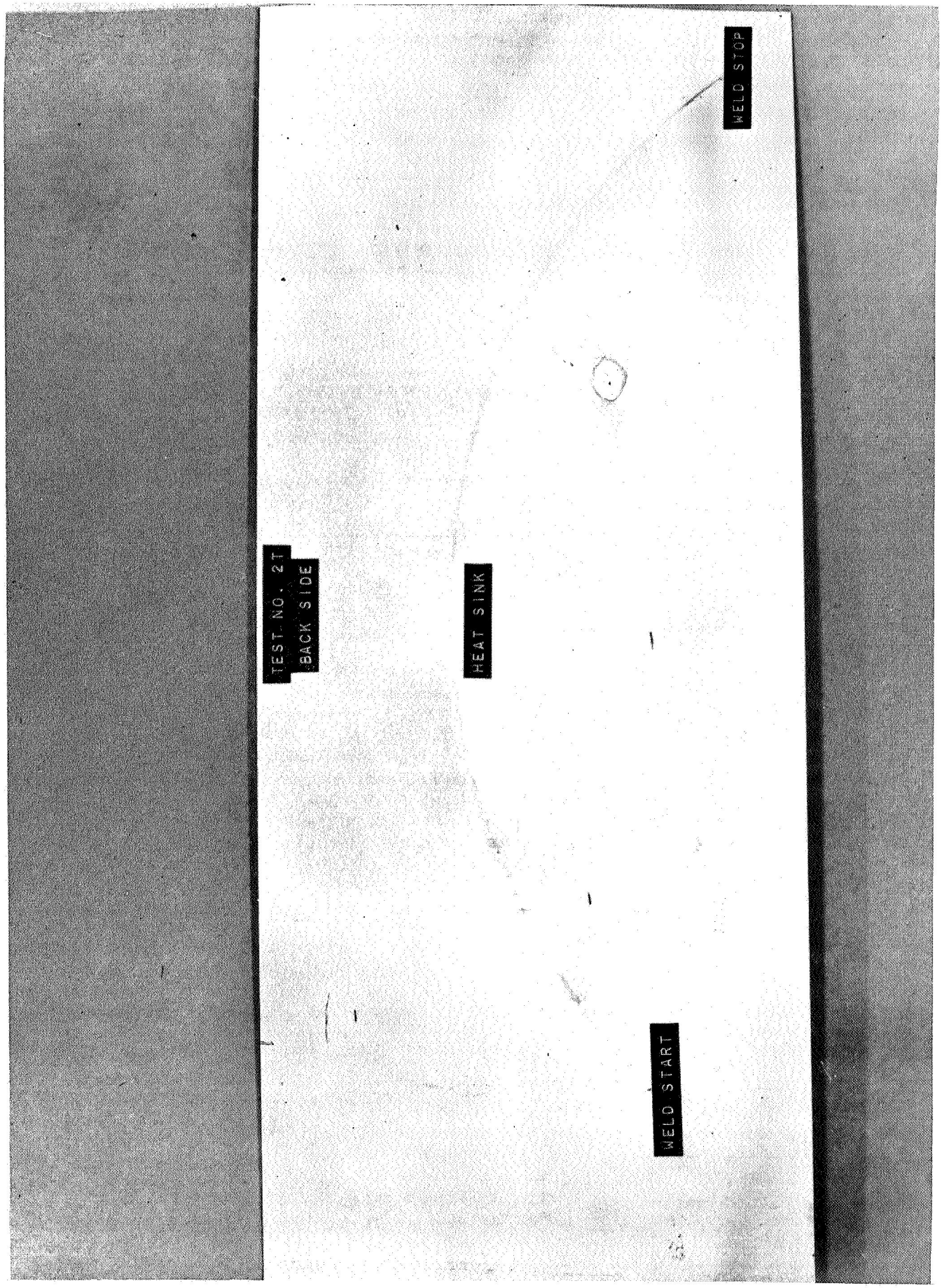


Figure 137: Weld bead, backside, test number 2T.

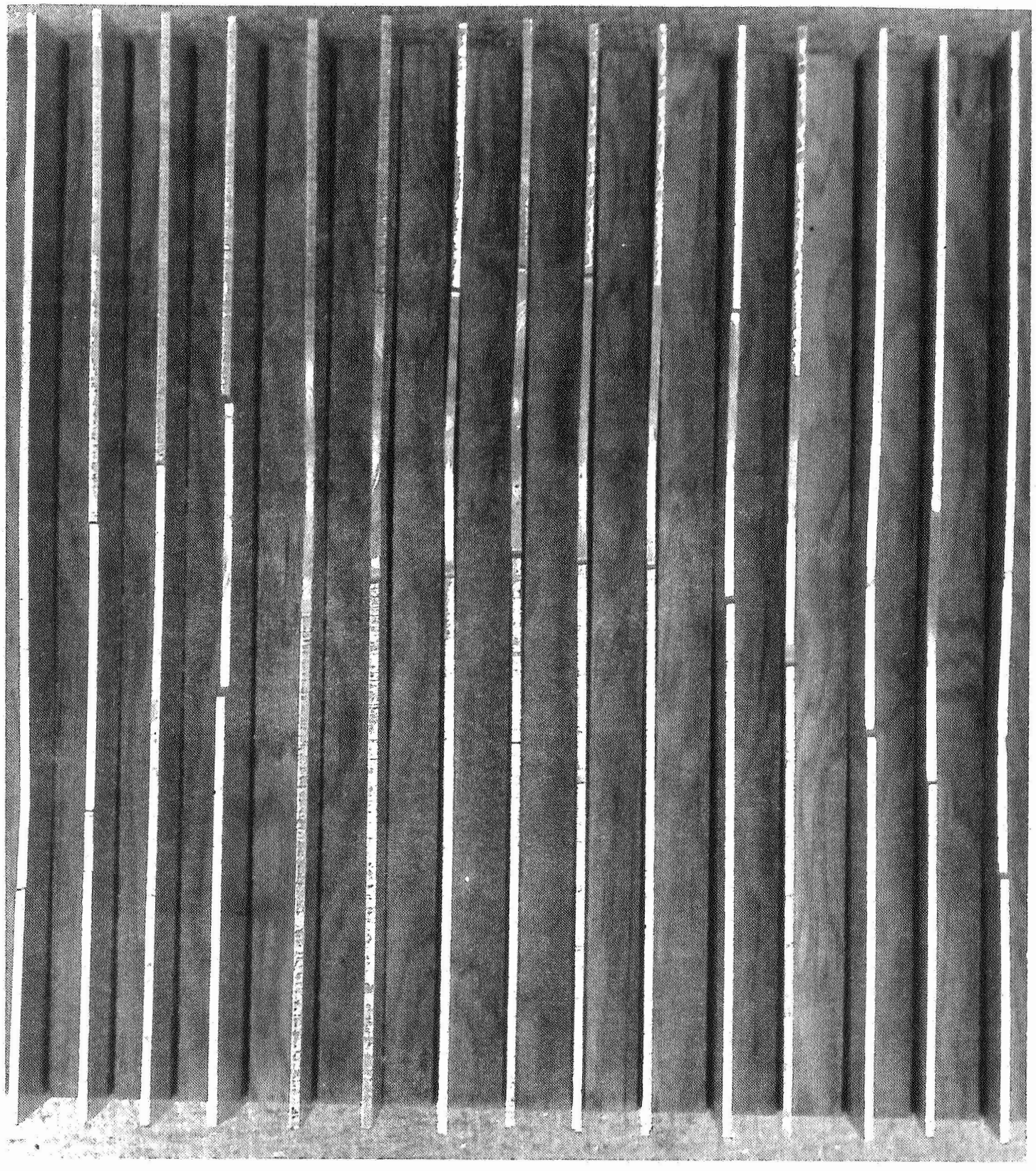


Figure 138: Cross Sections, Test number 2T.

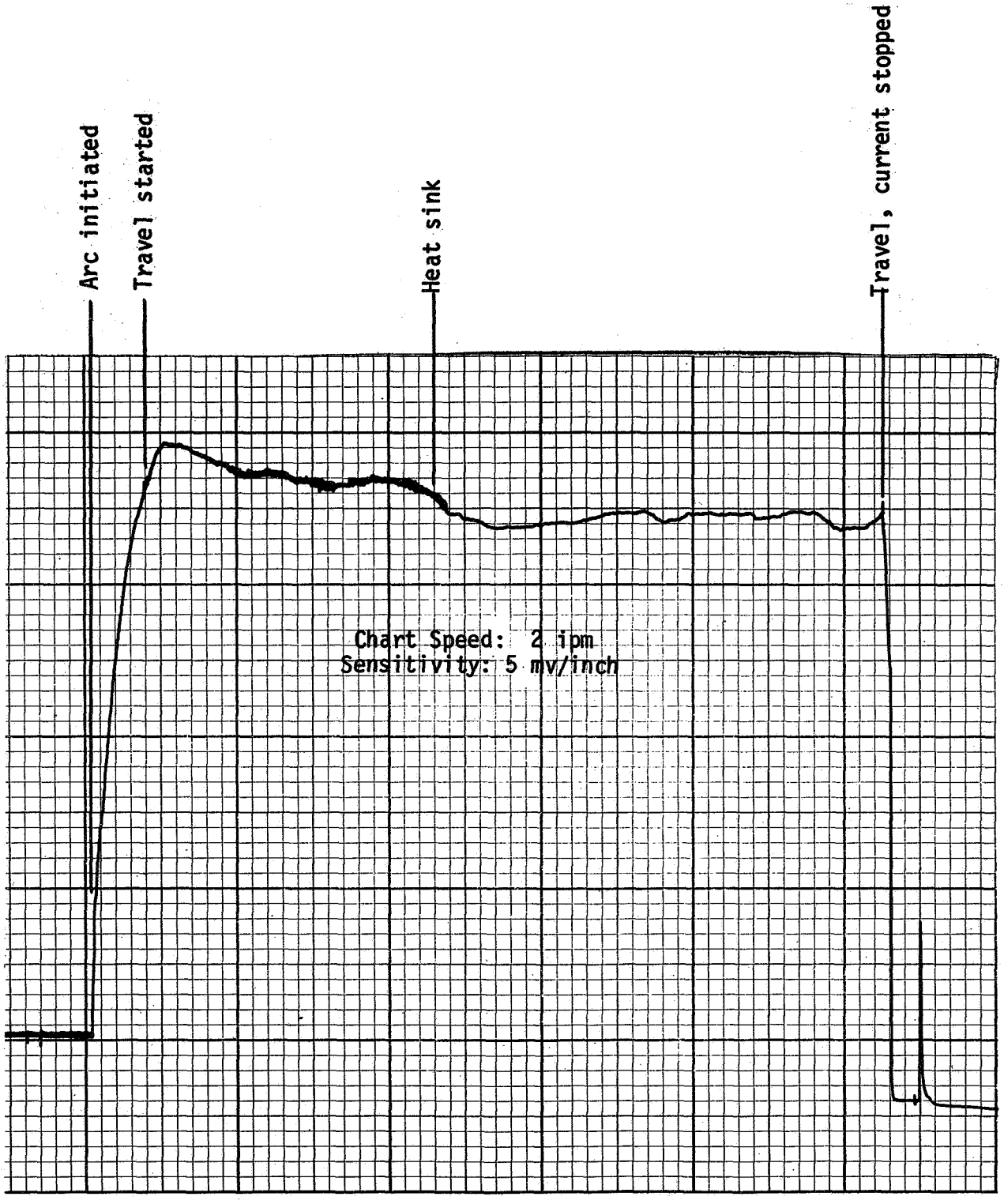


Figure 139: Hybrid thermocouple output, test number 3T.

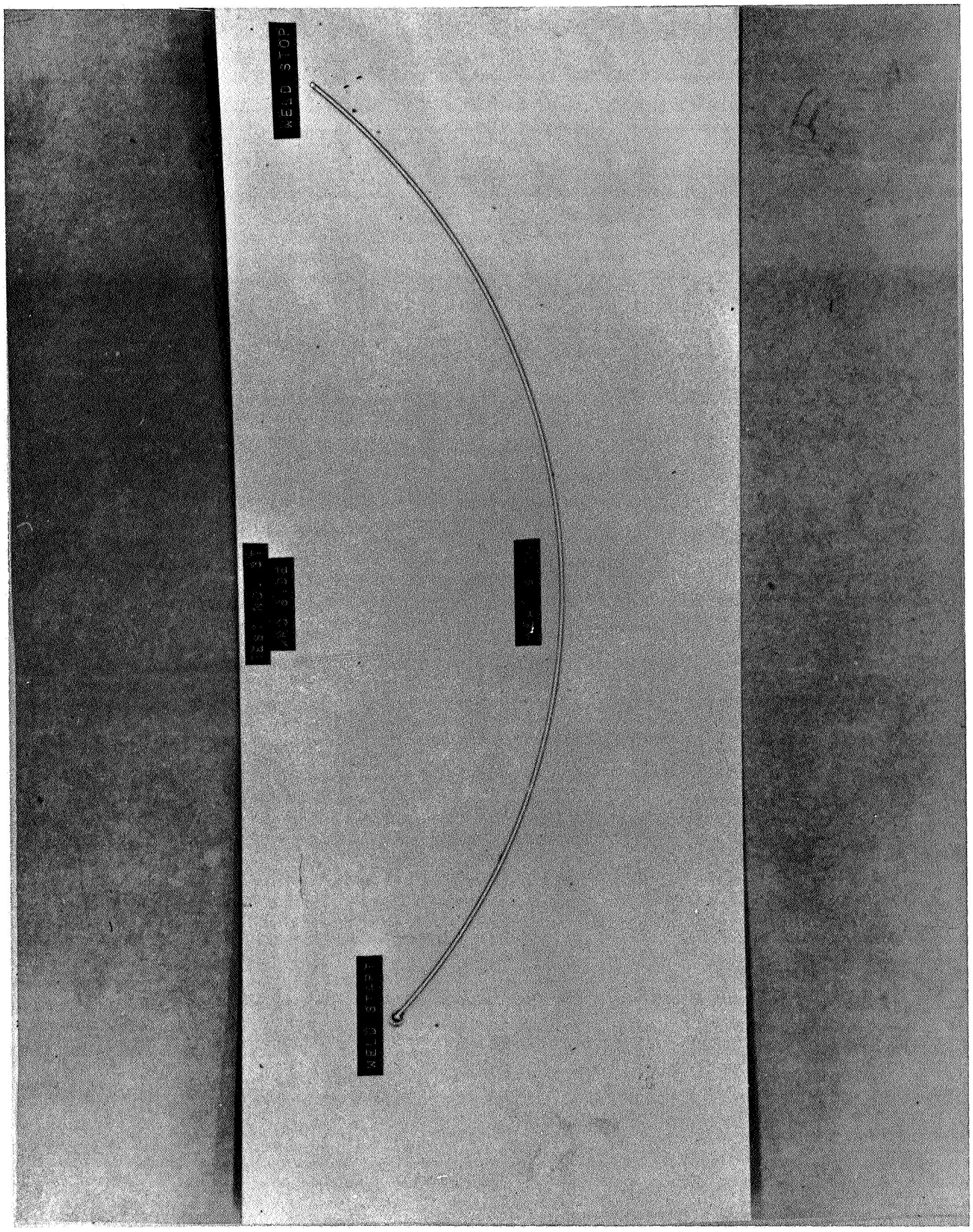


Figure 140: Weld bead, arc side, test number 3T

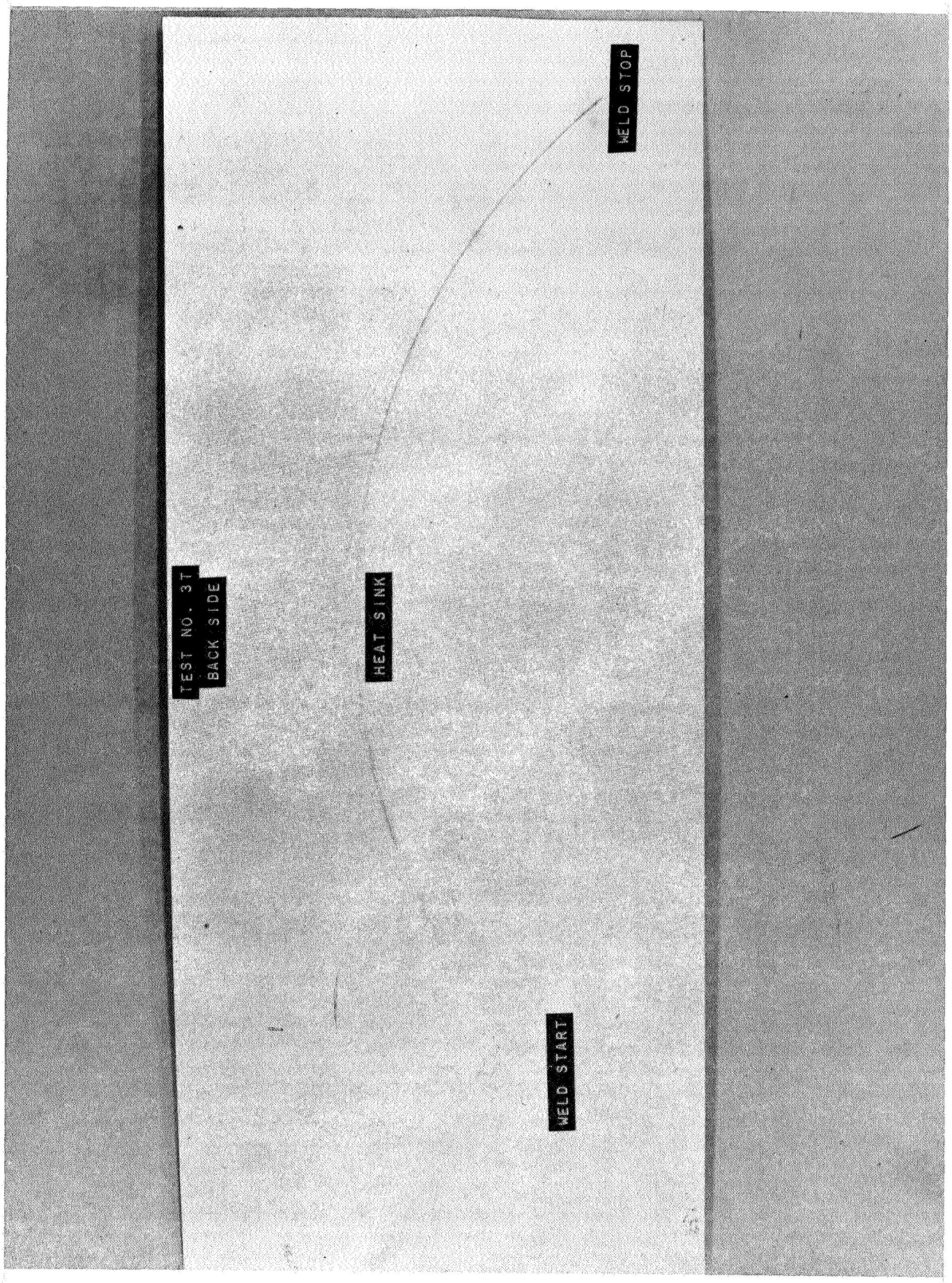


Figure 141: Weld bead, backside, test number 3T.

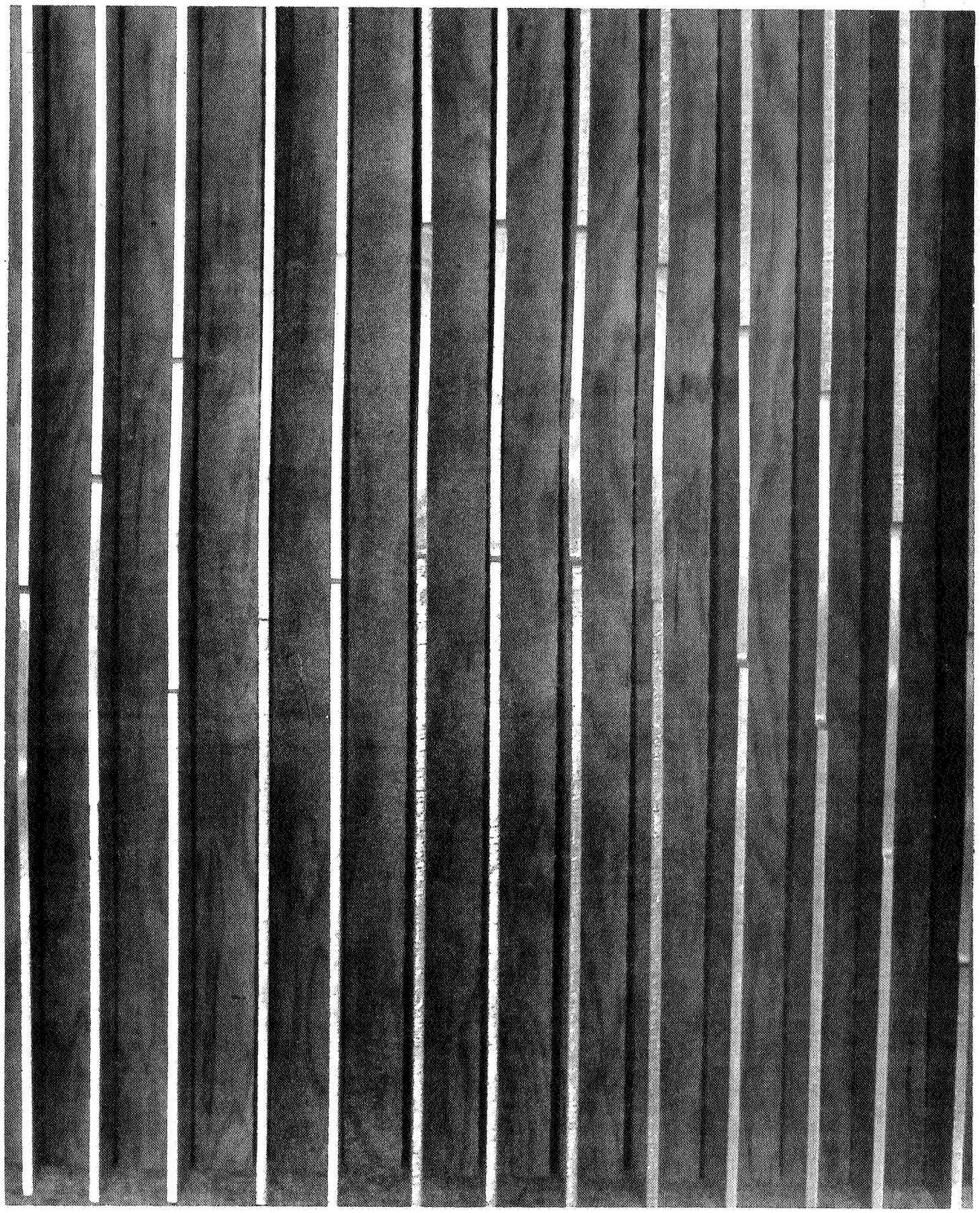


Figure 142: Cross Sections, Test Number 3T.

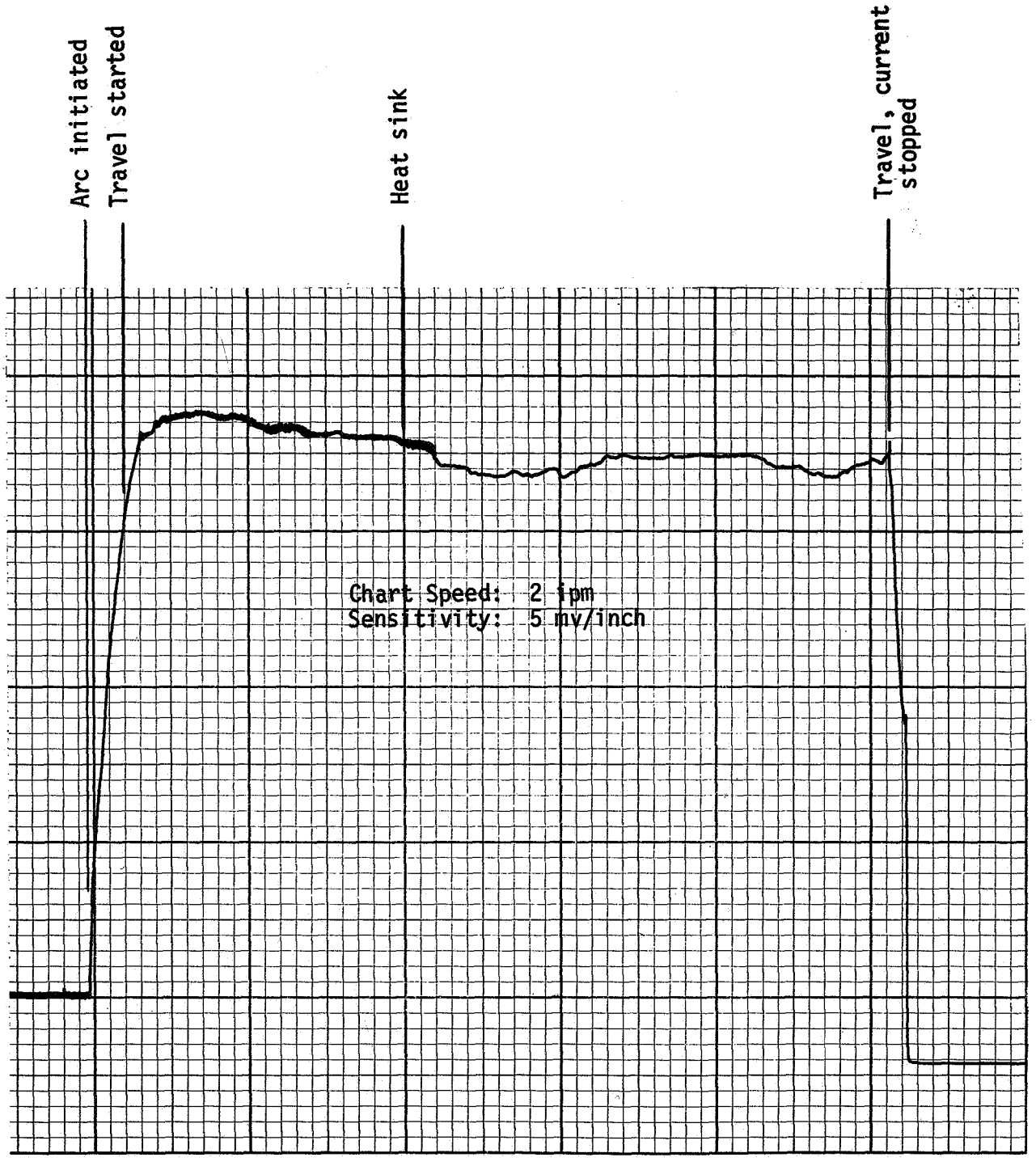


Figure 143: Hybrid thermocouple output, test number 4T.

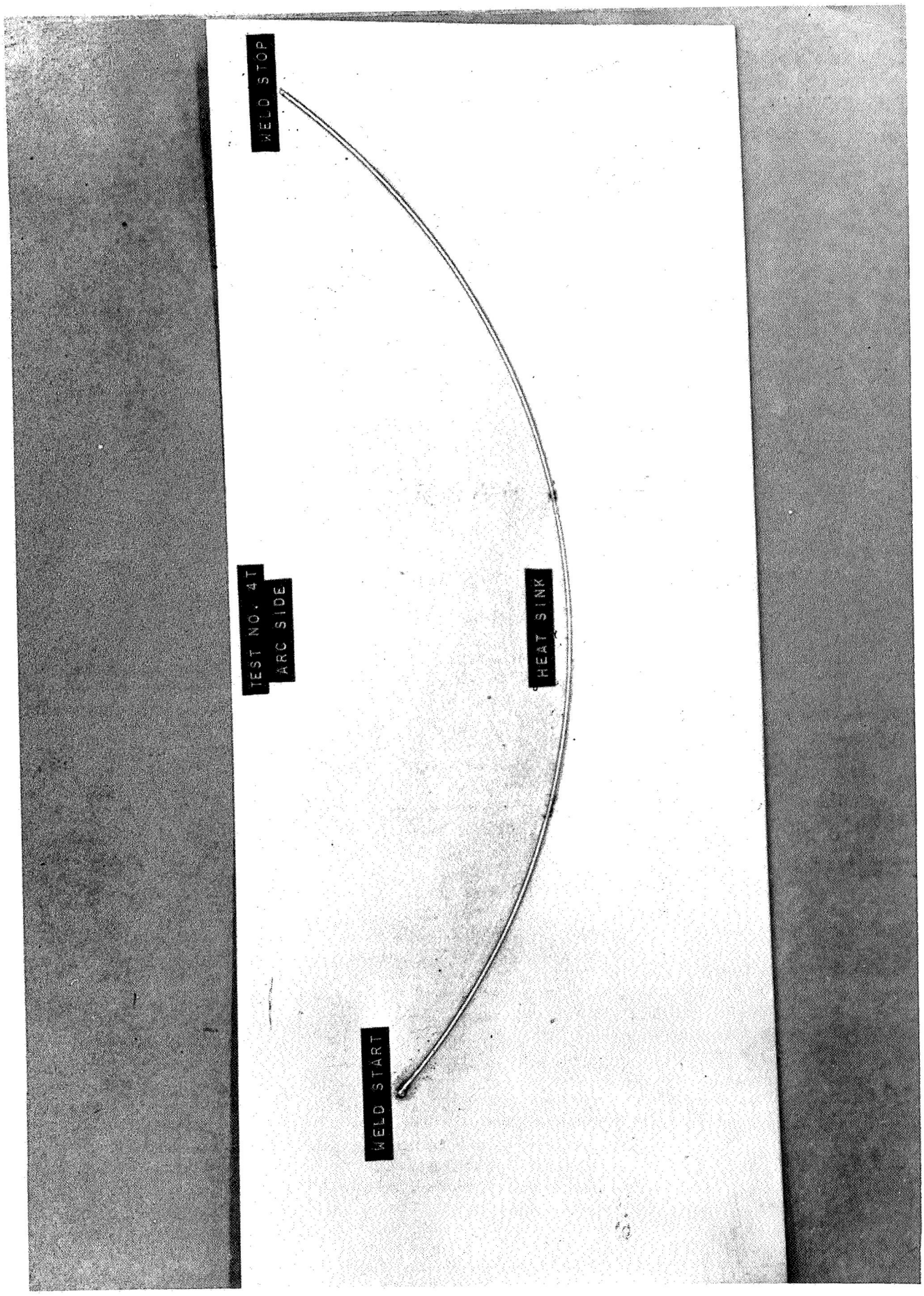


Figure 144: Weld bead, arcside, test number 4T.

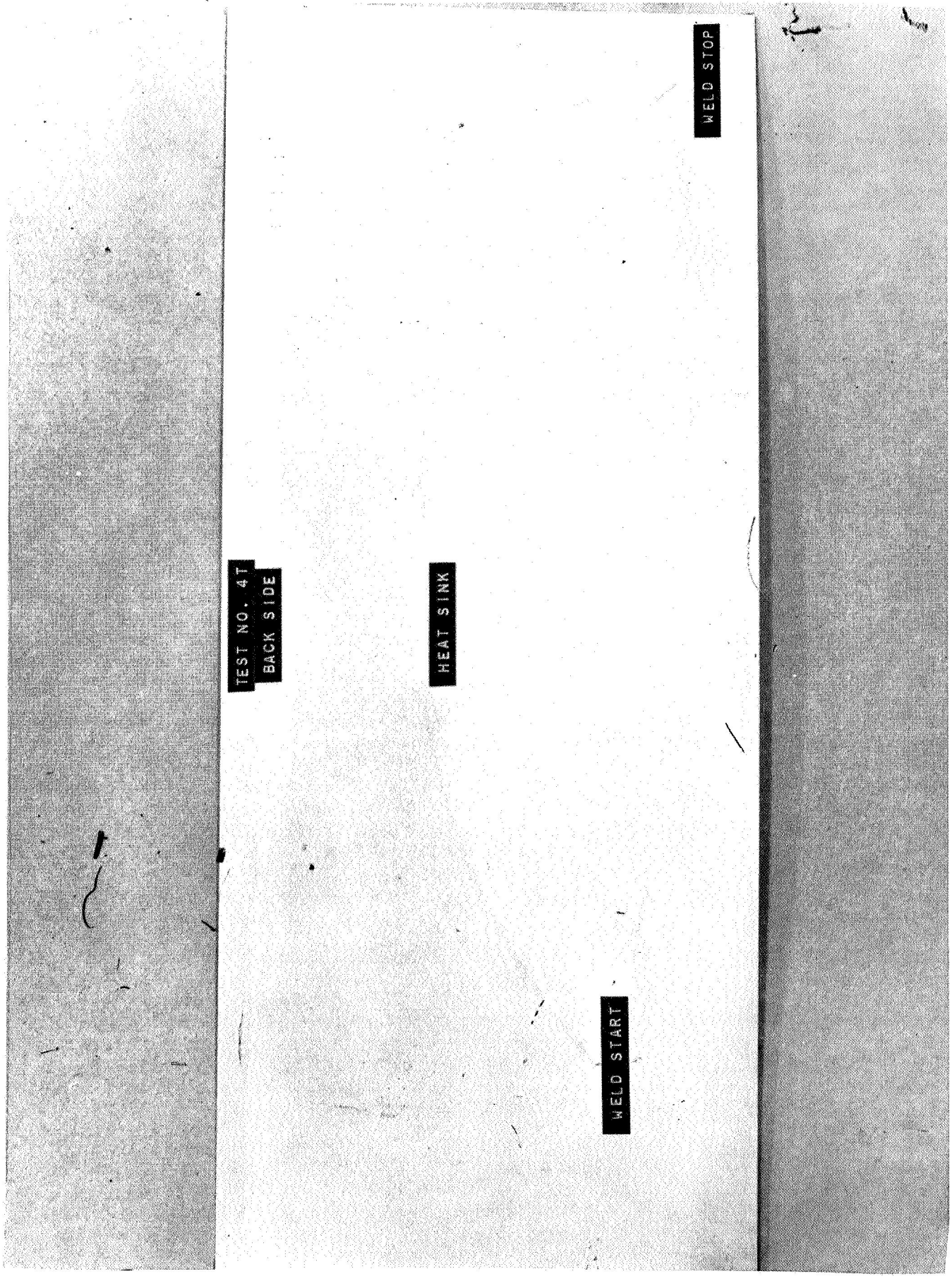


Figure 145: Weld bead, backside, test number 4T

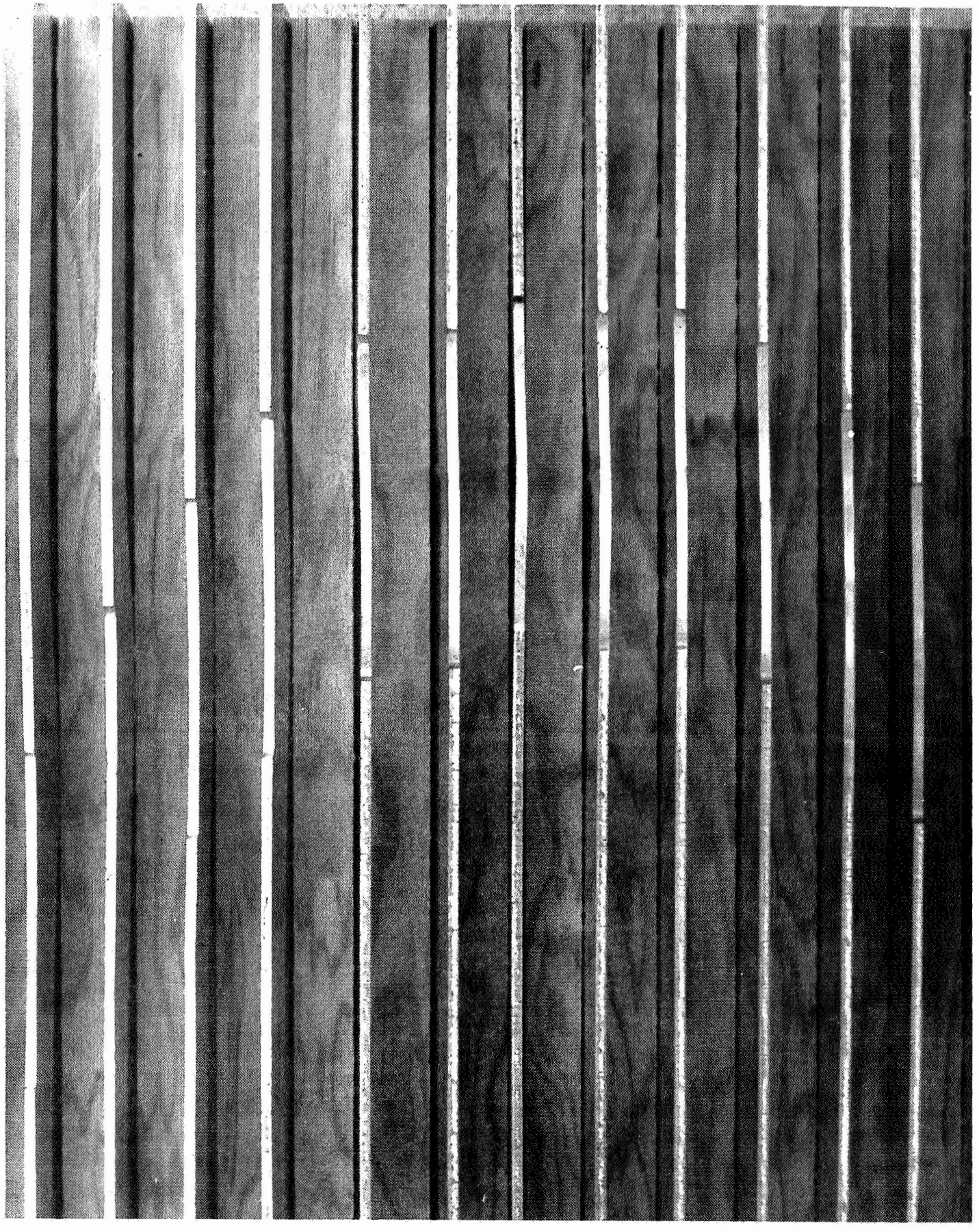


Figure 146: Cross Sections, Test Number 4T.

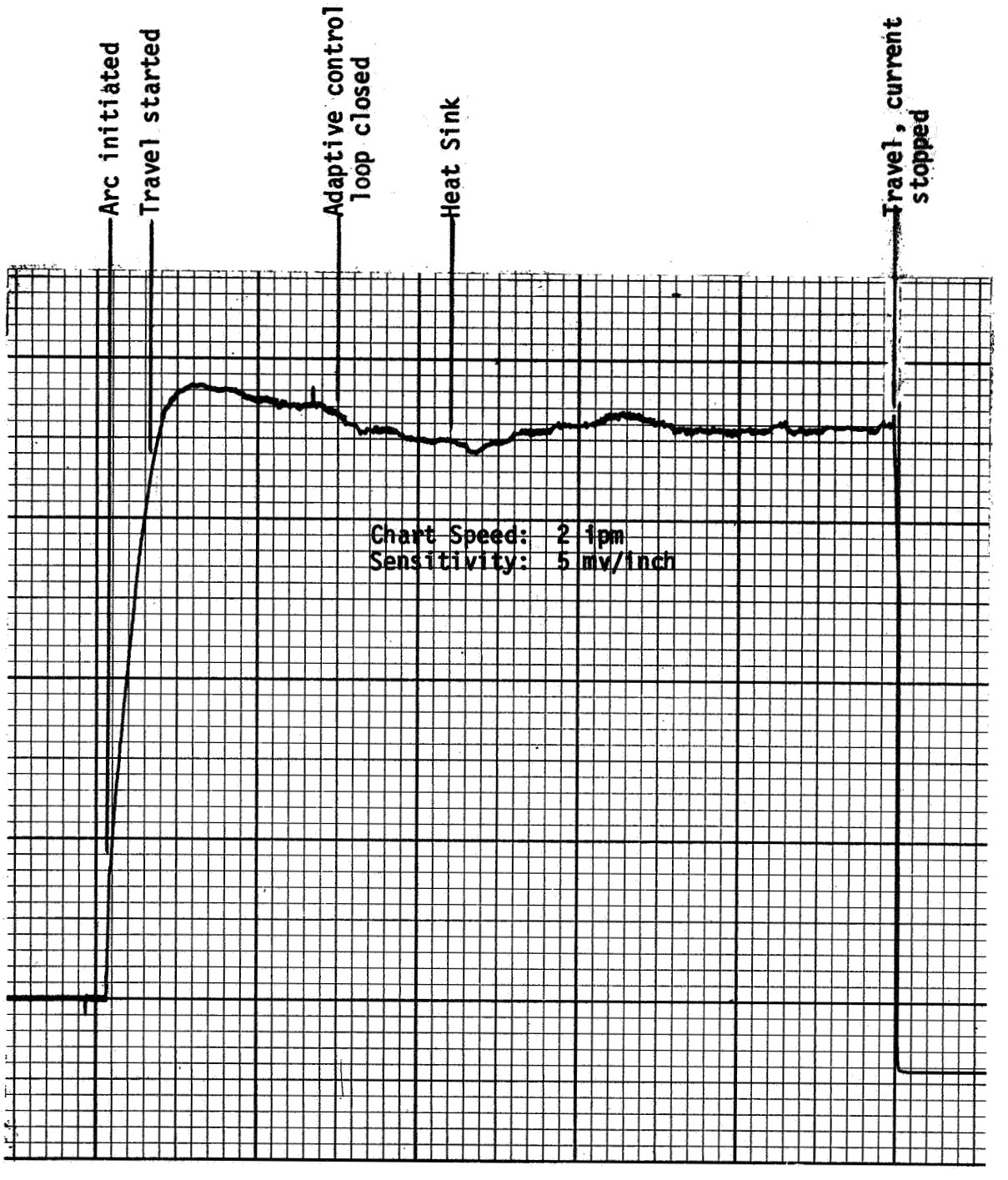


Figure 147: Hybrid thermocouple output, test number 5T.

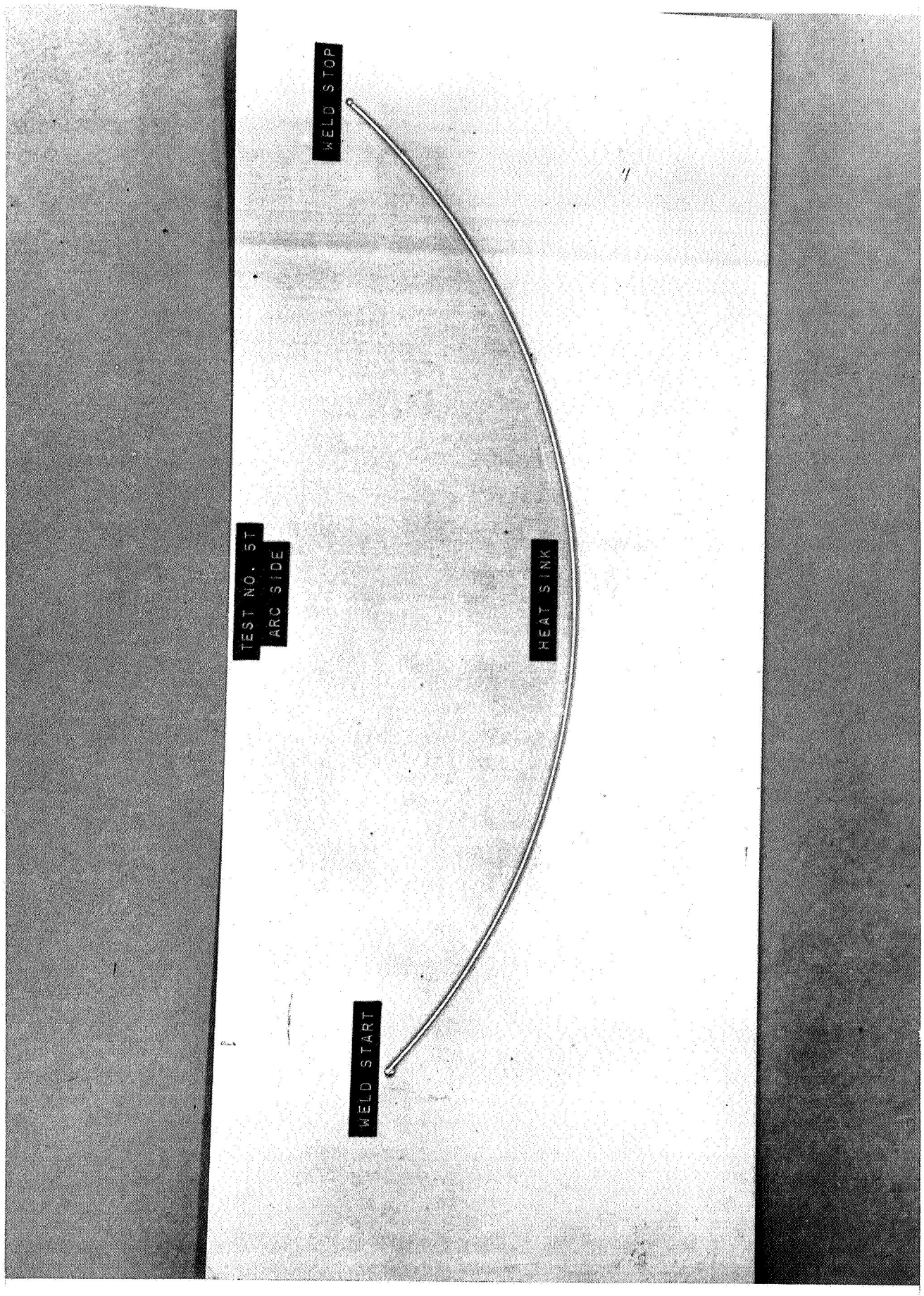


Figure 148: Weld bead, arc side, test number 5T.

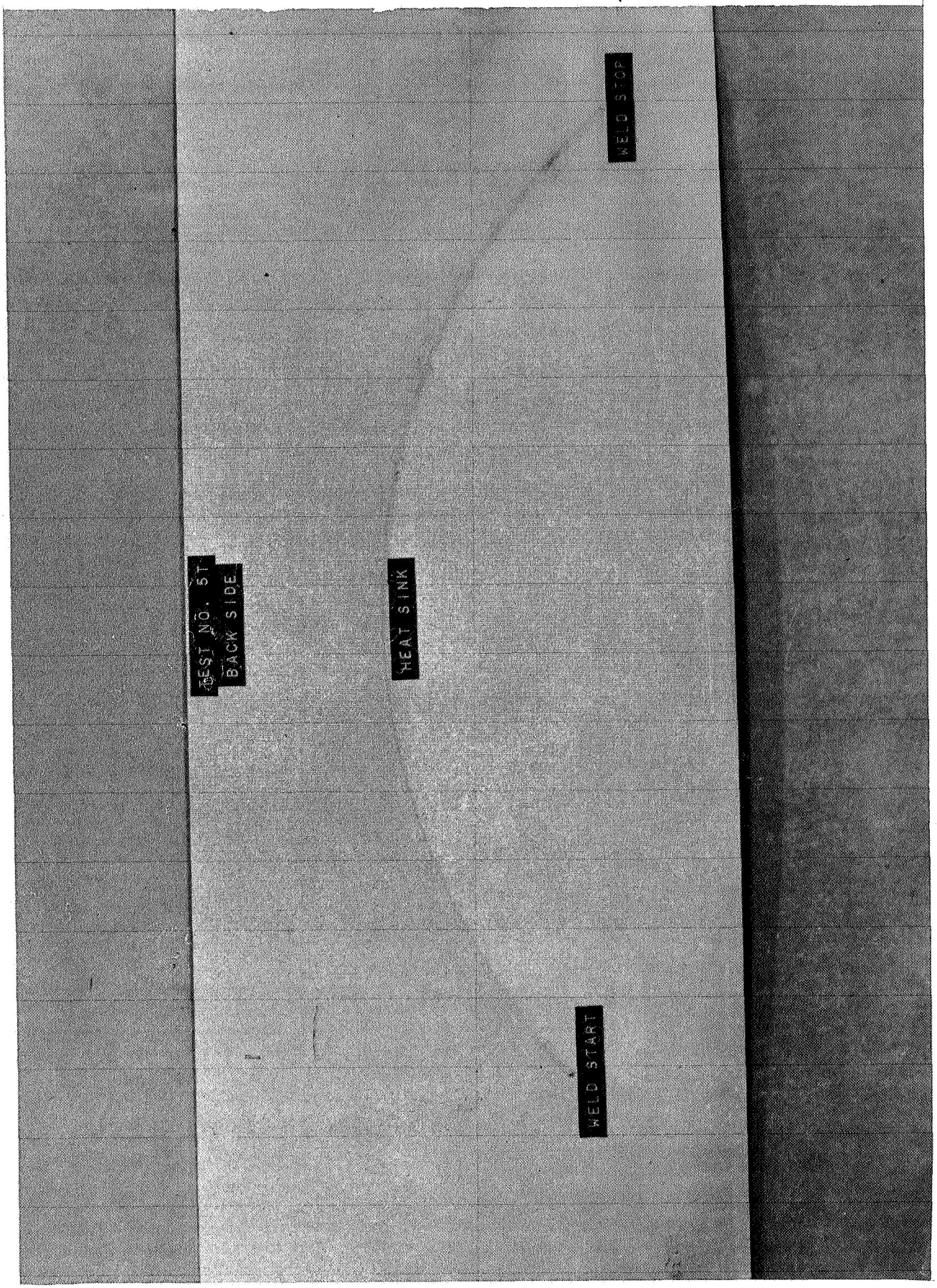


Figure 149: Weld bead, backside, test number 5T.

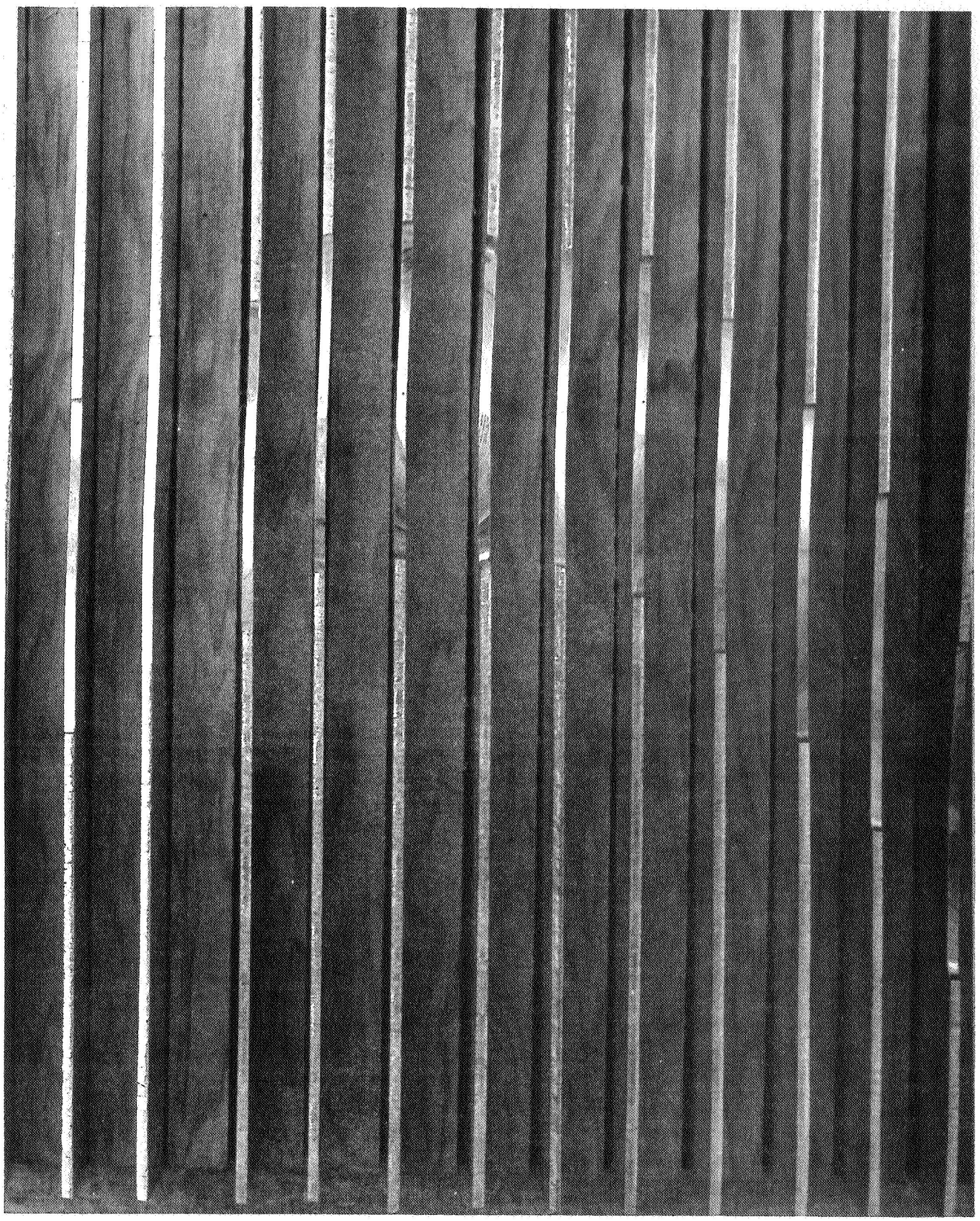


Figure 150: Cross Sections, Test Number 5T.

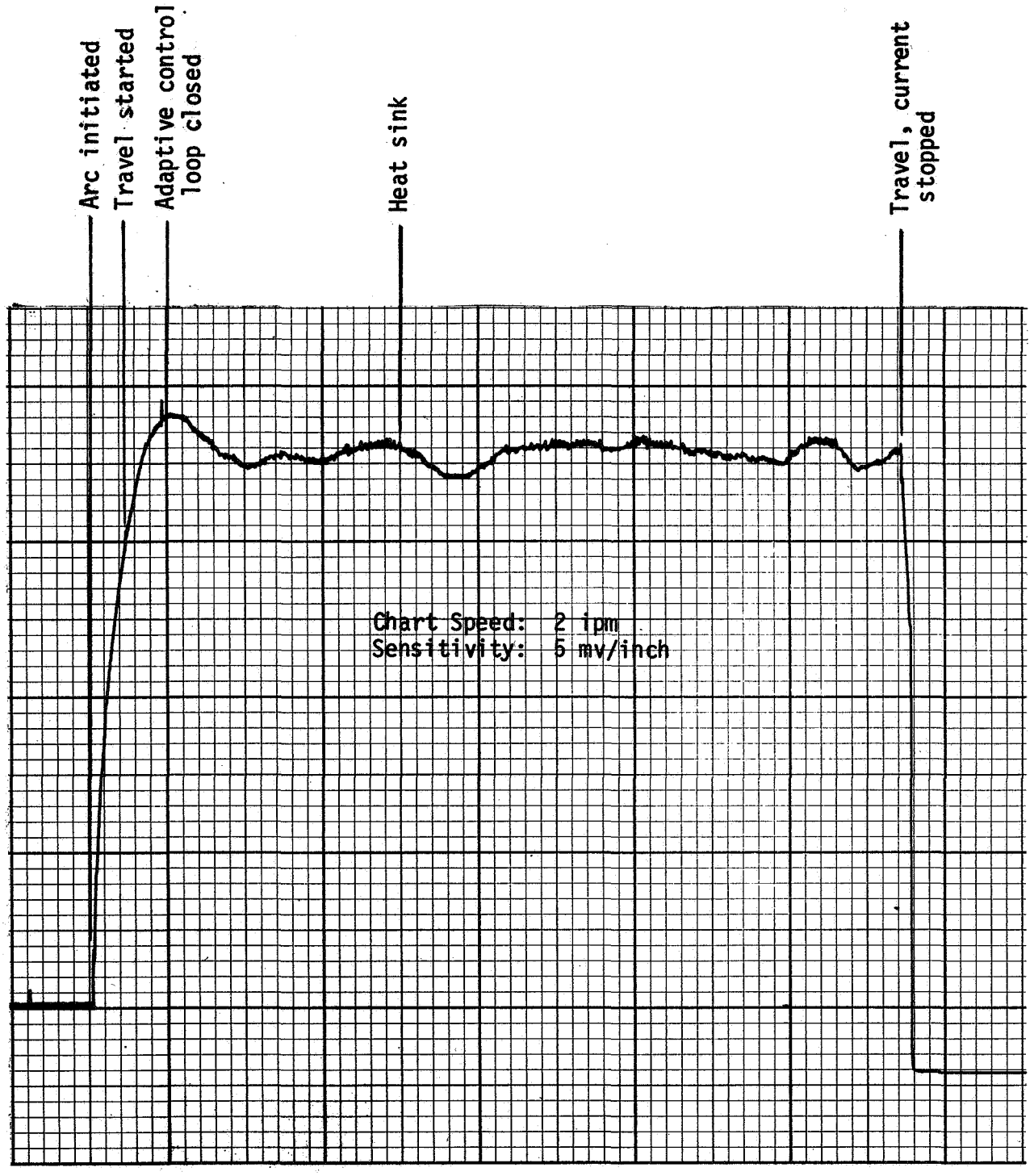


Figure 151: Hybrid thermocouple output, test number 6T.

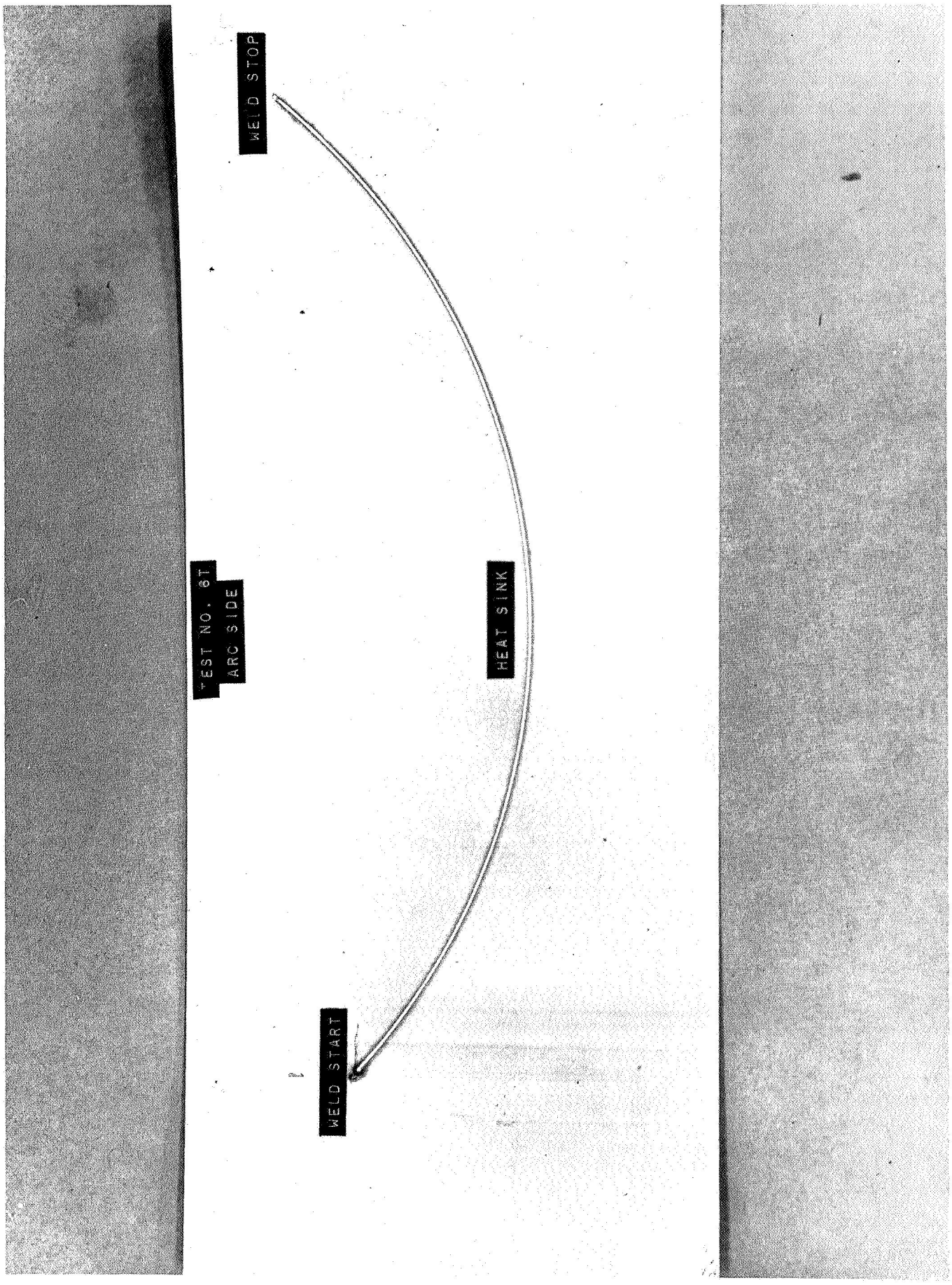


Figure 152: Weld bead, arc side, test number 6T

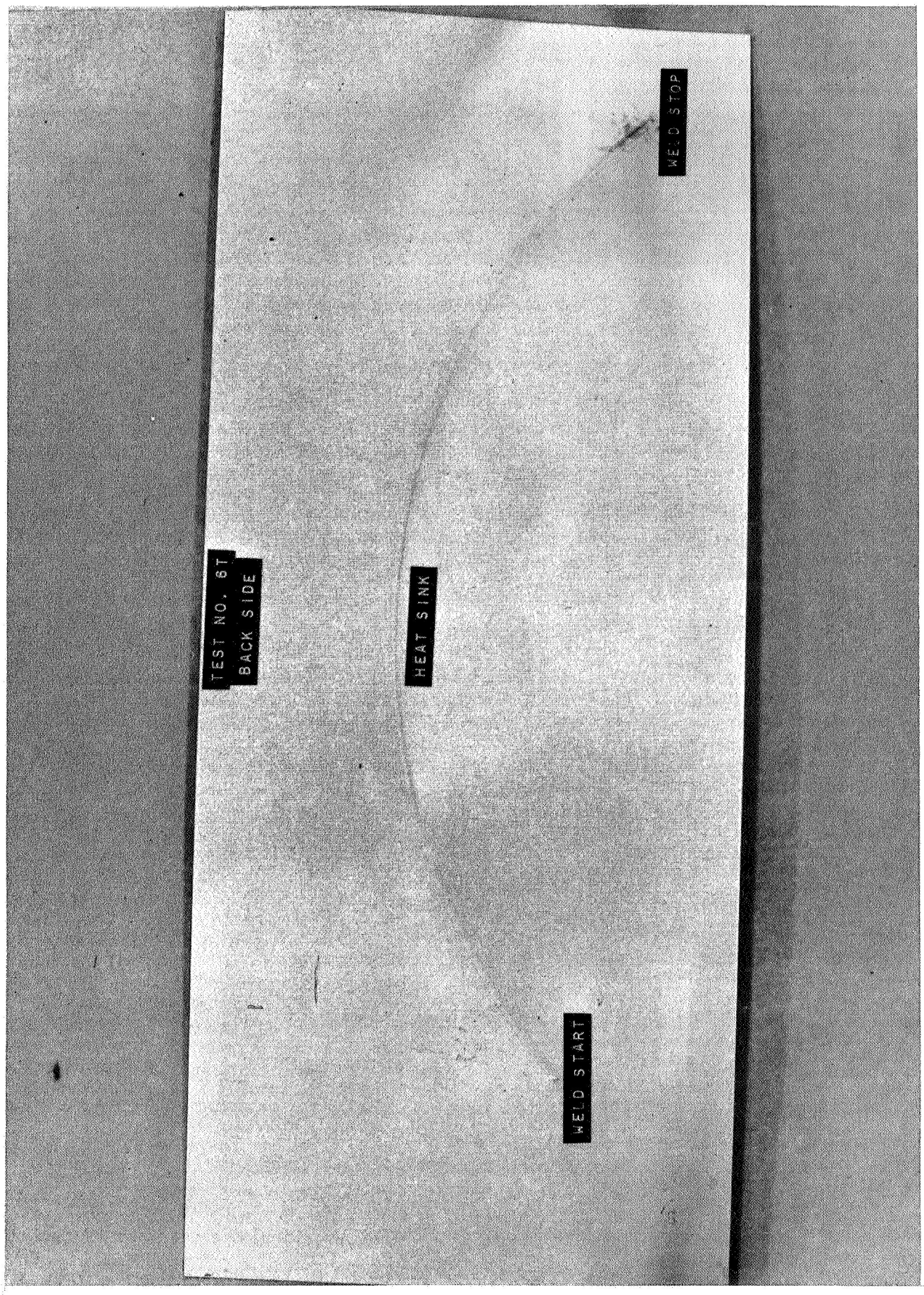


Figure 153: Weld bead, backside, test number 6T.

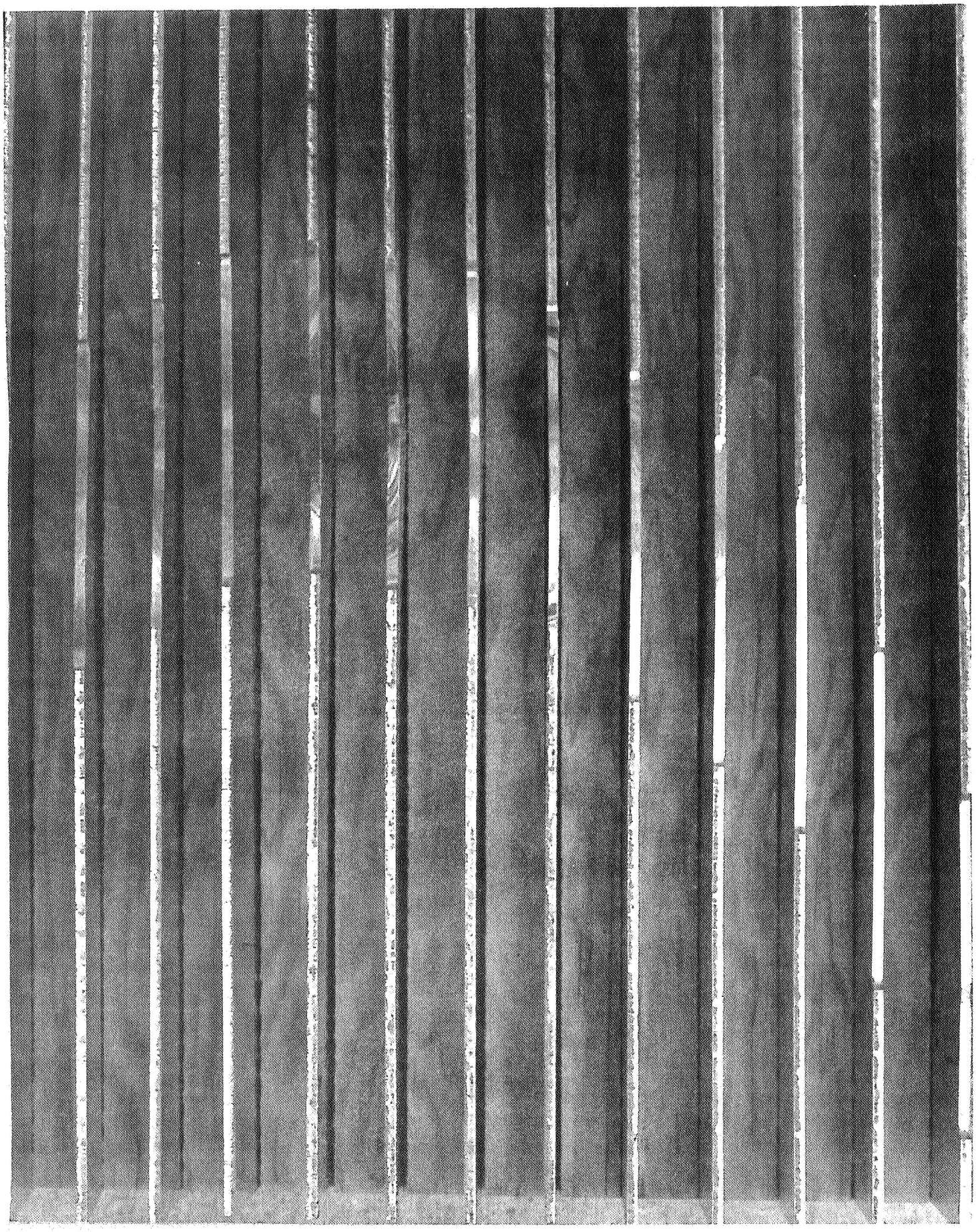


Figure 154: Cross Sections, Test Number 6T.

Figures 155 through 166. As can be seen from the thermocouple recording (Figure 155, 159 and 163), tighter control was realized with the increased gain. Again, all of these tests were conducted with the adaptive loop closed.

5.3.4 TEST NUMBER 10T, 11T, 12T, 13T, 14T

On tests number 10T through 14T, the adaptive controller reference setting was adjusted in an attempt to optimize the penetration level. On tests number 10T, 11T, and 12T the reference voltage was decreased. On tests number 13T and 14T the reference voltage was increased slightly. The thermocouple recordings, front and backside views and cross sections for these tests are shown in Figure 167 through 186.

5.3.5 TEST NUMBER 15T

Test number 15T was identical to the previous tests except that a preheat pass of 10 amperes was made without adaptive control. The purpose of this test was to simulate heat buildup in the workpiece. The thermocouple recording for the preheat pass is shown in Figure 187. The thermocouple recording, front and backside views, and cross sections of the completed weld are shown in Figures 188 through 191.

5.3.6 DISCUSSION

The tests conducted on thin plates proved the adaptive control system's ability to maintain full penetration welds on thin material. The adaptive controller gain was shown to be critical relative to tightness of control.

6.0 CONCLUSIONS AND RECOMMENDATIONS

A hybrid thermocouple probe assembly was designed and fabricated to provide an accurate and simple method of monitoring workpiece temperature during the welding process. The system was demonstrated to: (1) be insensitive to radiated arc interference and the effect of variations in surface emissivity, (2) provide an essentially instantaneous response, and (3) be free from interference due to surface oxides.

An adaptive controller was designed and fabricated to amplify the hybrid thermocouple signal and actuate a small instrument servo motor, which was geared to a potentiometer for varying either the travel speed or weld current. The adaptive system was demonstrated to be capable of providing accurate and stable

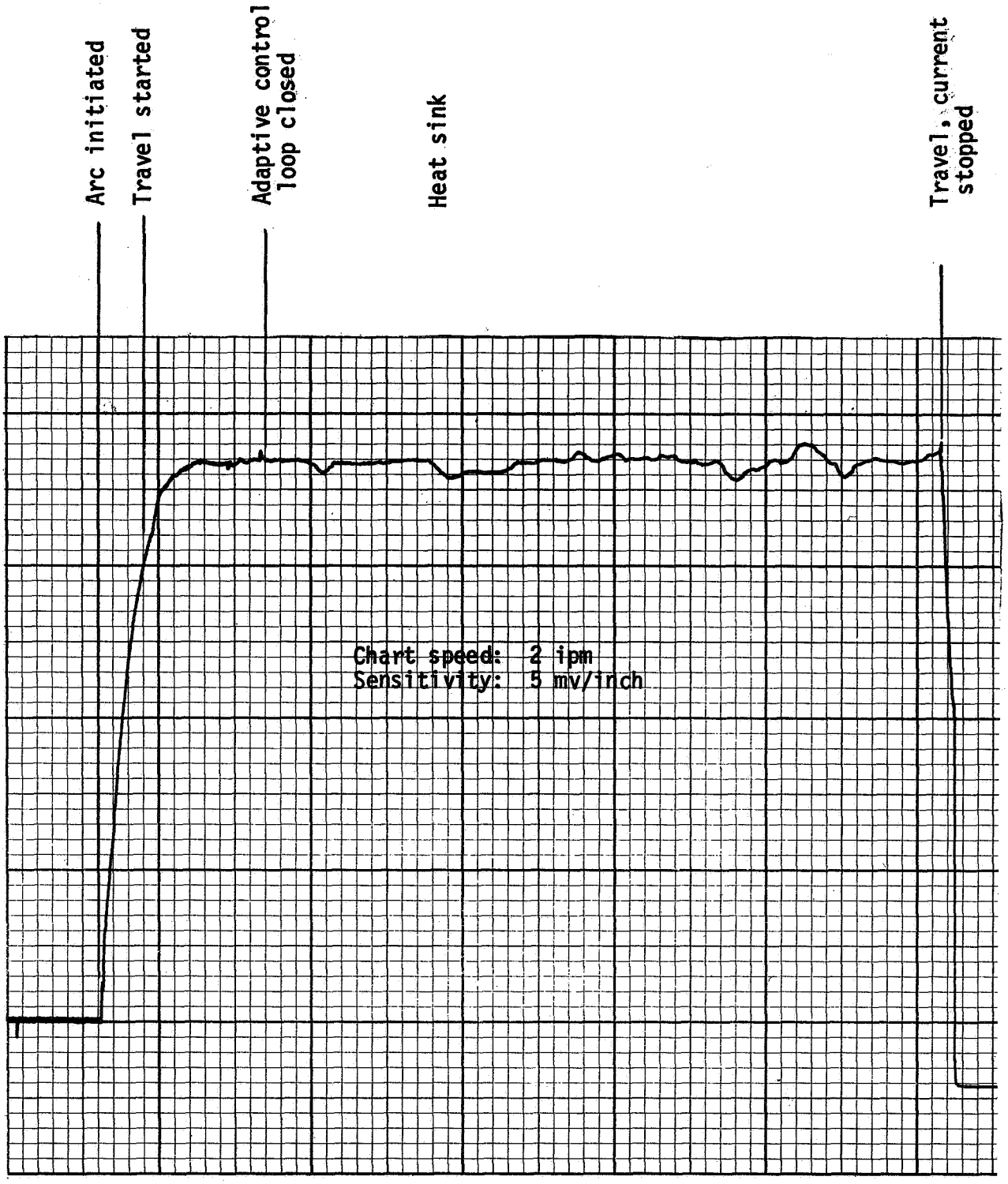


Figure 155: Hybrid thermocouple output, test number 7T.

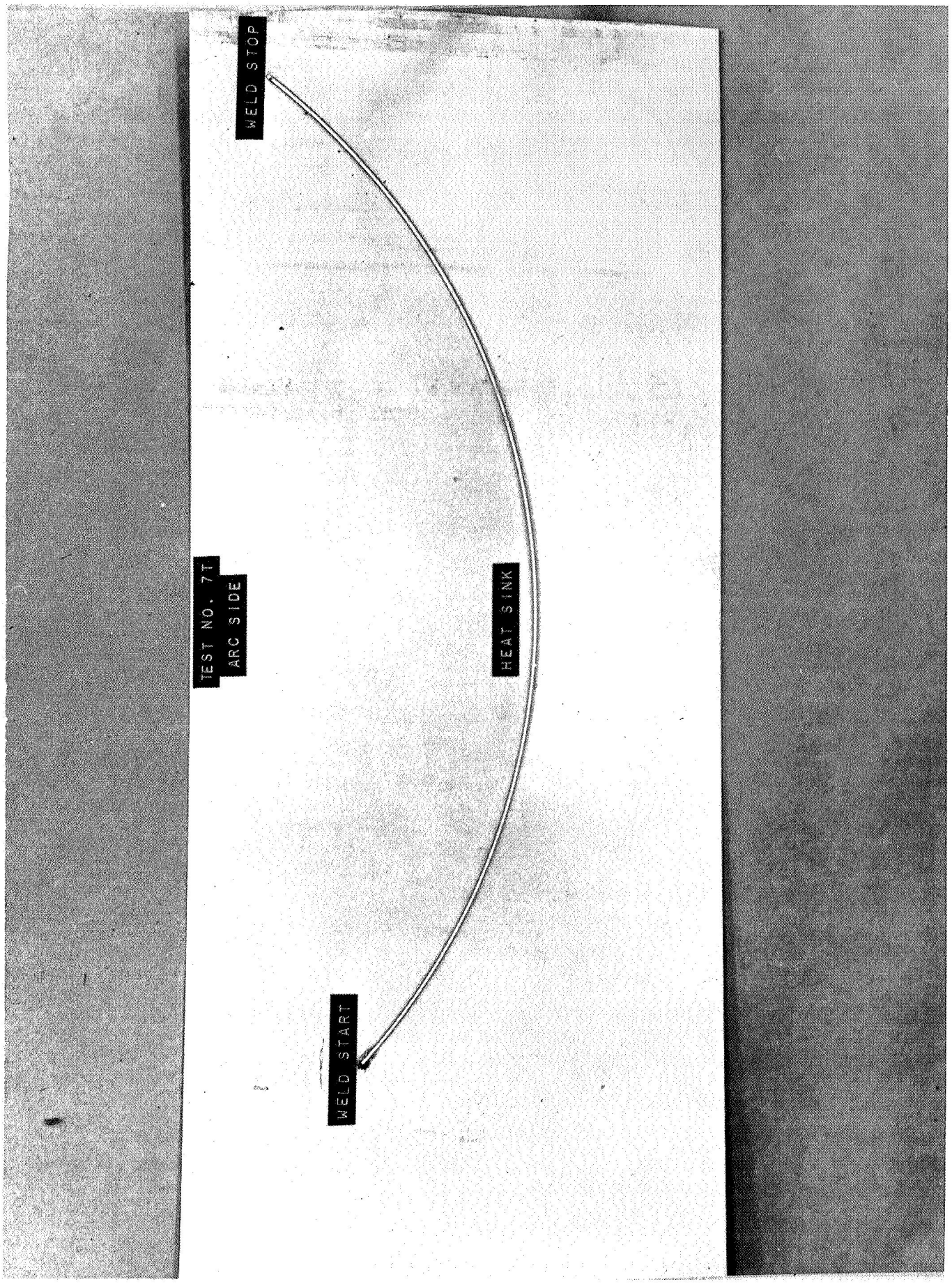


Figure 156: Weld bead, arc side, test number 7T.

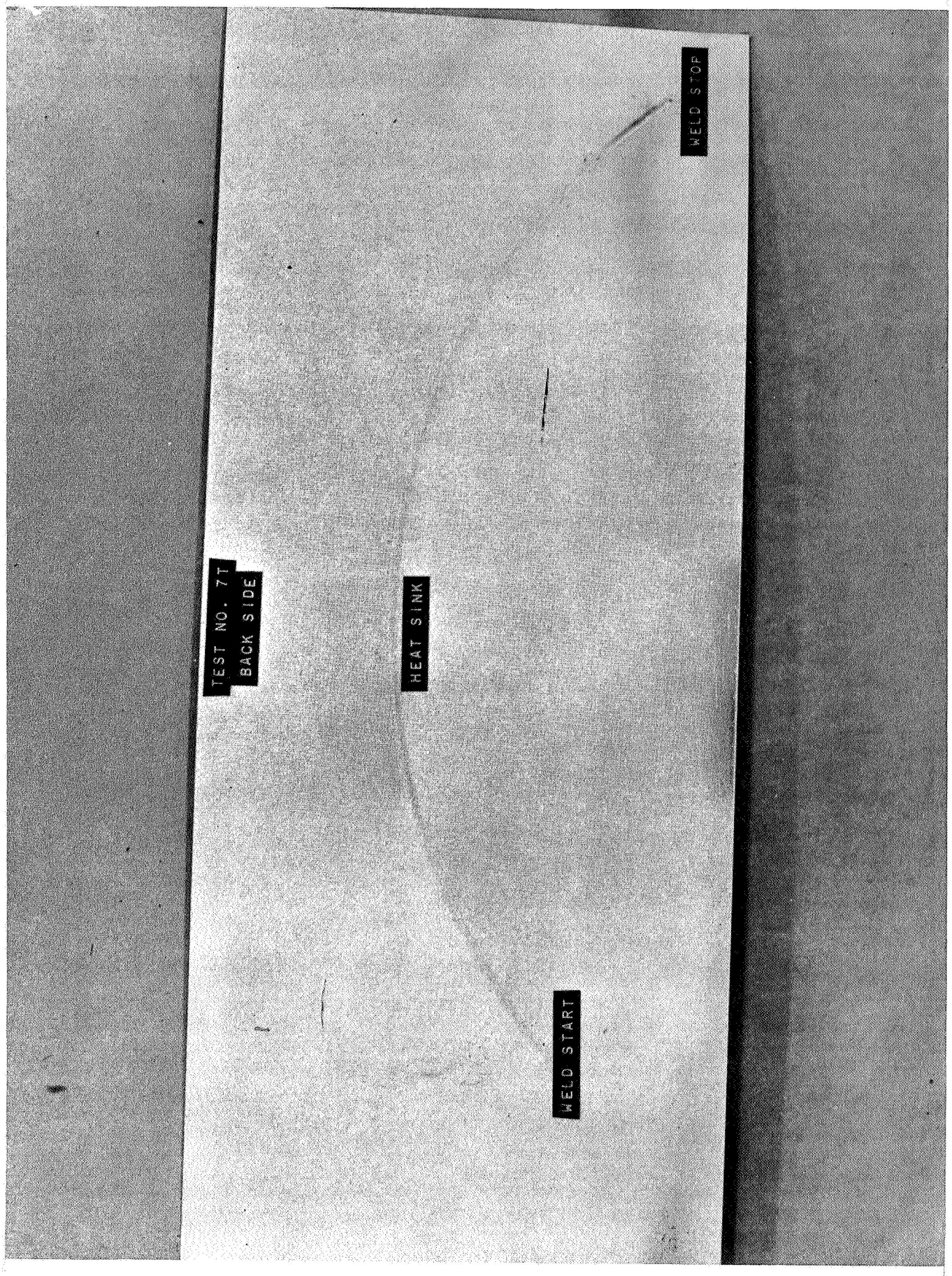


Figure 157: Weld bead, backside, test number 7T

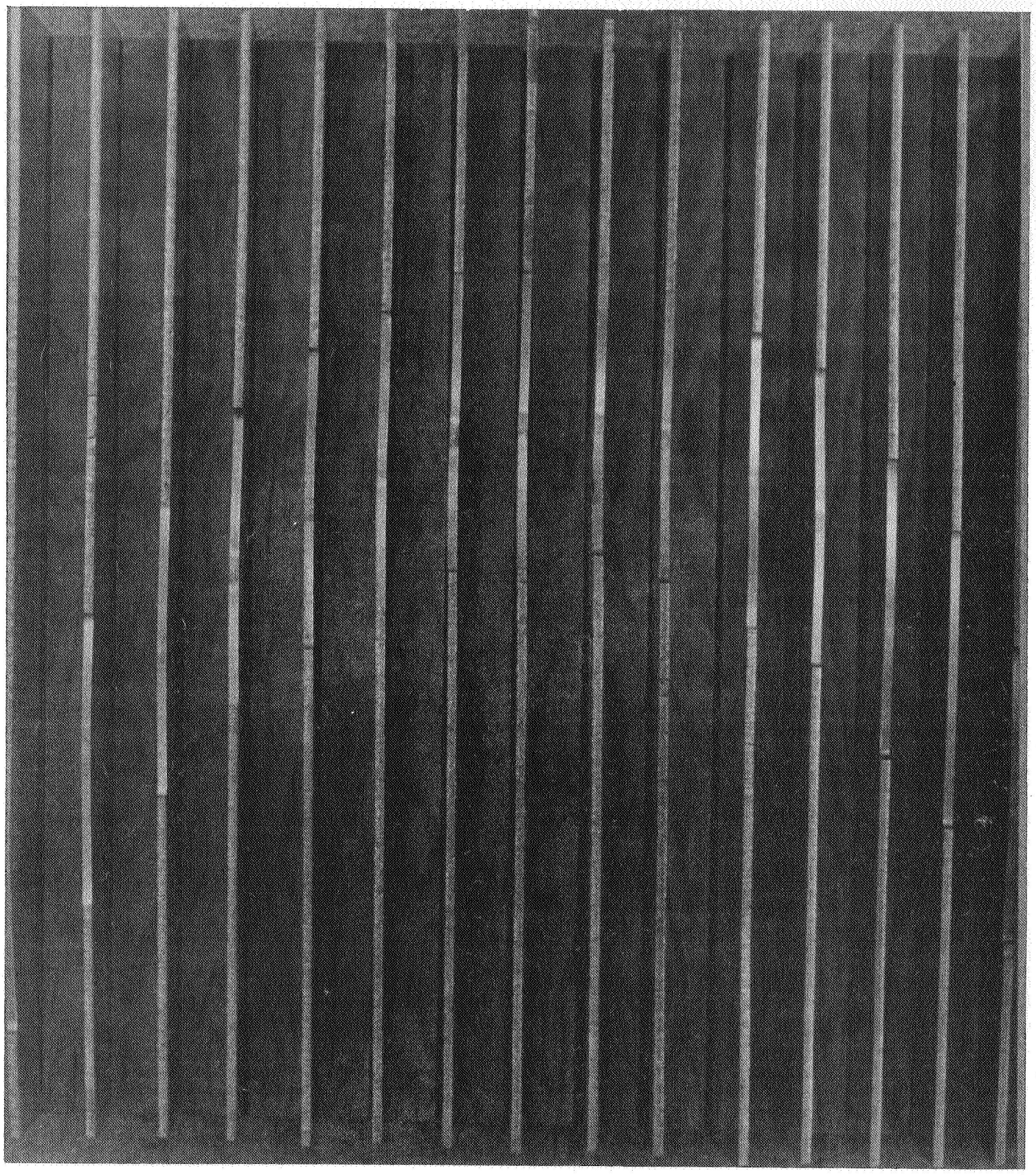


Figure 158: Cross Sections, Test Number 7T.

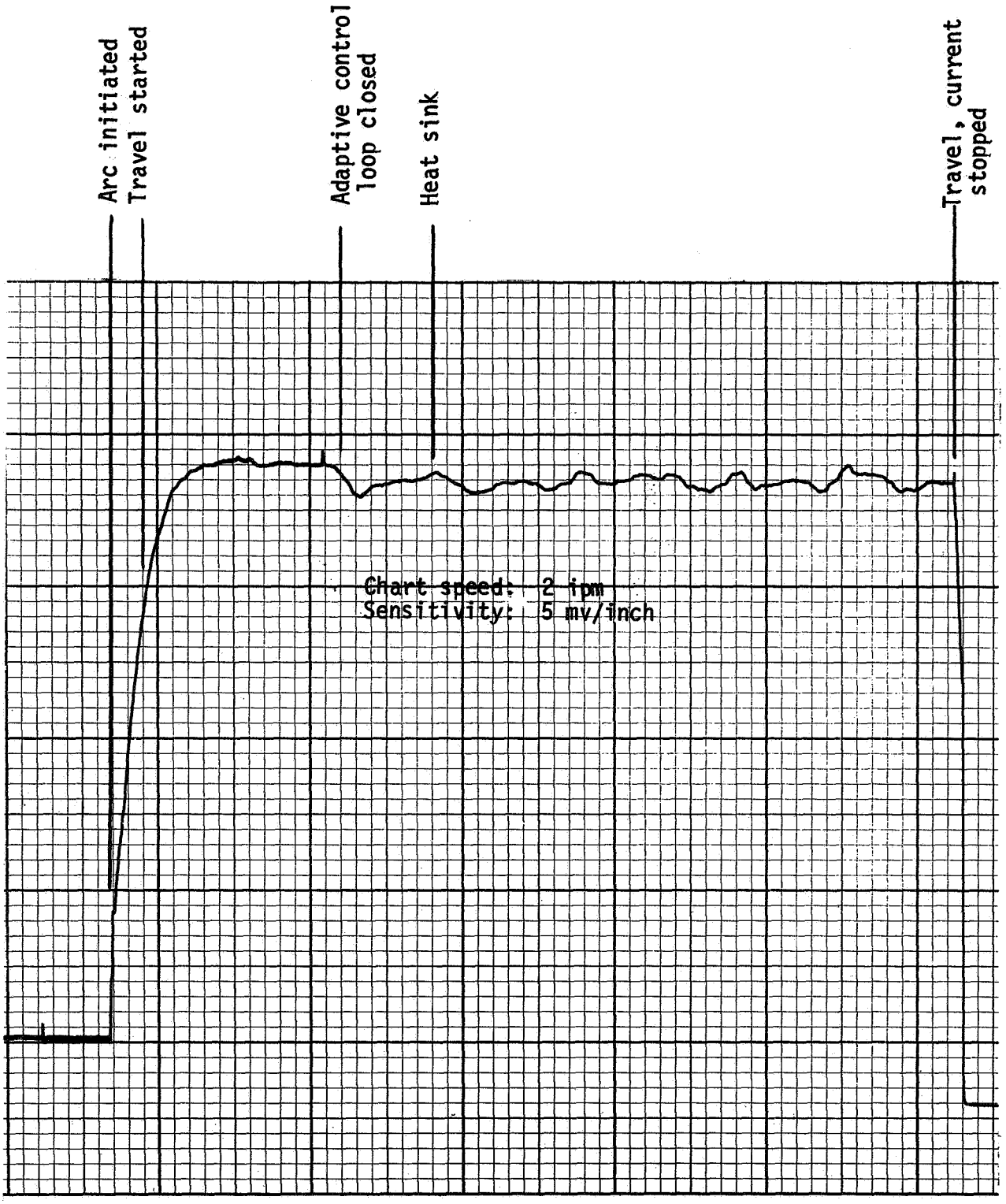


Figure 159: Hybrid thermocouple output, test number 8T.

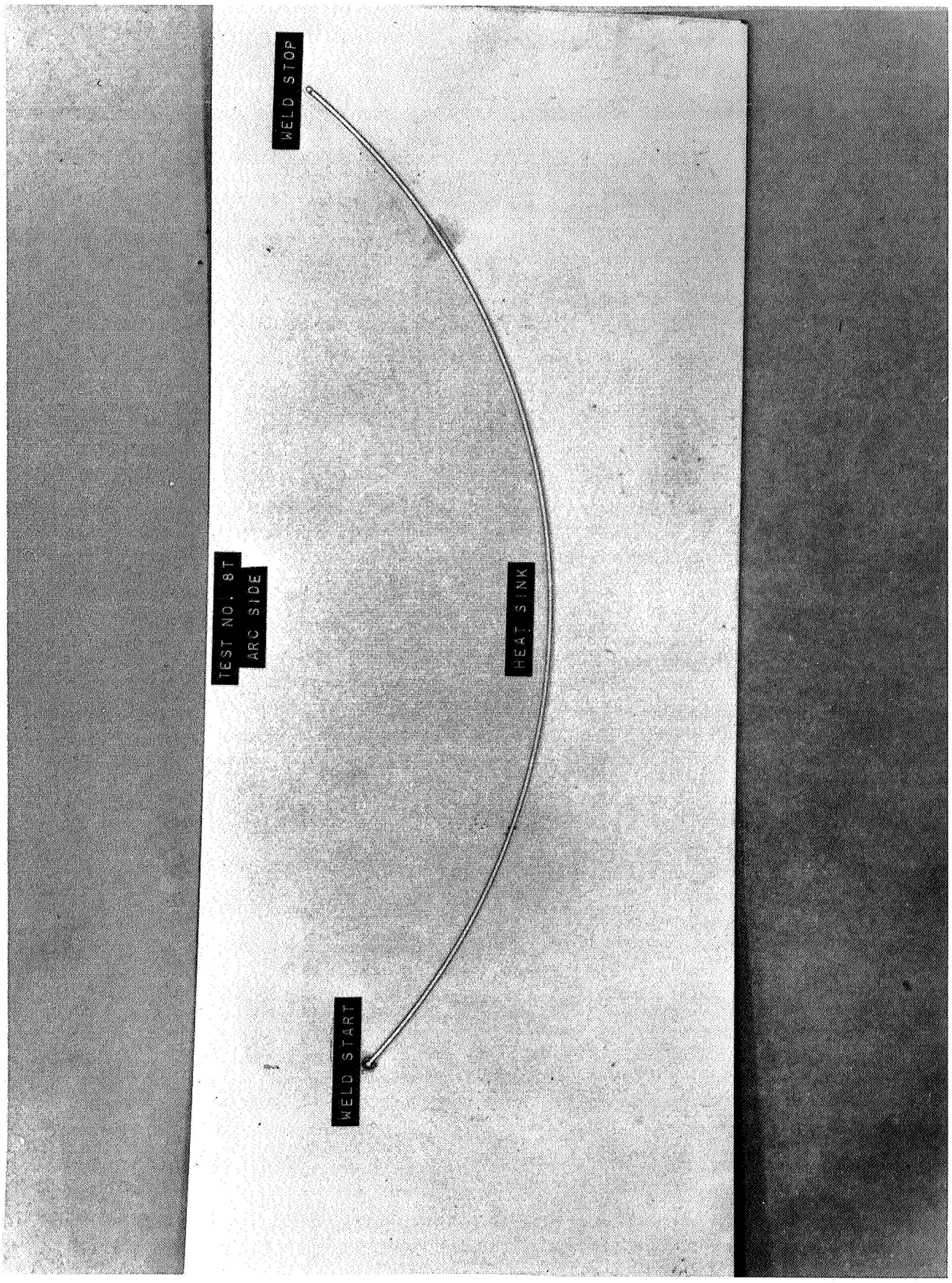


Figure 160: Weld bead, arc side, test number 8T.

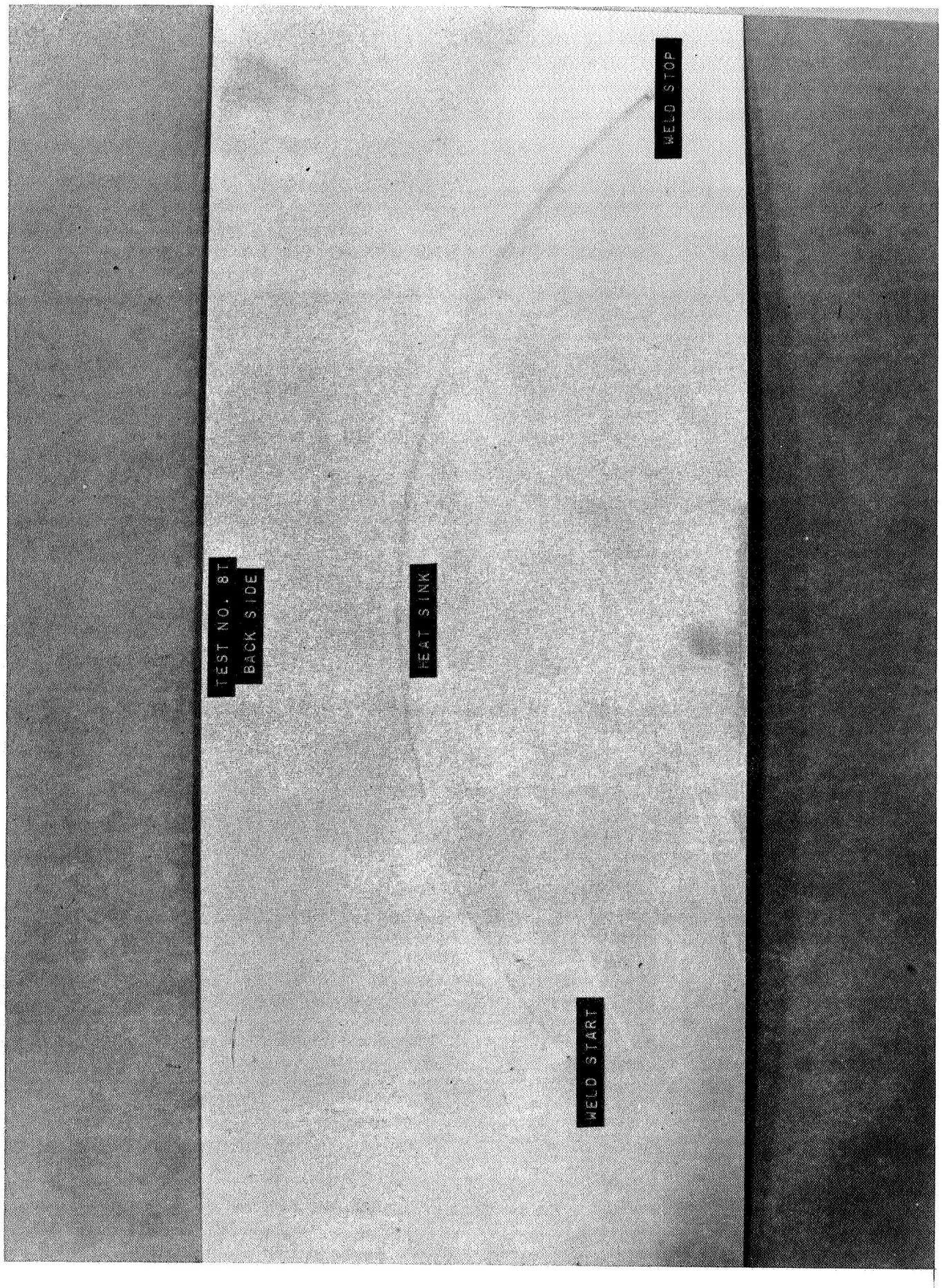


Figure 161: Weld bead, backside, test number 8T.

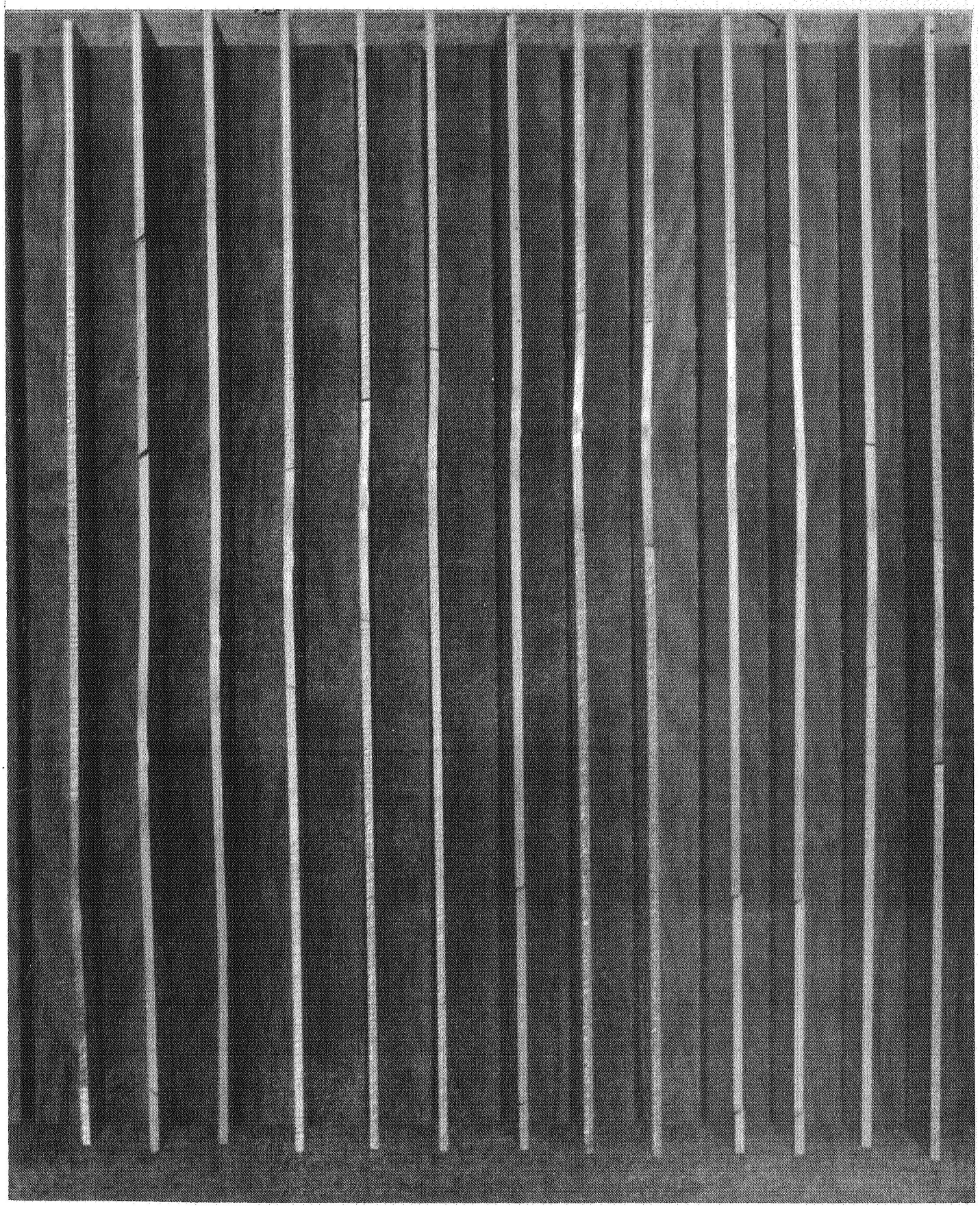


Figure 162: Cross Sections, Test Number 8T.

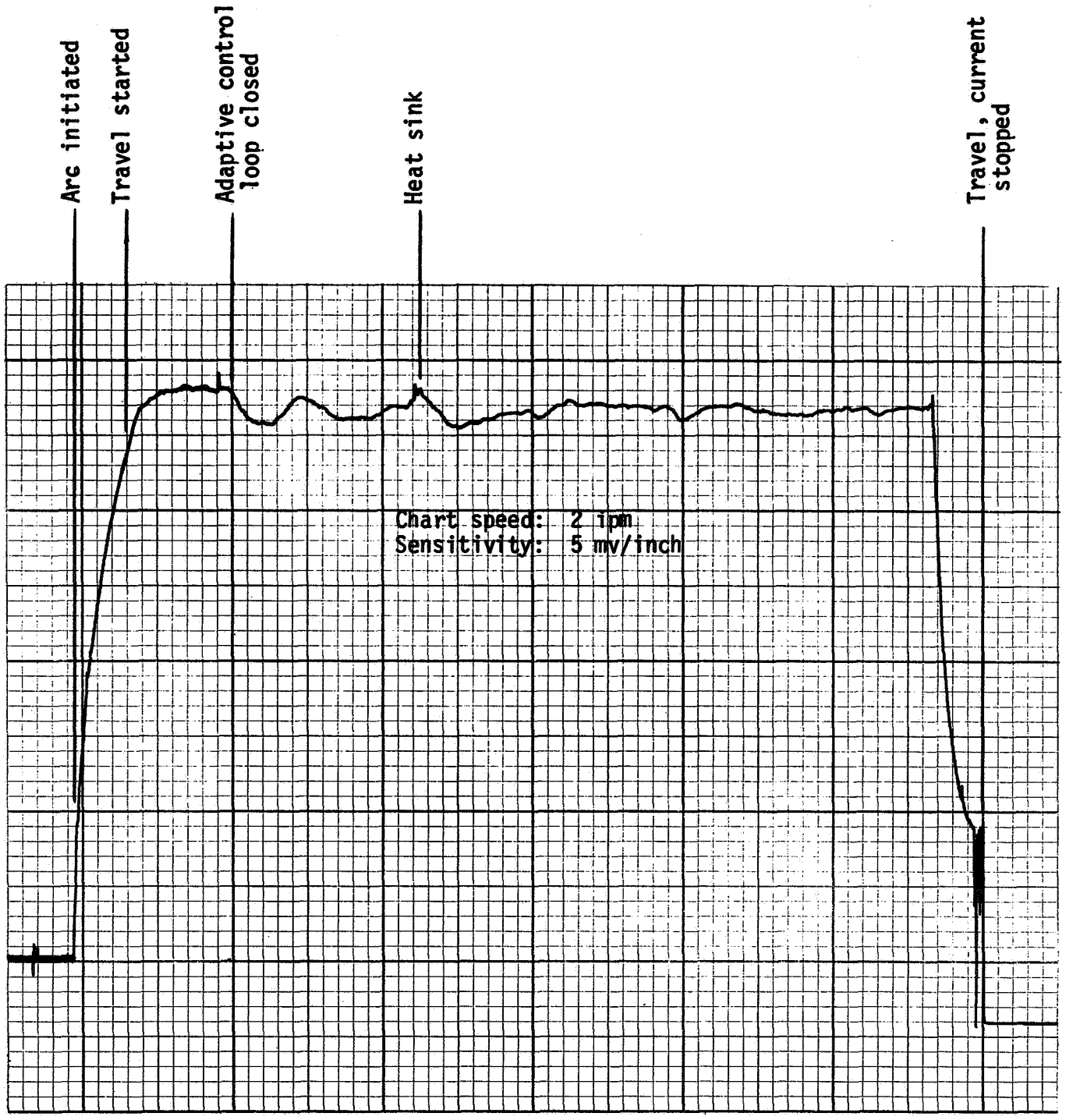


Figure 163: Hybrid thermocouple output, test number 9T.

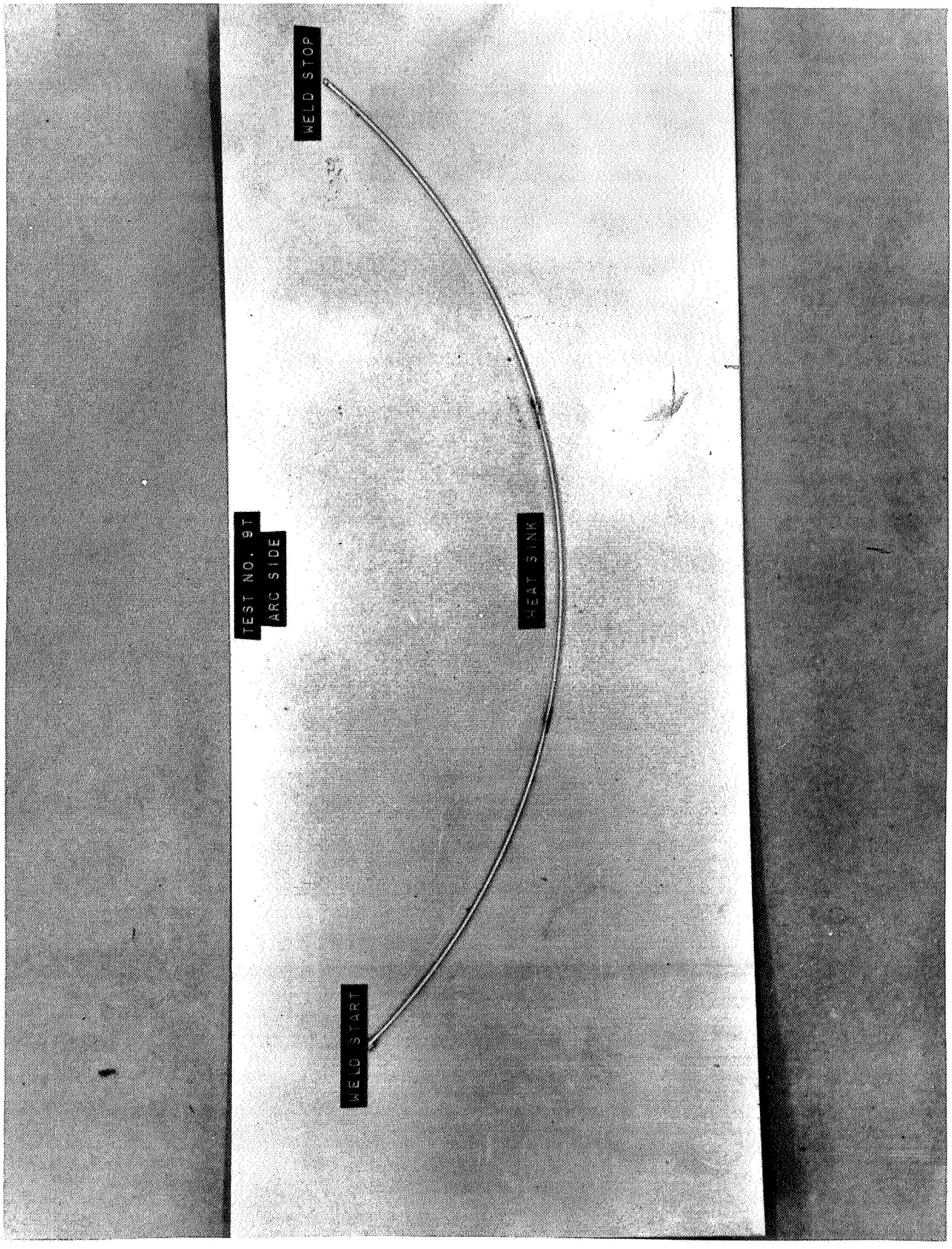


Figure 164: Weld bead, arc side, test number 9T.

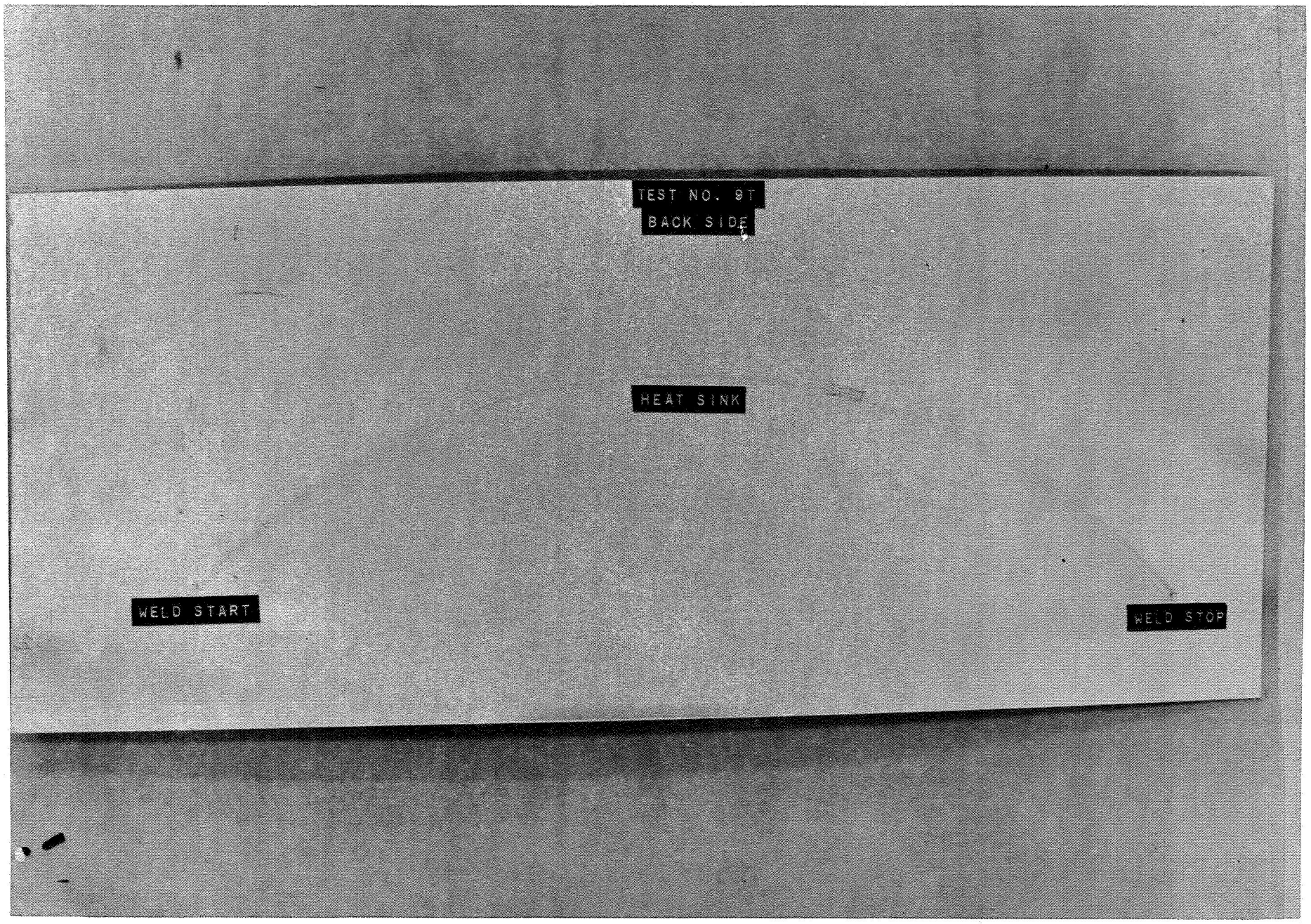


Figure 165: Weld bead, backside, test number 9T.

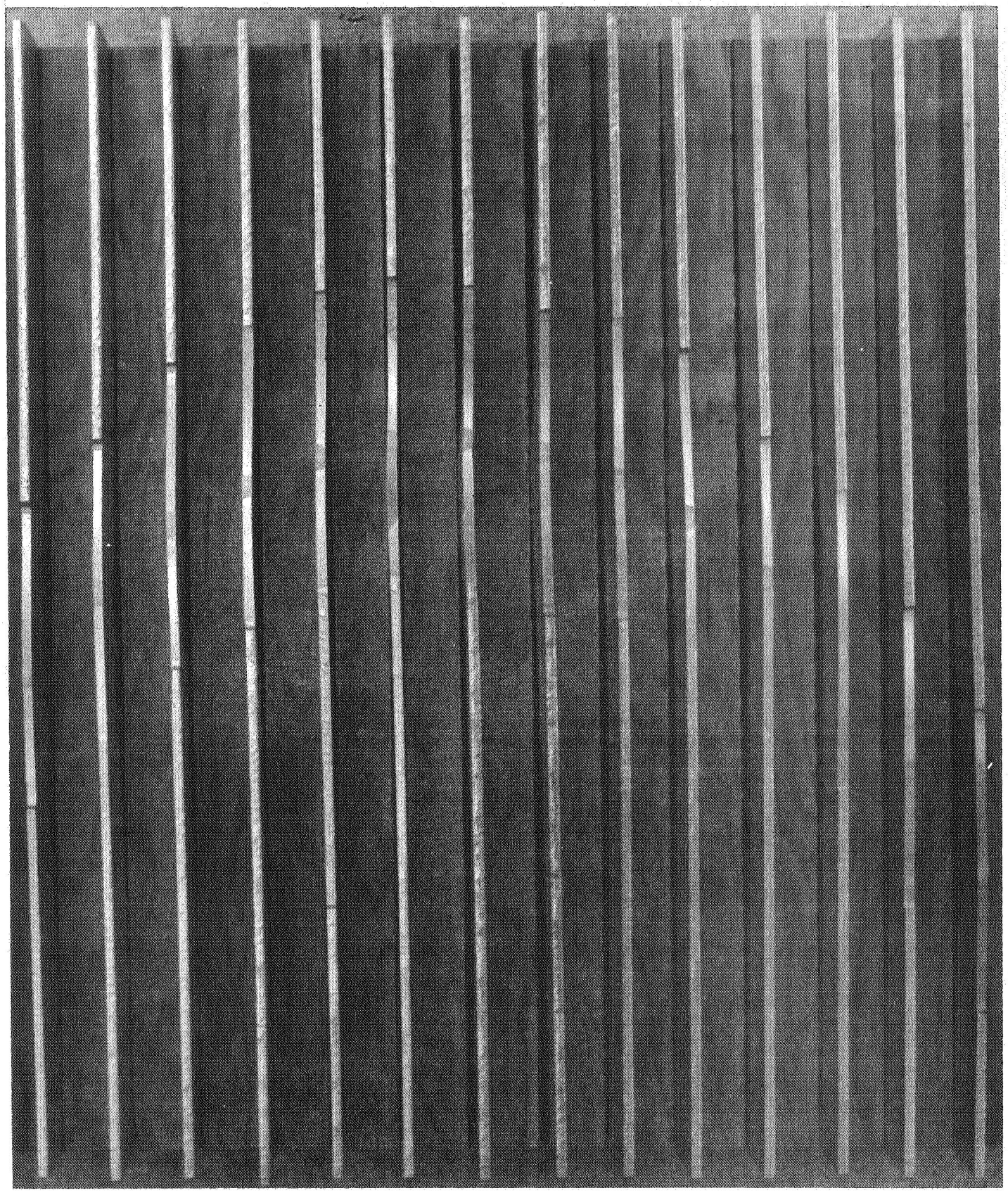


Figure 166: Cross Sections, Test Number 9T.

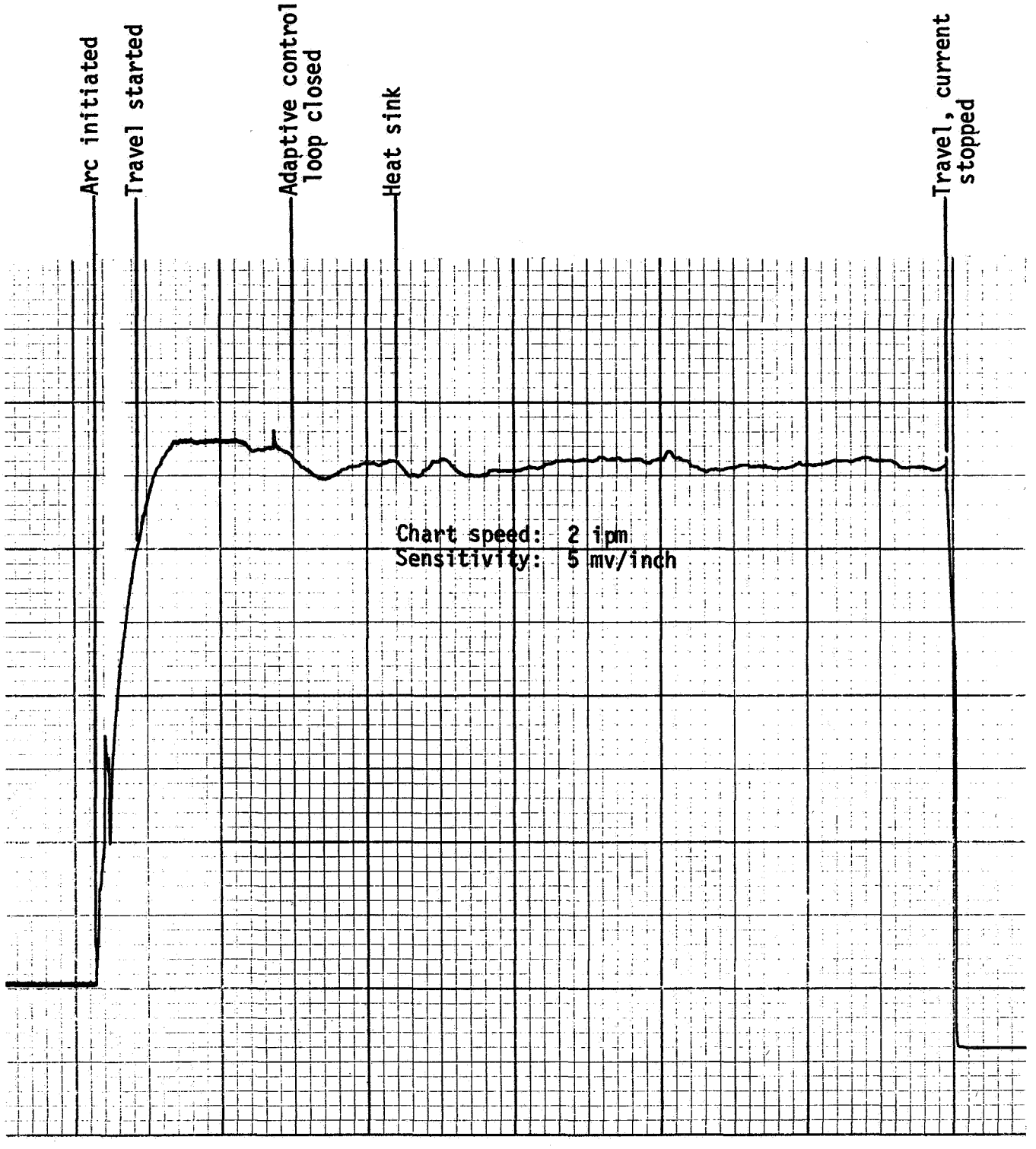


Figure 167: Hybrid thermocouple output, test number 10T.

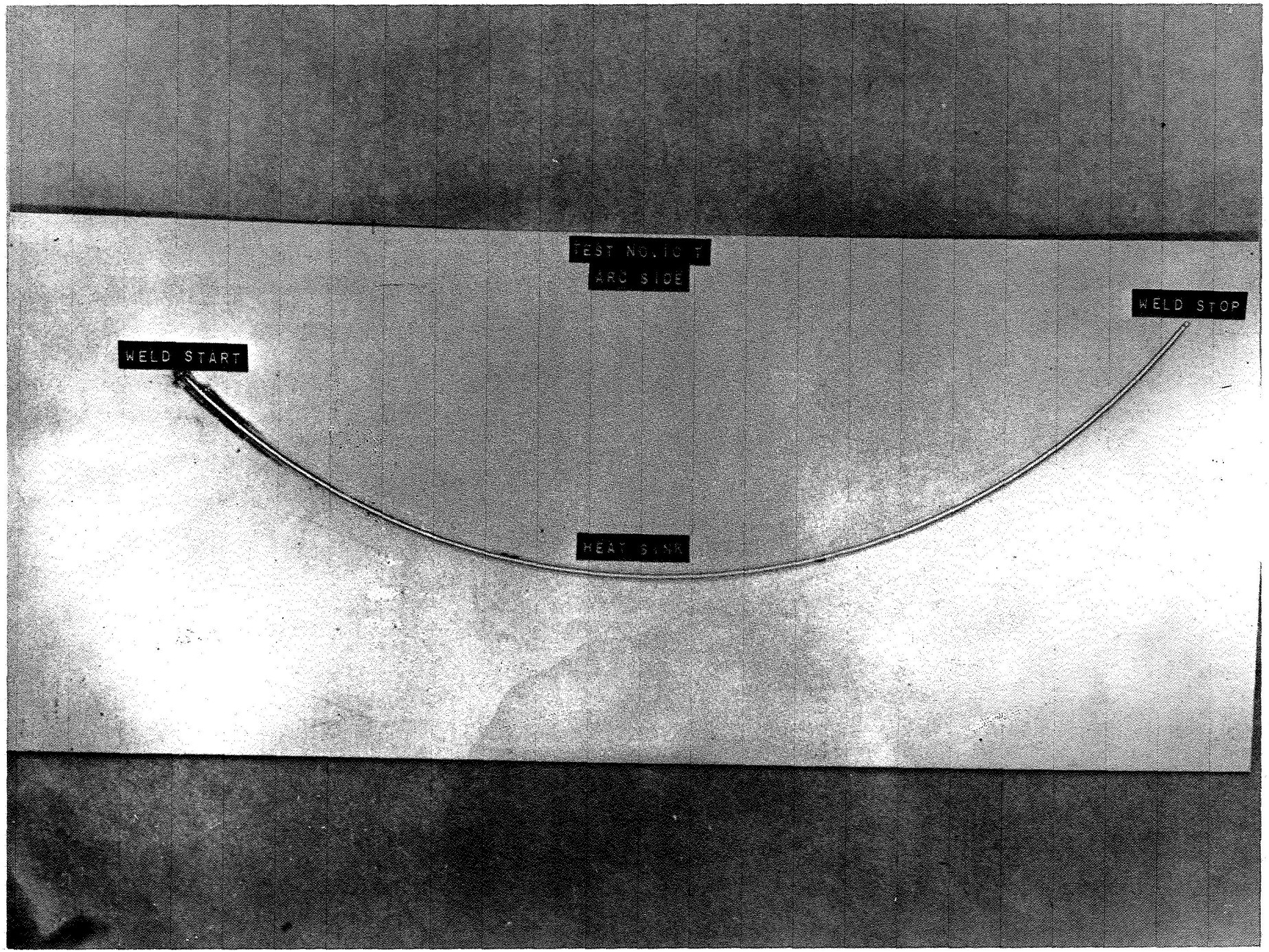


Figure 168: Weld bead, arc side, test number 10T.

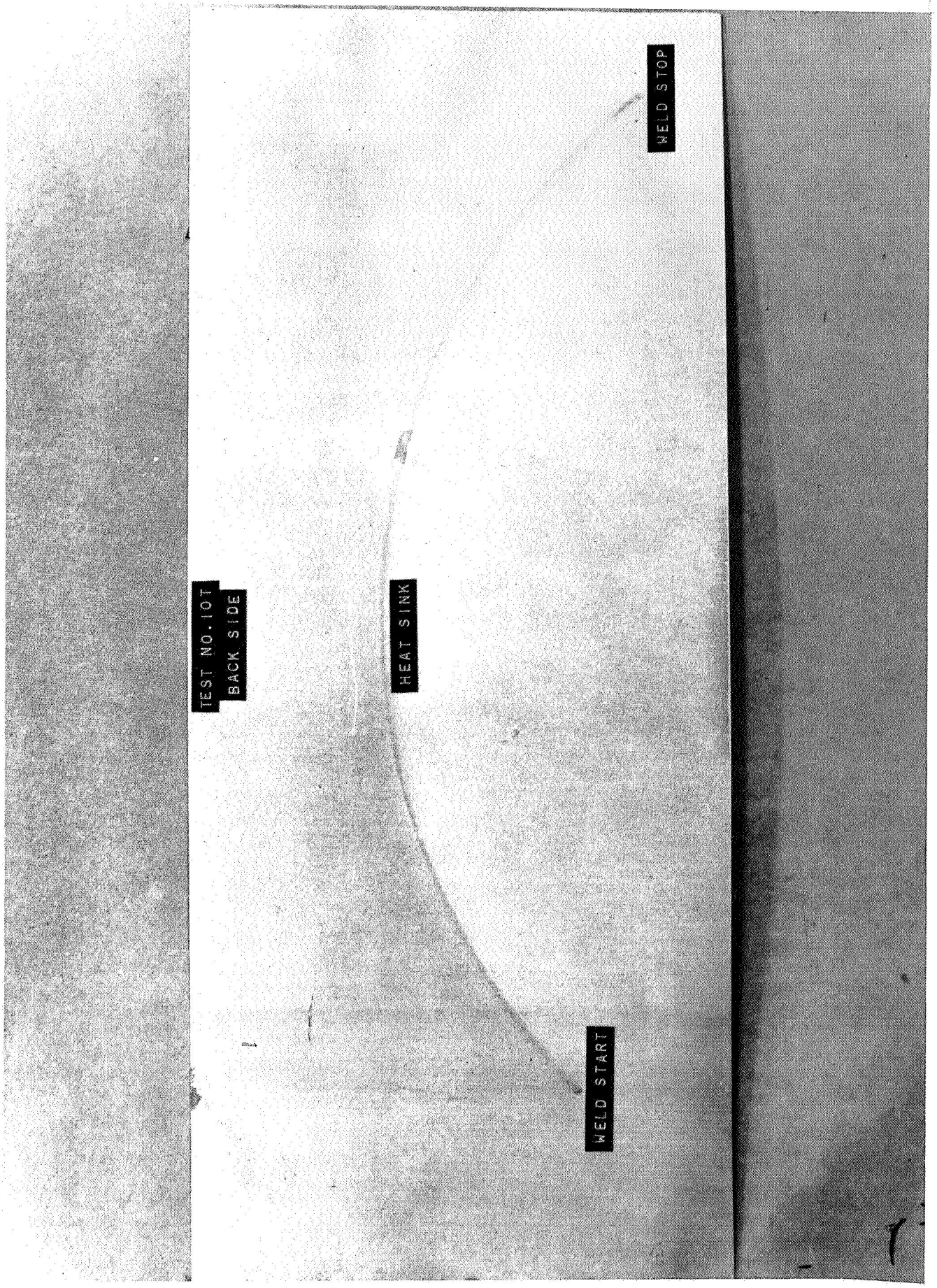


Figure 169: Weld bead, backside, test number 10T.

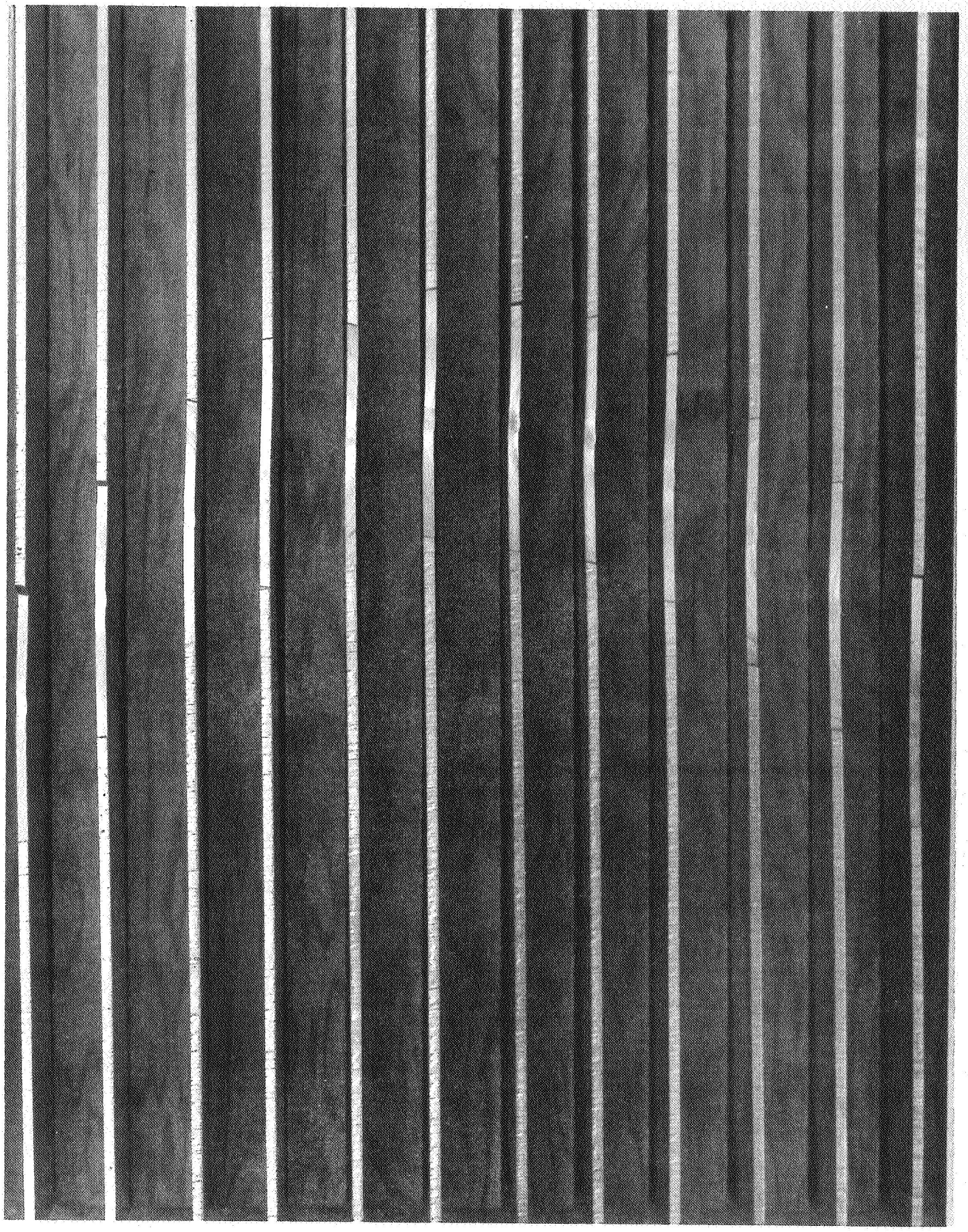


Figure 170: Cross Sections, Test Number 10T

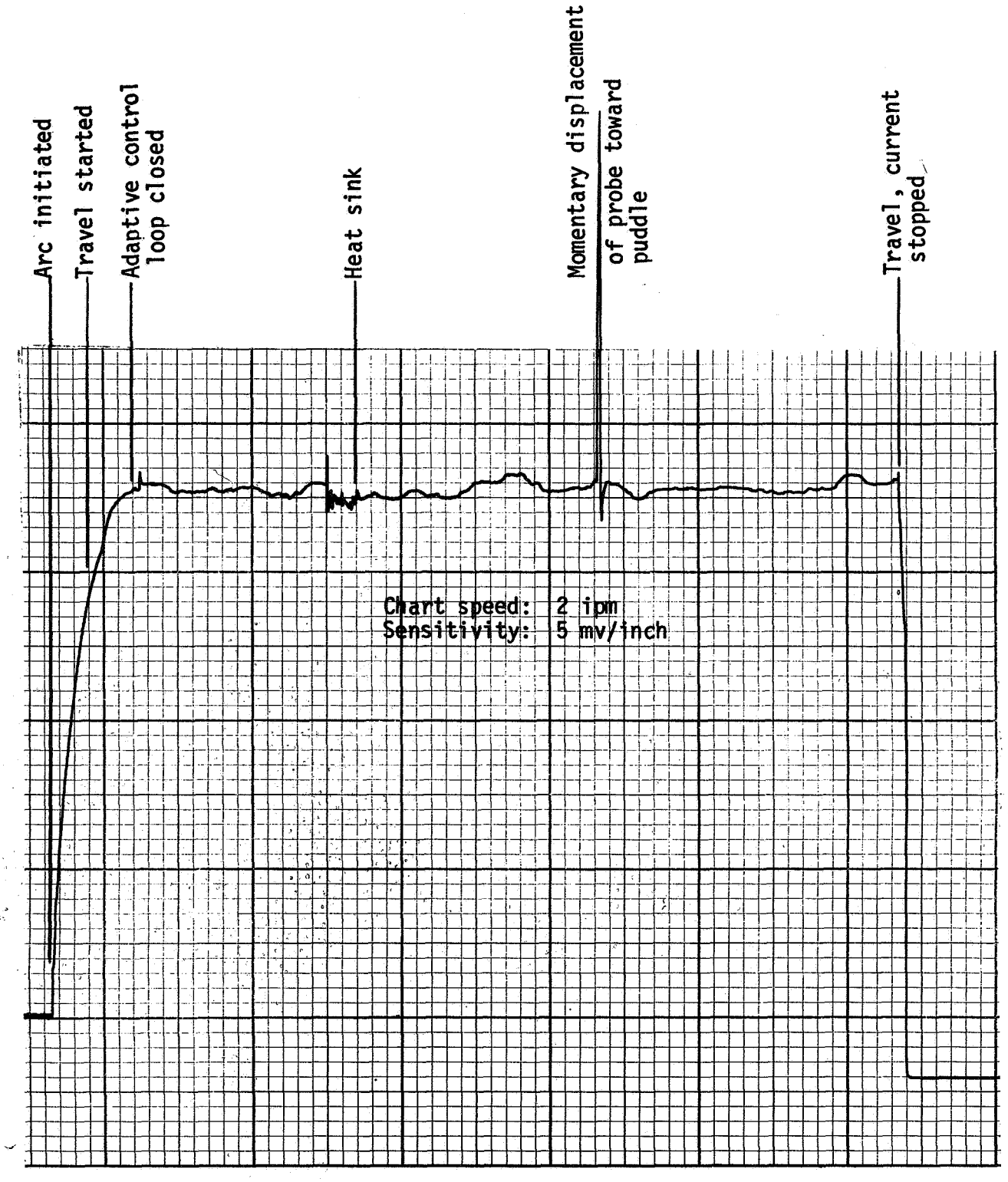


Figure 171: Hybrid thermocouple output, test number 11T.

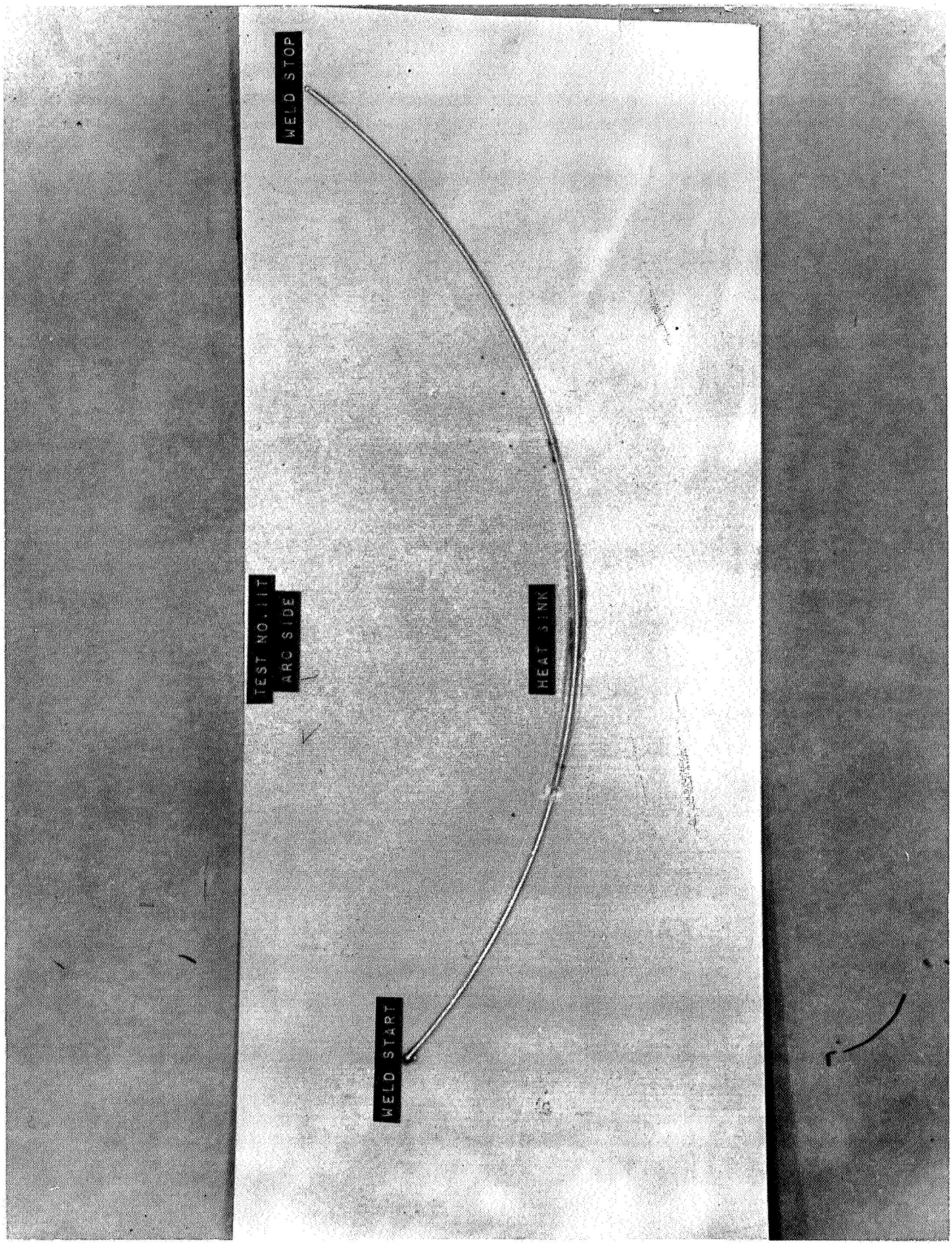


Figure 172: Weld bead, arc side, test number 11T.

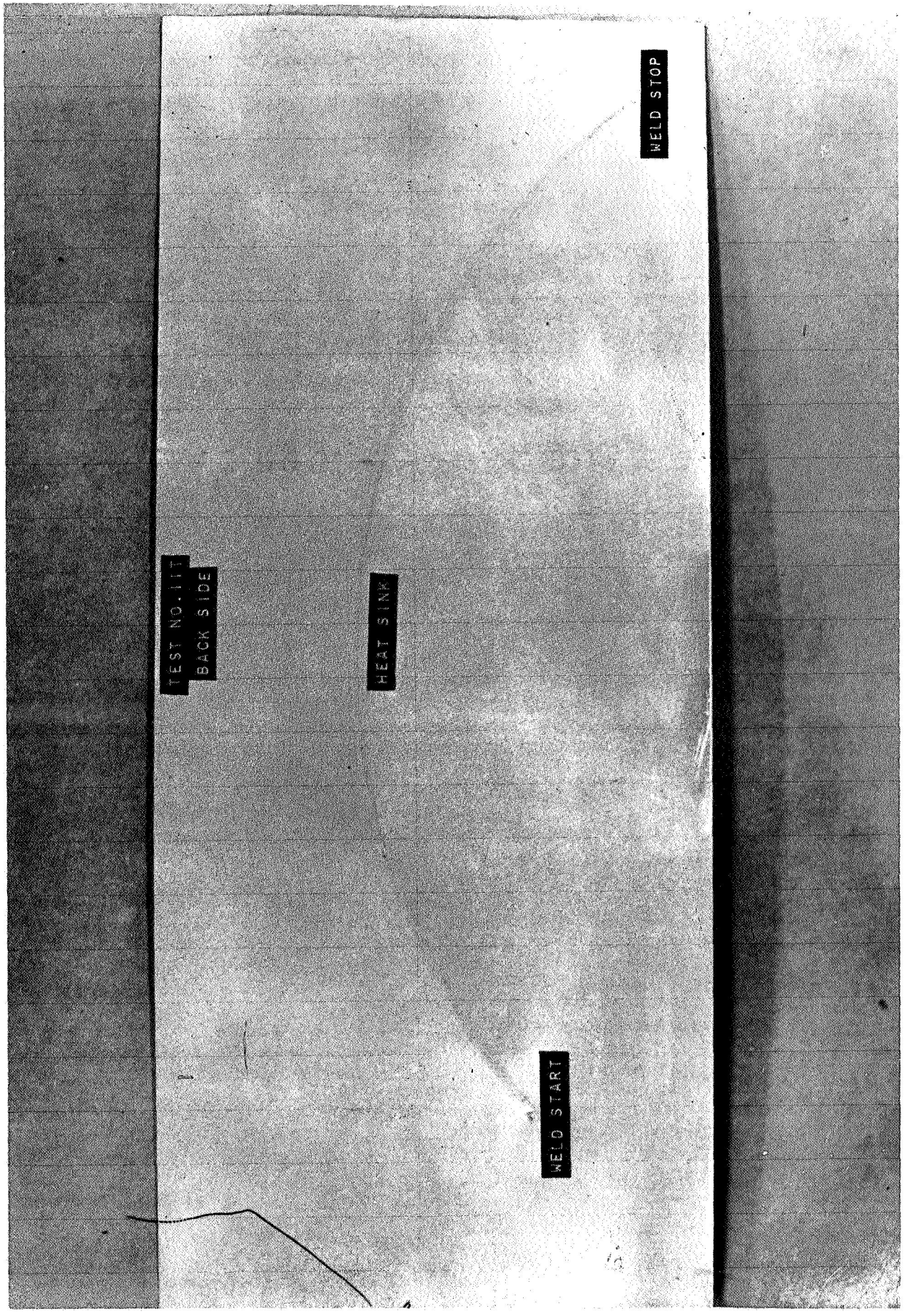


Figure 173; Weld bead, backside, test number 11T.

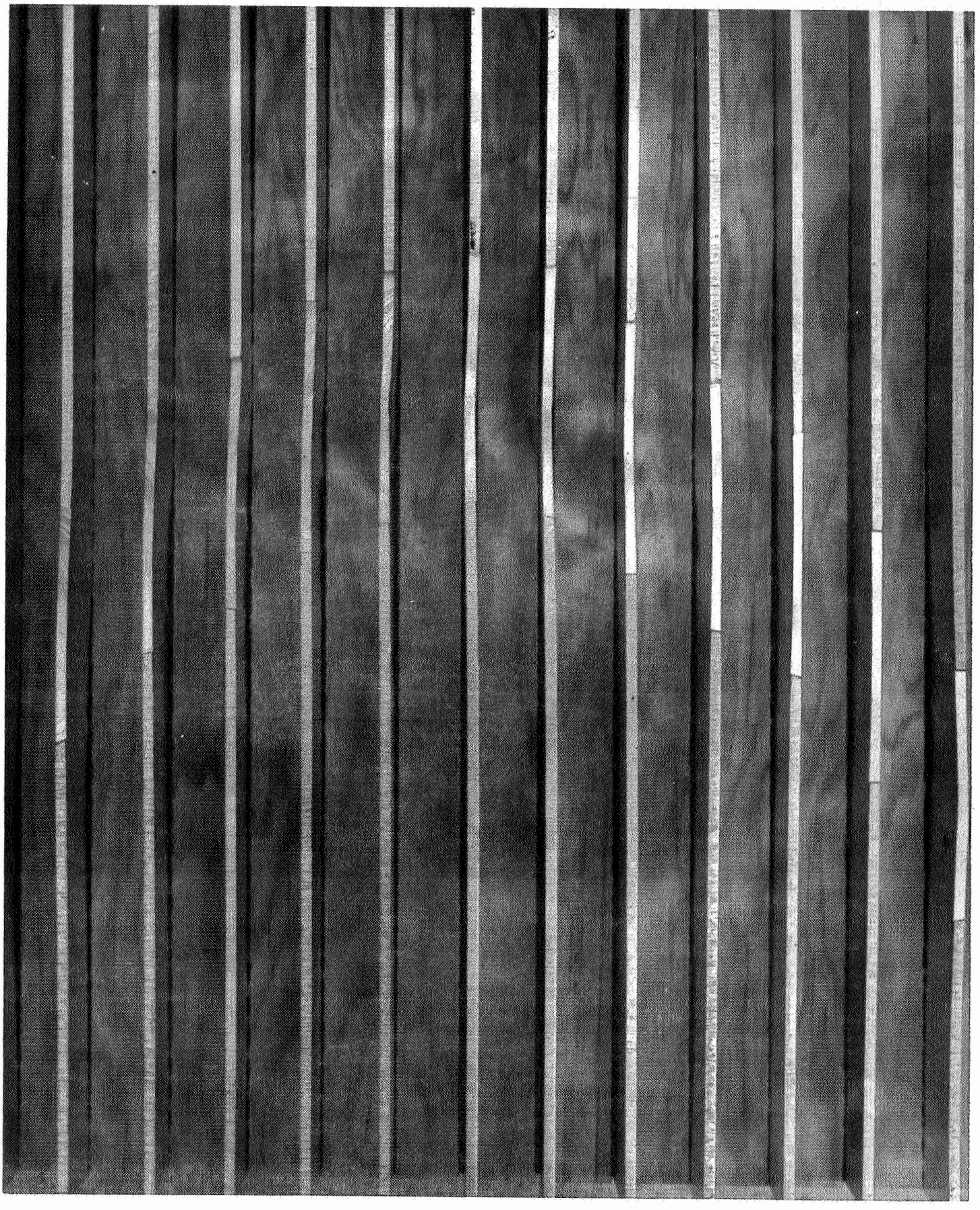


Figure 174: Cross Sections, Test Number 11T.

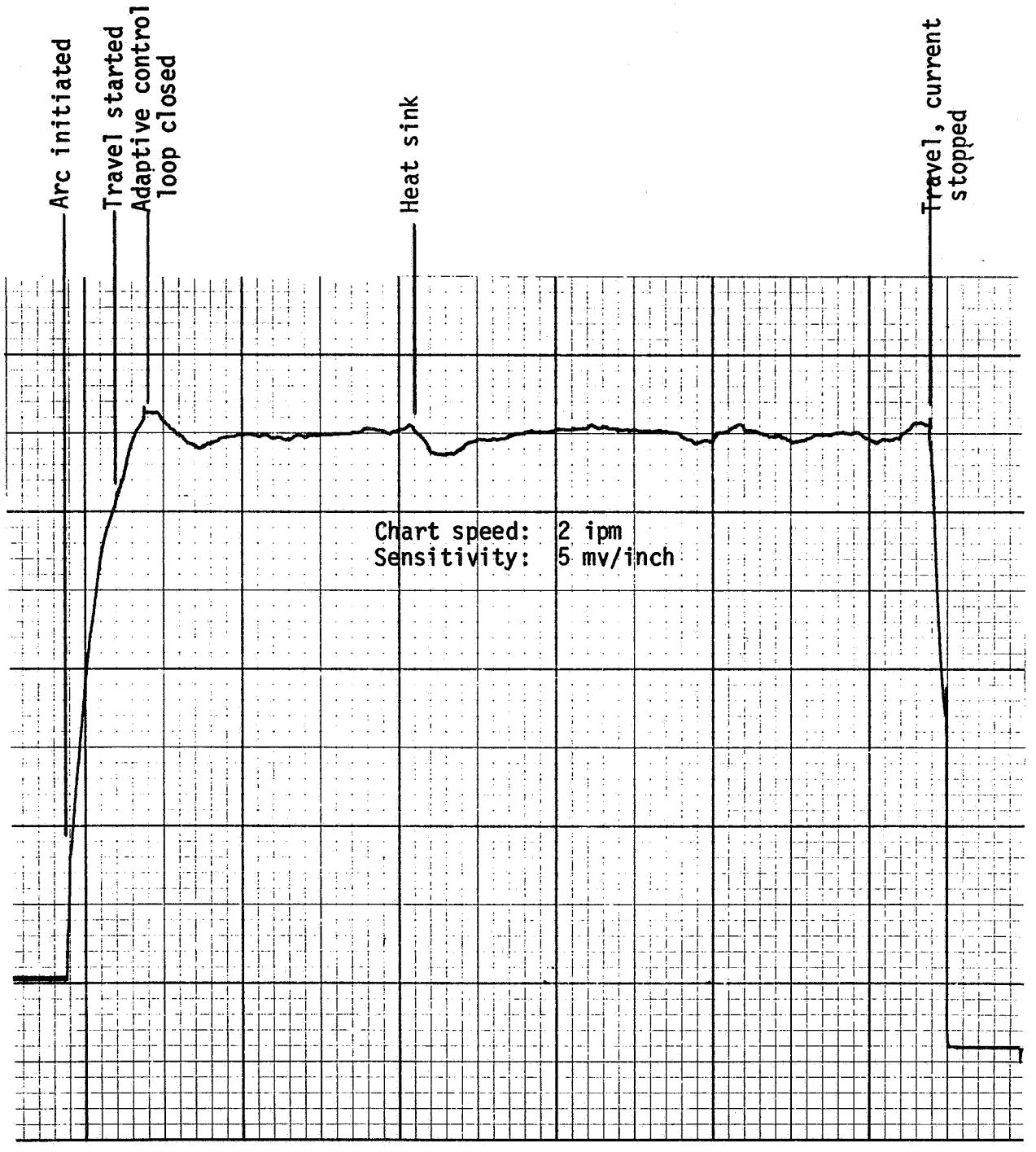


Figure 175: Hybrid thermocouple output, test number 12T.

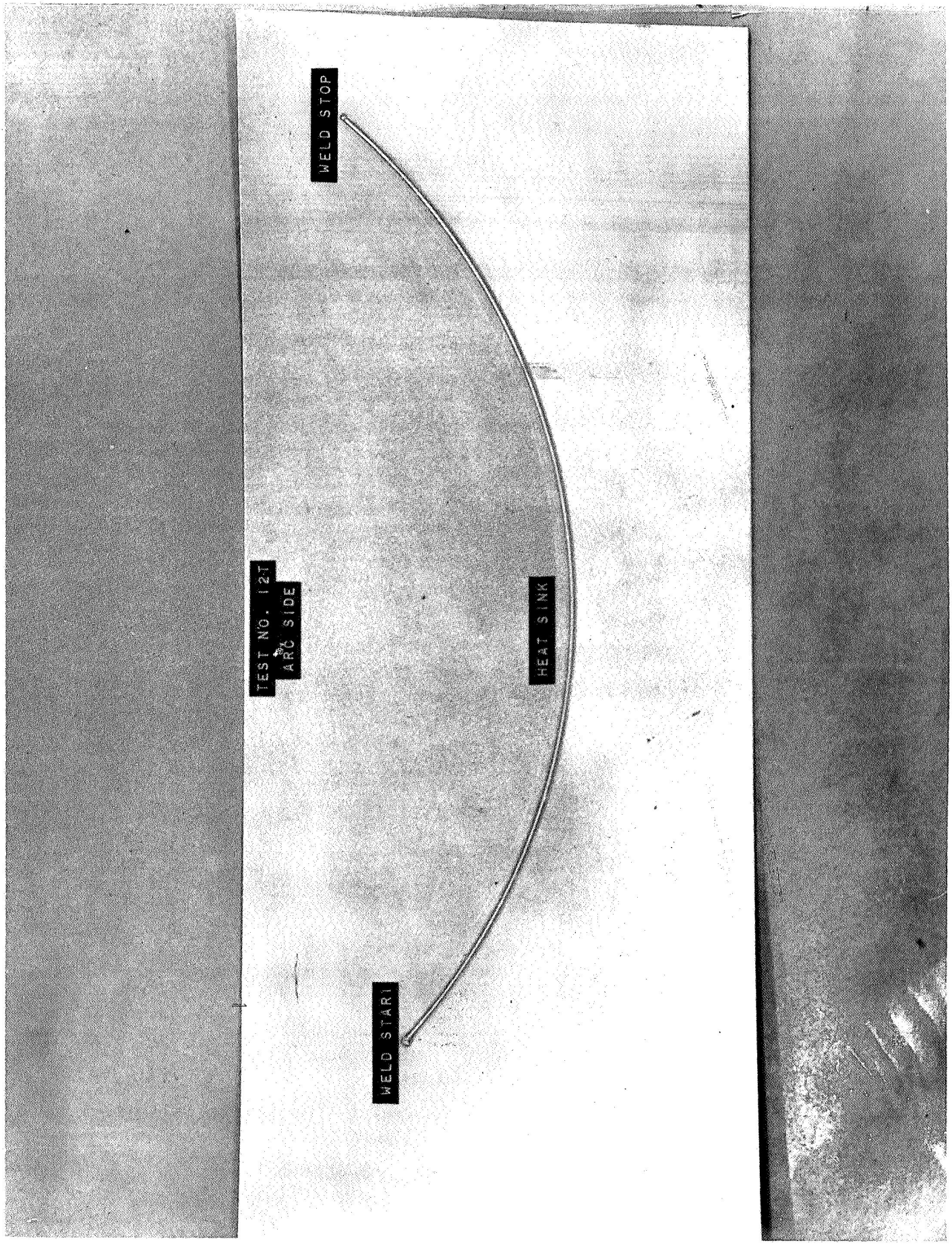


Figure 176: Weld bead, arc side, test number 12T.

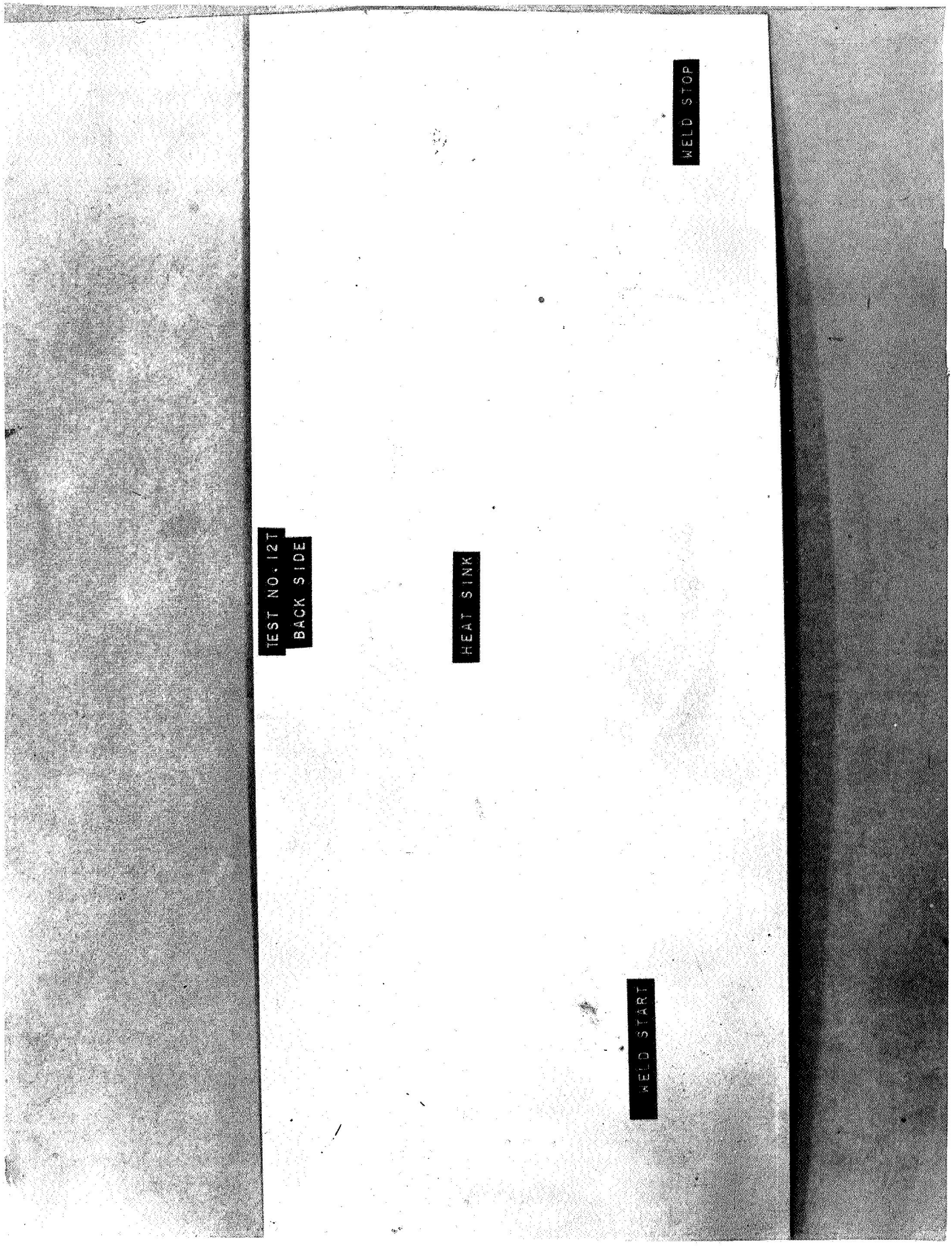


Figure 177. Weld bead, backside, test number 12T.

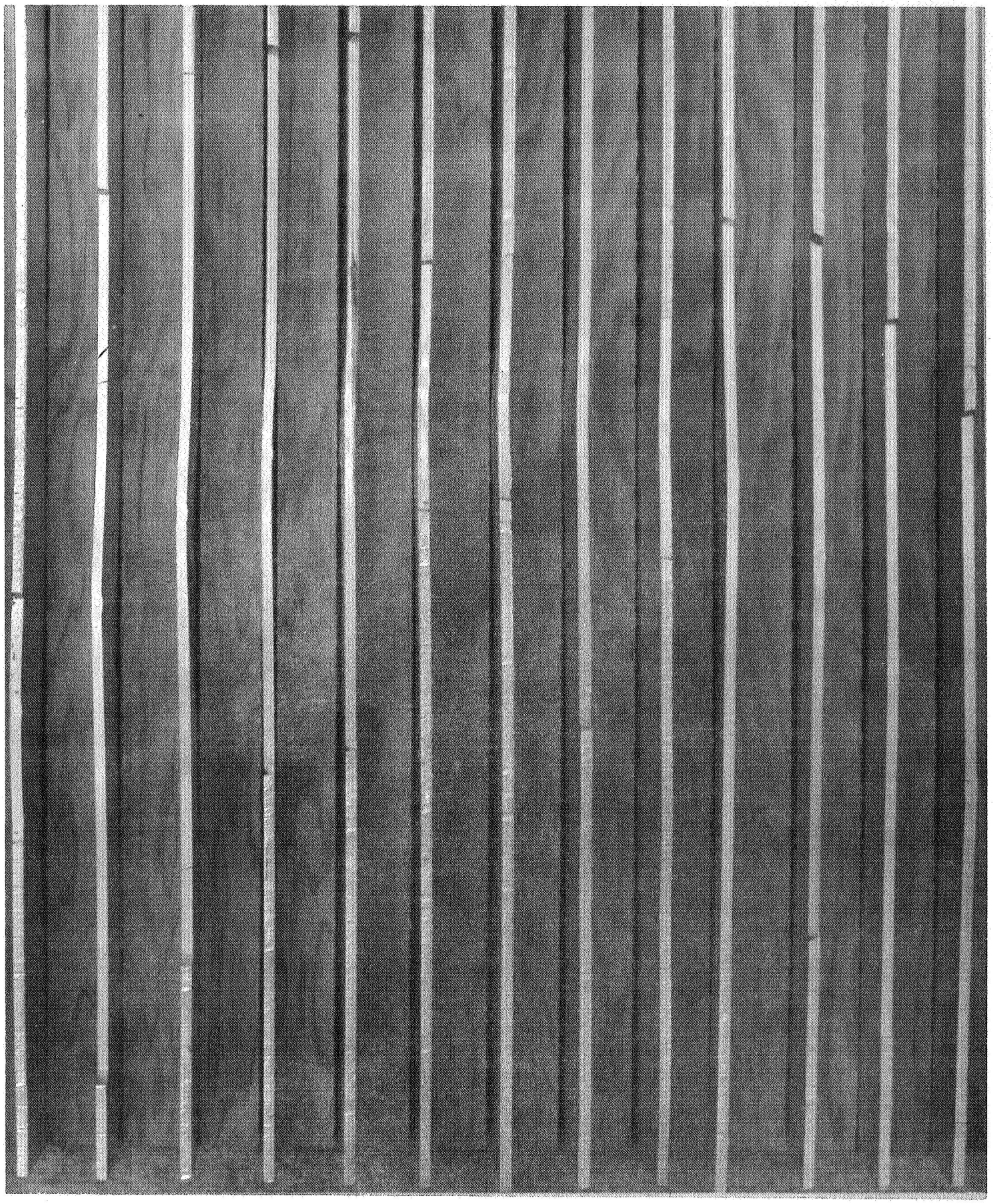


Figure 178: Cross Sections, Test Number 12T.

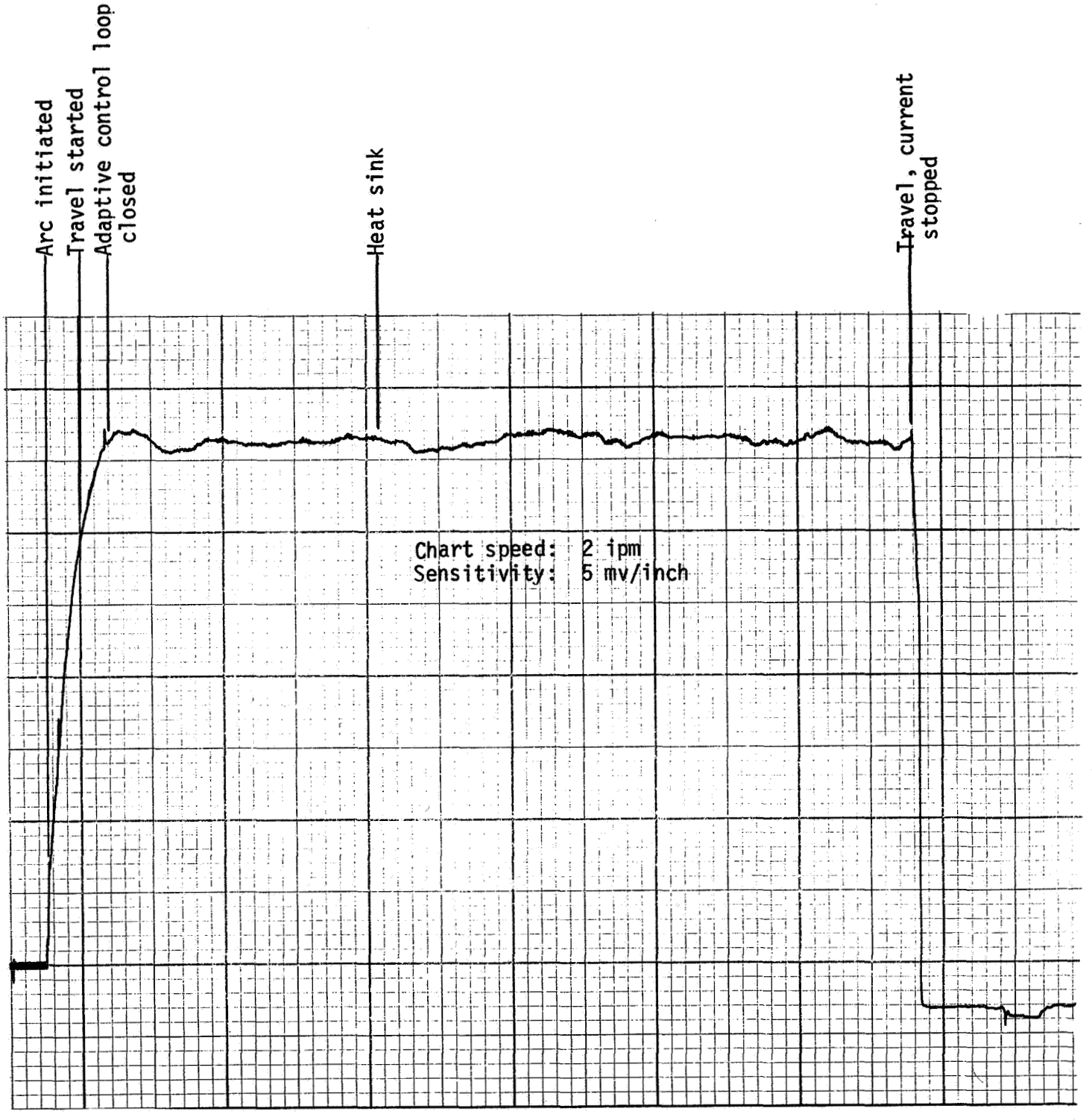


Figure 179: Hybrid thermocouple output, test number 13T

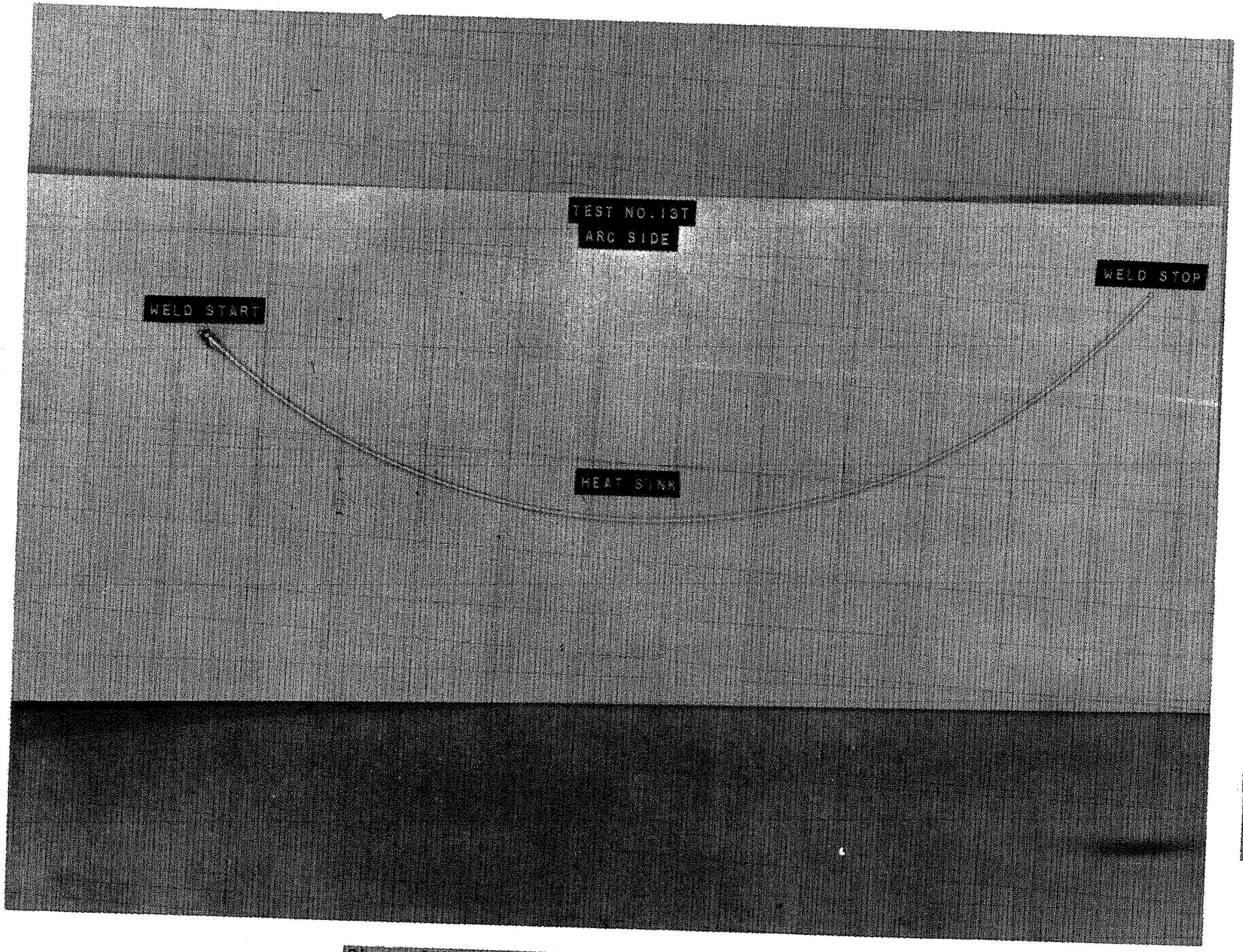


Figure 180: Weld bead, arc side, test number 13T.

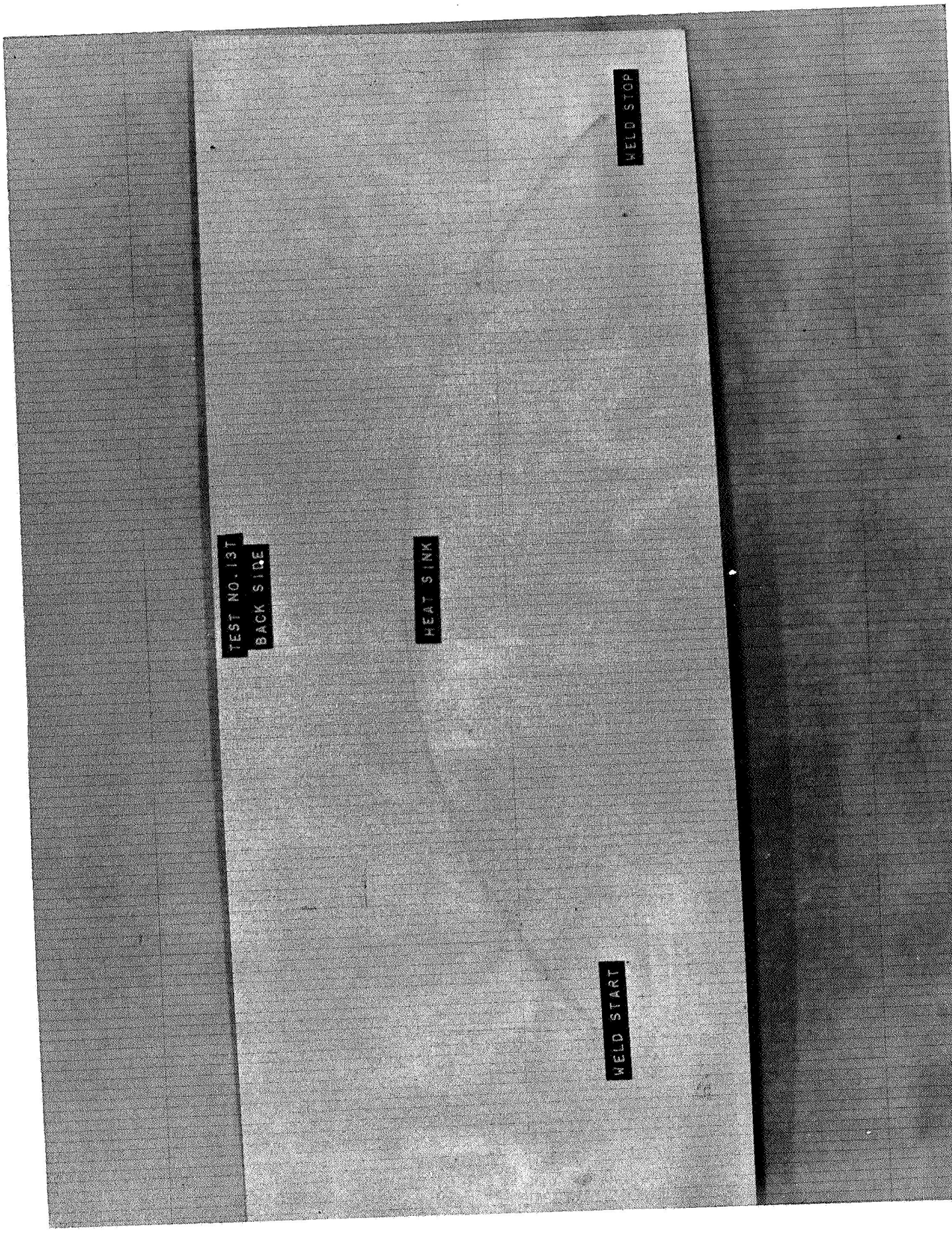


Figure 181. Weld bead, backside, test number 13T.

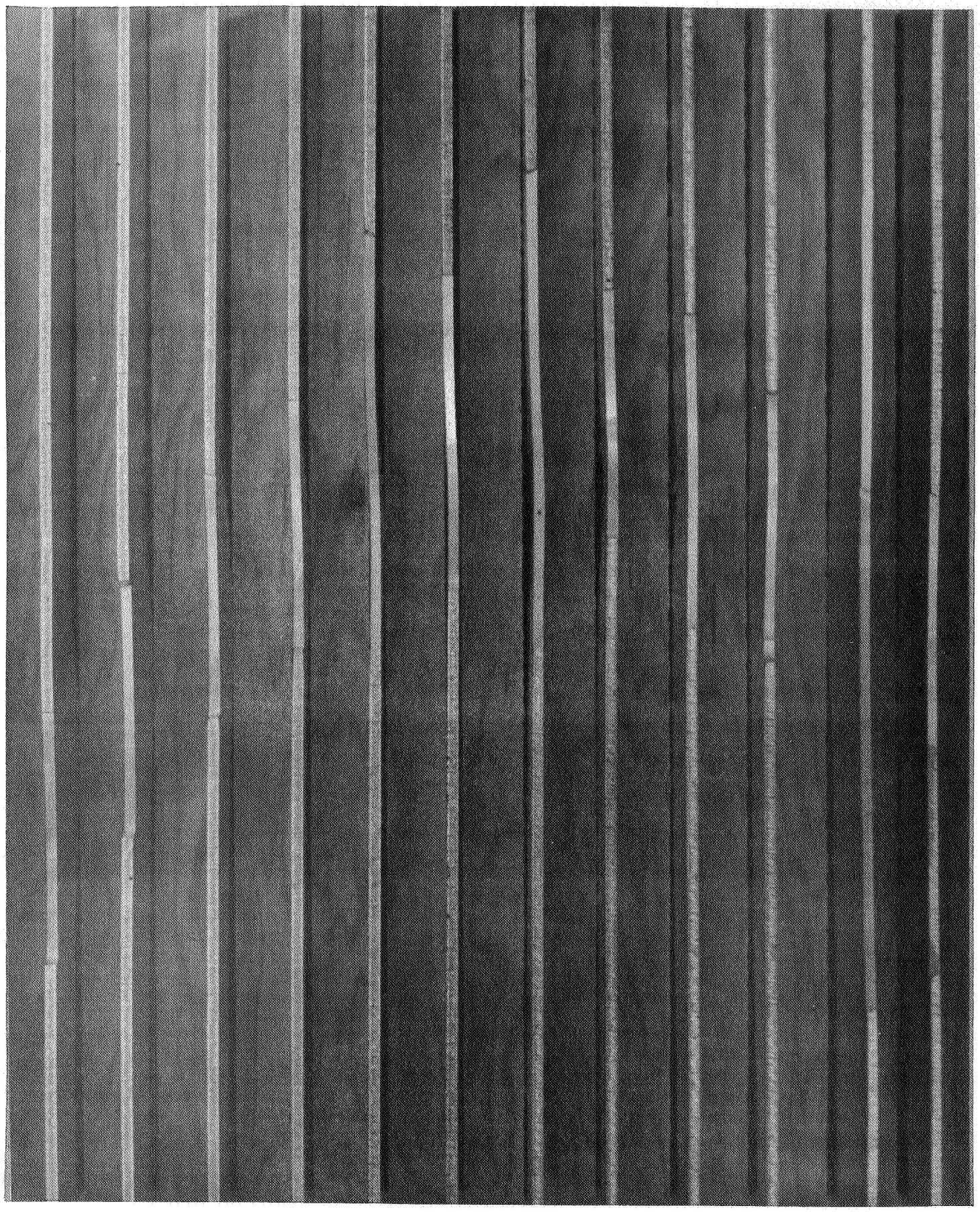


Figure 182: Cross Sections, Test Number 13T.

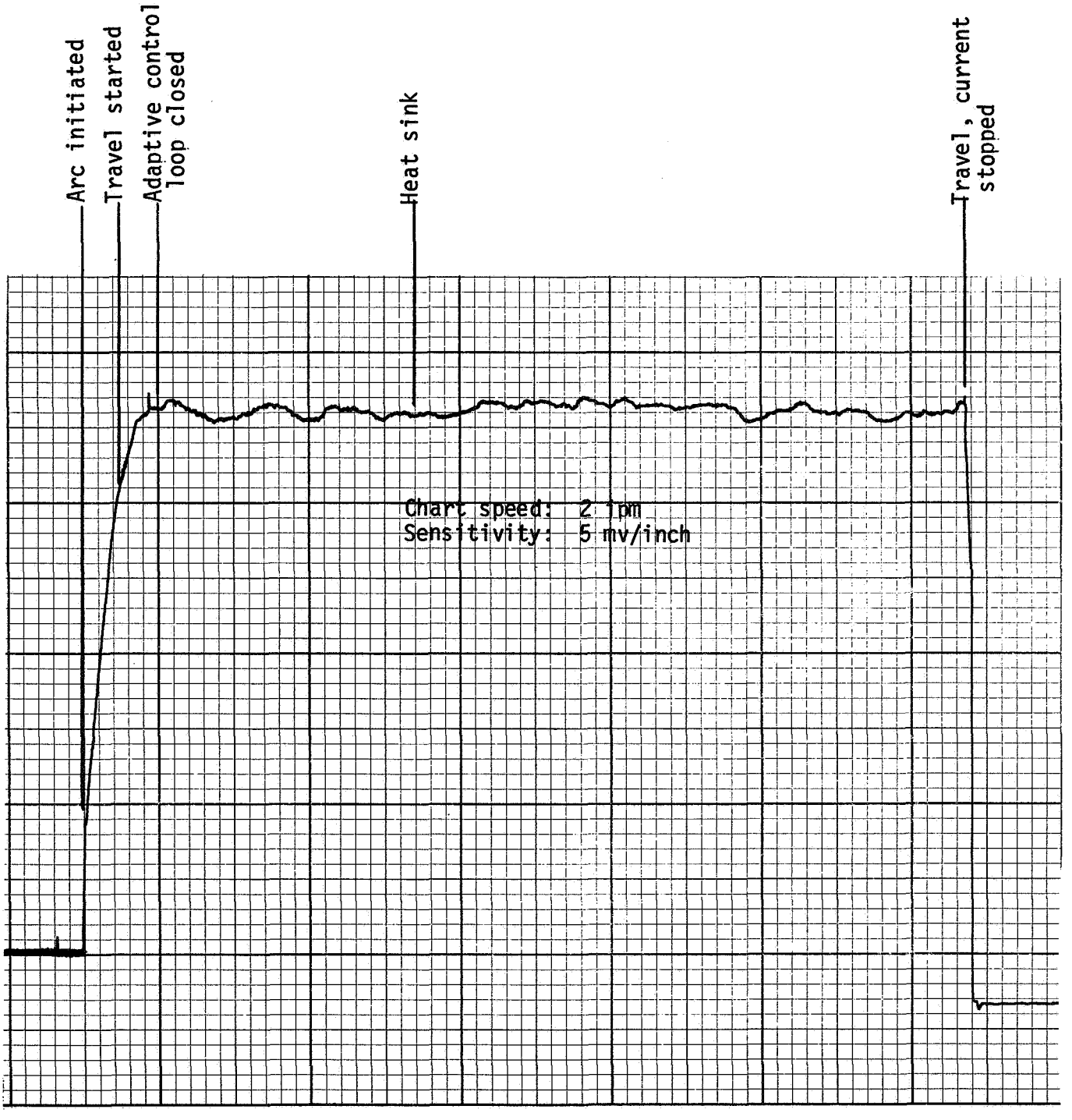


Figure 183: Hybrid thermocouple output, test number 14T.

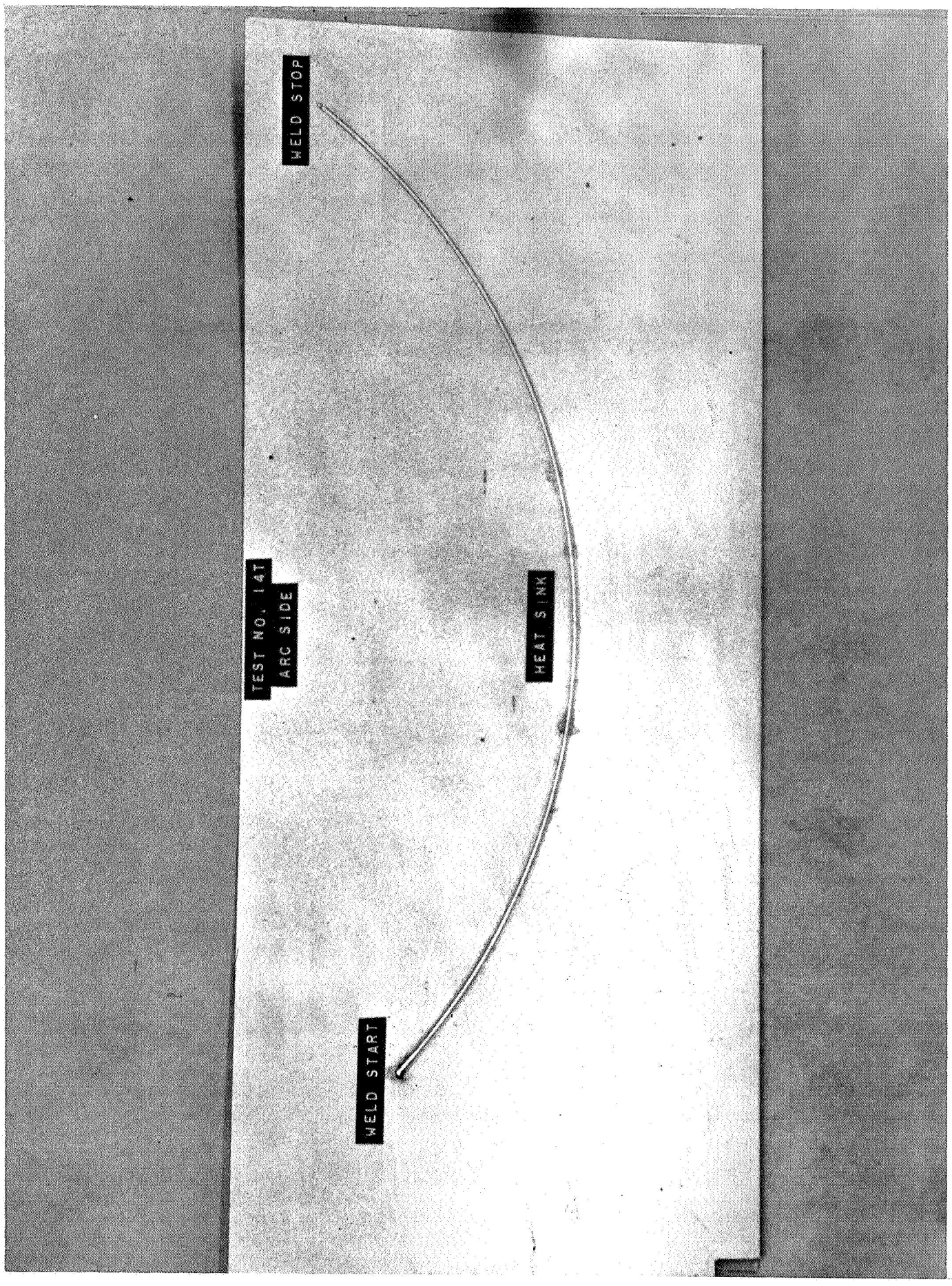


Figure 184: Weld bead, arc side, test number 14T.

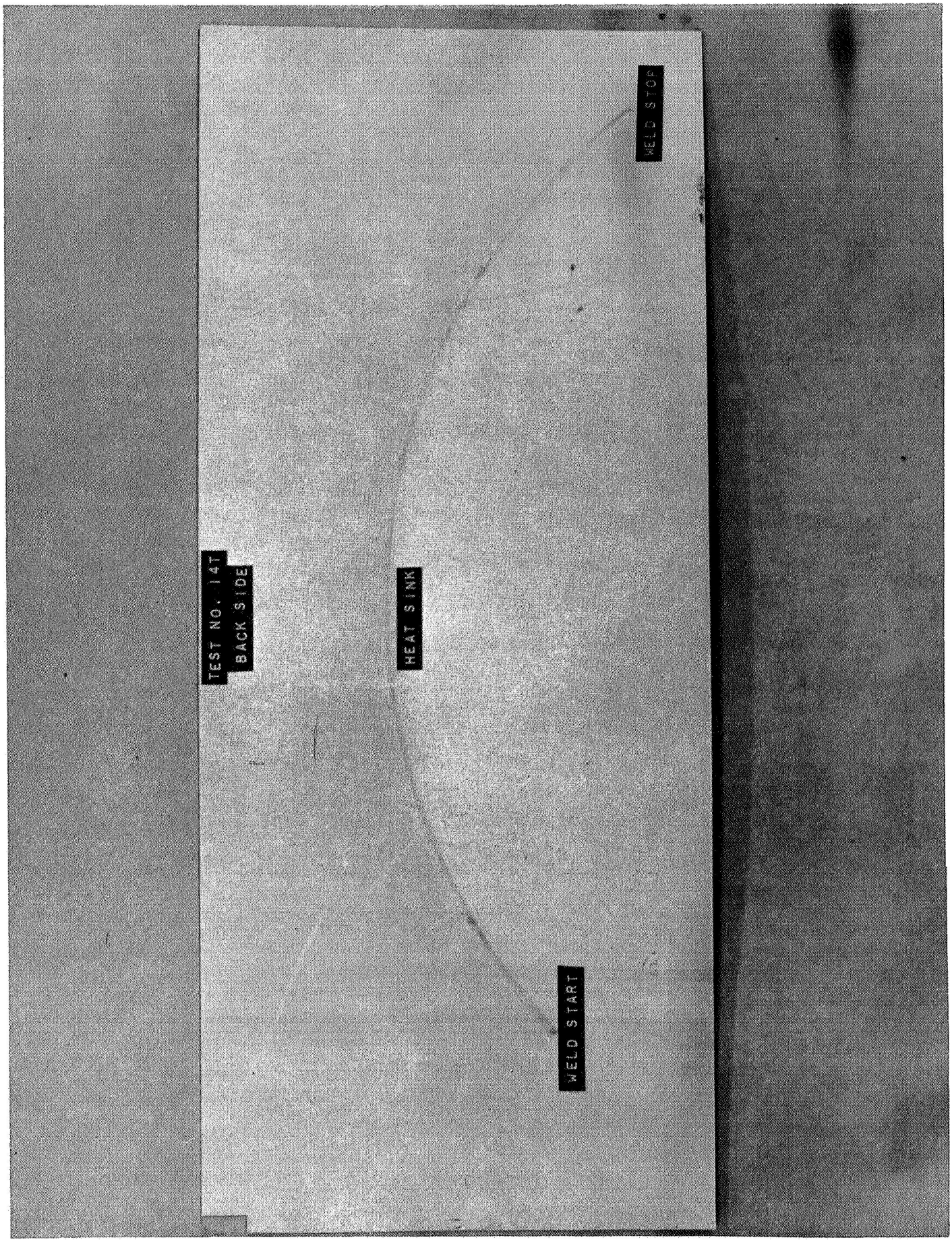


Figure 185: Weld bead, backside, test number 14T.

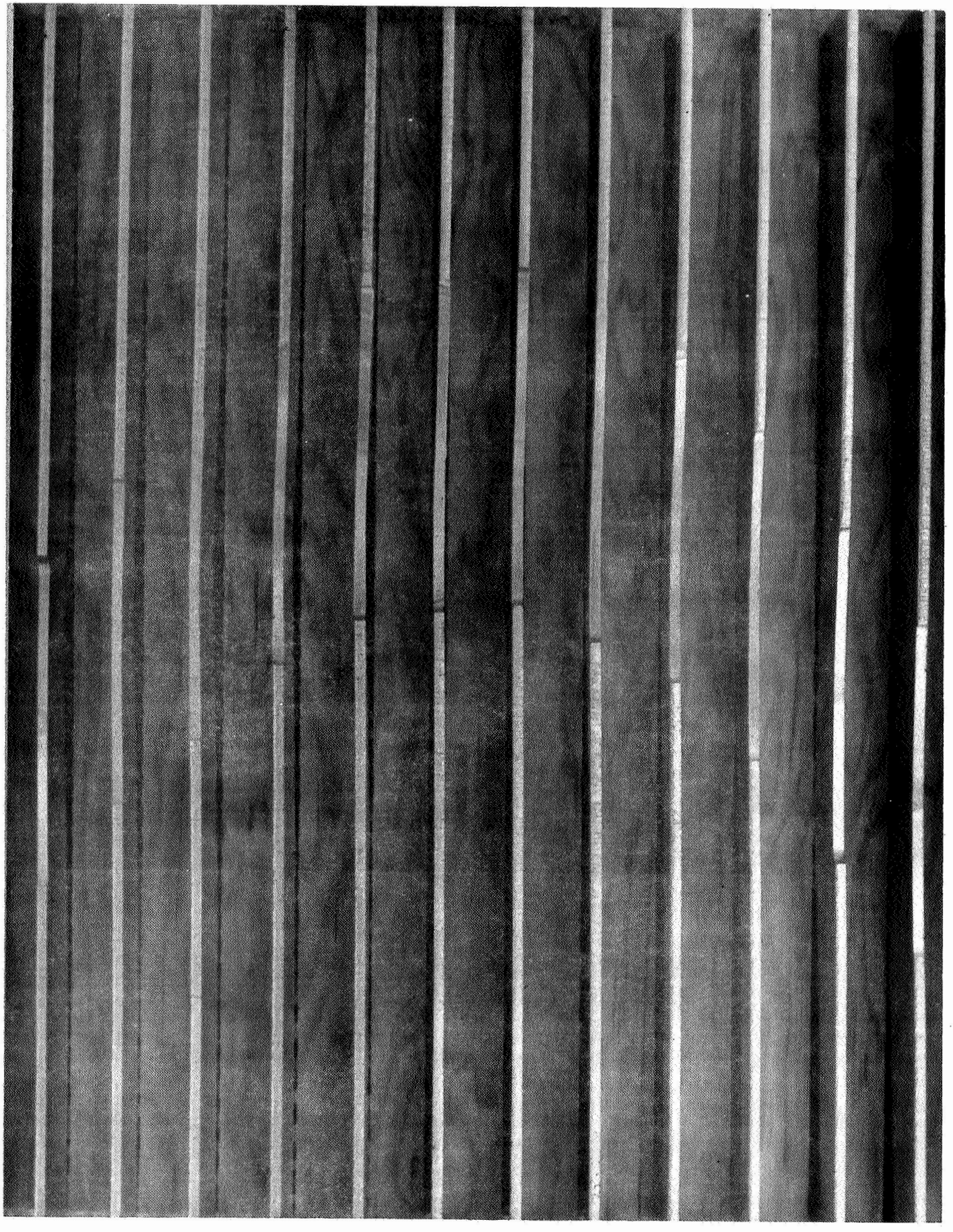


Figure 186: Cross Sections, Test Number 14T.

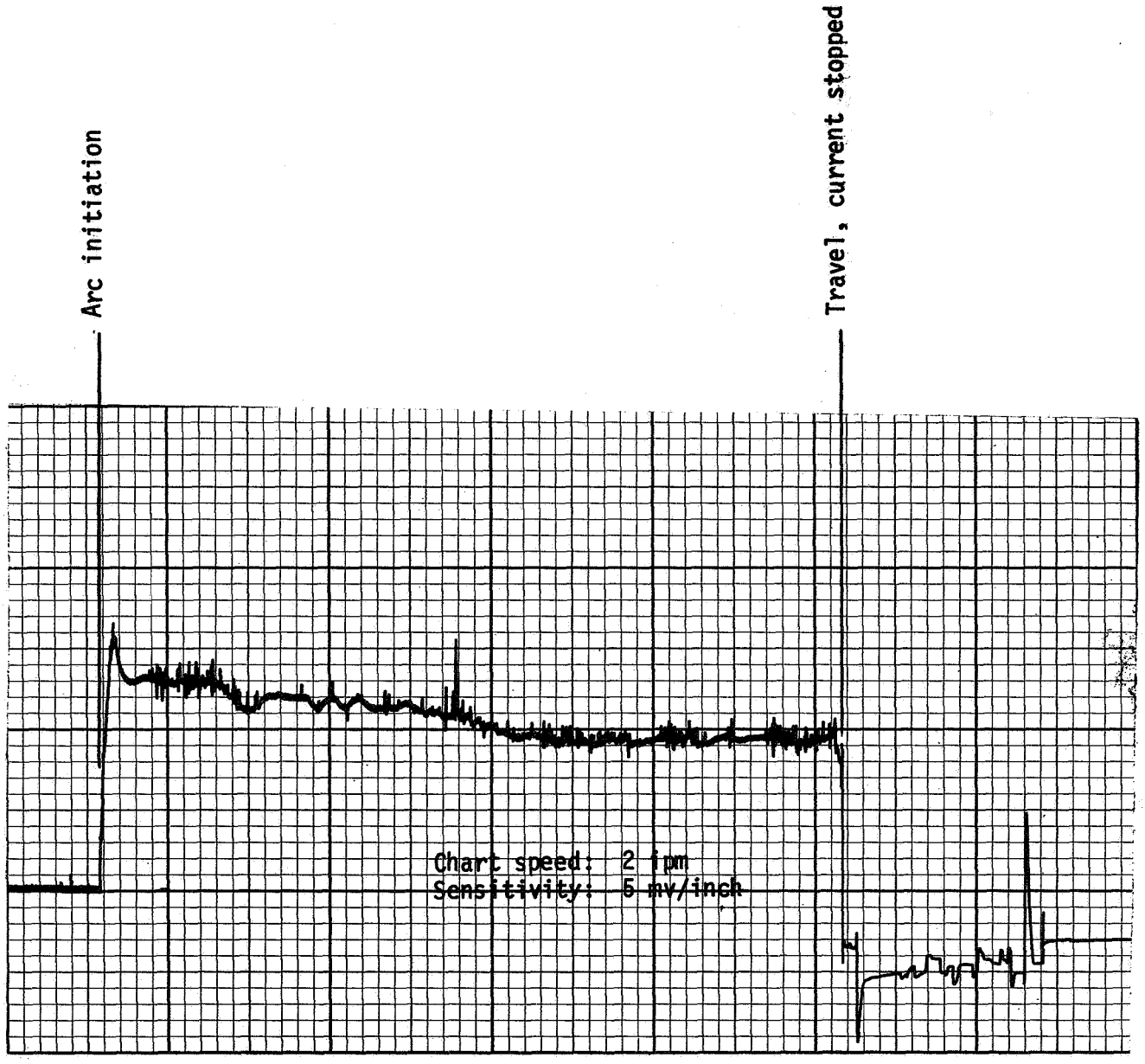
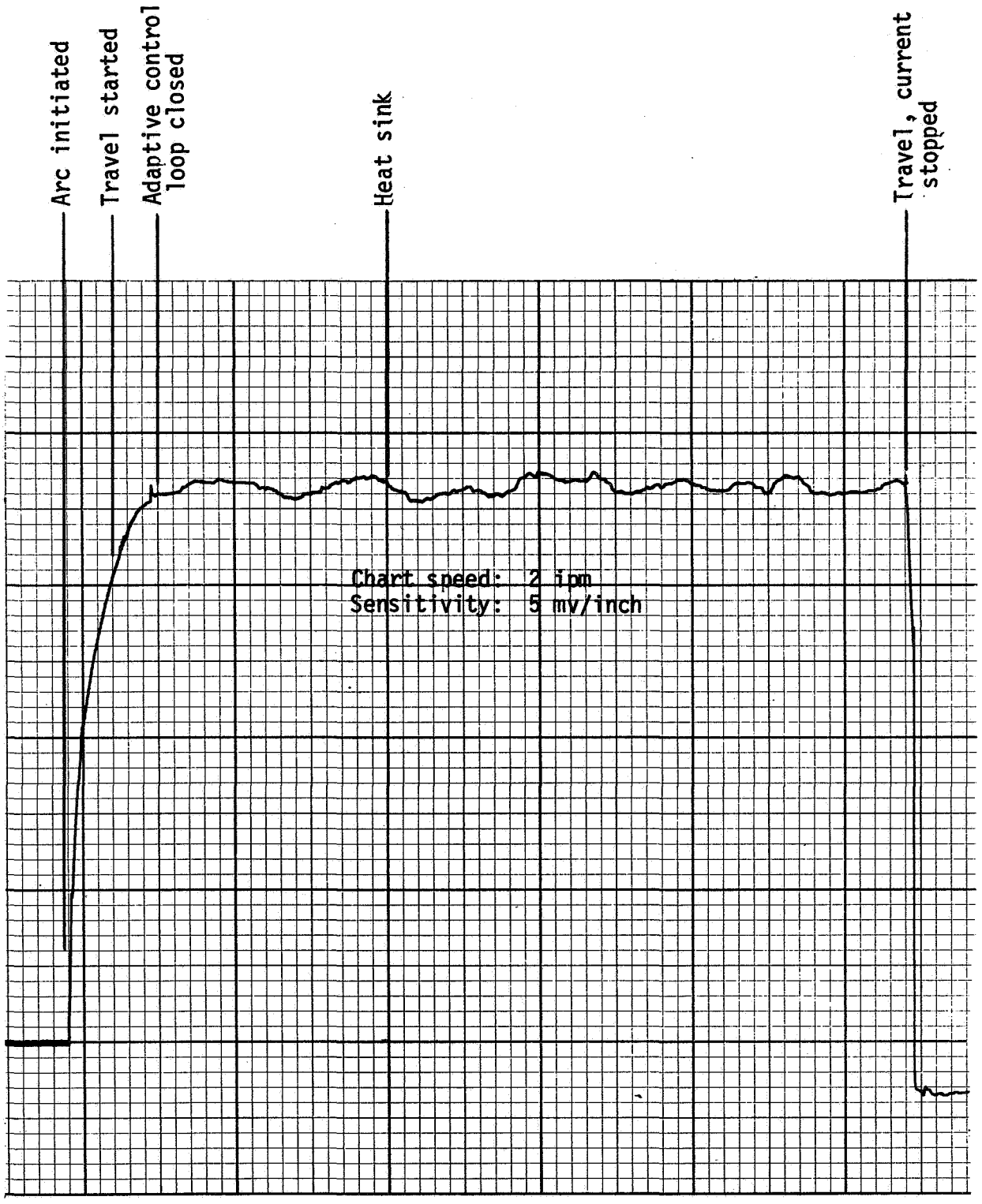


Figure 187; Hybrid thermocouple output, test number 15T, preheat pass.


Arc initiated
Travel started
Adaptive control loop closed
Heat sink
Travel, current stopped
Chart speed: 2 ipm
Sensitivity: 5 mv/inch

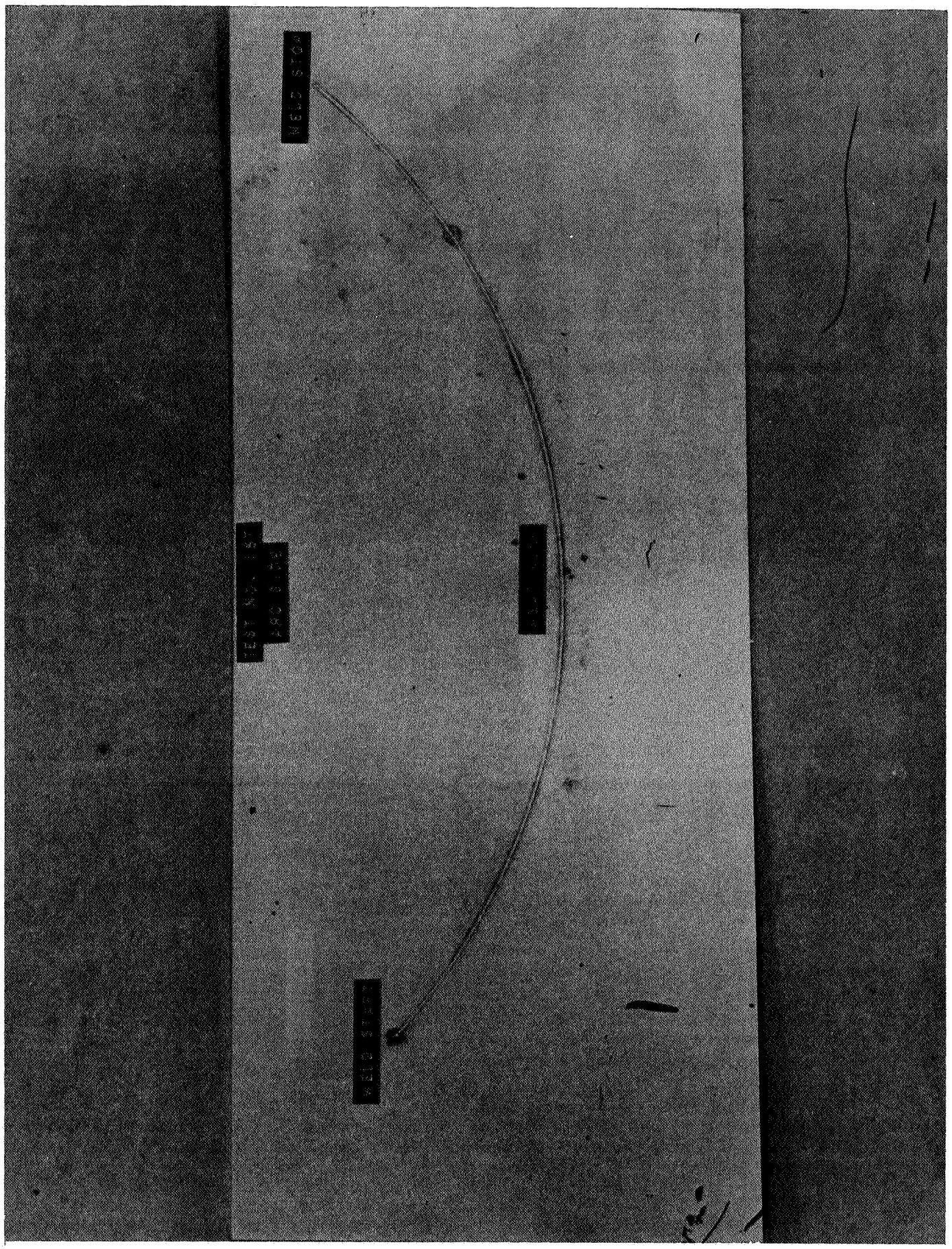


Figure 180. Weld bead, arc side, test number 151.

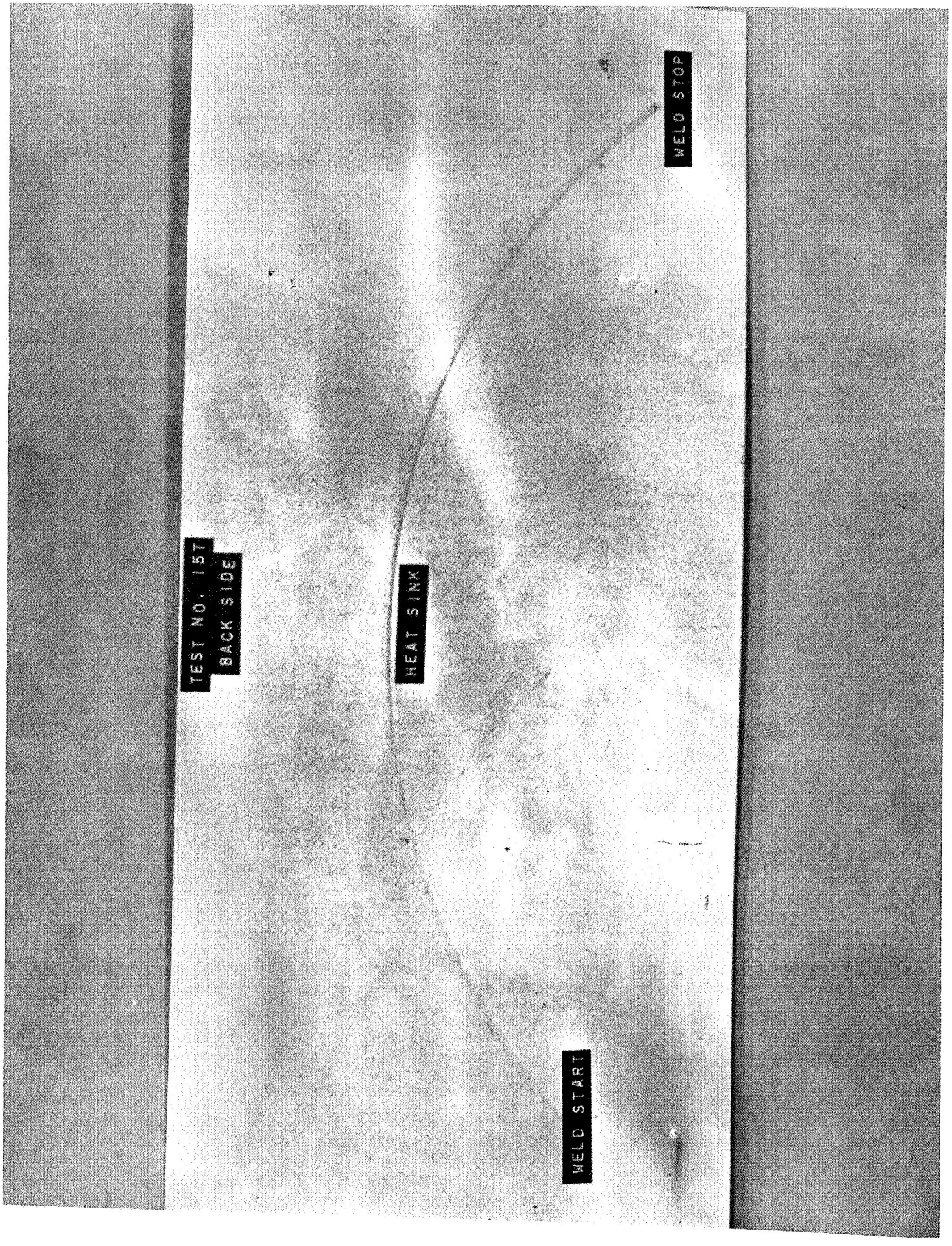


Figure 190: Weld bead, backside, test number 15T

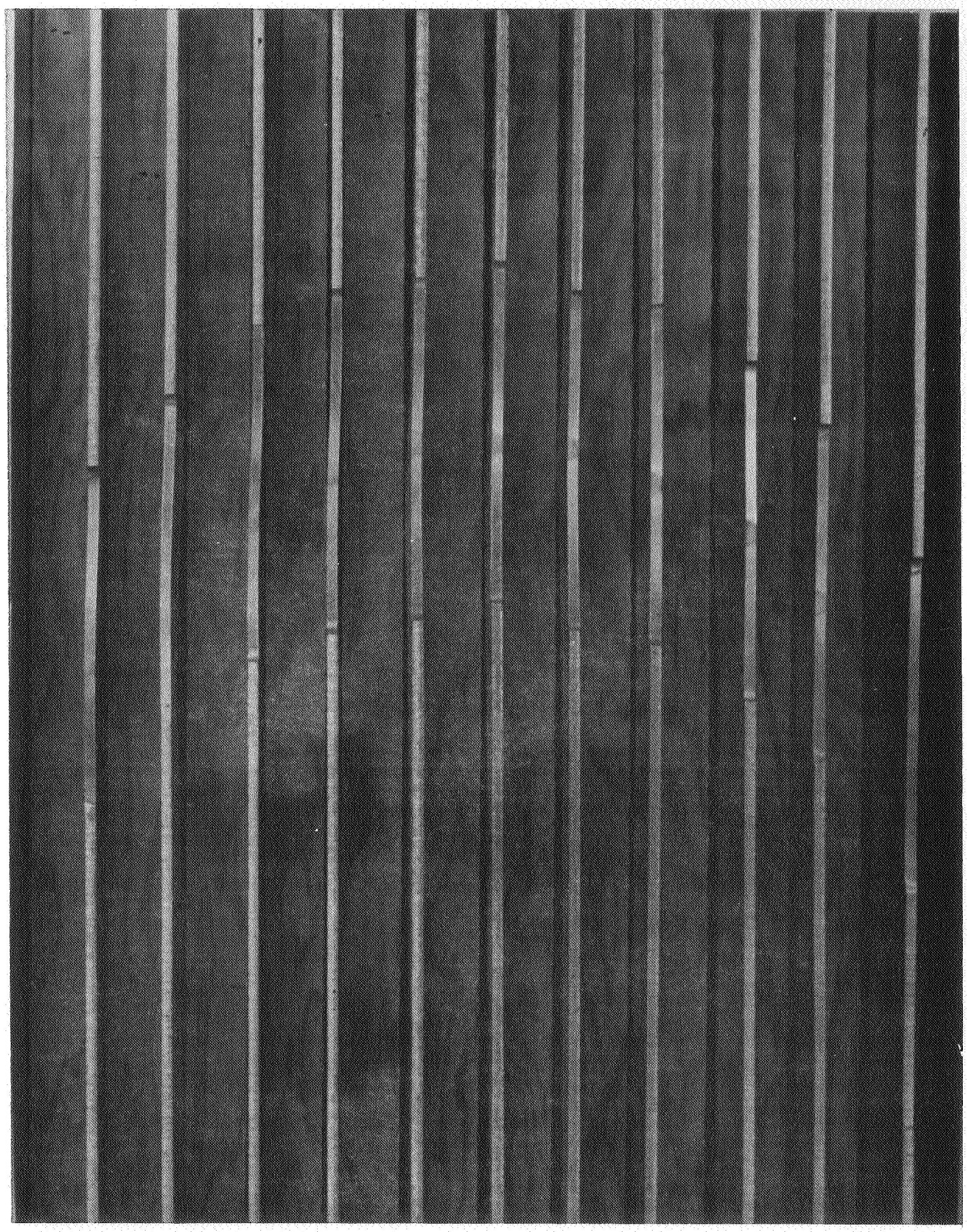


Figure 191: Cross Sections, Test Number 15T.

control of temperature at the probe position for wide variations in fitup, fixture, and material thickness.

Experimentation was conducted to demonstrate that the hybrid thermocouple signal was proportional to penetration on partial or full penetration welds made on 0.090 inch thick 2219 aluminum samples. On all of these experiments automatic voltage control was used to maintain constant arc voltage, and the transducer signal was used to automatically alter the weld current in such a manner as to maintain the mean temperature (and hence depth of penetration), at the probe, constant. While experimentation was limited to 0.090 inch thick samples, it was concluded that similiar results could be achieved on all samples less than approximately 0.125 inch thickness.

Results of experimentation conducted on samples of 0.250 and 0.312 inch thickness indicated that the hybrid thermocouple signal could be correlated with partial penetration for varying conditions of heat sinck. The system was found to operate with only marginal satisfaction, however, on the 0.250 and 0.312 inch thick samples when 100% penetration was attempted.

Experiments were conducted to establish the feasibility of utilizing a continuous intrinsic thermocouple in conjunction with a backup bar for penetration control on welds requiring backup for chilling purposes. Also, preliminary investigation was conducted to determine the feasibility of a recently developed thermocouple wire, trademarked Magic Wire, being used in the backup bar type of control.

In the majority of experiments conducted under this program, the temperature at a single point, located with respect to the molten puddle, was monitored. However, a dual probe could be easily implemented such that a continuous measure of a temperature gradient could be obtained; thereby providing a continuous signal proportional to thermal transients in the workpiece. This signal could then be used in a feedback loop to control an auxiliary workpiece cooling system; and hence provide automatic control of the time-temperature relationship in the vicinity of the molten puddle. The result would be better control of the grained cast structure and heat affected zones in the weldment.

While all experimentation conducted under this program was limited to 2219

aluminum, the same technique is applicable to other materials as well. For example, in the welding of stainless steel tubing a constantan probe could be utilized to provde an intrinsic iron-constantan thermocouple transducer. For other welding materials a different type probe material may be advisable.

7.0 REFERENCES

7.1 NASA Specification: Development of Weld Intelligence System and Controls, MR & T SK114.

7.2 "Infrared Temperature Sensing Systems For Automatic Fusion Welding", P.W. Ramsey, J.J. Chyle, J. N. Kuhr, P. S. Myers, M. Weiss and W. Groth, Weding Journal, August, 1963.

7.3 "Time-Temperature Characteristics In Aluminum Weldments", Final Report, Contract No. NAS8-11930, Control No. DCN 1-5-30-12723-01. Report prepared by Harvey Engineering Laboratories.

7.4 "Temperature Equipment, Measurement System (TEMS), Magic Wire", Report prepared by Continental Sensing, Inc., 1960 North Ruby Street, Melrose Park, Illinois.

7.5 "The Science of Arc Welding", Clarence E. Jackson, Welding Journal, pp 129S - 140S, April, 1960.

7.6 "Induktive Temperature Messung", G. Keinath, Arch. tech. Messen V215-2 (1934).

7.7 "Temperature Measurement with Eddy Currents", Raymond J. Mouly, TEMPERATURE - ITS MEASUREMENT AND CONTROL IN SCIENCE AND INDUSTRY, Vol 3, Part 2, 1962, Reinhold Publishing Corp., New York, N. Y. pp 1009-1013

7.8 NASA memo number R-ME-ME-198-64 by W. M. McCampbell.

7.9 "Cooling Rates and Peak Temperatures in Welds", C. M. Adams, Jr., Welding Journal, May, 1958, pp 2105-2155.

8.0 PUBLICATIONS, PATENTS, AND PRESENTATIONS

8.1 "The Development of a Weld Intelligence System", W. M. McCampbell, G. E. Cook, L. E. Nordholt, and G. J. Merrick, pp 1395-1445, Welding Journal Vol. 45, No. 3 (March, 1966). Paper presented at AWS 1965 National Fall Meeting held in Birmingham, Ala., during October 4-7, 1965.

8.2 "System Maintains Constant Penetration During Fusion Welding", W. M. McCampbell and G. E. Cook, NASA TECH BRIEF, Brief number 67-10091, April, 1967.

8.3 "Thermocouple Probe Controls Welding Torch", G. E. Cook and W. M. McCampbell, p. 98, CONTROL ENGINEERING, Vol. 14, no. 11, Nov., 1967.

8.4 "Intrinsic Thermocouple Monitors Temperature In Aluminum Welding", G. E. Cook and W. M. McCampbell, To be published in METAL PROGRESS.

8.5 Disclosure of Invention for "Automatic Control System for Maintaining Constant Penetration During Fusion Welding", George E. Cook and William M. McCampbell.

9.0 PERSONNEL AND ACKNOWLEDGEMENTS

9.1 MERRICK ENGINEERING PERSONNEL

9.1.1 Dr. George E. Cook, Vice President and Director of Engineering, served as project manager for this program.

9.1.2 Mr. George J. Merrick, President, administration, and project engineer.

9.1.3 Mr. L. E. Nordholt, Vice President and Director of Engineering, project engineer.

9.1.4 Mr. C. K. Wortman, welding technician.

9.1.5 Mr. Glen G. Griffin, electrical designer.

9.1.6 Mr. William Akin, research analyst.

9.1.7 Mr. Jim Petty, welding technician.

9.2 NASA PERSONNEL

9.2.1 This program was administered under the technical direction of the Manufacturing Engineering Laboratory with Mr. William M. McCampbell (R-ME-ME) as technical representative.

9.2.2 Mr. Kirby Platter served in administrative liaison.

9.3 SUBCONTRACT TO VANDERBILT UNIVERSITY

Vanderbilt University provided assistance in the investigation of eddy current temperature transducers and in the preliminary design of the adaptive controller.